Optimization and automation of the ligase cycling reaction

Zur Erlangung des Grades eines Doktors der Naturwissenschaften (Dr. rer. nat.)
genehmigte Dissertation von Niels Carsten Schlichting aus Berlin
Tag der Einreichung: 24.02.2020, Tag der Prüfung: 24.06.2020

1. Gutachten: Prof. Dr. Johannes Kabisch
2. Gutachten: Prof. Dr. Beatrix Süß
Darmstadt – D 17

TECHNISCHE UNIVERSITÄT DARMSTADT

Biology Department
Computer gestützte Synthetische Biologie
Prof. Dr. Johannes Kabisch

Optimization and automation of the ligase cycling reaction

Doctoral thesis by Niels Carsten Schlichting

1. Review: Prof. Dr. Johannes Kabisch
2. Review: Prof. Dr. Beatrix Süß

Date of submission: 24.02.2020
Date of thesis defense: 24.06.2020

Darmstadt – D 17

Acknowledgement

First, I want to thank Prof. Dr. Johannes Kabisch for the great opportunity to be a member of his group and to be involved in the development of automated methods. He always encouraged me to got one step further. Thanks to his open door policy he enabled an agile working environment and improved my research with his knowledge and valuable ideas for scientific and pragmatic solutions. Additionally, I am thankful for his support to write this thesis and to present the derived data in a consistent and professional way.

Special thanks goes to my second reviewer Prof. Dr. Beatrix Süß for her warm welcome, her support during my phD and for being a helpful advisor.

I also want to thank Prof. Dr. Barbara Drossel and Prof. Dr. Viktor Stein for being the auditors for the defense of my thesis.

For all the great moments I want to thank the whole group of Prof. Dr. Johannes Kabisch. The team spirit, organizational skills and personal interactions were brilliant and very important for my work. Thank you very much! Extraordinary thanks goes to Florian Nadler, Thomas Zoll, Stefan Bruder, Felix Bracharz and their detailed hints and inspiring philosophical discussions. Special thanks goes to Thomas Zoll, Albert Koch and Aaron Eiermann for supporting me to work with the robotic platform and to design the workflow for the automated DNA assembly.

Additionally, I am grateful for the help of Francois-Xavier Lehr and Darius Zibulski to develop a cell-free version of the LCR.

I want to thank Prof. Dr. Heinz Köppl and Prof. Dr. Beatrix Süß for the opportunity to let me be a member of the diverse and fantastic project CompuGene. Together with post-docs, phD candidates and students this project enabled a unique environment to work interdisciplinary and to achieve goals beyond my personal knowledge. Especially I want to thank Felix Reinhardt, Sven Jager, Michael Schmidt, Maximilian Dombrowsky, Johannes Falk, Lara Becker and Tim Prangemeyer for the valuable and mind-opening discussions. Also thanks to the HMWK Hessen to grant this brilliant project.

Finally, I want to thank my family and friends for being patient, their encouragement and helpful comments to realize this thesis.

Ehrenwörtliche Erklärung:

Ich erkläre hiermit ehrenwörtlich, dass ich die vorliegende Arbeit entsprechend den Regeln guter wissenschaftlicher Praxis selbstständig und ohne unzulässige Hilfe Dritter angefertigt habe.
Sämtliche aus fremden Quellen direkt oder indirekt übernommenen Gedanken sowie sämtliche von Anderen direkt oder indirekt übernommenen Daten, Techniken und Materialien sind als solche kenntlich gemacht. Die Arbeit wurde bisher bei keiner anderen Hochschule zu Prüfungszwecken eingereicht.

Darmstadt, 24.02.2020

N. C. Schlichting

Contents

Zusammenfassung

Im Feld der Biologie, und speziell in der Synthetischen Biologie, ist die Verwendung von sogenannten *Design-Build-Test-Learn* (DBTL)-Zyklen eine generelle Methodik um z. B. diverse genetische Konstrukte zu generieren und zu optimieren. Die Geschwindigkeit für solch einen DBTL-Zyklus ist hauptsächlich dadurch limitiert, inwiefern DNA Fragmente erfolgreich zu komplexeren Produkten assembliert werden können. Eine Möglichkeit dies zu gewährleisten ist die Automatisierung der DNA Assemblierung mit Hilfe von Robotik-Plattformen und wird zunehmend verwendet. Unglücklicherweise werden dafür weitestgehend Assemblierungsmethoden verwendet, die einen aufwändigen Planungsprozess benötigen, die Wiederverwendung der genutzten DNA Fragmente erschweren oder sogar genetische Narben in den Produkten hinterlassen. Eine Assemblierungsmethode, die alle drei genannten Limitationen umgeht, ist die *Ligase Cycling Reaction* (LCR) und wird daher in dieser Arbeit verwendet.
Im Kontrast zu gängigen Assemblierungsmethoden müssen keine Konstrukt-spezifischen DNA Fragmente entwickelt werden. Zudem bleiben keine genetischen Narben in der finalen Sequenz zurück. Zur Festlegung der Assemblierungsreihenfolge werden einzelsträngige DNA Brücken, sogenannte *Bridging Oligos* (BOs), genutzt um bis zu 20 DNA Fragmente in einer Reaktion zu ligieren. Dazu wird der Mix aus Fragmenten, BOs und einer Ligase unter spezifischen Salzbedingungen zyklisiert erhitzt und abgekühlt um das Denaturieren der DNA Fragmente, das Hybridisieren der BOs mit den Fragment-Einzelsträngen sowie die Ligationsreaktion zu ermöglichen. Letztendlich wird das Produkt nach der Transformation von *Escherichia coli* (*E. coli*) mit der LCR erhalten. Somit ist die LCR eine Verkettung einer *in vitro* sowie *in vivo* Prozedur. Diese Methodik wurde bereits 2018 von Robinson *et al.* mit einer Robotik-Plattform automatisiert. Jedoch wurden teilweise niedrige Assemblierungseffizienzen erreicht was mit einem hohen zeitlichen und finanziellen Aufwand für das Identifizieren von korrekt assemblierten Konstrukten verbunden ist. Die Optimierung der LCR Reaktion und die darauffolgende Automatisierung mit Hilfe der Robotik-Plattform des CompuGene-Projektes ist der Fokus dieser Arbeit und soll die Reproduzierbarkeit, Robustheit und den Durchsatz von DNA-Assemblierungen verbessern. Zusätzlich wird eine *in vitro* LCR Methode entwickelt, um den *in vivo* Einfluss von *E. coli* auszuschließend und das limitierende Transformieren und Ausplattieren der *in vivo* LCR zum umgehen.
Durch die Verwendung des publizierten LCR Protokolls von de Kok *et al.* (2014) konnten bis zu zehn DNA Fragmente in einer Reaktion erfolgreich assembliert werden. Jedoch waren manche

Assemblierungen nicht erfolgreich oder die Effizienz der Reaktion war gering. Daher wurde ein verbessertes LCR Protokoll entwickelt: im Gegensatz zum ursprünglichen Protokoll erhöhte das Weglassen der Detergenzien Dimethylsulfoxid (DMSO) und Betain die Effizienz und die Anzahl der Transformanten. Dieser Einfluss konnte bei Assemblierungen verschiedener Plasmide gezeigt werden. Weiterhin führte eine Erhöhung der Annealing Temperatur zu verbesserten Ergebnissen bezüglich der Transformantenmenge. Das neue LCR Protokoll wurde anschließend verwendet um ein Protokoll für ein automatisiertes Assemblieren und Ausplattieren von 96 Konstrukten innerhalb von 19 h mit Hilfe der Robotik-Plattform zu ermöglichen. Dieser Prozess wurde im Trockenmodus entwickelt und erfordert noch eine Validierung. Um die Automatisierung weiterhin zu unterstützen, wurde zudem eine Software zur automatischen Erzeugung von BOs und von voll-kombinatorischen *in silico* LCRs entwickelt. Diese Software und der Robotik-Prozess der *in vivo* LCR bildet mitunter auch die Grundlage für die entwickelte *in vitro* LCR: basierend auf diesem zell-freien System könnten innerhalb von 19 h ca. 5× mehr LCR Reaktionen durchgeführt und analysiert werden als mit dem *in vivo* Ansatz. In Zukunft stellt die *in vitro* LCR die Methode der Wahl dar um automatisiert im Hochdurchsatz DBTL-Zyklen von genetischen Schaltern und Schaltkreisen durchzuführen.

Summary

Modern approaches in the field of biology, especially the field of synthetic biology, are based on design-build-test-learn (DBTL)-cycles to, *e.g.*, generate optimized genetic constructs for various applications. The overall speed of one cycle mainly depends on the ability to physically assemble DNA with a high efficiency in a short time period. This is achievable by automation approaches. Several automated DNA assemblies are described in the literature but are related to laborious *in silico* planning, are usually limiting the reusage of the DNA parts or are introducing scars into the final sequence. To overcome those restrictions and to enable a rapid automation, an easy-to-plan and scar-less assembly method has to be utilized. The ligase cycling reaction (LCR) is the most promising candidate and is the scope of this thesis.
For the LCR, no construct specific DNA parts have to be designed and no scars are incorporated into the desired construct. Single-stranded bridges made of DNA (bridging oligos (BOs)) are utilized to specify the order of up to 20 parts in a one-pot reaction. A thermal cycling protocol enables the strand separation of the DNA parts, the annealing of the BOs and the *in vitro* ligation. The desired product is finally derived by transforming the LCR mixture into *Escherichia coli* (*E. coli*). Due to the benefits of this assembly technique, the LCR was already implemented from Robinson *et al.* on a robotic platform in 2018. According to the authors and the results presented in this thesis, the assembly efficiency for some LCR reactions is low. This issue is associated with a tremendously increased effort to obtain the desired sequence. The reasons for low efficiencies are determined within this thesis to optimize the LCR. Furthermore, an alternative *in vitro* method for the cumbersome *in vivo* approach is developed and is based on a cell-free system to screen for correctly assembled constructs. In the end, a workflow for an automated LCR is designed and initially validated on a robotic platform.
Overall, up to ten DNA parts were assembled in a one-pot reaction by applying the LCR protocol described in the literature by de Kok *et al.* (2014). Nevertheless, some assemblies were not successful and an improved LCR assembly protocol was developed. In contrast to the literature, to omit the secondary structures inhibitors dimethyl sulfoxide (DMSO) and betaine had tremendously increased the efficiency and the total number of colonies for the assembly of various plasmid designs. Furthermore, to shift the annealing temperature to the activity optimum of the utilized ligase was beneficial. The new LCR protocol was implemented in an automated assembly and plating workflow for a robotic platform to theoretically build 96 DNA constructs within 19 h and needs to be further validated. To support the automation process, a software

for the BO design of combinatorial LCR assemblies was build. As an additional scope, an *in vitro* LCR method was designed and validated by using a cell-free system for the test-learn steps of the DBTL-cycles. In comparison to the automated *in vivo* workflow, ca. 5× more LCR assemblies are screenable within the same time frame of 19 h and the same hardware setup. In future, the optimized LCR protocol and the robotic workflow for the *in vivo* LCR can be adapted for the *in vitro* LCR approach and represents the method of choice for automated high-throughput DBTL-cycles of genetic switches and circuits.

Abbreviations and lists

Abbreviations

ATP	adenosine triphosphate
BASIC	BioPart assembly standard for idempotent cloning
BO	bridging oligo
CFPS	cell free protein synthesis
CFU	colony forming unit
cPCR	colony polymerase chain reaction
CPEC	circular polymerase extension cloning
DBTL	design-build-test-learn
DMSO	dimethyl sulfoxide
ds	double stranded
dsDNA	double stranded DNA
EDTA	ethylenediaminetetraacetic acid
GMO	genetically modified organism
GOI	gene of interest
LB	Lysogeny broth
LCR	ligase cycling reaction
NAD^+	nicotinamide adenine dinucleotide
OD	optical density
ORF	open reading frame
ORI	origin of replication
PCR	polymerase chain reaction
POI	product of interest
RBS	ribosome binding site
RCA	rolling circle amplification
RT	room temperature
SLiCE	seamless ligation cloning extract
ssDNA	single stranded DNA
T4-PNK	T4-polynucleotide kinase
TAE	TRIS acetate EDTA
TAR	transformation-associated recombination
T_m	melting temperature
TRIS	trihydroxyaminomethan
TXTL	cell-free transcription-translation
w/o	without

Genes

ampR	*ampicillin resistance gene*
mRFP1	*monomeric red fluorescent protein 1*
GFP	*green fluorescent protein*
kanR	*kanamycin resistance gene*
recA	*recombinase A*
sfGFP	*superfolder green fluorescent protein*
specR	*spectinomycin resistance*

List of Figures

List of Tables

1 Introduction

One of the goals of synthetic biology is to specify, design, build and test genetic circuits and to optimize the microbial production of, *e.g.*, biofuels [53], therapeutics [77, 110], to support the development of new microbial or plant production strains [113, 124] or to promote a cell free protein synthesis (CFPS) with cell extracts derived from various hosts [42]. Genetic circuits consist of DNA parts which are assembled to functional genes, pathways with regulatory elements and complete genomes [23, 115]. The circuits are build with the help of computational methods [51, 69, 116, 123] to predict constructs with a low susceptibility regarding, *e.g.*, context dependent perturbations [7]. All these computer-aided approaches are based on the design-build-test-learn (DBTL) cycle to support a robust *in vivo* functionality of the circuit and accelerates synthetic biology approaches like an increased yield of a product of interest (POI). As a prerequisite for a computational design, the lowest level building bricks, the DNA parts, need to be characterized precisely according to their switching behavior [6], retro-activity [18], host-dependency [7] and environmental context [28, 35, 58]. The DNA parts are derived by chemical synthesis [43] or *in vitro* amplification from an existing template via polymerase chain reaction (PCR). For the utilization of *de novo* DNA parts, synthesis is mandatory.
The DNA synthesis utilizes oligonucleotides derived by the phosphoramidite method [84] and is applicable for a total size of 2000 bp [43] and they are commercially provided as 'synthetic genes', 'gene fragments' or 'GeneStrands'. Larger genes, circuits or even complete genomes can be ordered and are obtained by joining several synthetic genes by ligations and PCR amplifications. Until today, this step-by-step synthesis approach is still laborious and expensive [43, 57]. Furthermore, to receive large synthetic constructs can take weeks or even months (personal experience). To rapidly build the designed circuits, an automated and robust DNA assembly method is needed to join synthetic genes and PCR products [23, 43, 115]. For this thesis, a robust DNA assembly is defined as a high efficient method with a low rate of misassemblies, a high reproducibility and a low impact of intra- and intermolecular crosstalk of all utilized components.

1.1 DNA assembly in synthetic biology

1.1.1 Status quo and limitations for rapid prototyping approaches

The synthesis of DNA,and especially the robust assembly of DNA parts, are the scaffold of all synthetic biology approaches [43, 63, 114] and '[...] the limit of what synthetic biology can achieve is becoming determined by our ability to physically assemble DNA.' [23]. By DNA assembly methods already designed *in silico* constructs are physically build to test their *in vivo* or *in vitro* behavior and are mainly representing the 'build' process of a DBTL cycle [29].
Nowadays, several assembly methods are used for the build process, *e.g.*, BioPart assembly standard for idempotent cloning (BASIC) [102], Golden Gate assembly [24,25], Gibson assembly [34] or circular polymerase extension cloning (CPEC) [80], and are based on specific DNA part modifications like overhangs [34] or restriction sites [80, 102] (Table 1.1). Usually, the DNA parts for the mentioned assembly methods have to be redesigned for each desired construct (Figure 1.1). For restriction-ligation-based methods, the utilized sequences have to be analyzed and modified to remove unwanted restriction sites [37]. Altogether, the introduced assembly methods are disadvantageous for the reusability and automation. Furthermore, scars can remain after the assembly. This results in unpredictable behavior of the translation if the scar is located nearby a sensitive functional sequence like an ribosome binding site (RBS) or for the design of fusion-proteins due to introduced shifts of an open reading frame (ORF) [23, 88].
In contrast, the ligase cycling reaction (LCR) [11, 16, 74, 83] fits the prerequisites for robust and automated assemblies [81]. For this DNA assembly method, no specific modifications of the DNA parts are necessary and no scars are introduced. In total, the LCR fits for the automated assembly of genetic constructs.

Table 1.1: Most common DNA assembly methods, their mechanisms and drawbacks. BASIC: BioPart assembly standard for idempotent cloning, CPEC: circular polymerase extension cloning, LCR: ligase cycling reaction, SLiCE: seamless ligation cloning extract, TAR: transformation associated recombination.

Assembly method	Mechanism	Drawbacks
Golden Gate [24, 25]	type IIs restriction	scars, limited reusability of parts
BASIC [102]	type IIs restriction	scars, limited reusability of parts
CPEC [80]	overhangs, PCR amplification	scars, limited reusability of parts
Gibson [34]	overhangs, ligation	limited reusability of parts
SLiCE [126]	homologous recombination	$\leq$5 parts in one reaction, limited reusability of parts
TAR [55]	homologous recombination	mutation prone, 2-3 days, limited reusability of parts
LCR [11, 16, 74, 83]	ligation	no automated design tool available

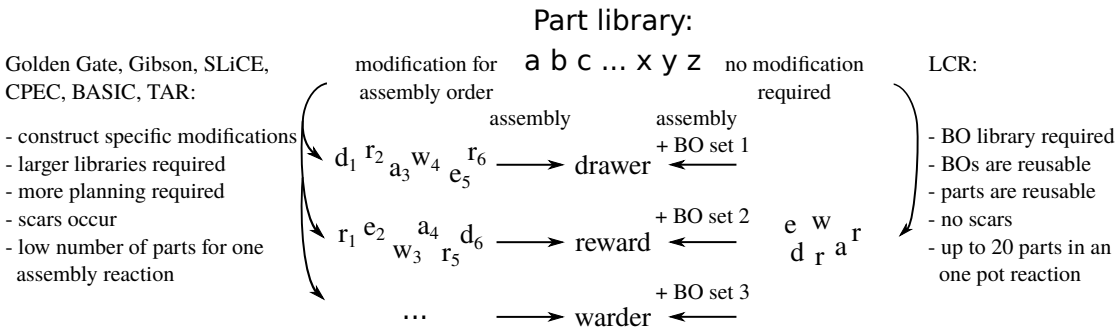

Figure 1.1: Commonly utilized assembly methods like GoldenGate, Gibson assembly® etc. are hampering the usage of a DNA library due to specific modifications of the DNA parts. The LCR allows a DNA library based on unmodified DNA parts. By using the DNA library and specific BOs several constructs can be build with the same parts. The parts are illustrated by letters of the alphabet. Furthermore, no remnant scars are introduced in the final construct. BO: bridging oligo, LCR: ligase cycling reaction, TAR: transformation associated recombination.

1.1.2 Automation in synthetic biology

The automation in the field of biology is one way to ensure fast and robust methodical approaches. It is considered as a mandatory tool to meet the modern demands of high throughput methods in biological research and also to tackle the low reproducibility of published results [47]. Currently,

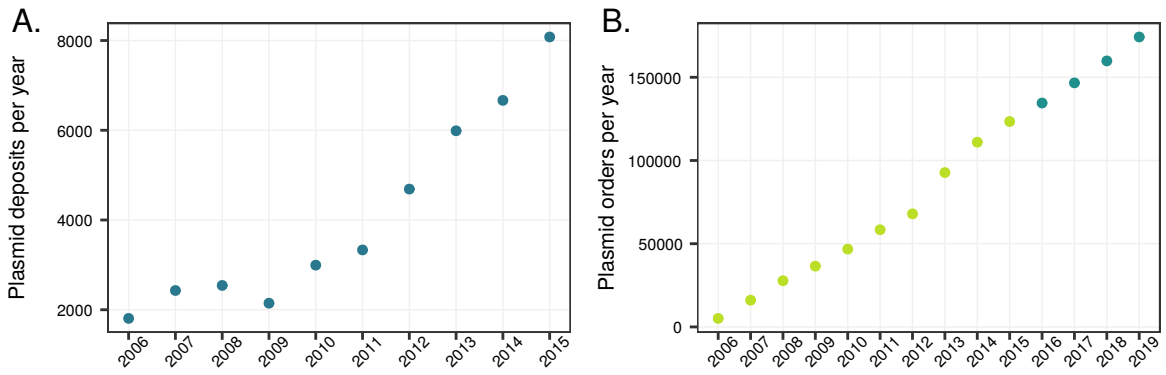

Figure 1.2: Plasmid deposits and orders of the Addgene repository [50]. **A.** Plasmid deposits from 2006 to 2015 [57]. **B.** Amount of orders from 2006 to 2019. The raw data from 2006 to 2015 is derived from [49, 57]. Data points from 2016 to 2019 are estimated with a growth rate of 9 %. They are based on the announced and predicted growth from Addgene in 2018 (https://blog.addgene.org/celebrating-15-years-of-scientific-sharing). For all other data points, the raw data of [49, 57] was plotted.

the implementation of automation technologies is well established in the industry but is limited in the field of academia due to a high financial effort for highly specialized devices. This is usually undesirable for the research of public facilities like universities because it hampers the flexibility in use. Especially, the lack of a universal, scar-less and easy-to-design assembly method to build constructs in a high throughput scale is still an urgent bottleneck [114]. For the

design of circuits, various software tools were developed, provided and utilized which allow a full combinatorial design with and without a rational strategy [26, 69, 100, 109]. The utilization of these tools result in a vast workload for classical wet-lab cloning and can be estimated by the dynamics of the plasmid repository of Addgene [50]. A tremendous increase of the total amount of build, deposited and ordered plasmids is observed (Figure 1.2, data from [49, 57]). This highlights the need for automated DNA assemblies and probably even represents the impact of the increasing utilization of automation approaches. On the other hand, computer-aided tools have to be optimized to lower the amount of assemblies by omitting irrational designs. A promising DNA assembly method for the automation is the LCR. Unfortunately, low effort was spent so far to strengthen this method and to automatically design and build genetic constructs.

1.2 Ligase cycling reaction

1.2.1 Ligase cycling reaction and ligase chain reaction

The LCR fulfills relevant criteria like a fast and robust DNA assembly and fits the automation approach to enable a rapid build process for synthetic DNA circuits. A similar method is utilized in the field of molecular biology and is also named LCR. This LCR, the ligase chain reaction, also applies oligonucleotides and a ligase but with the purpose to synthesize DNA fragments [121], to sequence DNA [13] or to detect DNA mutations [33]. For these methods, the ligation is coupled with an amplification step by a PCR. Unfortunately, the same abbreviation 'LCR' is utilized. Nevertheless, the method of interest of this thesis is the ligase cycling reaction (LCR). It is closely related to the ligase chain reaction whereby *E. coli* is utilized to amplify the product. In the following, the abbreviation 'LCR' is consistently utilized for the DNA assembly reaction method 'ligase cycling reaction'.
According to the mechanistic principle of the LCR (Figure 1.3A), no construct-specific modifications of the DNA parts are necessary besides that all DNA parts have to be phosphorylated on the 5'-end to enable the enzymatic ligation [20, 98]. No scars are incorporated and the utilization of DNA part libraries is possible (Figure 1.1). The order of assembly is determined by the addition of single stranded DNA (ssDNA) oligonucleotides which are spanning a bridge from one part to the next and are called bridging oligos (BOs) (Figure 1.3A). Based on the BOs, the LCR offers a DNA assembly with a full modularity. To shuffle the order of already existing DNA parts, new BOs have to be ordered only. This reduces the experimental workload by omitting an additional DNA part synthesis or PCR amplification. Further, 12 kbp constructs consisting of up to 20 fragments can be assembled in a one-pot reaction. For the ligation of the DNA parts, a thermostable prokaryotic ligase is utilized in combination with repetitive thermal cycling and the transformation of *E. coli* (Figure 1.3) [11, 16]. In 2014, de Kok *et al.* [16] published this LCR method and is the baseline condition for the following sections.

1.2.2 Ligation of DNA fragments

First, the dsDNA is heated up to separate the strands and to allow the hybridizations of the forwarded BOs with the ssDNAs of two DNA parts in the annealing step. The ligase recognizes the 5'-phosphorylated end at the single nick on the opposite strand of the bound BO followed by a binding [19,71] (Figure 1.3B) and a conformational change of the DNA by bending [68]. To bind to the DNA, the ligase recognizes two recognition sites which are asymmetrically placed around the nick. On the 5'-end, 7-12 bp and on the 3'-end 3-8 bp are mandatory for the binding event of helix-hairpin-helix motifs [20]. The ligase is sensitive to a missing 5'-phosphorylation [20, 71] or a gap $\geq$ 1 nt [97]. Both tremendously decrease the ligation efficiency. On the other hand, this increases the fidelity of this ligation method due to a high sensitivity to mismatches, unspecific hybridizations and overlapping bases at the ligation site. After the ligation of the nicked strands of two DNA parts, the forwarded BO is separated from the template by a denaturation step at 94 °C. In the next cycles, the ligated strands serve as template for joining the forward strands. By 25 denaturation-annealing-ligation cycles most DNA parts are ligated to a double stranded (ds) construct. Afterwards, the assembled sequence is obtained by transforming the LCR mixture into *E. coli* and by screening the obtained colonies via PCR or by sequencing.

1.2.3 Melting temperature of the bridging oligos

In the LCR, a stable hybridization of the BOs with the ssDNA parts is mainly influenced by the annealing temperature, the melting temperature (T_m) of the BOs and the salt concentrations. At a given BO-T_m, the BOs are in a folded state if the annealing temperature is too low. No hybridization with the DNA part is achieved and no ligation will appear. By increasing the annealing temperature equal to the T_m of the BOs, 50 % of them are unfolded [90] and can participate in the annealing process. A further increase of the annealing temperature results in less hybridizations and less efficient assemblies in the annealing time of 30 s. Concluding this, the interdependence of a precisely calculated T_m for the BOs and the utilized temperatures have to be considered carefully. Besides the adjustment of the BO length or the annealing temperature, T_m altering supplements can be utilized to influence this dynamic homeostasis. In the LCR, 8 % v/v and 0.45 M betaine are added to accelerate the strand separation time during cycling [11, 16]. Although this is regarded as beneficial for the ligase due to a shorter exposition to high temperatures, both additives are also lowering the T_m of the BOs [65,112]. No investigation on the synergistic effects of utilizing both additives, the BO-T_m and the annealing temperature was performed. Furthermore, the T_m calculations of a BO tremendously differ if another algorithm is applied for the design of BOs with the target T_m of 70 °C [90]. This is related to the simplified calculation models, estimations in the utilized formulas and the complexity of the multi-state melting behavior of oligonucleotides [90]. Those inaccuracies in the design process of the BOs are assumed to have an impact on the LCR assembly. Additionally, the Gibbs free energy ΔG is considered as the more significant design parameter for oligonucleotide-based

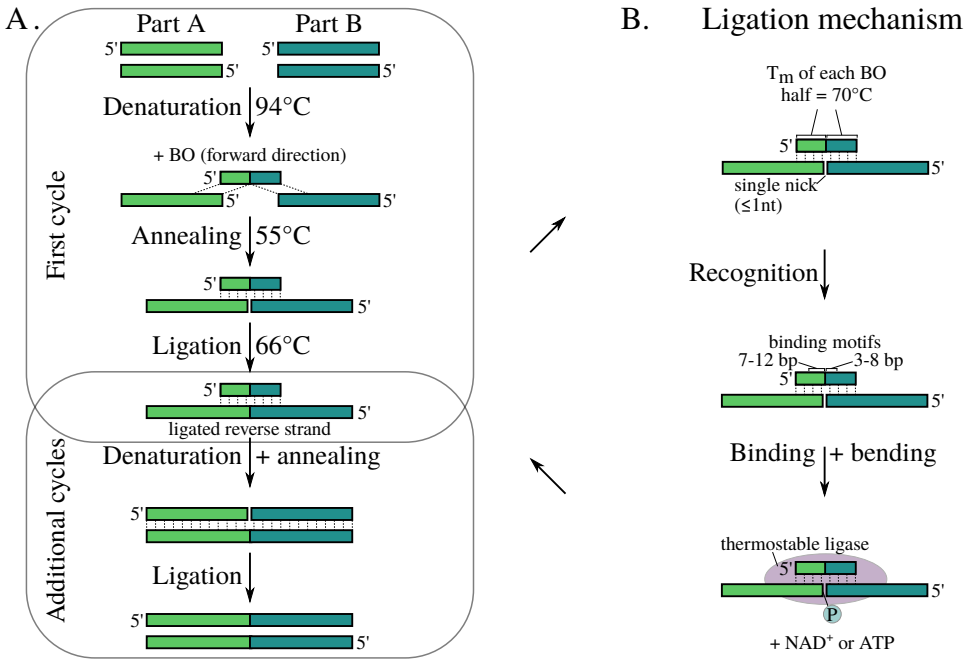

Figure 1.3: Principle of the ligase cycling reaction. **A.** DNA parts are denaturated by heating up the LCR mixture to 94 °C for 2 min and to obtain ssDNA. In the annealing step, the forwarded BOs are able to bind to the free ends of the two ssDNA parts and to form a single-nicked template for the DNA ligase. After the ligation with the help of the BO, the ligated reverse strands are serving as a template for the forward strands. Finally, the DNA parts are assembled to the desired construct. [16] **B.** To accomplish a stable complex of BO and ssDNA at the thermal conditions shown in A., each BO-half have a target T_m of 70 °C [16]. The BO binds at the ends of the single stranded DNA parts to form a dsDNA with a single nick. The thermostable ligase recognizes the nick and binds asymmetrically [20]. By utilizing NAD^+ or ATP, the ligase joins the DNA parts by utilizing the phosphorylated 5'-end ('P') of part A [98]. ATP: adenosine triphosphate, BO: bridging oligo, bp: basepairs, NAD^+: nicotinamide adenine dinucleotide, nt: nucleotide, T_m: melting temperature.

molecular reactions [40, 90], respectively the BOs. Altogether, investigations on the BO-T_m and ΔG, the utilized calculation rules and experimental temperatures are so far neglected for LCR assemblies. To determine the effects of varying these parameters is one scope of this thesis. Based on this, optimized LCR conditions can be postulated and validated to increase the robustness of this assembly method.

1.3 Automated LCR assembly

To address the automated assembly of genetic constructs, several computer-aided approaches are dealing with specifying, designing and building constructs but are mainly utilizing the aforementioned undesired restriction-ligation or homology based methods [41, 45, 69, 76, 103, 114, 122] (Figure 1.1). To address the assembly automation with the help of the LCR, several design tools for oligonucleotides or *in silico* assemblies are mentioned: Nowak *et al.* [70] offer a software for the assembly of sequence-optimized DNA parts to reduce secondary structures

without altering the coding usage. This tool is supposed to optimize the negative effects for synthetic gene synthesis and was not applied for LCR assemblies. Bode *et al.* [3] describe a tool with an analogous functionality. Another web-tool was provided by Hendling *et al.* [40]: it is applicable for the design of oligonucleotides and checks the T_m and ΔG crosstalk against all participating sequences and chosen genomes but is not suited for LCR designs. Besides the design of optimized BOs, studies were already applied to observe the influence of a wide range of LCR-parameters by using a design-of-experiment approach [16]. Within this study, the ΔG crosstalk is tackled by the secondary structure inhibitors dimethyl sulfoxide (DMSO) and betaine but was not considered as a limitation for BOs [65, 112]. So far, no comprehensive design tools are provided for the automated LCR assembly.

According to the build process, the LCR was already utilized for automation in 2018 [81] and is a promising DNA assembly method (Figure 1.1). Robinson *et al.* [81] offered a workflow for their utilized robotic platform, the management of DNA part libraries [107] and a design tool for BOs. This tool is available but it is not published so far. It is an easy-to-use web-based software which allows the user to adjust the T_m for each BO-half [1] by utilizing the design rules of de Kok *et al.* [16]. Interestingly, the assembly efficiencies in Robinson *et al.* are significantly lower than the proposed results of de Kok *et al.* (40 % vs. 95 %). This supports the mentioned discrepancy of published results and their reproducibility [47]. Obviously, more insights into the design of BOs and their impact on the robustness of the LCR are mandatory to validate or redefine the design and experimental parameters. Further, the utilized detergents DMSO and betaine are not regarded as automation-friendly for liquid-handling robotics [1, 10] due to the extreme viscosity or hygroscopic character. The omission of both additives without affecting the LCR efficiency would be beneficial and has to be investigated. For this, a screening system has to be utilized to detect the impact on the LCR.

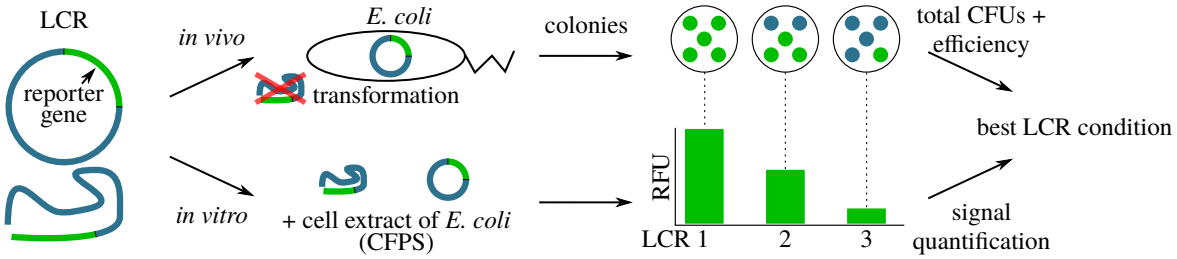

Figure 1.4: Investigation principle for assembly efficiencies. **A.** The classical *in vivo* approach utilizes a bacterial host to uptake the assembled circular construct with a reporter gene and to amplify it by plasmid propagation. Genes of fluorescent proteins are normally utilized as reporter molecules. After the transformation, colonies with a specific fluorescent phenotype are counted to determine the assembly efficiency and the total amount of colonies. This workflow usually takes 24 h. **B.** In contrast, to substitute the transformation of *E. coli* by a cell free protein synthesis (CFPS) step enables an *in vitro* readout within one day and a higher throughput. Circular and linear constructs are detectable and no origin of replication or selection marker is necessary. CFU: colony forming unit, ORI: origin of replication, RFU: relative fluorescence unit.

[1] https://parts.synbiochem.co.uk/plasmidGenie

1.3.1 Screening system to detect LCR efficiencies

By considering the kinetic parameters of the BOs and the thermal cycling of de Kok *et al.* [16], the positive effects of DMSO and betaine has to be validated. Otherwise, new criterion have to be defined. Furthermore, the influence of omitting DMSO and betaine while maintaining the LCR efficiency is of special interest. To enable a screening of varying those parameters, the classical approach is utilizing the transformation of a bacterial host like *E. coli* with the LCR mixture (Figure 1.4). This workflow results in an *in vivo* amplification system of circular constructs if an origin of replication (ORI) and selection marker are incorporated into the final sequence. Afterwards, the plasmid of several colonies is isolated and verified by PCR, restriction digestion or sequencing. The amount of colonies with the correct plasmid is divided by the sum of all analyzed colony forming units (CFUs) to obtain the assembly efficiency. This value is the main criterion to evaluate the relative success of a DNA assembly. A second criterion is the total amount of colonies after the transformation. Together, both criteria are utilized to analyze one assembly reaction and were already applied for various methods [16, 25, 102]. In case of similar efficiencies, the total amount of CFUs is utilized for a discrimination. By applying this verification workflow, no high throughput screening is possible or it is associated with high costs for sequencing. Additionally, the detection of linear constructs or constructs without an ORI or selection marker gene is limited. In summary, a detection system which facilitates a rapid prototyping of linear and circular assemblies without the time-consuming colony screening, plasmid isolation and sequencing is preferred.
For this, the utilization of a fluorescent reporter gene is useful and was already implemented for the development of DNA assemblies [41, 102]. Correct assembled plasmids are detectable by screening colonies or populations via fluorescence microscopy or fluorescence-based cytometry (Figure 1.4). In addition, cell free systems represent a useful tool to obtain assembly efficiencies by a CFPS. Cell free protein synthesis is increasingly utilized for the synthetic biology, rapid prototyping and circuit characterizations [42, 61, 96]. In contrast to the classical approach of transforming the LCR into a bacterial host, the assembled construct, including a gene of interest (GOI) or reporter gene, is transcribed and translated *in vitro* by a cell extract and is named cell-free transcription-translation (TXTL) [31, 66, 85]. By utilizing fluorescent reporter genes like the *green fluorescent protein* (*GFP*), an *in vitro* LCR system can detect and quantify correctly assembled constructs and overcome the limitations of the *in vivo* LCR (Figure 1.4). Improved LCR conditions are detectable by an increased fluorescent signal due to a higher quantity of assembled sequences. Currently, no CFPS approach for the LCR is described. The workflow for this is investigated and described in details in section 3.3.

1.4 Research objective

To fulfill the rapid design and build of synthetic circuits in the field of biology, the automated, robust and easy-to-design DNA assembly is a mandatory tool [47]. Unfortunately, the current workflows for DNA assembly automation are error-prone due to the complex design, the introduction of scars in the final sequence or are unreproducible [114]. Common assemblies like, *i.e.*, Golden Gate assembly [24, 25], Gibson assembly [34], CPEC [80] and SLiCE [126], are based on construct specific DNA part modifications or require a massive *in silico* planning process. In contrast, the ligase cycling reaction (LCR) [11, 16, 74, 83] offers a promising opportunity to tackle those drawbacks by assembling unmodified DNA parts in a desired order with the help of single stranded oligonucleotides, the bridging oligos (BOs) (Figures 1.1 and 1.3). Up to 20 DNA parts can be arranged in a one-pot *in vitro* reaction without restriction. Due to those unique features, the LCR was already implemented for the design and build automation of DNA constructs for metabolic engineering [81]. Unfortunately, low assembly efficiencies of $\leq$40 % were revealed which tremendously increase the overall screening effort to obtain correctly assembled constructs. Investigations of the impact of the utilized LCR protocol are necessary to address the low robustness.

To optimize the LCR assembly, the experimental parameters like the annealing and ligation temperature, the amount of cycles, the effects and the stability of the supplements, and the design rules of BOs are varied to determine their impact. For this, a reliable and rapid screening system is obligatory and is achievable by the utilization of fluorescent reporter genes (Figure 1.4). To determine the impact of altering the LCR parameters, the two evaluation criteria 'efficiency' and 'the total amount of colonies' are utilized. Both are obtained by observing the fluorescent phenotype of colonies derived from the transformation of *E. coli* and plating the suspension on agar plates with a selection marker.

Based on the LCR optimization results, new improved parameters are postulated and their applicability is validated by the assembly of additional DNA constructs (section 3.1). Afterwards, the validated protocol is the scaffold for the automated *in silico* design of BOs for combinatorial LCR assemblies (subsection 3.4.1) and the development of an *in vitro* LCR to further accelerate the design-build-test-learn cycle of synthetic circuits (section 3.3). The *in vitro* method substitutes the cumbersome transformation step of the *in vivo* LCR by an rolling circle amplification (RCA) and a cell free protein synthesis (CFPS). Finally, workflows for the developed *in vitro* and *in vivo* LCR protocol are designed and implemented on the robotic platform of Prof. Dr. Kabisch for an automated DNA assembly and also includes the computer-aided *in silico* design of DNA constructs and BOs in a combinatorial approach (section 3.4).

2 Material and methods

2.1 Materials

2.1.1 Equipment

Table 2.1: Equipment

Equipment	Fabricator	Model
Autoclave	Systec GmbH (Linden, Germany)	VX-75
Camera	Sony	Cyber-Shot DSC-QX10
Shaking incubator	VWR (Darmstadt, Germany) New Brunswick™ (Upland, California, USA)	Incu-Line Tower Innova© 44
Centrifuges	VWR (Darmstadt, Germany) B. Braun Biotech International GmbH (Melsungen, Germany)	Mega Star 3.0R Sigma 6K15
Electroporation chamber	Bio-Rad Laboratories, Inc. (Hercules, CA, USA)	MicroPulser
Heat incubator	Eppendorf AG (Hamburg, Germany)	Thermomixer comfort
Laboratory balances	Sartorius AG (Göttingen, Germany) Shimadzu (Gießen, Germany)	Quintix® AUW120D
Magnetic stirrer (heatable)	IKA-Werke GmbH & Co. KG (Staufen, Germany)	IKAMAG RCT basic
pH-meter	HANNA Instruments Germany GmbH (Kehl am Rhein, Germany)	HI 2211 pH/ORP Meter
Thermal cycler	Bio-Rad Laboratories, Inc. (Hercules, CA, USA)	DNA Engine Tetrad2
Power supply for electrophoresis	Amersham Biosciences Europe GmbH (Freiburg, Germany)	EPS 301
Safety workbench	Thermo Fisher Scientific™ (Dreieich, Germany)	HeraSafe KS15
UV/-photometer	Mettler-Toledo GmbH (Gießen, Germany)	UV5 Nano
UV-table		

Table 2.1: Equipment (continued)

Equipment	Fabricator	Model
Vortex	Heidolph Instruments GmbH & Co. KG (Schwabach, Germany)	REAX top
Plate reader (for *in vitro* LCR)	BMG LABTECH GmbH (Allmendgrün, Germany)	CLARIOstar®
Robotic platform (Analytik Jena AG, Jena, Germany), also see Figure 2.3		
Robotic arm	Precise Automation (Fremont, CA, USA)	PreciseFlex PF750
Nanoliterdispenser	Dispendix GmbH (Cellink; Stuttgart, Germany)	I-DOT One
Plate reader	BMG LABTECH GmbH (Allmendgrün, Germany)	PHERAstar® FSX
Cytometer	Beckman Coulter® (Krefeld, Germany)	CytoFLEX S®
Pipetting robot	Analytik Jena AG (Jena, Germany)	CyBio FeliX
Thermal cycler	Analytik Jena AG (Jena, Germany)	Biometra TRobot
Incubator	Thermo Fisher Scientific™ (Dreieich, Germany)	Cytomat™ 2

2.1.2 Substances

Table 2.2: Substances

Method and Component	Fabricator
Agarose gel elektrophoresis:	
Roti®garose	Carl Roth GmbH & Co KG (Karlsruhe, Germany)
DNA-ladder (1000 bp)	New England Biolabs (Ipswich, MA, USA)
SERVA DNA Stain G	SERVA Electrophoresis GmbH (Heidelberg, Germany)
Selection marker:	
Ampicillin sodium salt	Carl Roth GmbH & Co KG (Karlsruhe, Germany)
Spectinomycin dihydrochloride	Alfa Aesar, Thermo Fisher Scientific™ (Dreieich, Germany)
Kanamycin sulphate	Carl Roth GmbH & Co KG (Karlsruhe, Germany)
Chloroamphenicol	Carl Roth GmbH & Co KG (Karlsruhe, Germany)
X-GalNAc (blue-white screening)	Sigma-Aldrich Chemie GmbH (Taufkirchen, Germany)
Cell culture:	
Glycerol (99.5 %, water-free)	Carl Roth GmbH & Co KG (Karlsruhe, Germany)
Lysogeny broth (LB) powder ($10\,g\,L^{-1}$ NaCl)	Sigma-Aldrich Chemie GmbH (Taufkirchen, Germany)
Agar agar, Kobe I	Carl Roth GmbH & Co KG (Karlsruhe, Germany)
CCMB80 buffer:	
Potassium acetate	Sigma-Aldrich Chemie GmbH (Taufkirchen, Germany)
Calcium chloride	Sigma-Aldrich Chemie GmbH (Taufkirchen, Germany)
Manganese(II) chloride	Sigma-Aldrich Chemie GmbH (Taufkirchen, Germany)
Magnesium chloride	Sigma-Aldrich Chemie GmbH (Taufkirchen, Germany)
Glycerol (99.5 %, water-free)	Carl Roth GmbH & Co KG (Karlsruhe, Germany)

Table 2.2: Substances (continued)

Method	Fabricator
Cell extract of *E. coli* (adapted from [106]):	
2× YT	Sigma-Aldrich Chemie GmbH (Taufkirchen, Germany)
Potassium phosphate monobasic solution (1 M)	Sigma-Aldrich Chemie GmbH (Taufkirchen, Germany)
Potassium phosphate dibasic solution (1 M)	Sigma-Aldrich Chemie GmbH (Taufkirchen, Germany)
TRIS base	Sigma-Aldrich Chemie GmbH (Taufkirchen, Germany)
1,4-Dithiothreitol (DTT)	Carl Roth GmbH & Co KG (Karlsruhe, Germany)
L-Glutamic acid hemimagnesium salt tetrahydrate (Mg-Glu)	Carl Roth GmbH & Co KG (Karlsruhe, Germany)
L-Glutamic acid potassium salt monohydrate (K-Glu)	Carl Roth GmbH & Co KG (Karlsruhe, Germany)
Acetic acid 100%	Carl Roth GmbH & Co KG (Karlsruhe, Germany)
ATP dipotassium salt dihydrate	Sigma-Aldrich Chemie GmbH (Taufkirchen, Germany)
GTP disodium salt hydrate	Sigma-Aldrich Chemie GmbH (Taufkirchen, Germany)
CTP disodium salt hydrate	Sigma-Aldrich Chemie GmbH (Taufkirchen, Germany)
UTP trisodium salt dihydrate	Sigma-Aldrich Chemie GmbH (Taufkirchen, Germany)
tRNA	Sigma-Aldrich Chemie GmbH (Taufkirchen, Germany)
CoA	Sigma-Aldrich Chemie GmbH (Taufkirchen, Germany)
NAD^+	Sigma-Aldrich Chemie GmbH (Taufkirchen, Germany)
cAMP	Sigma-Aldrich Chemie GmbH (Taufkirchen, Germany)
Folinic acid	Sigma-Aldrich Chemie GmbH (Taufkirchen, Germany)
Spermidin	Sigma-Aldrich Chemie GmbH (Taufkirchen, Germany)
3-PGA	Sigma-Aldrich Chemie GmbH (Taufkirchen, Germany)
DNA restriction enzymes/buffers, DNA isolation, DNA ligation:	
EcoRV	New England Biolabs (Ipswich, MA, USA)
DpnI	New England Biolabs (Ipswich, MA, USA)
Polymerase chain reaction (PCR):	
dNTPs	Carl Roth GmbH & Co KG (Karlsruhe, Germany)
Q5® High-Fidelity Polymerase	New England Biolabs (Ipswich, MA, USA)
Taq polymerase	New England Biolabs (Ipswich, MA, USA)
PCR-clean-up:	
Monarch® PCR & DNA Cleanup Kit	New England Biolabs (Ipswich, MA, USA)
Plasmid isolation:	
innuPREP Plasmid Mini Kit 2.0	Analytik Jena AG (Jena, Germany)
Rolling circle amplification:	
illustra GenomiPhi™ V2 DNA Amplification Kit	GE Healthcare UK Limited, Buckinghamshire, UK

Table 2.2: Substances (continued)

Method	Fabricator
Ligase cycling reaction:	
Ampligase®	Lucigen, Wisconsin, USA
10×-Ampligase® buffer	Lucigen, Wisconsin, USA
HiFi *Taq* ligase	New England Biolabs (Ipswich, MA, USA)
10×-HiFi *Taq* ligase buffer	New England Biolabs (Ipswich, MA, USA)
DMSO	Carl Roth GmbH & Co KG (Karlsruhe, Germany)
Betaine, BioUltra, ≥99.0% (NT)	Sigma-Aldrich Chemie GmbH (Taufkirchen, Germany)
NAD^+, ≥95%	Carl Roth GmbH & Co KG (Karlsruhe, Germany)
$MgCl^{2+}$, ≥98.5%, anhydrous	Carl Roth GmbH & Co KG (Karlsruhe, Germany)

2.1.3 Media and solutions

Table 2.3: Media and solutions

Medium	Composition
Lysogeny broth (LB), liquid:	*ad* 1 L *A. dest.*:
LB-powder (10 g L^{-1} NaCl)	25 g
TAE (TRIS acetate EDTA) buffer:	*ad* 1 L *A. dest.*:
Acetic acid	1.14 mL
Na_2EDTA	1.11 mM
TRIS	40 mM
E. coli cell extract	
2× YT + phosphate (2× YT+P):	*ad* 1 L *A. dest.*:
2× YT (31 g L^{-1})	31 g
1 M Potassium phosphate dibasic solution (40 mM)	22 mL
1 M Potassium phosphate monobasic solution (22 mM)	40 mL
S30-A buffer:	*ad* 1 L *A. dest.*; add 2 mL DTT directly before usage and after autoclavation:
Mg-Glu (14 mM)	5.44 g
K-Glu (60 mM)	12.20 g
2 M TRIS base pH 7.7 (50 mM)	25 mL
L-amino acid solution :	*ad* 42 mL *A. dest.*:
140 mM leucine (5 mM leucine)	1.5 mL
168 mM all other amino acids (6 mM others)	1.5 mL
Nucleotide mix:	*ad* 1.5 mL *A. dest.*:
ATP dipotassium salt dihydrate (156 mM)	145 mg
GTP disodium salt hydrate (156 mM)	133 mg
CTP disodium salt dihydrate (94 mM)	79.4 mg
UTP trisodium salt dihydrate (94 mM)	82.6 mg
tRNA solution (50 mg mL^{-1}):	*ad* 0.6 mL *A. dest.*:
tRNA	30 mg
CoA solution (65 mM):	*ad* 0.6 mL *A. dest.*:
CoA	30 mg
NAD^+ solution, pH 7.5-8:	*ad* 0.3 mL *A. dest.*:
NAD^+ (175 mM)	34.83 mg
2 M TRIS base pH 7.7	27 µL
cAMP solution, pH 8 (650 mM):	*ad* 0.2 mL *A. dest.*:
cAMP	42.8 mg
2 M TRIS base pH 7.7	73 µL
Folinic acid solution (33.9 mM):	*ad* 1.15 mL *A. dest.*:
Folinic acid calcium salt	20 mg

Table 2.3: Media and solutions (continued)

Medium	Composition
Spermidin solution (1 M):	*ad* 155 µL *A. dest.*:
Spermidin	23.55 µL
3-Phosphoglyceric acid (3-PGA) solution, pH 7.5:	*ad* 3.2 mL *A. dest.*:
3-PGA (1.4 M)	1.03 g
2 M TRIS base	1.73 mL
Energy solution, pH 7.5:	
2 M HEPES	3.6 mL
Nucleotide mix	1.39 mL
tRNA solution	576 µL
CoA solution	576 µL
NAD^+ solution	276 µL
cAMP solution	170 µL
Folinic acid solution	288 µL
Spermidin solution	144 µL
3-PGA solution	3.09 mL
A. dest.	144 µL
Cell extract buffer:	
500 mM Mg-Glu	94.26 µL
3 M K-Glu	251.37 µL
Amino acid solution	531.56 µL
Energy solution	336.66 µL
100 mM DTT	70 µL
40 % m/v PEG-8000	235.66 µL
A. dest.	459.33 µL

2.1.4 Used organisms and strains

Table 2.4: Used organisms and strains

Organism	Genotype	Origin
NEB® 10-β *E. coli*	*Δ(ara-leu) 7697 araD139 fhuA ΔlacX74 galK16 galE15 e14- ϕ80dlacZΔM15 recA1 relA1 endA1 nupG rpsL (StrR) rph spoT1 Δ(mrr-hsdRMS-mcrBC)*	New England Biolabs (Ipswich, MA, USA)
E. coli TOP 10	*F^- mcrA Δ(mrr–hsdRMS–mcrBC) ϕ80dlacZ ΔM15 ΔlacX74 nupG rexA1 araD139 Δ(ara-leu)7697 galK16 rpsL(str^R) end A1 fhuA2λ^-*	Invitrogen, Life Technologies (Carlsbad, CA, USA)
E. coli BL21 Rosetta™(DE3)	*F- ompT hsdSB(rB- mB-) gal dcm (DE3) pRARE (CamR)*	Sigma-Aldrich Chemie GmbH (Taufkirchen, Germany)

2.1.5 Software

Table 2.5: Software

Software	Fabricator	Purpose
`Geneious` (v. 11.0.5) [52]	Biomatters, Ltd.	*In silico* cloning
`Inkscape` 0.92.4	The Inkscape Project	Figures
`R`, version 3.6.1	R Core Team	Plots
`RStudio`, version 1.2.5033	RStudio, Inc.	Plots

2.2 Methods

2.2.1 Cultivation and conservation of cells

Escherichia coli cells were cultured in liquid LB medium (in culture tubes) with or without antibiotics at 37 °C and 200 rpm. For solid media, 1.5 % m/v of agarose was used. When necessary, antibiotics were added (ampicillin: 100 µg mL^{-1}, kanamycin: 50 µg mL^{-1}, spectinomycin: 100 µg mL^{-1}). Overnight cultivations of all strains were inoculated with 1-2 µL of a glycerol stock or by pcking a colony with a sterile tooth pick followed by an incubation for 16 h. Bacteria were stored on agar plates at 4 °C or in glycerol stocks at −80 °C. For glycerol stocks of *E. coli*, 800 µL of an overnight culture were mixed with 200 µL of 100 % glycerol.

2.2.2 Competent *E. coli*

To get electrocompetent cells, *E. coli* TOP10 or NEB® 10-β *E. coli* cells from an overnight cultivation were used to inoculate liquid LB medium supplemented with streptomycin (100 µg mL^{-1}). After reaching an OD_{600} of 0.5-0.7, the cell suspension was transferred into 50 mL tubes and stored for 30 min on ice. Subsequently, the cells were sedimented by centfriguation (4 °C, 15 min) and the supernatant was discarded. Afterwards, the cells were resuspended in 15 % v/v glycerol (4 °C) by using one volume of the main culture. Centrifugation and resuspension were performed again for three times with stepwise reduced volume of 15 % v/v glycerol (0.5 and 0.05 volume units of the main culture) ending in resuspending the cell pellet with the residual glycerol after decantation. The cells were aliquoted in single aliquots of 30 µL or masteraliquots with a cell volume for 1 to 20 transformations with a volume of 30 µL for one transformation. Subsequently, the aliquots were stored at −80 °C.
For chemically competent *E. coli* cells, the protocol from OpenWetWare[1] was adapted to prepare the CCMB80 buffer for the washing procedure. For this buffer, 10 mM of potassium chloride, 80 mM of calcium chloride, 20 mM manganese(II) chloride, 10 mM magnesium choride and 10 % v/v glycerol were mixed in *A. dest.* and the pH was adjusted to 6.4 with 0.1 M HCl. The buffer was sterilized by filtration (0.2 µM filter) and stored at 4 °C. For harvesting, an OD_{600} of 0.5 was used. The centrifugation and aliquotation were performed as described for the electrocompetent *E. coli* cells.

2.2.3 Electroporation of *E. coli*

30 µL of electrocompetent *E. coli* cells were incubated with the plasmid DNA for 2 min on ice. Afterwards, a dry and ice-cold electroporation cuvette was filled with the cell/DNA suspension followed by the electric pulse (2.5 kV, time: 5 ms). Immediately, 470 µL of LB medium (room temperature) were added to the cells followed by an incubation step at 37 °C for 1 h and shaking.

[1] https://openwetware.org/mediawiki/index.php?title=TOP10_chemically_competent_cells&oldid=677117

Finally, the suspension was plated on agar with selection markers. For a blue-white screening, 40 µg mL^{-1} X-Gal and 200 nM IPTG were added before the plating. The plates were incubated for 16 h at 37 °C and stored at 4 °C afterwards.

2.2.4 Chemical transformation of *E. coli*

For a chemical transformation, 30 µL of chemically competent *E. coli* cells were incubated with the plasmid DNA in a 96-well PCR plate for 30 min on ice. Subsequently, a heat shock was applied for 30 s at 42 °C. After 10 min on ice, 170 µL of LB medium was added to each well with transformed cells. The total volume per well was directly transferred to a 96-well flat-bottom MTP with a plastic lid. Afterwards, the 96-well MTP was incubated for 1 h at 37 °C and 800 rpm in a thermomix (Eppendorf) followed by spreading the cells on agar plates with a selection marker. For a blue-white screening, 40 µg mL^{-1} X-Gal and 200 nM IPTG were added before the plating. The plates were incubated for 16 h at 37 °C and stored at 4 °C afterwards

2.2.5 Plasmid isolation from *E. coli*

Plasmid isolation was performed by using the innuPREP Plasmid Mini Kit 2.0 (Analytik Jena). 4 mL of an overnight culture were used for the isolation; for overday cultures, 2 mL LB were inoculated and used for the isolation. For the isolation, the cell pellets were resuspended in 250 µL resuspension buffer after the centrifugation step of 1 min at 6000 g. The lysis was achieved by adding 250 µL of the lysis buffer followed by an incubation step of 4 min at room temperature. Afterwards, 350 µL binding buffer were added and mixed with the lysed cells by inverting. The suspension was centrifuged for 8 min at 17 000 g to generate a cell pellet. The supernatant was transferred to a purification column of the kit. Subsequently, the DNA was bound to the column by spinning the tube for 1 min at 11 000 g. The bound DNA was washed by adding 500 µL of the washing buffer A and a centrifugation step for 1 min at 11 000 g. After a second washing step with 700 µL of washing buffer B and a centrifugation step for 1 min at 11 000 g, residual buffer was removed by centrifuging for 2 min at 17 000 g. The column was transferred into a microcentrifuge tube and 50 to 100 µL of the elution buffer was added to elute the DNA by a centrifugation for 1 min at 11 000 g. Finally, the plasmid was stored at −20 °C.

2.2.6 Quantity and purity of DNA

Concentrations and purities of DNA from isolations and PCR amplifications were obtained by photometric measurements with the UV5 Nano (Analytik Jena AG). 2 µL of DNA were used to load the pedestal and to measure the DNA quantity. The 260/280 nm and 260/230 nm ratios were utilized to determine the purity. Afterwards, the purified DNA was checked for the correct size by gel electrophoresis.

2.2.7 Agarose gel electrophoresis

For an electrophoresis, 1 % m/v agarose in TRIS acetate EDTA (TAE) buffer was used for a gel electrophoresis. To stain the DNA, 1.5 µL SERVA Stain was added to 30 µL to the liquid agarose before pouring the gel. The electrophoresis was performed in TAE buffer for about 30 min at 100 V. A DNA ladder served as a reference for the determination of the DNA size. Afterwards, gels were documented by using a UV-light table and a digital camera.

2.2.8 Polymerase chain reaction (PCR) and colony PCR

For a PCR, 0.1 mM of dNTPs, 0.25 mM of each primer, 2.5 U Q5® High-Fidelity Polymerase, 5× Q5® buffer and 0.5 µL DNA template were mixed. To get the total volume, *A. dest.* was used to fill up the reaction mixture to 50 µL. Initial denaturation was achieved after 3 min at 95 °C for plasmid or chromosomal DNA as template. The following denaturation step at 95 °C for 15 s, the attenuation and elongation at 95 °C were repeated for 35 cycles. The attenuation temperature and the elongation time depended on the T_m of the primers and the amplicon size. The PCR was ended by a final elongation for 2 min at 72 °C.
In case of a colony PCR (cPCR), a part of a colony was transferred to a PCR tube with 5 µL *A. dest.*with a sterile tooth pick. The volume in one PCR tube was filled up to 25 µL and the PCR mix described above. The high-fidelity Q5® polymerase and buffer was substituted by the *Taq* polymerase and its 10×C buffer. For the initial denaturation step of the thermal cycling, the duration was prolonged to 5 min followed by the protocol described for PCRs.

2.2.9 Clean-up of PCR products

The purification of a PCR amplified DNA fragment was realized by using a column-based Monarch® PCR & DNA Cleanup Kit or the corresponding kit for gel extractions. Binding buffer was mixed with the PCR reaction in a 2:1 ration for fragments with more than 2000 bp and in a 5:1 ratio for smaller fragments. The mixture was transferred to a column in a microcentrifuge tube. The DNA was bound to the column by a centrifugation step for 1 min at 13 000 g. Subsequently, 200 µL washing buffer was added to the column followed by a centrifugation for 1 min at 13 000 g. This washing procedure was repeated. Afterwards, the column was transferred to a microcentrifuge tube to elute the DNA with 20 to 60 µL elution buffer. The column with the elution buffer was incubated for 1 min at room temperature followed by a centrifugation for 1 min at 13 000 g. Finally, the DNA was stored at −20 °C.
In case of a gel extraction, the excised gel was solved by adding 400 µL of the Gel Dissolving Buffer to 100 µg gel followed by an incubation at 50 °C for 5 to 10 min. After loading the column with the PCR or solved gel, the column was washed twice with 700 µL washing buffer (30 s, 13 000 g) and residual buffer was removed afterwards by an additonal centrifugation for 1 min at 13 000 g. Elution was performed by using 30 to 60 µL of elution buffer.

2.2.10 Ligase cycling reaction

According to the literature [11, 16], baseline conditions for the LCR were initially utilized and optimized in section 3.1. The baseline protocol utilized 3 nM for each DNA part, 30 nM of each BO, the Ampligase®, the Ampligase® buffer, 8 % v/v DMSO and 0.45 M betaine in a total volume of 25 µL. Betaine and DMSO were solved in *A. dest.* and stored in aliquots at −20 °C. A thermal cycler (DNA Engine Tetrad®2), cycling block (96-well Alpha™ Unit) and low-profile PCR stripes (all from Bio-Rad Laboratories GmbH, Muenchen, Germany) were utilized for the cycling and to reduce evaporation effects. The LCR was cycled for 25 cycles as shown in Figure 2.1. Afterwards, the LCR was utilized for the electroporation or chemical transformation of *E. coli*, the *in vitro* LCR approach (section 3.3) or was frozen at −20 °C.

Initial denaturation :	94° C	2 min	
Denaturation :	94° C	10 s	┐
Annealing :	55° C	30 s	├ 25x
Ligation :	66° C	1 min	┘
Hold :	10° C	∞	

Figure 2.1: Cycling parameters of the baseline LCR. This setup was used for the initial LCRs to optimize the LCR. This is further descibed in subsection 2.2.15 and in section 3.1.

2.2.11 Cell extract generation from *E. coli*

For the *in vitro* LCRs, a cell-free system was utilized. For this, a cell extract was generated from the strain BL-21 Rosetta™ *E. coli* cells. For this, a modified protocol of [106] was utilized. An overnight culture of 50 mL with 2×YT+P medium was inoculated by utilizing a cryostock. As antibiotics, 34 µg mL^{-1} of chloramphenicol and 50 µg mL^{-1} kanamycin were added. After the growth for 16 h at 37 °C and 200 rpm, 800 mL of 2×YT+P medium was inoculated with the preculture. Additionally, antibiotics were added to the main culture as mentioned for the overnight culture. The cells were grown to OD_{600}=3-3.5 in a 5 L flask at 37 °C and 200 rpm (3.5 to 4 h). The following steps were performed at 4 °C. The main culture volume was split into four centrifuge beakers with ca. 200 mL each and were centrifuged at 5000 g for 12 min. After the subsequent decanting of the supernatant, each pellet was resuspended with 40 mL of S30A-buffer with 2 mM DTT. The DTT has to be added right before the previous step. The cell pellets were resuspended by rigorous shaking by hand. In between, the beakers were cooled down on ice. Afterwards, the beakers with the suspended cells were centrifuged for 12 min at 5000 g. The washing step with the same volume of S30A-buffer + 2 mM DTT was repeated. The pellets were then resuspended by shaking in 10 mL S30A-buffer + 2 mM DTT and pooled in two 50 mL centrifuge tubes. A centrifugation for 20 min at 3499 g resulted in cell pellets. The supernatant was decanted and the centrifugation tubes were centrifuged again for 2 min at 2000 g. Residual supernatant was removed with a pipette. Subsequently, the cells

were resuspended by a volume of S30A-buffer + 2 mM DTT equals to the mass of the pellet (1 g of cells→ +1 mL buffer). The cells were split and transferred à 1 mL in pre-chilled 2 mL microcentrifuge tubes and lysed by sonification.
For the sonification of the cells, an amplitude of 50 % with 10 s-pulse and 10 s-pause cycles were applied. The total sum of energy for the sonification has to be around 700 J. A successful lysis is achieved when the suspension is turning aqueous/transparent. After this, the microcentrifuge tubes were centrifuged for 10 min at 12 000 g at 4 °C. The supernatant was transferred with a pipette to microcentrifuge tubes and the extract was incubated for 80 min at 37 °C and 220 rpm in a thermomixer. A final centrifugation step for 10 min at 12 000 g and 4 °C resulted in the cell extract. For this, the supernatant was removed with a pipette and pooled followed by aliquoting. The 35 µL aliquots were stored at −80 °C.
The cell extract buffer was mixed according to the literature [106] and is shown in Table 2.3. A step-by-step protocol for the generation of the cell extract and the buffer and how to perform a CFPS is described in subsection 6.1.4.

2.2.12 Rolling circle amplification

To amplify the fluroescence signal for the *in vitro* LCR read-out, the rolling circle amplification (RCA) was applied. The RCA was performed prior to the CFPS. For the RCA, the illustra GenomiPhi™ V2 DNA Amplification Kit (GE Healthcare UK Limited, Buckinghamshire, UK) was utilized. The enzyme mix was aliquoted and stored at −80 °C and the buffers were stored as aliquots at −20 °C. According to the instructions of this kit, 1 µL of plasmid or LCR was mixed with 9 µL of the sample buffer. The mixture was heated up for 3 min at 95 °C and subsequently was cooled down on ice. After the addition of 9 µL reaction buffer and 1 µL enzyme mix, the RCA was performed by incubating the suspension for 90 min at 30 °C followed by a 10 min deactivation step at 65 °C. In case that an LCR was utilized as a template, the incubation step was prolonged from 90 to 180 min. After the RCA, the cell extract was added to perform a CFPS. To enable an automation of the RCA and to lower the financial costs, the volumes of sample buffer, reaction buffer and enzyme mix were reduced step-by-step and is described in more details in section 3.3. A comparison of the protocol described above and the protocol with reduced volumes is presented in Table 3.3.1. The low final reaction volume requires conic reaction wells. For this, a 384-PCR-plate was utilized (384 Well Multiply® PCR-plate, Sarstedt AG & Co. KG, Sarstedt, Germany) and optical sealing foils (#4360954; MicroAmp™ Optical Adhesive Film; Thermo Fisher Scientific™, Dreieich, Germany) scale due to evaporation effects. Furthermore, a protocol of RCA and CFPS is described in subsection 6.1.4.

2.2.13 Cell free protein synthesis

A CFPS with the *E. coli* cell extract was initially performed according to the literature [106]. Following steps were performed on ice: 0.7 µL cell extract and 0.84 µL cell extract buffer (recipe

for the buffer in Table 2.3) were mixed with 0.46 µL of DNA or LCR product in a well of a 384-well PCR plate (384 Well Multiply® PCR-plate, Sarstedt AG & Co. KG, Sarstedt, Germany). An optical sealing foil was utilized to seal the plate (#4360954; MicroAmp™ Optical Adhesive Film; Thermo Fisher Scientific™, Dreieich, Germany).
The protein synthesis was performed by incubating the plate without shaking for at least 3 h at 29 °C in an incubator or in the plate reader. The DNA contained the fluorescent reporter gene *sfGFP* to enable a signal detection by fluorescence measurements with the plate reader. Due to the utilization of a non-optical plate, a top-measurement with an extinction at 470 nm and an emission at 515 nm was utilized.
The protocol for the CFPS is altered to reduce the required volume for the *in vitro* LCR approach presented in section 3.3. This optimized protocol is shown in Table 3.2.

2.2.14 *In silico* experiments and DNA-sequencing

For the design of primers, BOs and *in silico* cloning, the software `Geneious` (v. 11.0.5, www.geneious.com, [52]) was used. All oligonucleotides were ordered as salt-free custom DNA oligos from Eurofins Genomics (Ebersberg, Germany). Sequencing was performed by utilizing Mix2Seq tubes of Eurofins Genomics (Ebersberg, Germany).

2.2.15 Toy-model plasmid for the optimization of the LCR

The LCR optimization experiments shown in section 3.1 were performed by assembling a toy-model plasmid consisting of seven DNA parts (Figure 3.1B) with a total length of 4918 bp. As a plasmid backbone, the cloning vector CloneJet pJET1.2/blunt was utilized (2974 bp; Thermo Fischer Scientific, Massachusetts, USA). Two reporter genes were incorporated as 'inserts' two enable a bi-colored screening of correctly assembled plasmids (*sfGFP* from pYTK001, *mRFP1* from pYTK090 [59]). Both genes were split into subparts to obtain a high size heterogenity (79 bp to 2974 bp). As a terminator, the BioBrick *BBa_B0015* was present in both reporter genes to simulate an assembly with redundant sequences. A spacer sequence of 37 bp was incorporated at the 3'-end of *mRFP1* to disable the ligation of the *mRFP1* (part 3, Figure 3.1B) with the backbone (part 7, Figure 3.1B). For the *in silico* designs, `Geneious` was utilized (v. 11.0.5, http://www.geneious.com, [52]). Amplification primers (Eurofins Genomics, Ebersberg, Germany) were 5'-modified by the T4-polynucleotidekinase/-buffer (New England Biolabs, Ipswich, USA) prior to the amplification via PCR (Q5® High-Fidelity Polymerase, New England Biolabs, Ipswich, USA). Each primer was phosphorylated in a single tube with a total volume of 50 µL, a primer-concentration of 1 µM, 2 mM ATP and 10 U of T4-PNK for 1 h at 37 °C and 20 min at 65 °C. The promoter of *mRFP1* (part 1, Figure 3.1B) was made of an ordered forward and reverse primer (lyophilized, salt-free). The primers for the promoter of *mRFP1* were phosphorylated separately prior to the annealing to dsDNA for 3 min at 95 °C and 70 cycles of 20 s with an incremental decrease of 1 °C. The backbone pJET1.2/blunt was PCR-amplified

using a digested pJET1.2/blunt+*lacZ* plasmid to enable the detection of plasmid carry-over by blue-white screening. All PCR products were treated by a DpnI-digested directly after the cycling for 60 min at 37 °C and an inactivation for 20 min at 80 °C. For the toy-model plasmid, the amplification primers are presented in Supplementary Tables 6.1. A GenBank file of the plasmid is published in Schlichting *et al.* [95].

A baseline LCR assembly was mixed according to the recipe of de Kok *et al.* [16] to get a reaction mixture with specific final concentrations of 1× ligase buffer, 0.5 mM NAD^+, 3 nM of non-backbone parts, 0.45 M betaine and 8 % v/v DMSO. In contrast to de Kok *et al.* [16], the concentration of the backbone pJET1.2/blunt was adjusted to 0.3 nM. The 10×-Ampligase® reaction buffer was self-made and based on the recipe of the supplier (Lucigen, Wisconsin, USA). Due to the unknown stability of nicotinamide adenine dinucleotide at −20 °C, it was added separately afterwards. Bridging oligo sets were solved and mixed in nuclease-free water with 1.5 µM of each BO. The sets were heated up for 10 min at 70 °C and cooled down on ice before the addition to the LCR mixes. At last, 10 U of Ampligase® (Lucigen, Wisconsin, USA) was added. Afterwards, each LCR was split into 3 µL reactions in separate reaction tubes. After the cycling, the LCRs were cooled down on ice and were transformed in *E. coli*.

For the cycling, a thermal cycler (DNA Engine Tetrad®2), cycling block (96-well Alpha™ Unit) and low-profile PCR stripes (all from Bio-Rad Laboratories GmbH, Muenchen, Germany) were utilized. The heat and cooling rate for all LCRs were 3 °C s^{-1}. The cycling was started by a denaturation at 94 °C for 2 min. Afterwards, the LCRs were cycled 25 × at 94 °C for 10 s, 55 °C for 30 s and 66 °C for 1 min. After cooling down the LCRs on ice, 30 µL electro-competent or chemically-competent NEB® 10-β *E. coli* cells (self-made batches; New England Biolabs, Ipswich, USA) were added to each tube with the LCR mix. For the electroporation, the total volume was pipetted to cuvettes for electroporation with a diameter of 1 mm. The electroporations were performed by applying an electric pulse of 2.5 kV. The chemical transformations were achieved by using 96-well PCR-plates and a cycling block for the heat-shock. For the heat-shock, the 96-well plates were put on ice for 30 min, followed by a 30 s heat-shock at 42 °C. After a cool down on ice for 10 min each transformation mix was transferred to 96-MTPs (flat bottom) with 170 µL SOC medium per well for the recovery step at 37 °C for 1 h. The electroporation mix was transferred to 470 µL SOC medium and the transformed were recovered as described for the chemical transformation. Finally, the transformation mix was plated on Lysogeny Broth (Miller) plates with 1 % m/v agar and 100 µg mL^{-1} ampicillin. The plates were incubated for 15 h at 37 °C.

To observe the alterations of parameters, the efficiencies of all LCRs were determined by investigating the phenotype of CFUs by fluorescence microscopy as depicted in Figure 1.4 (microscope: Axio Vert.A1, Carl Zeiss Microscopy GmbH, Jena, Germany, 50×-magnification; LEDs for sfGFP/mRFP1: 470/540−580 nm). To calculate the assembly efficiency, the phenotypes of all CFUs derived by each LCR transformation were screened. For more than 100 CFUs per agar plate, 100 colonies were screened randomly by first specifying the CFUs of interest. The CFUs were

then observed by fluorescence microscopy and the efficiency was calculated by dividing the number of red+green CFUs by the amount of investigated CFUs. The amount of CFUs per LCR was derived from the total CFUs on each agar plate and the volume of the plated cells. For the validation of the phenotype-genotype correlation, plasmids from 120 CFUs with different phenotypes were purified (Monarch® Plasmid Miniprep Kit; New England Biolabs, Ipswich, USA) and analyzed by Sanger sequencing (Eurofins Genomics, Ebersberg, Germany).

2.2.16 Validation experiments for the improved LCR protocol

To validate the improved LCR protocols, two additional plasmids were designed and both were split into three and seven parts (Supplementary Figures 6.15 and 6.16). The sequences of the amplification primers for the validation plasmids are shown in Supplementary Tables 6.5 and 6.6. GenBank files of both plasmids are published in Schlichting *et al.* [95]. As reporter genes, both plasmids consist of *lacZ* and one or two selection markers. Correctly assembled plasmids result in a blue phenotype; misassemblies have a white phenotype and do not grow on agar plates with the second antibiotic. As for the previous LCR investigations with the toy-model plasmid, 3 µL LCR were chemically transformed into 30 µL NEB® 10-β *E. coli* cells.
Validation plasmid 1 ('VP1') were assembled followed by a chemical transformation and plating on 1 % m/v agar plates containing 100 µg mL^{-1} spectinomycin after 1 h of recovery. After the incubation for 16 h at 37 °C, forty colonies were transferred to agar plates with 100 µg mL^{-1}, 50 µg mL^{-1} kanamycin, 40 µg mL^{-1} X-Gal and 200 nM IPTG. The resulting colonies after 16 h at 37 °C with a blue phenotype were regarded as CFUs with the correct plasmid. Empty spots were treated as colonies with a misassembled plasmid due to the lack of the kanamycin resistance. From ten blue colonies of the agar plate with both antibiotics, the plasmids were isolated and analyzed by Sanger sequencing. Additionally, four plasmids of colonies with the false phenotype and/or kanamycin sensitivity were sequenced after Sanger.
Validation plasmid 2 ('VP2') the chemically transformed cells were plated on 1 % m/v agar plates with 100 µg mL^{-1} spectinomycin, 40 µg mL^{-1} X-Gal and 200 nM IPTG. After the incubation for 16 h at 37 °C, all obtained CFUs were screened visually to detect a blue or white phenotype. A blue phenotype was regarded as a correct assembly and white colonies as CFUs with misassembled plasmids. Sanger sequencing of ten plasmids from colonies with the correct phenotype and four plasmids from false phenotypes were isolated and analyzed by Sanger sequencing.

Installation of the `CloneFlow` plugin for the automated bridging oligo design in `Geneious`

Together with bachelor students of informatics (TU Darmstadt) and Felix Reinhardt (phD student Computational Biology and Systems, Fakultät der Biologie, TU Darmstadt), the software was build for `Geneious` versions $\geq$ 10 with `Java` v8. The plugin also requires `Python`3. 7. 2 for the calculation of the BO T_ms. The installation of `CloneFlow` is achieved by drag and drop

of the installation file[1] to the main window of Geneious or by selecting the file via Tools→Plugins→Plugins And Features→install plugin from a gplugin file.
After the successful installation, a pop-up window appears with information about the plugin and 'CloneFlow Plugin' is shown in the 'Installed Plugins' list. Afterwards, the tool can be started by clicking on 'CloneFlow' in the 'Tools' menu. Another option to start the plugin is to add it by customizing the gray toolbar. Right click on the gray bar shows 'Customize'. Subsequently, 'CloneFlow' can be chosen for a continuous appearance in the toolbar. To design BOs, the DNA parts of interest are preselected before starting the plugin or are added by a search afterwards. The latter approach is described in more details in subsection 3.4.2.

Installation of the CloneFlow server for the design of bridging oligos with low secondary structures

The CloneFlow server is a stand-alone tool for the upload and management of DNA parts sequences and the automated BO design. It is a modular system and allows the user to design a human-readable phosphorylation protocol for amplification primers, to find crosstalk optimized BOs with a specified target T_m and to generate an LCR protocol in a csv-format (Figure 3.35A). The server and can be set up on Linux systems or virtual machines with Ubuntu16, Ubuntu18 and Mint. The calculations in the server environment are based on Python3.5. An installation file for setting up the server is available in subsection 6.3.1 and can be executed by the following command:

```
sudo python3 installserver.py
```

By following the instructions in the installation terminal the server will be installed. All software packages are installed automatically. Afterwards the pSQL database and the Django-based server will be prepared to enable the storage of sequences and to allow the user management. In the last installation step, the credentials for the log in as a superuser are created. For this, a superuser name, password and an e-mail address have to be entered. The superuser data is necessary to log in as an administrator of the CloneFlow server. If the installation was successful, two terminals should be running in parallel. Afterwards, the local server can be accessed by using the internet browser Mozilla Firefox only. This issue is located to the security settings of other browsers where local servers are forbidden or disabled in the default browser settings or browser-specific ports are allowed. Due to this, Mozilla Firefox is the recommended browser. By opening Mozilla Firefox, CloneFlow can be accessed by typing the default IP-address and port (127.0.0.1:8001) or by typing 'localhost' and pressing enter. The welcome page of CloneFlow is shown and the user can log in by using the credentials

[1] Installation file for the CloneFlow plugin available at https://gitlab.com/kabischlab.de/lcr-publication-synthetic-biology/blob/master/LCR_Plugin_geneious_v1.1.zip [95]

used to set up the superuser during the previous steps. The superuser is the administrator for the `CloneFlow` server and has to prepare templates for the BO-design.
Before running a first job with `CloneFlow`, a few things have to be considered and customized. Adding an e-mail address to receive notifications of finished `CloneFlow` jobs or to reset the password for registered users is recommended but not mandatory. To use the right management is a complex part and is only of interest if the administrator wants to restrict permissions for a shared use with, *i.e.*, colleagues of other working groups or guests. `CloneFlow` is based on the open-source web framework `Django`. This framework offers a rights management system and allows a superuser to create new groups, adjust the permissions and assign users to the groups. For this, already existing users or a new one can be created and assigned to existing or newly created groups. The rights management settings are only accessible as an admin or as a member of the superuser group. In the administration area, various setting can be customized by the admin to enable or disable rights for, *e.g.*, single users or user groups. Especially the admin has to care about the DNA library settings: by default, every new user has the right to edit or delete DNA parts and BOs. This allows all users to delete sensitive data or are able to edit metadata after the upload of the DNA parts or the design of BOs. Restoring these changes is not possible and should be considered by the administrator.

2.2.17 Automated DNA assembly with the LCR

To enable the automated DNA assembly, a robotic platform was utilized (Figure 2.3). Besides the cytometer, each device of the platform is utilized. The workflow for the LCR is based on the results of the *in vivo* LCR optimization (section 3.1). The automated methods for dispensing, transformation of *E. coli* and agar plating is described in the next paragraphs.

2.2.18 Combinatorial DNA dispensing with a nanoliter dispenser

By utilizing the nanoliter dispenser 'I-DOT' (Figure 2.2A), up to 96 liquids, *e.g.*, DNA parts, BOs, ligase buffer, ligase, NAD^+ and water, can be filled into the 'pure columns' of the source plate. On the bottom of each column is a 90 µm orifice. By applying an air pressure pulse a drop with a specific volume is transferred from the source well to the desired wells in the target plate (Figure 2.2B). As an additional feature, parallel dispensing of eight liquids is further accelerating the overall dispensing procedure (Figure 2.2C). The unit of the applied pressure pulse is $\mathrm{bar\,s^{-1}}$ and is named 'Laske'-unit. The sum of drops per well results in the desired volume and is automatically calculated by the device itself and the previously calibrated liquid class.
To prepare the combinations for the LCR assembly, the nanoliter dispensing unit is utilized. Depending on the physical properties of the liquid, a liquid class has to be created and assigned to each liquid. The calibration of the liquid classes is error-prone due to manually produced columns, batch-dependent differences and is considered as a parameter with a high impact on

accurate dispensing of liquid-handling devices [1, 10]. Although it was not investigated, the accuracy of the dispensing can be increased by performing the calibration at least in triplicates and by considering a low, mid and high Laske value (50, 175, 300 Laske). If the volume of a liquid is constantly used for one reaction like, *e.g.*, the buffer volume, the liquid class should be adjusted for this specific volume only. This is achievable by first calibrate the liquid class as described before. Afterwards, the liquid of interest has to be dispensed with the I-DOT into one well of a target plate or onto the surface of the target tray of the device. The liquid volume can be measured by aspirating it with a pipette. If the volume is too low or high, the parameters of the liquid class are adjusted manually until the aspirated volume is equal to the desired volume. For this workaround, it is mandatory to utilize a calibrated pipette.
To mix the LCRs, the library plate with all desired liquids is imported into the platform. The dispensing robot 'Felix 1' transfers the desired liquids after a resuspension step to the I-DOT source plate in a column-wise pattern (Figure 3.37). For this, the user defines a dispensing protocol including the names of the liquids. Furthermore, a second file with the positions of the liquids in the library plate is created by the user. Based on both files, all desired liquids are transferred to the I-DOT source plate followed by the dispensing into a 96-well PCR plate. A user-defined `csv`-protocol is utilized to dispense the liquids. After the dispensing, drops of the liquids can remain on the surface of the inner walls of the source wells due to an imprecise drop release during the dispensing. Before the cycling, the PCR plate with the liquid is transferred to the plate reader of the platform. By double orbital shaking, the drops on the walls are released, collected on the bottom of each well and the total volume is mixed to ensure a more homogeneous reaction mixture. To prevent the evaporation in the subsequent thermal cycling, the dispensed volume is layered by paraffin. During the cycling (parameters shown in Figure 2.1 in subsection 2.2.10), the residual volumes of the I-DOT source plate are backfilled into the library plate to enable an efficient and sustainable utilization of the DNA library.

2.2.19 Automated transformation of *E. coli* and dilution plating

Up to 96 LCRs are chemically transformed into *E. coli* by the heat-shock method [38, 39]. The optimal heat-shock duration of 30 s and an LCR-to-cells ratio of 1:10 were investigated in section 3.2 (Figures 3.17 and 3.18). The user prepares a one-well plate or a 96-well/PCR plate with the desired cell volume and stores it with a lid or not on the cooling position. Each well of the PCR plate with the cycled LCRs is mixed with a user-defined cell volume. Afterwards, the cell-LCR mix is incubated for 30 min at 4 °C, the heat-shock is applied followed by an additional incubation. To recover the cells, a specific volume of the medium is transferred to the wells. For this, the volume is automatically calculated to not exceed a maximum volume of 200 µL per well. This volume depends on the sum of the user-defined volume of competent cells, the reaction volume of the LCR and the volume of the paraffin layer. Finally, the suspension is transferred to a 96-well plate for the recovery step.

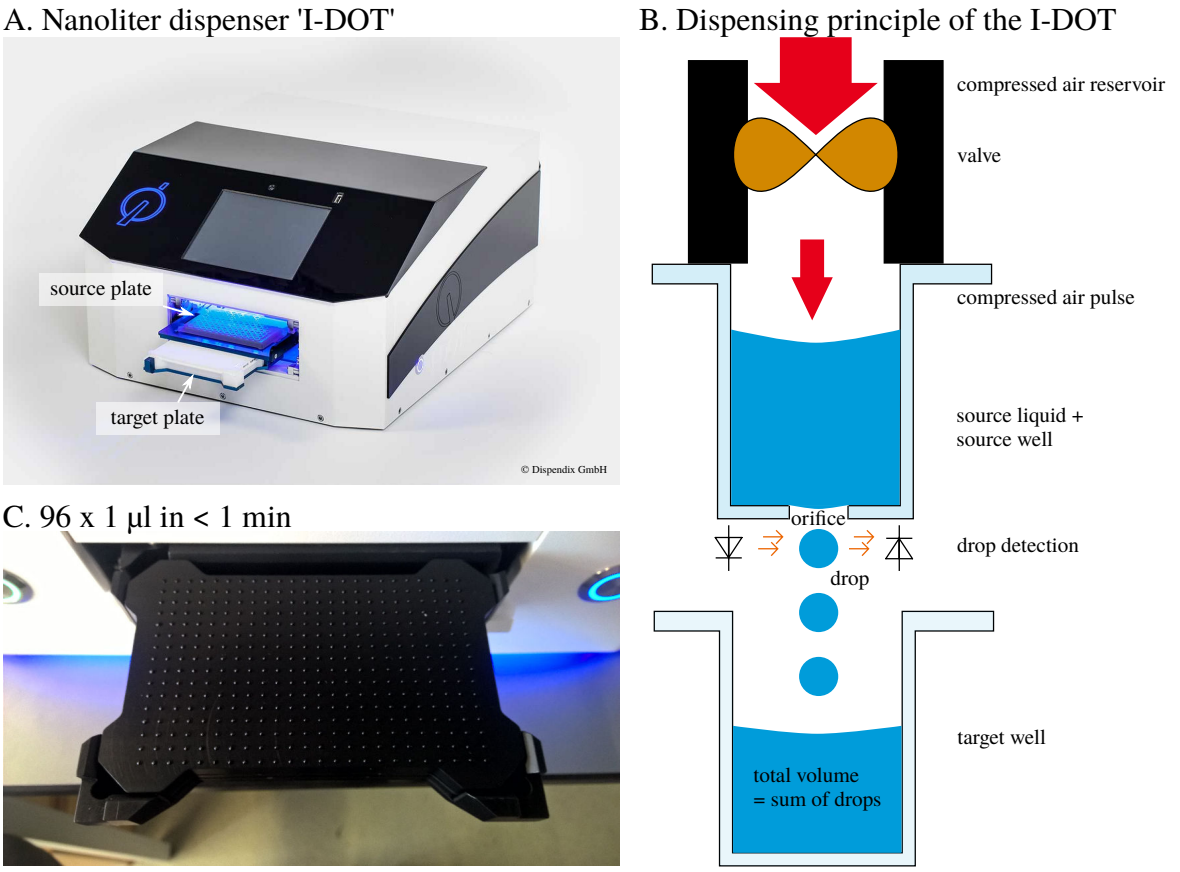

Figure 2.2: Nanoliter dispensing with the I-DOT. **A.** The I-DOT device from Dispendix GmbH with a source and target plate. The target plate is placed underneath the source plate. To dispense a liquid, the source plate is moved horizontally to place the source liquid above the target wells. **B.** Dispensing principle for one liquid of interest. Maximal 80 µL can be filled into one source well. After calibrating the liquid class, a certain amount of drops is released from the source liquid by applying pressure pulses. In total, eight source liquids are dispensed in parallel. The drops are formed due to an 90 µm orifice on the bottom of the source well. The sum of drops is determined for each source liquid by an LED-based drop detection. **C.** Within 1 min, 96 $\times$ 1 µL of water can be dispensed from one source well. By utilizing eight source wells with water in one column of the source plate, the duration is shortened to ca. 10 s due to the presence of eight independent dispensing heads.
The figure is modified from the master thesis of Markus Susenburger: Susenburger, M., Computational Optimization of the Ligase Cycling Reaction for Automation. Masterarbeit, 2018, TU Darmstadt.

After the recovery, the transformed cells are transferred to 4-well plates with agar and a selection marker. In case that the expected number of colonies is too high for one well with agar, the user can adjust the workflow to generate two plating dilutions per transformation. For this, two volumes between 5 and 200 µL can be chosen whereby the sum is restricted to be higher than 200 µL (maximal working volume for a well of the utilized 96 MTP). Based on this, each transformed LCR will be split in the same pattern. Before transferring the transformed cells to the agar plates, 100 to 500 µL of the recovery medium are added to each well with agar to support an equal distribution of the cells. Afterwards, the two predefined split volumes are pipetted on the agar with the layer of recovery medium. The transformed cells are spread by the

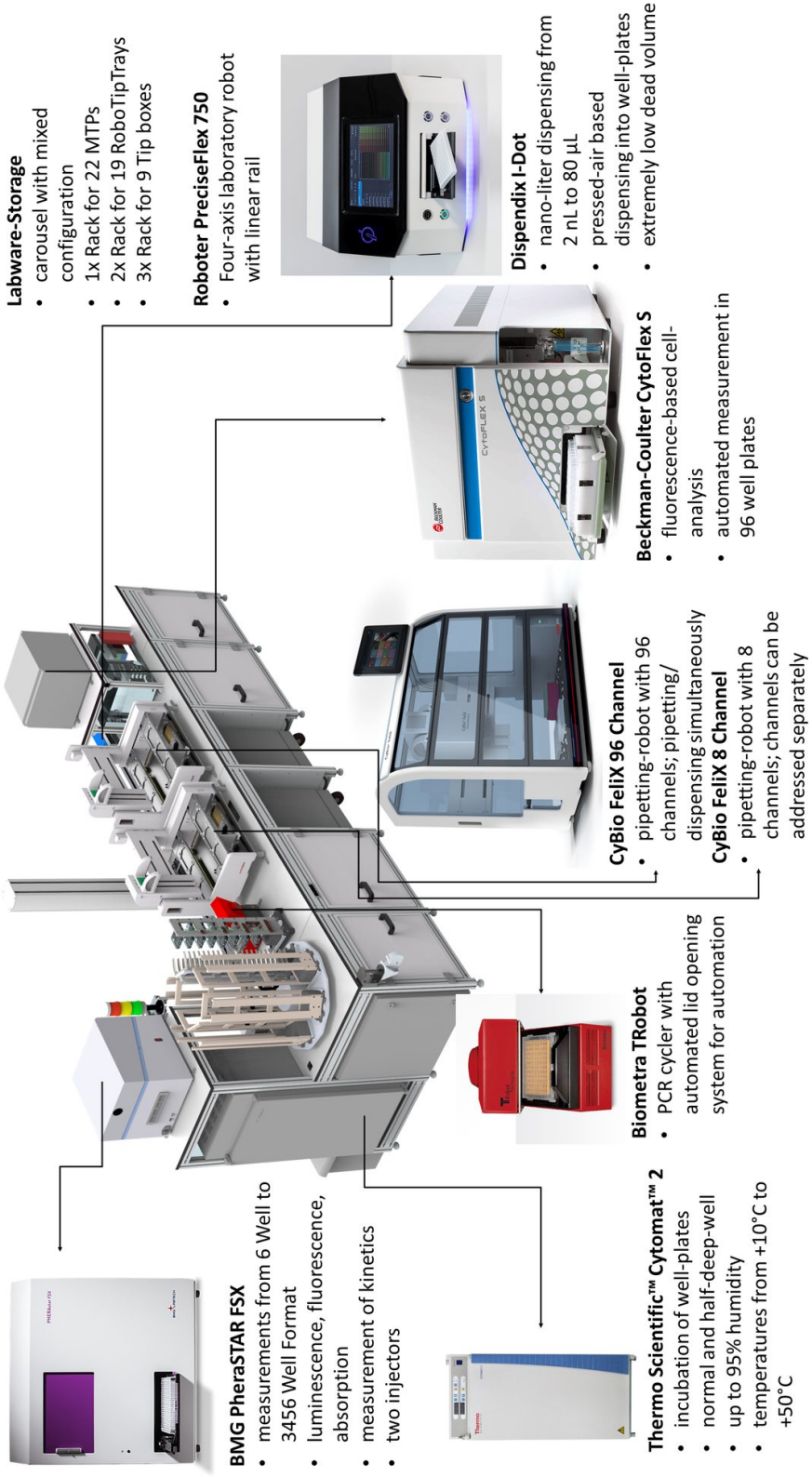

Figure 2.3: Robotic platform. Figure kindly provided by Thomas Zoll (PhD student of Prof. Dr. Kabisch).

liquid medium on the surface of the solid agar and the following shaking step in the incubator. After the last agar plate was stored in the incubator, the shaking continues for an additional hour.

3 Results and discussion

3.1 *In vivo* optimization of the LCR

To optimize DNA assemblies for the construction of synthetic circuits, several *in vitro* and *in vivo* issues during the DBTL cycles have to be considered. For the DNA assembly using the LCR, the construct of interest is build *in vitro* by a ligase and thermal cycling of a defined mix of DNA parts and BOs. Afterwards, the assembly mix is transformed into a microbial host for the uptake and propagation of the circular product. Due to this, the LCR workflow is an *in vivo* method. In the assembly steps of the LCR, a sequence-dependent crosstalk of the involved DNA parts and BOs along with the applied thermal conditions are supposed to have an impact on the LCR assembly. Furthermore, the influence of the transformation of the LCR into, *e.g.*, *E. coli*, underlies the endogenous abilities of the chosen host to process DNA by post-assembly alterations or even ligations [54, 117]. These assumptions are investigated and discussed in this chapter and present the results of the published study of Schlichting et. al [95]. The study presented in the following sections initially utilizes the LCR conditions published 2017 [11, 16] and are called 'baseline conditions'. Based on these initial LCRs, the impact of several BO design rules, their ΔG crosstalk and the inter-dependencies of the applied design rules and experimental temperatures are investigated. For this, a toy-model plasmid system was developed and utilized. This plasmid enabled a fast DBTL cycle and is based on fluorescence (Figure 3.1). Afterwards, the new LCR conditions were validated by the assembly of two additional plasmids to confirm the optimized protocol. Prior to performing the optimization experiments, the toy-model plasmid was designed and a standard process of performing an LCR was investigated.
The toy-model plasmid with the repetitive terminator sequence was designed to simulate a challenging assembly (Figure 3.1B). The plasmid consisted of the two reporter genes *sfGFP* and *mRFP1*. Both were split into three subparts to design an assembly of the toy-plasmid with DNA parts in range of 79 bp to 2974 bp. As the terminator, the BioBrick *BBa_B0015* is present in both genes. To get insights into the LCR, several BO sets were designed and experimental parameters were varied to assemble the toy-model plasmid. For this, the phenotype of $\sim$100 CFUs per LCR were observed by fluorescence microscopy to estimate the efficiency for each experimental setting. The number of colonies per LCR was determined by counting all CFUs per plate. This amount was used for an extrapolation by using the dilution-factor. Within this study, 61 experimental conditions were utilized to determine improved assembly conditions for the

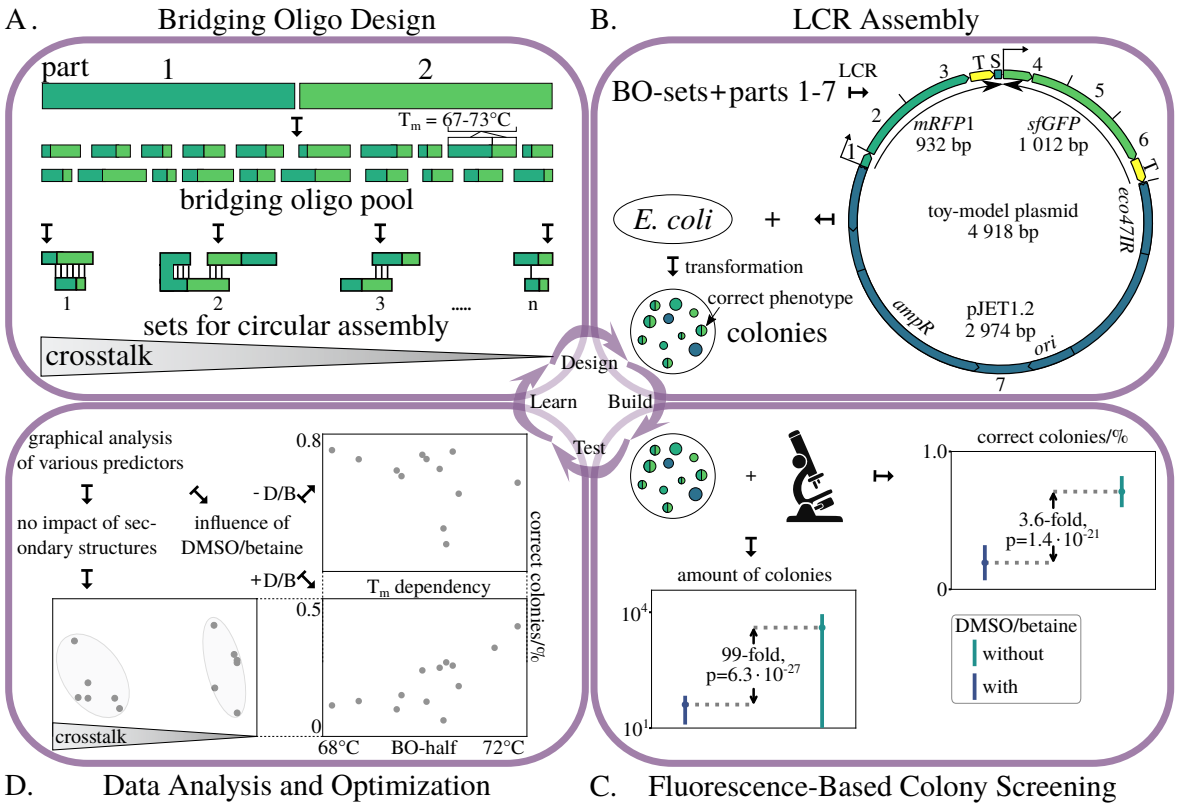

Figure 3.1: Workflow for the *in vivo* LCR optimization experiments. **A.** Bridging oligo sets were designed using general design rules with the focus on ΔG-related BO-crosstalk while maintaining a T_m of $70 \pm 3\,^{\circ}\mathrm{C}$. **B.** The BOs were utilized for the LCR-assembly of a seven or three parted toy-model plasmid with *sfGFP* and *mRFP1* as reporter genes. To simulate repetitive sequences, the same terminator *BBa_B0015* (T) was chosen for both reporter genes. A DNA-spacer S (37 bp) was incorporated at the 3'-end of *mRFP1* to disable the ligation with the plasmid backbone (part 7). A GenBank file of the plasmid is available in the supplement of Schlichting *et al.* [95]. **C.** A negative impact of 8 % v/v DMSO and 0.45 M betaine was oberserved for the toy-plasmid assembly. The p-values were derived from a Kolmogorov-Smirnov test between the two sets of data shown in Supplementary Figure 6.4. **D.** No ΔG-related influence was observed in the LCRs. The assembly was mainly affected by the target T_m of the BOs. This was investigated by design new BOs and utilizing them for the assembly of the toy-plasmid. *ampR*: gene for ampicillin resistance, *eco47IR*: gene for a restriction enzyme (reduction of religations of the backbone), *mRFP1*: *monomeric red fluorescent protein 1*, *ori*: *origin of replication*, *sfGFP*: *superfolder green fluorescent protein*, T_m: melting temperature.
This figure is modified after Schlichting *et al.* [95].

toy-model plasmid. Around 15 000 CFUs were screened by fluorescence microscopy. Contrary to the recommended backbone concentration of 3 nM [11, 16], 0.3 nM of the backbone was added to each LCR reaction to reduce religations. This increase of the insert-to-backbone ratio is described as beneficial for other DNA assembly methods [46, 126]. In the control reactions where the Ampligase® was omitted, no colonies with fluorescence were detected (Figure 3.2). Furthermore, no carry-over of the pJET1.2/blunt backbone was revealed by blue-white screening of ∼1000 CFUs without fluorescence. No carry-over is expected for the DNA parts of the reporter genes *sfGFP* and *mRFP1* due to a change of the antibiotic selection marker.

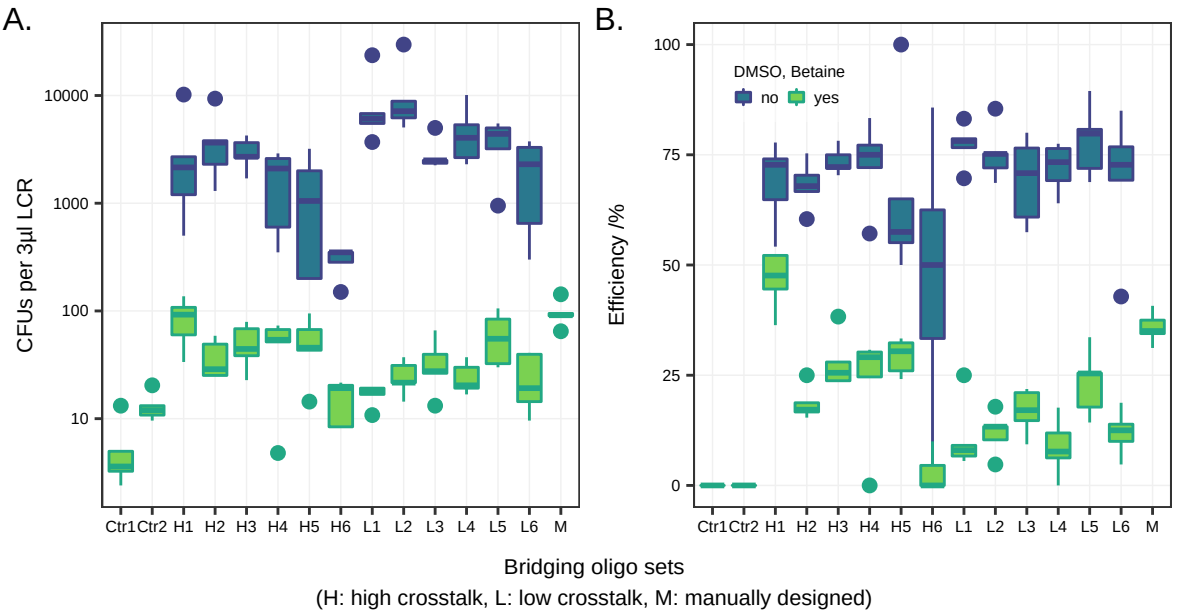

Figure 3.2: Boxplots of LCRs of a seven part toy-plasmid by utilizing BO-sets with high crosstalk (sets H1-H6) and low crosstalk (sets L1-L6). Each LCR was performed as a quintuplet. The standard deviation for each LCR is indicated by error bars. In addition to these twelve sets, a 13^{th} set ('manually' set M) was utilized for the baseline LCR with DMSO and betaine. **A.** All LCRs without DMSO/betaine resulted in higher efficiencies in comparison to the LCRs with both detergents. No correlation between crosstalk and BO performance was found. Interestingly, BO-set dependent differences were found for the baseline LCRs without DMSO/betaine, *e.g.*, BO-set H1 resulted in a higher efficiency in contrast to the utilization of BO-set L1. The negative control reactions with BOs but without ligase (Ctr1) and another control reaction without BOs and ligase (Ctr2) resulted in no fluorescent colonies. **B.** LCRs without DMSO/betaine resulted in more colonies in comparison to the baseline-conditions. The raw data of the LCRs presented here are shown in Supplementary Figure 6.4. The sequences of all BO-sets are shown in Supplementary Table 6.2.
This figure is plotted by using the raw data of Schlichting *et al.* [95].

As a mandatory prerequisite for the fluorescence-based is the correlation of the phenotype and genotype of a colony. For this, the plasmids from 120 CFUs were isolated, sequenced and analyzed. No true/false-positive and true/false-negative results were observed. Sixty colonies with a bicolored phenotype (red AND green fluorescence) contained the toy-model plasmid and its seven subparts in the desired orientation and order. To validate the colonies with the false phenotypes 'only red', 'only green' and 'non-fluorescent', twenty plasmids of each were analyzed. They were lacking at least one of the *sfGFP*- or *mRFP1*-subparts and showed a red or green fluorescence (but not both) or showed no fluorescence due to religations of the backbone. Colonies with no fluorescence were also observed for plasmids lacking at least one subpart of both reporter genes in other assemblies within this thesis. Point-mutations in the sequence of the analyzed LCR products were regarded as alterations by the amplification primers, the polymerase or *E. coli* and were not considered as LCR-related.
The sequence analysis of plasmids from CFUs with a 'only green' phenotype revealed one or more missing subparts of the *mRFP1*. Interestingly, the missing parts were not completely absent

in the LCR product. Remnant basepairs at both ends of the missing DNA part were observed in a range of 10 to 100 bp. For the 20 analyzed plasmids of CFUs with the phenotype 'only red', the sequences lacked the full *sfGFP* and the incorporated spacer sequence at the 3'-end of the *mRFP1*. Obviously, *E. coli* recognizes the two identical terminator sequences and deletes it via *recA*-independent recombination [5, 21].
As already mentioned, sequence analysis of misassembled plasmids revealed remnant bases or even longer fragments of the missing DNA parts. These issues are possibly related to the heterogeneous mixture of the DNA parts and debris derived from their PCR amplification, the utilized primers and templates. The negative impact of residual amplification primers in the LCR is presented in more details in section 3.2 and Figures 3.10 and 3.11. Furthermore, *E. coli* is able to circularize DNA in the transformation process [54, 117]. The transformation of the LCR mix results in a ligation by *E. coli* and the growth of colonies with the religated backbone or plasmids with missing DNA parts. For example, this was detected in the negative control reaction without utilizing a ligase and is shown in Figure 3.2. Concluding this, the carry-over of the mentioned species of DNA along with the influence of *E. coli* results in misassemblies and also in correctly assembled plasmids.
Overall, the fluorescence-based screening system is a robust and rapid method (screening of ca. 500 CFUs h^{-1}) to obtain insights of LCR assembly efficiencies and the impact of varying the experimental parameters. Furthermore, the correlation of the genotype of the assembled plasmid with the phenotype of colonies offers a screening system without applying next generation sequencing approaches. The discrimination of the phenotypes is achievable by several methods like fluorescence microscopy or photometric analysis and the utilization of software tools for the detection of fluorescent colonies (`OpenCFU` [32]; `CellProfiler` [8]).

3.1.1 Bridging oligo crosstalk and melting temperature

The assembly order in the LCR is defined by BOs and they are normally designed by the experimenter. The design rules are based on published protocols [11, 16]. One rule is to adjust the BO-half length until it matches the target T_m of 70 °C. Nevertheless, the free energy ΔG is presumed to be a parameter with a higher impact for oligonucleotide-based reactions [40, 90]. In the LCR, the influence of ΔG is reduced by using 8 % v/v DMSO and 0.45 M betaine [11, 16]. Nevertheless, this ΔG-related crosstalk and the need of ΔG-optimized BOs is unknown. In this study, BOs were designed following the rules of de Kok *et al.* [16]: they were designed in forward direction and the LCR-specific concentrations of 10 mM Mg^{2+}, 50 mM Na^{+}, 3 nM DNA parts, 30 nM BOs and 0 mM dNTPs. All BOs were ordered freeze-dried from Eurofins Genomics (Ebersberg, Germany) as salt-free DNA oligonucleotides. A manually BO-set was designed with `Primer3` [111]. This tool is included in the software suite `Geneious`. For the T_m calculation and salt correction of all BOs sets, the formulas of SantaLucia [89] were utilized. `Primer3` only accepts one DNA concentration. The LCR experiment is based on different concentrations

of DNA parts and BOs. Corresponding to this issue, only the BO concentration of 30 nM was entered. This manually designed set is named BO set 'M'. To investigate the BO crosstalk,

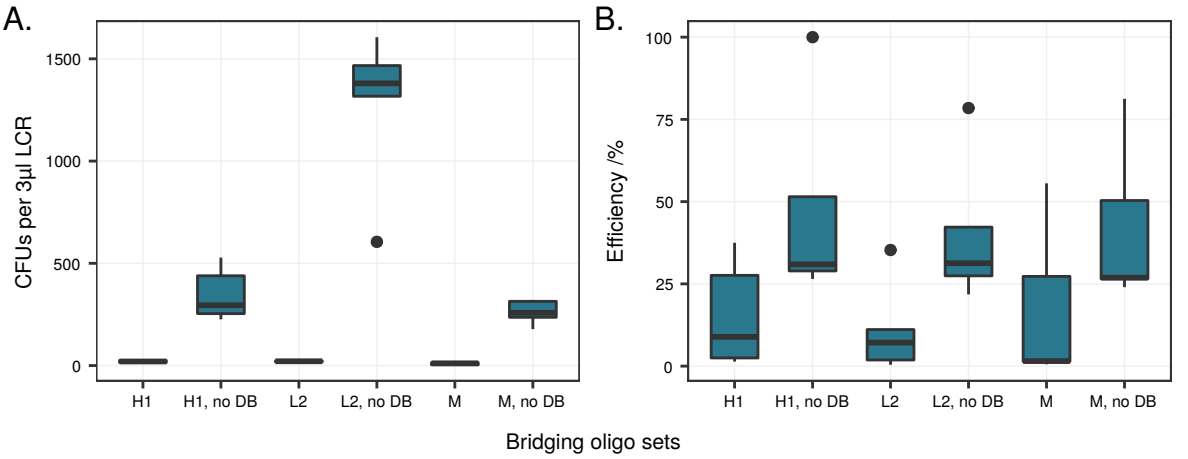

Figure 3.3: Influence of DMSO and betaine in the LCR. All LCRs were performed as quintuplets using the same batches of DNA parts, electrocompetent cells and a master-mix (excluding the BO-sets and the ligase). **A.** For all three BO-sets (H1, L2 and the manually set) the DMSO/betaine-free LCRs were more efficient. As observed in Supplementary Figure 3.2, the efficiency of the set 'H1' was higher than the manual set 'M' and set 'L2' in the baseline LCR (with DMSO and betaine). **B.** The omission of DMSO/betaine highly increased the total amount of colonies. This is consistent with the results shown in Supplementary Figures 3.2B and 6.6H for DMSO/betaine-free conditions: a lower T_m is beneficial and resulted in more colonies. All BO sequences are shown in Supplementary Table 6.2. DB: DMSO and betaine.
This figure is plotted by using the raw data of Schlichting *et al.* [95].

additional sets were designed by minimizing or maximizing ΔG-dependent crosstalk between oligonucleotides with a target T_m in the range of 67 °C and 73 °C. The crosstalk is defined as the sum of all minimum free energies (MFEs) when cofolding each BO of one set with each BO in this set and with itself. As a temperature for the calculations, the annealing temperature of the baseline LCR was utilized (55 °C [16]). For the design of the crosstalk minimized BOs, the SantaLucia parameters [89] were utilized for the T_m calculation and salt correction as described for the manually set. In contrast to the manually designed one, the DNA part concentration was also adjusted to fit the experimental parameters. For all BO designs, the influence of DMSO and betaine were not included. Sets with low crosstalk are denoted by an 'L' and sets with high crosstalk by an 'H'. All BO-sets, sequences and melting temperatures for the crosstalk investigations are provided in Supplementary Table 6.2. Further information for the calculation of the crosstalk is given in the supplement of Schlichting *et al.* [95].
One manually designed BO-set and twelve automatically designed ones (Supplementary Table 6.2) were utilized to assemble the seven part split of the toy-model plasmid (Figure 3.1B) and to investigate the influence of BOs with high and low crosstalk. For this, the baseline protocol (Table 3.1) with and without 8 % v/v DMSO and 0.45 M betaine were applied.
For the LCRs with both detergents, 3.6× lower efficiencies and 99× fewer colonies per 3 µL LCR were obtained for assemblies with DMSO and betaine ($p < 0.001$, Figure 3.1C; raw data

in Supplementary Figure 6.4). For a validation, the diverse LCRs of BO set 'H1' and 'L2' were repeated in a more consistent approach with the same batch of DNA parts and the same batch of electrocompetent cells (Figure 3.3 and Supplementary Figure 6.11). The LCRs were analyzed graphically to investigate the origin of those diverse results. First, no ΔG-related impact was observed for the LCRs with or without DMSO and betaine (Supplementary Figures 6.5, 6.6, 6.7, 6.8, 6.9 and 6.10). Furthermore, the need for a guanosine or cytosine at the 3'-end of the BOs was not proven as mandatory and is contrary to the literature [16].
The success rate of LCRs with DMSO and betaine were shown to be dependent on the utilized BO-set. The utilization of the BO-set 'L1' resulted in lower efficiencies in comparison to 'H1' (Figure 3.2A). According to the graphical analysis, this difference is related to the higher average T_m per BO-half of the latter set (Supplementary Figure 6.6C). The impact of the melting temperature of the BOs was further observable for the other utilized sets. Obviously, higher T_ms are beneficial for the LCRs with DMSO/betaine. Additionally, a higher T_m than 72 °C is supposed to result in more efficient assemblies. This is theoretically confirmed by the T_m-recalculation of the BO-set utilized by de Kok *et al* [16]. Considering the calculation parameters (SantaLucia 1998 for the T_m calculation [89] and Owczarzy *et al.* [72]), the BO-set of their study supposed to have a melting temperature of 70 °C but a value of 72.2 °C was recalculated. Applying the formulas of the study presented here (SantaLucia 1998 [89] only), the average T_m of this BO-set is 74.8 °C. These comparisons are depicted in Figure 3.4. Concluding the investigations of LCRs with DMSO and betaine, a T_m higher than 68 °C per BO-half was advantageous for the assembly reaction. The manually BO set ('M') was designed with a target T_m of 70 °C by utilizing `Primer3` of the *in silico* software `Geneious`, the T_m formula of SantaLucia 1998 [89] and the salt correction of Owczarzy *et al.* [72]. The average T_m shown in Supplementary Figure 3.4B is lower than the expected T_m of 70 °C. `Geneious` allows the user to adjust only one DNA concentration for the T_m calculation. This value is utilized for both the DNA part and oligonucleotide concentration and results in a lower T_m in comparison to the formulas applied in this study.
Besides the too low T_m of the BOs, an additional hypothesis of low LCR efficiencies in the baseline LCR is related to temperature interval of the annealing step at 55 °C and the following ligation step at 66 °C. Already bound BOs during the annealing will be separated until the ligation temperature is reached and may results in less templates for the ligase. According to this, in LCRs with BOs with a lower T_m are supposed to be more affected and this should negatively influence the results in comparison to sets with higher T_ms. In Figure 3.5, this theory was validated by reducing the ligation temperature for LCRs with BO-sets with high and low melting temperatures. Although the ligase is described as being less active at the decreased ligation temperature of 60 °C[1], the assembly efficiency was increased for LCRs utilizing BOs with a higher T_m. This was validated by using three BO-sets with different melting temperatures

[1] according to the manufacturer 70 °C is the optimal temperature of the utilized ligase: https://www.epibio.com/docs/default-source/forum-archive/forum-03-1—nucleic-acid-ligation.pdf?sfvrsn=6

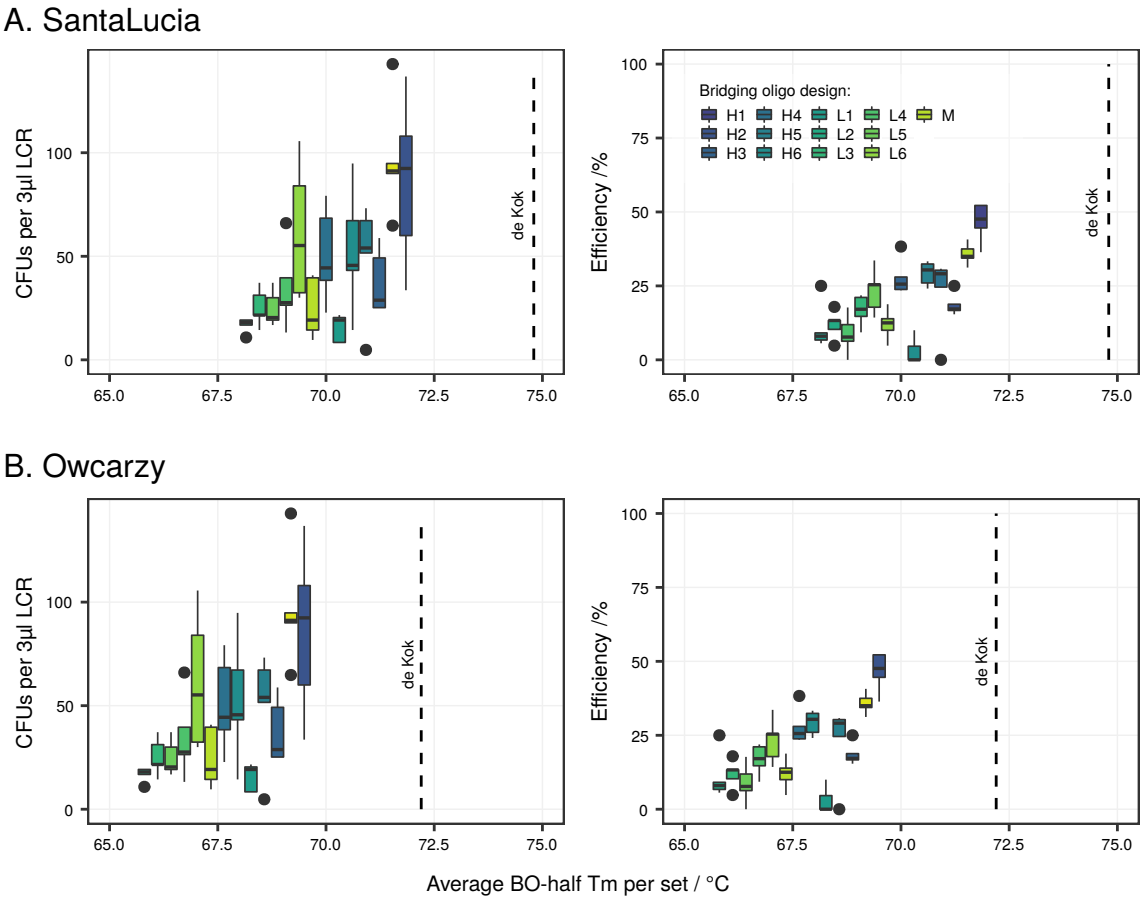

Figure 3.4: Effect of salt corrections on the melting temperature. The results for the LCRs with 8 % v/v DMSO and 0.45 M betaine are shown. Thirteen BO-sets were utilized (H1-H6: high crosstalk; L1-L6 low crosstalk; M: manually designed set). The thermodynamic calculation parameters for A. and B. were derived from SantaLucia [89]. For the salt correction, two different algorithms were utilized. **A**. SantaLucia [89] salt correction. **B**. Owczarzy [72] salt correction (utilized in de Kok *et al.* [16]). The optimized melting temperature is indicated by the dotted line and is obtained from recalculating the optimized BO-set of the de Kok *et al.* study [16]. BO: bridging oligo, CFU: colony forming unit, DMSO: dimethyl sulfoxide, T_m: melting temperature of one BO-half.
This figure is plotted by using the raw data of Schlichting *et al.* [95].

(Figure 3.5). Increasing the annealing temperature, which would also decrease the interval, was assumed to be disadvantageous due to accelerated separation of bound BOs and was not investigated.

Various mechanisms are thought to be disadvantageous for the low amount of colonies in LCRs with DMSO and betaine. First, a lower assembly efficiency directly results in less plasmids. Second, the utilization of both detergents negatively influences the electroporation process and is shown in Supplementary Figure 6.11. An already cycled LCR reaction without DMSO/-betaine was mixed with both substances followed by the electroporation. In contrast to the transformation of the LCR without DMSO/betaine (but with *A. dest.*), 3-4× less colonies with a similar efficiency were obtained. This effect is probably related to the decreased volume-ratio

of transforming 3 µL LCR in 30 µL competent cells. In contrast to this, 2.5 µL LCR are added to 50 µL cells in the published protocols [11, 16]. Strain-dependent influences of detergents like DMSO on transformations were already described and are related to their electrophysical properties [38]. This issue is assumed to explain the observed negative impact of the chosen LCR-cells ratio. Direct negative effects of DMSO and betaine on the utilized *E. coli* strain are not plausible due to no detectable impact on the strain if chemically transformation was performed (Supplementary Figure 6.14). In case of LCRs with DMSO and betaine, the yield of colonies can be increased by a dialysis step of the LCR for 30 min using *aq. dest.* and a nitrocellulose membrane. According to the results for crosstalk minimized BOs in the LCR, this optimization

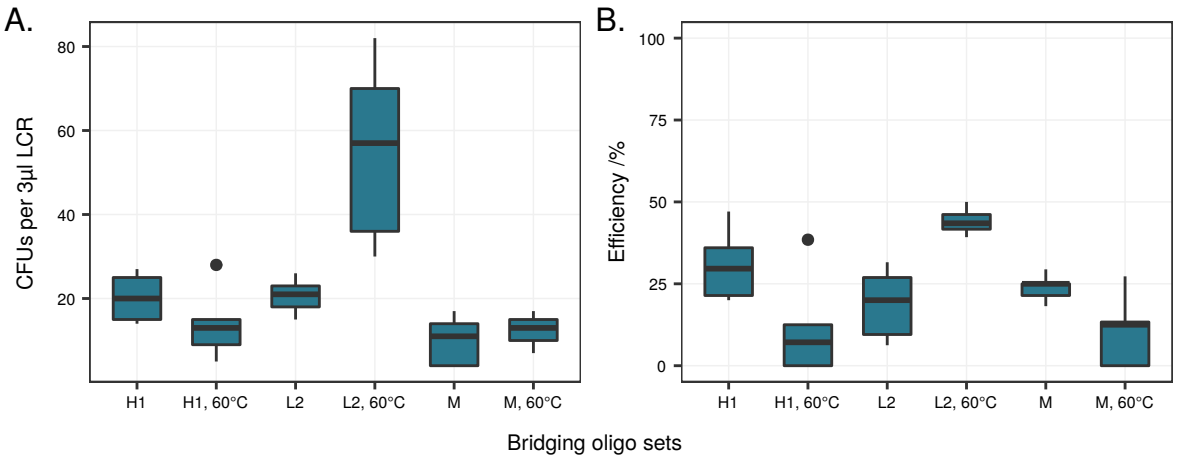

Figure 3.5: Impact of the ligation temperature on LCR performance with DMSO and betaine. All LCRs were performed as quintuplets. For the BO-set L2, a lower ligation temperature of 60 °C is beneficial for the efficiencies and total amount of colonies. This set had a lower T_m of 68.6 °C compared to the manually designed set 'M' with a T_m of 71.4 °C and the set H1 with a T_m of 71.9 °C. Due to the lowered ligation temperature, more BOs of set L2 remained attached to the DNA parts to guide the ligase. All BO sequences are shown in Supplementary Table 6.2.
This figure is plotted by using the raw data of Schlichting *et al.* [95].

strategy is negligible for the assembly of the predefined split of the toy-model plasmid. Of more interest, the addition of DMSO and betaine is not recommended for the assembly of the seven parted toy-model plasmid. Due to this, the applied experimental conditions like the annealing step, ligation step and target T_m of BOs have to be validated as being optimal for the new LCR without the DMSO and betaine.

3.1.2 A higher annealing temperature increases the amount of correct colonies

An approach to experimentally define the optimal annealing temperature of oligonucleotide-based molecular reactions like, *e.g.*, PCRs, is to perform a thermal cycling with a temperature gradient. This was applied for the LCR to investigate the influence of the annealing temperature. Furthermore, three BO sets with an average T_m of 67.8 °C, 69.9 °C and 71.8 °C were designed from the already existing BO pool for the crosstalk investigations to determine the impact of

different T_ms (sequences in Supplementary Table 6.3). The BO sets were used to assemble the seven parted toy-model plasmid in an annealing temperature range of 56.5 to 70.6 °C followed by a chemical transformation of NEB® 10-β *E. coli*. As shown in Figure 3.6B, the efficiency of

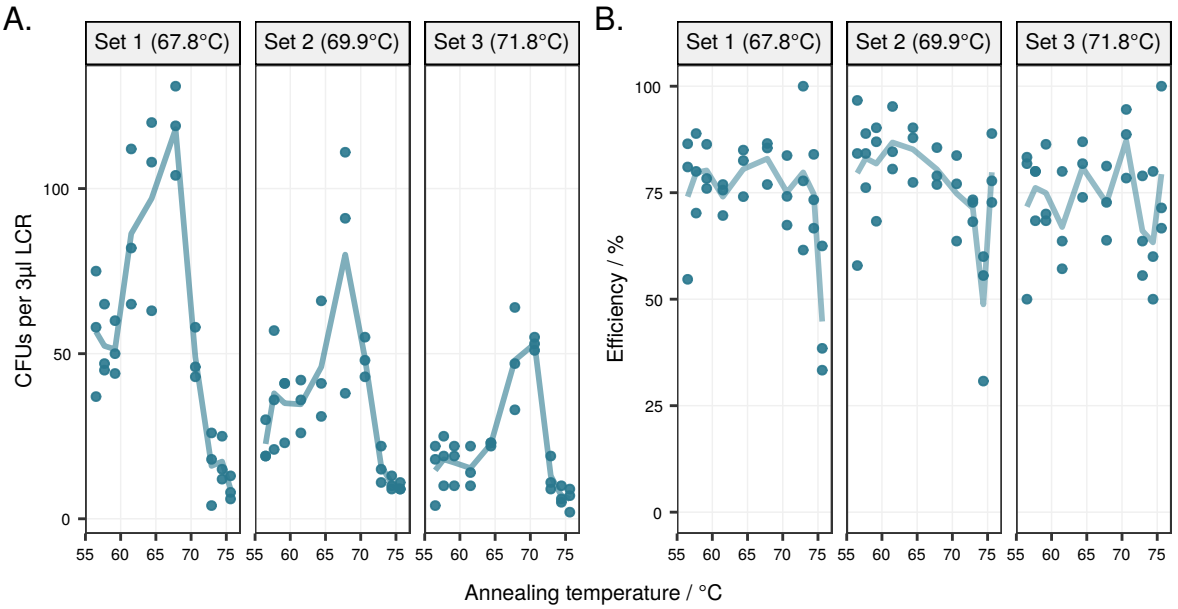

Figure 3.6: Gradient-LCR: adjustment of the annealing temperature for a DMSO/betaine-free LCR assembly of the seven part toy-model with three BO-sets. The annealing temperatures steps were 56.5, 57.7, 59.2, 61.5, 64.4, 67.8, 70.6, 72.9, 74.4 and 75.6 °C. The means are connected by a line. **A.** As already observed in B (and Figure 6.6H), the total amount of colonies was increased with a lower BO-T_m. Overall, the LCRs using these BO-sets resulted in a global maximum of colonies in a range of ∼68 °C with 2× more colonies (also shown in Supplementary Figure 6.12). **B.** For the three BO-sets the LCR-efficiency was at a similar level. It started decreasing at an annealing temperature of more than 70.6 °C. The LCRs were performed as triplets using the same DNA-parts and chemically competent cells. BO: bridging oligo, CFU: colony forming unit, DMSO: dimethyl sulfoxide, T_m: melting temperature of a BO-half.
This figure is plotted by using the raw data of Schlichting *et al.* [95].

the three utilized BO sets were similar in the annealing temperature range of 56.5 to 70.6 °C but seemed to decrease at higher temperatures. Consistent with previous results (Figure 6.6H), the number of colonies was reduced when a BO-set with a higher T_m was utilized (Figure 3.6A). Interestingly, a maximum amount of CFUs was observed for all LCRs in the range of 66-71 °C and was further validated for the BO sets '67.8 °C' and '71.8 °C' (Supplementary Figure 6.12). Within this range, the highest activity of the applied ligase is described and this assumes a positive effect of prolonging the overall duration for ligations by increasing the annealing temperature in the LCR. The increased annealing temperature doubled the colony yield for every LCR setup without decreasing the efficiency. Nevertheless, the total amount of CFUs at an annealing at 67.9 °C was dependent on the average T_m of the utilized BO-sets and can be observed in more details in Supplementary Figure 6.13: the set '67.8 °C' resulted in ca. 115 CFUs whereas the other sets '69.9 °C' and '71.8 °C' resulted in ca. 80 and 50 colonies. Further, a slightly higher efficiency was observed for the LCRs with the '67.8 °C'-set.

These results imply that a further decrease of the average T_m of BOs is advantageous for the yield of CFUs and the assembly efficiency. The validation experiments for this hypothesis utilized newly designed sets within a BO-T_m range of 62 °C to 67.3 °C to assemble the same seven part split of the toy-model plasmid at the annealing temperature of 66 °C. The sequences of the BO sets are presented in Supplementary Table 6.4. Unexpectedly, the number of CFUs and the

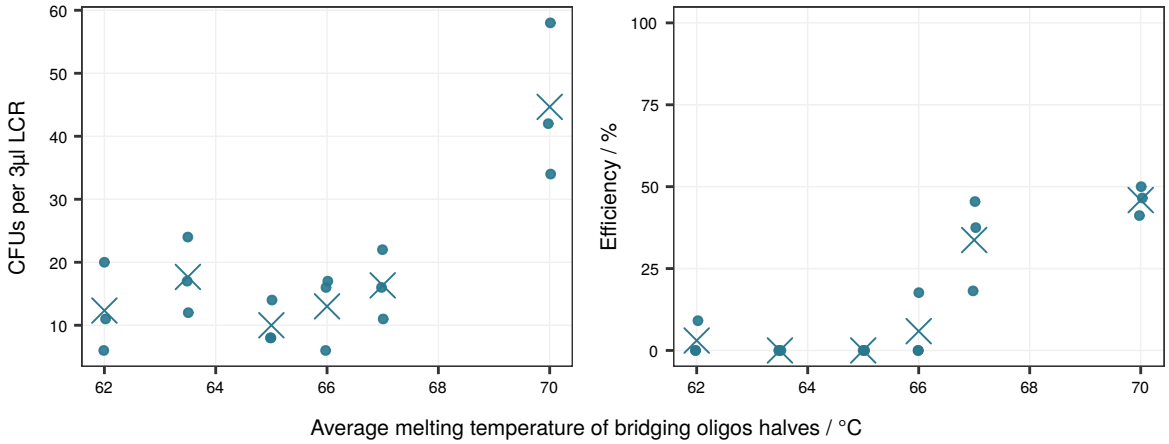

Figure 3.7: To decrease the BO-T_m from 67.3 °C to 62.0 °C is disadvantageous for LCRs at the annealing temperature of 66 °C. As reference, the BO-set '69.9 °C' from Figure 3.6 was utilized. Further decrease of the BO-T_m did not improve the LCR at the optimized annealing temperature of 66 °C. In comparison to the results shown in Figure 3.6, the LCR with the BO-set '69.9 °C' was less efficient due to loss of function by repeated freeze-thaw cycles of the DNA parts and/or BOs. The sequences of the BO-sets '62.0 °C' to '67.3 °C' are shown in Supplementary Table 6.4. The LCRs were performed as triplets using the same DNA-parts and chemically competent cells. BO: bridging oligo, CFU: colony forming unit, DMSO: dimethyl sulfoxide, T_m: melting temperature of a BO-half.
This figure is plotted by using the raw data of Schlichting *et al.* [95].

efficiencies for the reference set '69.9 °C' were depleted (Figure 3.7) in comparison to the results shown in Figure 3.6 although the same batch of DNA parts, LCR ingredients and competent cells were utilized. Probably, this is due to the additional freeze-thaw cycle in between the experiments which are known issues for DNA, oligonucleotides and BOs [15, 81]. Nevertheless, the investigations of a further decrease of the BO-T_m revealed no further optimization potential for the BO-design of LCRs without 8 % v/v DMSO and 0.45 M betaine (Figure 3.7).

3.1.3 Optimized LCR protocol is beneficial for another toy-model plasmid split

To validate the optimized experimental conditions, the toy-model was split into the DNA parts *sfGFP*, *mRFP1* and the backbone. The three parts were assembled by applying the baseline and optimized LCR protocol shown in Table 3.1. Additionally, the seven part split was assembled with both LCR protocols. The manually designed BO-set was utilized for the baseline conditions; the set '67.8 °C' of the gradient-LCR approach was used for the optimized LCR. All BOs were newly ordered and fresh aliquots of the ligase buffer, NAD^+ etc. were utilized. Both assemblies were transformed chemically in NEB® 10-β *E. coli* cells. As expected, the assembly of both splits

yielded more colonies and higher efficiencies for the optimized LCR protocol (Figure 3.8). The efficiencies of the seven part split was further decreased in comparison to the results presented before in Figure 3.6 and supports the hypothesis of a loss of function due to additional freeze-thaw cycles of the DNA parts. Nevertheless, the optimized protocol improved the assembly. To investigate the impact of the transformation method, the same LCRs were additionally

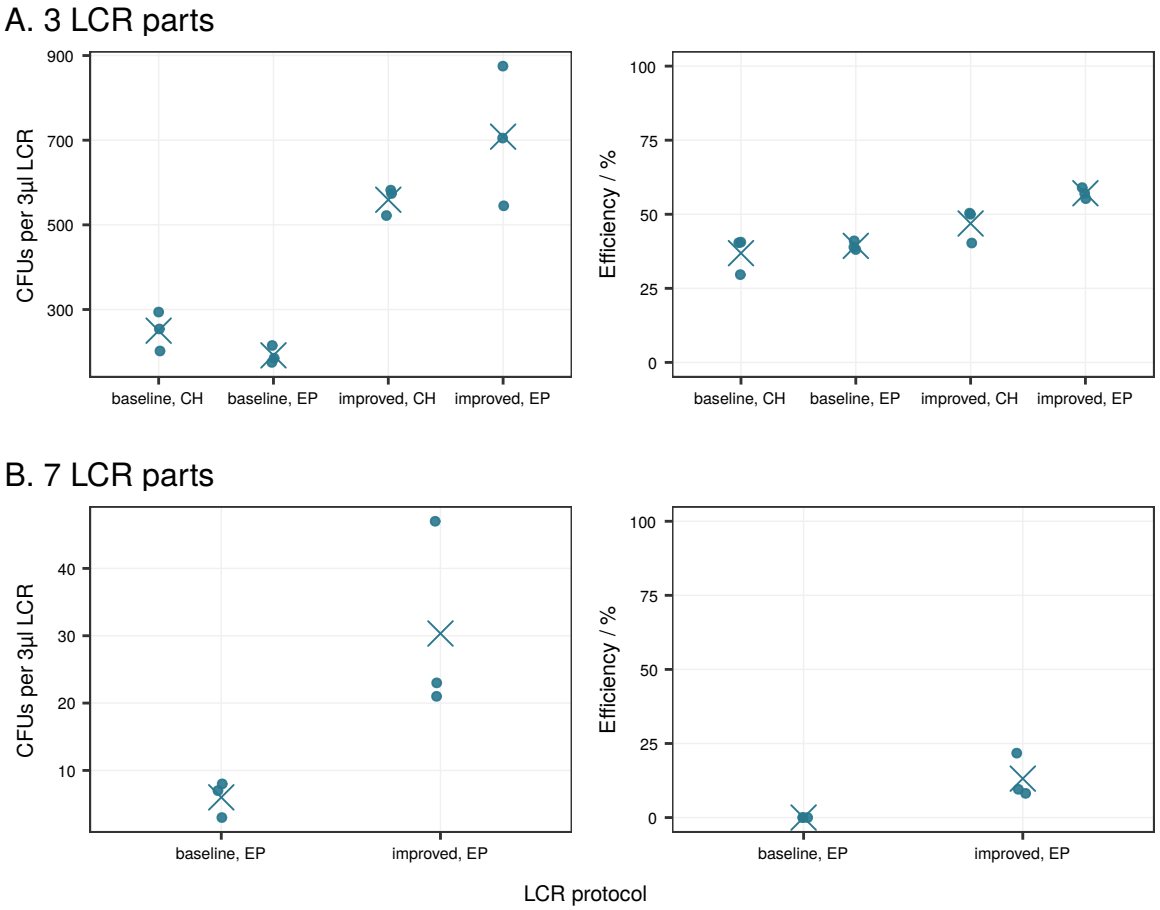

Figure 3.8: Results of the baseline and improved LCR-protocol for the toy-model plasmid ('TP'). **A.** For the three part split, the same LCRs were transformed in chemical ('CH') and in electrocompetent cells ('EP') to prove that the results are independent of the transformation method.**B.** For the seven part LCR only electroporation resulted in CFUs. For all LCRs, 3 µL were transformed in 30 µL cells. All LCRs were performed as triplicates. BO: bridging oligo, CFU: colony forming unit, DMSO: dimethyl sulfoxide, T_m: melting temperature of one BO-half.
This figure is plotted by using the raw data of Schlichting *et al.* [95].

transformed in electrocompetent NEB® 10-β *E. coli* cells by electroporation (Figure 3.8A). No colonies were obtained for the seven part split by using chemical transformation and is supporting the theory of the negative impact of freeze-thaw cycles. For the three part split, the choice of the transformation method does not affect the LCR efficiency but shows an impact on the CFU yield. Chemical transformation resulted in 2.5× more colonies for the optimized protocol whereas the electroporation resulted in 3.5× more CFUs (Figure 3.8A). According

to the investigations with another split of the utilized plasmid for the LCR optimizations, the optimized conditions are valid. Nevertheless, a validation of these findings requires additional comparative experiments by applying both protocols for constructs with different sequences.

3.1.4 Validation of the optimization experiments

Two validation plasmids were designed and split into a three part and seven part split. One reporter gene was the *lacZ*, which enables a blue white screening of colonies. Additionally, one or two selection markers were incorporated in the final sequence. The plasmids, amplification primers and BOs and are shown in Supplementary Figures 6.15 + 6.16 and Supplementary Tables 6.5,6.8, 6.6 and 6.9. By applying the baseline protocol, the improved protocol and a protocol with a higher target T_m for the BO design ('75 °C') in LCRs with DMSO and betaine the impact of the suggested improvements were investigated. The latter protocol is derived from the results shown in Supplementary Figures 6.7 and 3.4 where a higher T_m was assumed to be beneficial for LCRs with DMSO and betaine.

Table 3.1: Summary of the LCRs for the validation experiments using the toy-model plasmid and the validation plasmids 1 and 2 (Figure 3.1B, Supplementary Figures 6.15 and 6.16). Each plasmid was split into three and seven parts which were assembled by using the baseline and improved LCR protocol. The LCRs were transformed in chemically competent cells by a heat-shock. For results indicated by an *, the LCRs were transformed by electroporation due to low or no colonies when chemical transformation was used. BO: bridging oligo, CFU: colony forming unit, DMSO: dimethyl sulfoxide, T_m: melting temperature of a BO-half using the calculation of SantaLucia [89], TP: toy-model plasmid, VP1/2: validation plasmid 1 or 2. This table is modified after Schlichting *et al.* [95].

Factor	Unit	LCR protocol				TP		VP1		VP2	
		Baseline	75 °C	Improved	Protocol	3 parts	7 parts	3 parts	7 parts	3 parts	7 parts
						Efficiency (%)					
DMSO	% v/v	8	8	/	Baseline	37±6	0±0*	88±4	17±29*	98±2	93±12
Betaine	M	0.45	0.45	/	Improved	47±6	17±7*	96±1	98±3*	95±0	93±3
Annealing	°C	55.0	55.0	66.0		Total CFUs (per 3 µL LCR)					
Target T_m	°C	70.0	74.8	67.8	Baseline	250±46	6±3*	125±8	1±1*	365±63	12±2
					Improved	559±33	30±14*	493±19	323±70*	2023±331	189±26

By applying three protocols for the LCR assembly of the two validation plasmids 'VP1' and 'VP2', the impact of the improved experimental conditions were investigated. For both plasmids and splits, the improved LCR methods yielded more correct colonies (Figure 3.9 and Table 3.1). The efficiency was clearly improved for the seven part split of 'VP1'. No further positive effects for the efficiency were observed due to the high efficiency of the baseline LCR (>95 %). Related to this, the detection of an improved result is rather not possible. In contrast to this, the improved LCR conditions are beneficial for the total amount of CFUs. Dependent on the plasmid and split, 2× to 10× more colonies were obtained. Less positive effects on the efficiency and

amount of CFUs were observed for the '75 °C' protocol (Supplementary Figures 6.17 and 6.18). Nevertheless, two new protocols for LCRs with or without DMSO and betaine were validated as being advantageous whereby the protocol for LCRs without both additives was superior due to lower costs for the shorter BOs, less supplements, higher LCR efficiencies and higher yields of CFUs.
Sequence analysis of the assembled validation plasmids 'VP1' and 'VP2' was performed to enable and to prove the utilized phenotype-genotype screening. Ten plasmids of the seven part assemblies with a correct phenotype 'blue' and 'resistent to the antibiotic(s)' were sequenced after Sanger. No false-positive results were revealed for both whereas the analysis of four sequences from each validation plasmid were partly false-negative. Four false phenotypes 'white' of 'VP1' and three false phenotypes of 'VP2' were related to mutations in the promoter region of the *lacZ*. Due to its size of 80 bp it was ordered as oligonucleotides. Probably, the mutations are related to the synthesis of this part and are not related to the LCR. The fourth plasmid of 'VP2' lacked two subparts of the *lacZ* and was regarded as true-negative. Nevertheless, the LCR assembly investigations using both validation plasmids is a robust method to verify the protocol-derived differences of the LCR assemblies. The false-negative colonies are increasing the almost high efficiencies and not the total amount of CFUs. As discussed before, the assembly efficiency is not the relevant criterion to interpret the results of the validation experiments.
General issues like the size of the plasmid, genetic context, amount and size of DNA parts, purification grade and freeze-thaw cycles, a robust LCR assembly is influenced by the thermal experimental conditions and the target T_m of the utilized BOs. In this study, two new and optimized LCR protocols were developed and validated by assembling six splits of three plasmids and by comparing them to the published protocol. In contrast to the literature [11, 16], the utilization of 8 % v/v DMSO and 0.45 M betaine in the LCR is disadvantageous for all investigated assemblies. To omit both detergents, to increase the annealing temperature from 55 °C to 66 °C and to decrease the target T_m for a BO-half from 75 °C to 68 °C is the recommended protocol to optimize LCR assemblies.

3.1.5 The improved LCR protocol is applicable for other LCR constructs

To investigate DNA assemblies, no rapid detection system for assemblies and misassemblies is described in the literature. The utilization of the toy-model plasmid with the fluorescent reporter genes *sfGFP* and *mRFP1* is the first in-vivo approach which enables a fast and robust method to reveal misassembled and correctly assembled plasmids. Based on this, the impact of varying parameters is detectable by a fast and easy-to-adapt readout. This can be achieved by fluorescence microscopy or cytometry and is also applicable for other DNA assembly investigations.
The described toy-model system was utilized to investigate the role of ΔG-related crosstalk of BOs in the LCR. No impact of the BO-crosstalk was observed for the assembly of a seven part split and is assumed as negligible for LCR assemblies with predefined splits and DNA parts. An

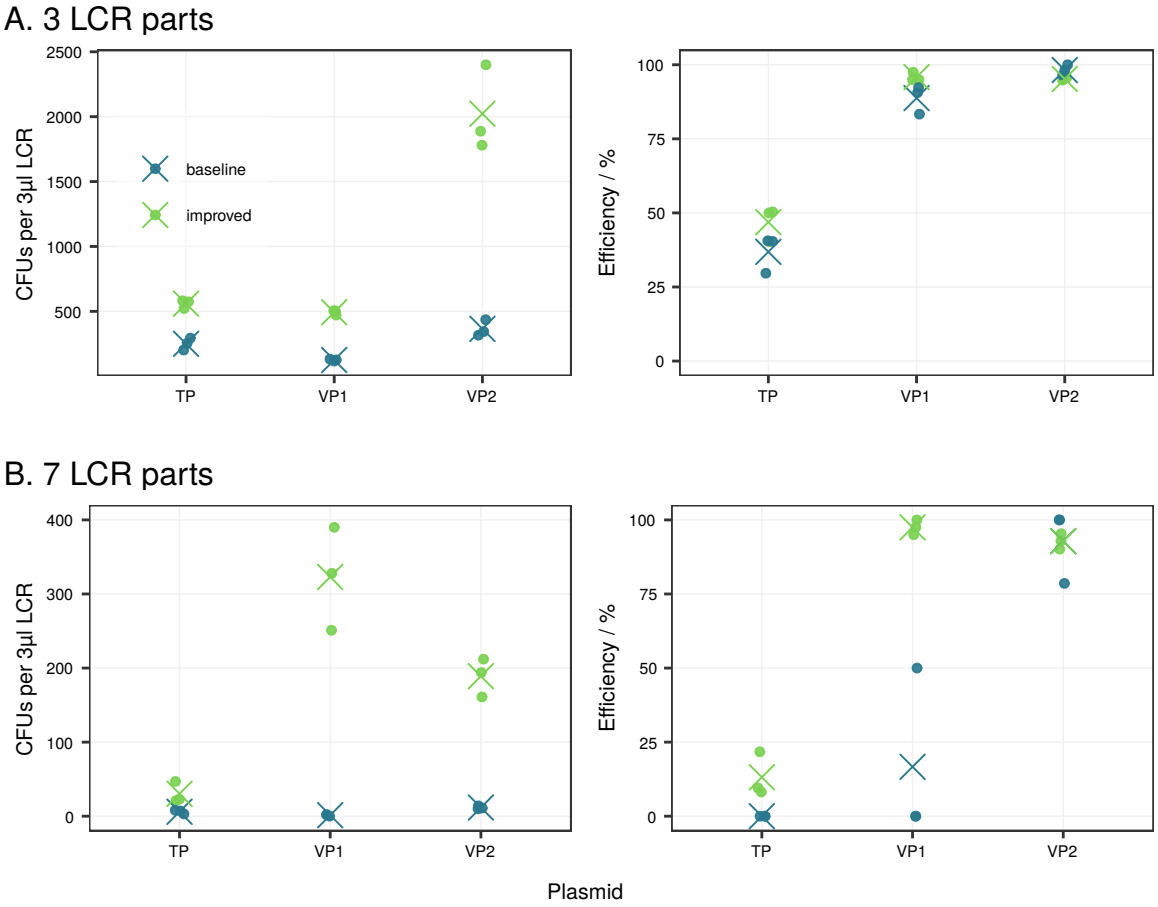

Figure 3.9: Comparison of the baseline and the improved LCR protocol for assembling the **A.** three part and **B.** seven part split of the toy-model plasmid (’TP’) and the validation plasmids 1 (’VP1’) and 2 (’VP2’). The improved protocol increased the total amount of (correct) colonies for all assemblies. The efficiencies were also improved, although the LCRs of the three part splits were similar for both protocols. LCRs were performed as triplicates and were transformed by chemical transformation. For the seven part split LCRs of the toy-model plasmid ’TP’ and validation plasmid ’VP1’ the LCRs were transformed by electroporation due to low or no colonies when chemical transformation was used. CFU: colony forming unit.
This figure is plotted by using the raw data of Schlichting *et al.* [95].

impact is conceivable for *de novo* designs of constructs where the ligation sites are not predefined. This was already reported for other DNA assemblies [37]. Besides this, the LCR of the toy-model plasmid is highly affected by the supplements DMSO and betaine, the T_m of the BOs and the temperatures for the annealing and the ligation step of the thermal cycling. Two new and optimized LCR protocols were derived from the results and were transferred to the assemblies of two additional plasmids. Both improved protocols were verified as being beneficial whereby the LCRs without DMSO and betaine were superior.
The recommended LCR protocol utilizes no DMSO/betaine and is based on an annealing step at 66 °C and the target T_m of 68 °C for each BO-half. The latter parameter is highly dependent of the utilized T_m calculation formulas: a target T_m of 68 °C is relevant for applying the calculations

of SantaLucia [89]; other systems differ significantly from this target T_m. To estimate the target T_m in another user-defined system, the T_m of the sequence 'TCCTCCCTGCAAGACGGTG' can be calculated. Afterwards, this value is the target T_m of the new system. Furthermore, to use a guanine or cytosine at the 3'-end of the BOs is not mandatory for high efficient assemblies and is contrary to the literature [16].
To conclude, a new toy-model plasmid was developed and utilized to investigate new improved protocols for the LCR assembly whereby the protocol without DMSO/betaine is the recommended one. This protocol was validated by the assembly of three plasmids and two different splits each. To ensure a robust assembly, a step-by-step protocol is offered on page 131. Furthermore, a software plugin was developed to design BOs with the optimal T_m (www.gitlab.com/kabischlab.de/lcr-publication-synthetic-biology). This plugin is described in more details in subsection 3.4.2. Further, more results of the *in vivo* optimizations are described in a guide for robust LCR assemblies in section 3.2.
A bottleneck of the presented *in vivo* screening system is the transformation of *E. coli*. Although it offers a fast readout method, this approach is accompanied by a high workload due to the generation of competent cells, plating and colony counting. To accelerate this, flow cytometry can be applied to omit the need of plating and counting. Another approach is to utilize cell-free systems [96] to screen for assemblies and misassemblies and to allow more insights in the LCR. This *in vitro* method was developed and applied for LCRs and is described in section 3.3. Prior to this, general guidelines for LCR assemblies are described and discussed in the next section.

3.2 Guidelines for robust *in vivo* LCR assemblies

To enable a robust LCR assembly it is mandatory to support the experimenter in the laboratory. Within this thesis, several bottlenecks and influencing parameters were obtained which can tremendously influence the success of an LCR assembly. As a summary, the following guidelines are helping the experimenter in achieving highly efficient LCR assemblies. These guidelines are based on information given in the literature or data of this thesis. For more detailed insights it is recommended to read the publications of Pachuk *et al.* [74], de Kok *et al.* [16], Chandran *et al.* [11], Robinson *et al.* [81] and the results presented in section 3.1. For the following LCR assemblies, the three part split of the toy-model plasmid was utilized (shown in Figure 3.1B).

3.2.1 Primer design, phosphorylation and ordering

Influence of amplification primers

Although it is not mentioned in the literature as an issue for LCRs, the carry-over of amplification primers can theoretically cause misassemblies: usually, PCRs are not primer-limited reactions and residual primers are remaining in the reaction mixture after the amplification. Depending on the purification method for these PCR products, the residual primers can be leftover in

the purified DNA part. Due to this, primers are transferred in low concentrations to the LCR where they can hybridize with the BOs. If so, the ligase will join the hybridized primers to the DNA-parts. This was hypothesized in subsection 2.2.15 (page 24) after the investigation of LCR misassemblies: residual bases at the 5'- and 3'-ends of missing subparts in a seven parted assembly were still existent and in a scale of 10 to 100 bp. In the first steps of the LCR, the ligation of a primer to a DNA part is only possible for reverse amplification primers due to the forward design of BOs. In the next cycles, also the forward amplification primers can be ligated. Finally, dead ends are build in the LCR which results in no fully assembled construct in the LCR. Those misassembled DNA chains are probably ligated by an unspecific blunt-end activity of the utilized ligase or by *E. coli* after the transformation and result in colonies with incomplete plasmids. Although the carry-over of primers from the utilized DNA part purification was not quantified, a proof-of-principle was performed to validate the negative impact of residual amplification primers in the LCR. The artificial addition of one reverse primer

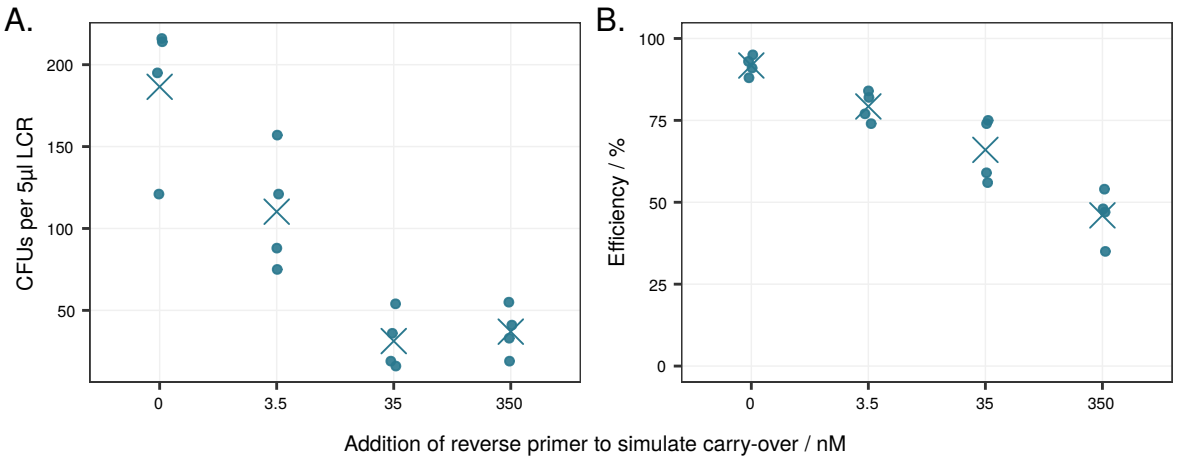

Figure 3.10: A three parted LCR of the toy-model plasmid was prepared (plasmid shown in Figure 3.1B). Different concentrations of the reverse amplification primer for *mRFP1* were added to the LCR mix right before the cycling. For this, a volume of *A. dest.* to fill up the total volume of an LCR mix was substituted by the primer to simulate a primer carry-over of 0, 3.5, 35 and 350 nM. Primers were solved in *A. dest.*. The '×' symbolizes the mean. CFUs: colony forming units, *mRFP1*: monomeric red fluorescent protein 1.

to the LCR assembly of a three parted plasmid can highly decrease the LCR assembly efficiency (Figure 3.10). For example, the impact of the lowest primer concentration of 3.5 nM (carry-over of 0.7 % if a primer concentration of 500 nM is used for a PCR reaction) decreased the amount of CFUs from 180 to 120 and the efficiency from 90 % to 80 %. An impact of the forward primer was not observed (Figure 3.11) and is probably related to the forward design of the BOs. Only the reverse primer hybridizes with the BO. This complex is build during the LCR by the thermal cycling followed by the participation in the ligation process. The primer of the BO-and-primer complex can directly be ligated in the first ligation cycles and this results in dead ends in early stages of the LCR. The proof-of-principle investigation shown in Figure 3.11 simulates the existence of only one reverse primer in a three parted LCR. Presumed that the

reverse primer of each PCR part is carried-over in an LCR, a high negative influence on the assembly results is expected. According to this, the existence of amplification primers in LCRs is a plausible reason for misassemblies and also one factor for decreasing efficiencies of assemblies with an increasing number of parts.
Several approaches are dealing with the avoidance of the carry-over of amplification primers in subsequent steps and are mainly achieved by gel excision or a digestion step after the PCR [27, 62, 119]. For the enzymatic digestion, the exonuclease I [60] and VII [12] are utilized to digest primers after the PCR. Although the digestion of residual amplification primers can decrease the carry-over, this is not straight-forwarded for the every-day use due to additional experimental steps and higher costs. The more rational way to reduce possible effects of residual amplification primers in the LCR mix is to optimize the grade of the PCR product by a gel extraction. Another approach is to design amplification primers with a relative low melting temperature in comparison to the melting temperature of the BOs. This supports the primer separation from the template in the LCR and though reduces unwanted hybridizations and ligations. The difference of the melting temperatures of the primers and BOs has to be as high as possible. For this, the melting temperature of the primers should be at 55 °C or less and the melting temperature of each BO-half at 68 °C for LCR conditions presented in section 3.1 to ensure high efficient PCRs and LCRs. Nevertheless, it is not proven to be a realistic issue in the LCR due to the fact, that the carry-over was not quantified so far. To utilize labeled primers and separate them from the PCR mix after the amplification allow an investigation of this issue and to probably highlight this bottleneck as one major limitation for high efficient LCRs.

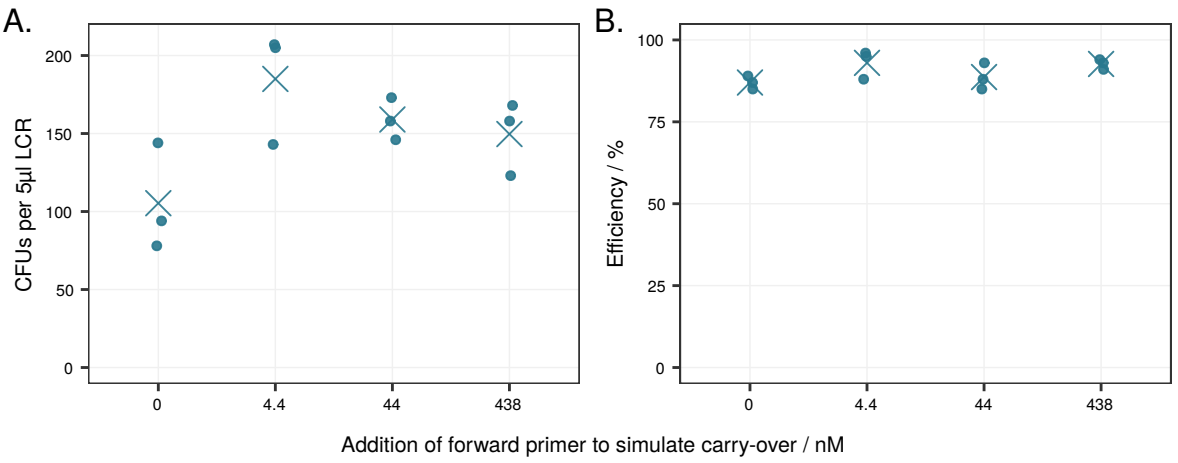

Figure 3.11: A three parted LCR of the toy-model plasmid was prepared (plasmid shown in Figure 3.1B). Different concentrations of the forward amplification primer for *mRFP1* was added to the LCR mix. For this, a volume of *A. dest.* to fill up the total volume of an LCR mix was substituted by the primer to simulate a primer carry-over of 0, 4.4, 44 and 438 nM. The '×' symbolizes the mean. CFUs: colony forming units, *mRFP1*: monomeric red fluorescent protein 1.

5'-phosphorylations of the DNA parts

5'-phosphorylated ends of the DNA parts are mandatory for the ligation of the utilized prokaryotic ligase [20, 71]. For linear constructs it is not necessary to use phosporylated primers for the 'left' 5'-end of the first DNA part and the 'right' 5'-end of the last DNA part. All other parts need phosphorylations on both 5'-ends. In general, the phosphorylation can be achieved by an enzymatic modification prior to the LCR and is the recommended approach. For this, the T4-polynucleotide kinase (T4-PNK) is the common way to add a 5'-phosphate-group to the DNA parts and is described in detail in the LCR protocol on page 131. Although it is possible to perform the modification with the dsDNA parts itself [11], it is recommended to phosphorylate the primers and to subsequently perform the PCR amplification. The phosphorylation efficiency is higher for short and single-stranded DNA in comparison to long and double-stranded DNA [108]. Additionally, low concentrations of primers in the phosphorylation reaction and freshly prepared ATP are increasing the yield of phosphorylated oligonucleotides. It is possible to phosphorylate a primer pair for one PCR product in one reaction for 1 h at 37 °C plus 20 min denaturation at 65 °C using a final concentration of 1 µM primer and 2 mM ATP. Before adding the ATP and the enzyme, it is beneficial to heat up the phosphorylation mix for 5 min at 70 °C and to cool it down on ice for at least 1 min to ensure a high percentage of unfolded primers.
An alternative route to get 5'-phosphorylated ends is to order modified primers or modified synthetic genes. This is useful, and also recommended, if the same DNA part is utilized multiple times (e.g., backbones, selection markers and reporter genes) or constructs build by a high number of parts. Although the assembly of enzymatically phosphorylated DNA parts routinely results in the desired construct, a high positive impact of the utilization of synthetically 5'-modified primers was investigated in comparison to enzymatically modified oligonucleotides (Figure 3.12). Nevertheless, the synthetic modification tremendously increases the costs for one DNA part and this has to be taken into account for LCR assemblies. Interestingly, the utilization of unphosphorylated 5'-primers resulted in similar efficiencies in comparison to the T4-PNK modified primers (Figure 3.12). This is probably related to the ability of *E. coli* to phosphorylate and ligate the unphosphorylated DNA parts by endogenous mechanisms during the transformation process and have to be further investigated by transferring these results to additional assemblies of other constructs.
Amplification primers and BOs are normally ordered from commercial suppliers. They are offering different types of purification grades and also offer special 'cloning'-primers with a higher purity. To order the oligonulceotides in a high purity is not assumed to be necessary for the LCR assembly. Nowadays, the synthesis of oligonucleotides is a standard process with low error rates. A 'low' purification grade of primers and BOs are sufficient for assemblies. This grade is also sufficient for primers with overhangs. To solve them in *A. dest.* is preferred over using TRIS-EDTA-buffer due to the $MgCl_2$-dependent ligation in the LCR [98]. Afterwards the storage at ≤ -20 °C is recommended. To accelerate the overall assembly process it is

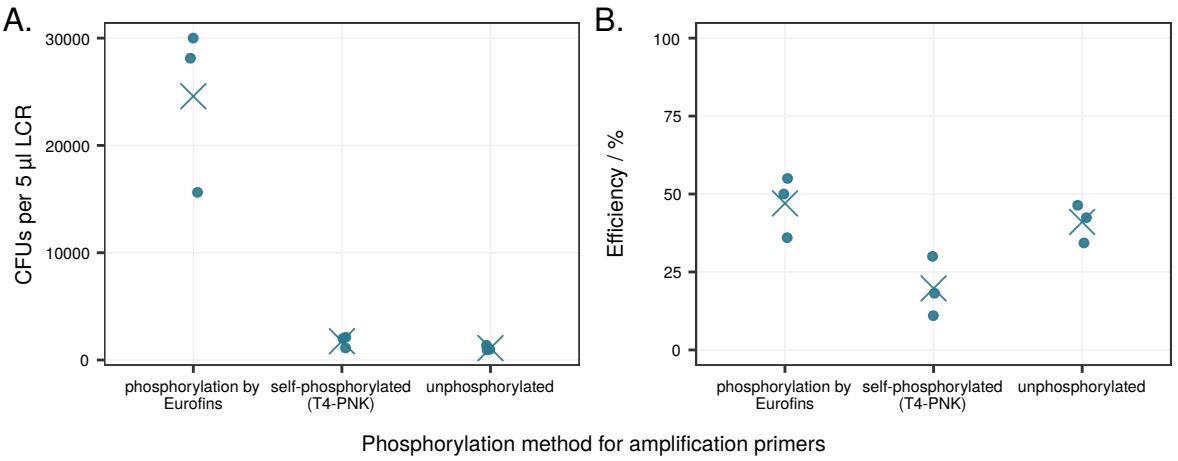

Figure 3.12: The amplification primers for the DNA parts of a three parted LCR were 5'-phosphorylated by the supplier Eurofins and compared to the enzymatically modified ones (T4-PNK). The latter modification method result in **A.** tremendous lower amount of total CFUs and a **B.** lower efficiency. Interestingly, unphosphorylated DNA parts were also assembled to the correct plasmid. The '×' symbolizes the mean. CFUs: colony forming units, T4-PNK: T4-polynucleotide kinase.

convenient to first order the amplification primers and afterwards the BOs. The BOs are much longer in comparison to the amplification primers (ca. 45-70 bases vs. 15-20 bases). The synthesis for longer oligonucleotides is more complex [70] and though the time of delivery of all oligonucleotides depends on the success of the BOs synthesis. For the LCR assemblies in this thesis the time during ordering and arrival of the BOs sometimes took weeks. To split the order allowed the PCR amplification in the meanwhile. Amplification primers are normally delivered within 2-3 days. To first order the shorter primers allows the experimenter to amplify the DNA parts while the oligonucleotide supplier produces the BOs. This approach probably saves time for the assembly but is accompanied by additional delivery costs and burden for the environment.

3.2.2 Bridging oligos

Some general advises has to be considered if other design rules than the improved conditions presented in section 3.1 are utilized. The BOs have the purpose to determine the order of the LCR assembly and are designed to build stable duplexes with the unwound ends of the DNA parts. To facilitate this, the interaction of the thermodynamic properties of the BOs, the experimental temperatures and the duration of the LCR cycling steps (denaturation, annealing and ligation) have to be adjusted if the bridging oligos are designed with custom parameters. These interdependencies were already described in section 3.1 and are further discussed in the following paragraphs.

Design rules for bridging oligos

The melting temperatures of DNA differ if DMSO and betaine are used. As shown in section 3.1 it is not recommended to utilize DMSO or betaine in the LCR. For these LCRs, the annealing temperature has to be increased to 66 °C in comparison to the baseline condition of 55 °C published by de Kok *et al.* [16]. Furthermore, it is recommended to adjust a target T_m of 68 °C for the design of each BO-half for LCRs without 8 % v/v DMSO and 0.45 M betaine. For this it is also necessary to use a thermostable ligase with a temperature optimum around 70 °C. Betaine and DMSO are decreasing the melting temperature of the BOs by accelerated strand separation [65, 112]. If both are omitted, more energy is needed to unfold them and afterwards they are able to build more stable duplexes with the DNA parts at higher temperatures. An increase of the annealing temperature to 66 °C is beneficial (Figure 3.6). Additionally, the higher temperature is closer to the optimum of the utilized Ampligase®[1]. In contrast, to modify the annealing temperature is not relevant for LCRs with DMSO and betaine. A higher annealing temperature would lead to less BO/DNA-part hybridizations and less template for the ligase.
As already mentioned, the target T_m for the BO design mainly depends on the utilization of DMSO, betaine, the thermal conditions and the T_m-calculation formula. The omission of DMSO and betaine results in the highest LCR efficiencies (Figure 3.9). Nevertheless, it was also showed that higher melting temperatures are beneficial for LCRs with DMSO and betaine (Figures 3.8, 6.17 and 6.18). Based on the utilized T_m-calculation formula, the target T_m for each BO-half has to be adjusted. It is recommended to utilize one of the following parameter sets for an LCR without or with DMSO/betaine. For both designs, and if adjustable for the applied software tool, the salt concentrations (monovalent: 50 mM, divalent: 10 mM), BO-concentration (30 nM and DNA part concentration (3 nM) have to be set according to the utilized conditions. The decreased concentration of the backbone (0.3 nM) is not considered for the calculations.

Without 8 % v/v DMSO and 0.45 M betaine:

1. T_m-calculation + salt correction of SantaLucia [89] $\approx$ 68 °C
2. T_m-calculation of SantaLucia [89] + salt correction of Owczarzy [72] $\approx$ 65 °C

With 8 % v/v DMSO and 0.45 M betaine:

1. T_m-calculation + salt correction of SantaLucia [89] $\approx$ 75 °C
2. T_m-calculation of SantaLucia [89] + salt correction of Owczarzy [72] $\approx$ 72 °C

As a critical criterion, the choice of thermodynamic formulas for the T_m-calculation of a BO is also influencing the assembly efficiency. Depending on the formula, for example the nearest-neighbour method from SantaLucia [89], BOs can be designed with a T_m of 68 °C for each half. If another formula is used with the same parameters and to recalculate the T_m of the previous designed BO-half, the T_m differs by a few degrees. This is demonstrated in Figure 3.4.

[1] http://www.epibio.com/docs/default-source/forum-archive/forum-03-1—nucleic-acid-ligation.pdf?sfvrsn=6

Depending on the experimental settings of the LCR, too high or low melting temperatures of the BOs will have a negative impact on the assembly. Nevertheless, it is possible to use all formulas for the design of BOs but the target T_m has to be specified for each calculation system. To simplify this, the sequence of an already designed BO-half with a target T_m of 68 °C can be utilized. First, to calculate the T_m sequence [1] by using any thermodynamic formula with adjusted salt and DNA concentrations results in a specific value. This value is the target T_m in the utilized system for a BO-half in LCRs without DMSO and betaine.
According to the literature, the BOs should have at least one G or C at the 3'-end [11, 16]. In the LCR investigations in section 3.1, no correlation of using BOs with or without a G or C at the 3'-end was observed (Figures 6.7, 6.8, 6.9 and 6.10). Thirteen BO sets were designed for the assembly of a seven part plasmid (plasmid shown in Figure 3.1B). Each set consisted of seven BOs with the minimum of zero G/C-3'-ends and the maximum of six G/C-3'-ends. A guanosine or cytosine at the 5'-end is also not necessary.

Impact of bridging oligo storage and age

The multiple usage of BOs for several assemblies is one benefit of the LCR. Further, to prepare mastermixes with all necessary BOs for the multiple assembly of the same construct is possible. This mastermix can be reused multiple times with multiple freeze-thaw cycles in between and was the standard approach for the LCRs shown here. Mastermixes of BOs are also mentioned as advantageous for high throughput approaches in the literature [81]. To prepare aliquots of BOs or mastermixes and to store them at −20 °C is recommended due to a negative impact of freeze-thaw cycles of oligonucleotides [15, 81]. The influence of the repeated freeze-thaw cycles can be estimated in Figure 3.13. For the assembly of a three parted LCR different production batches with the same production scale of 0.05 µM and a salt-free purification were utilized. The BOs of production batch 1 was freeze-thawed multiple times within 26 months. In contrast, the production batch 2 was utilized a few times. Although the freeze-thaw cycles of both BO batches were not counted, the utilization of the 26 months old batch resulted in less CFUs and is probably related to the additional freeze-thaw cycles. It is also plausible that the purity of the batches is different due to an improved purification method by the manufacturer Eurofins. Further investigations have to be performed to validate the effects of the BO age and freeze-thaw cycles. Nevertheless, the results of this initial experiment are supporting the hypothesis given by the literature that freeze-thaw cycles of BOs have a negative impact on LCR assemblies. Interestingly, the LCRs without BOs resulted in colonies and supports the hypothesis of an unspecific blunt-end activity of the ligase and/or the ligation by *E. coli*. A discrimination is not possible due to the no separate investigation. The transformation of *E. coli* is always the final step of this LCR approach.

[1] Bridging oligo half for the calibration (68 °C with the T_m calculation and salt correction of SantaLucia [89]): TCCTCCCTGCAAGACGGTG

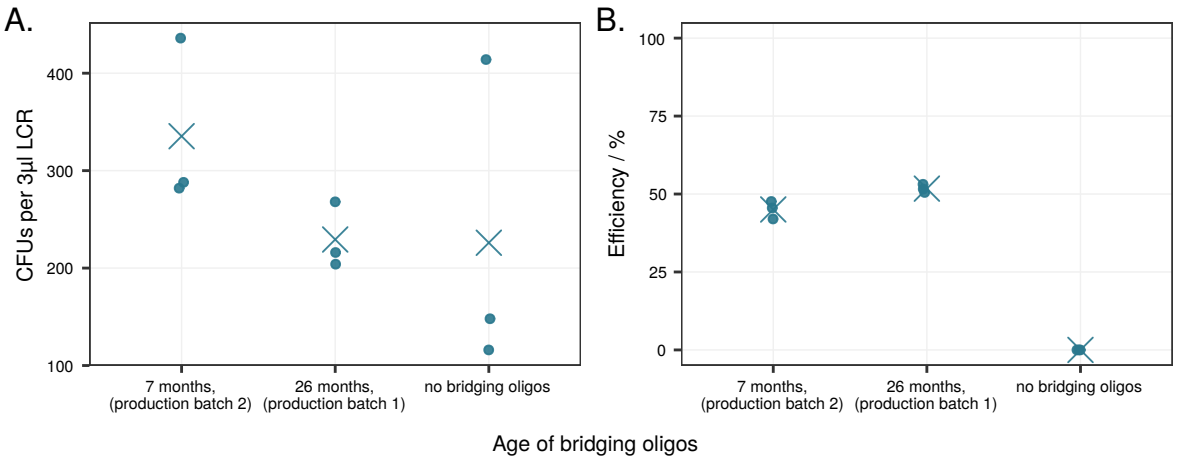

Figure 3.13: Two batches of different bridging oligo ages were used for the assembly of a three part split of a plasmid (Figure 3.1B) to investigate the influence of storage and different production batches. The bridging oligos were ordered from the same manufacturer in the same scale (0.05 µM) and purification grade (salt-free), were solved in *A. dest.* and stored at −20 °C. The production batch 1 was applied for more LCRs in comparison to the production batch 2. The latter oligonucleotides were frozen and thawed less times. Assemblies without bridging oligos resulted in CFUs and is probably related to the capability of *E. coli* to ligate DNA. For the LCRs, 3 µL LCR were transformed in 30 µL chemically competent *E. coli* cells. The '×' symbolizes the mean. CFUs: colony forming units.

3.2.3 DNA parts

In general, the design of cloning methods, respectively DNA assemblies, is a complex and complicated process. Sequence-related problems like homologous regions or palindromic repeats can hamper the assembly and even the previous steps like PCR amplifications or gene synthesis have to be considered as bottlenecks. There are free-available webtools with the focus on these issues and are not the scope of this thesis. Nevertheless, the following guideline helps the experimenter to circumvent usual problems in the wet-lab.

PCR amplification is a critical step in the LCR assembly

There are two approaches to generate the DNA parts for the LCR assembly: 1) the PCR amplification and 2) to order synthetic genes. For the PCR amplification, to utilize a high-fidelity polymerase has to be the standard due to low polymerase-related mutations of the products. Additionally, it is important to use a polymerase which does not add overhangs. Overhangs or chewed-back ends of PCR products cannot be ligated in the LCR due to its sensitivity to additional based or gaps at the nick of the ligation site [97]. The impact of this is higher for assemblies with an increasing number of parts. For example, if two fragments with 5 % overhangs each have to be assembled, the probability that two PCR products without overhangs are in proximity for a ligation event is 90 %. If six fragments with 5 % overhangs should be assembled, the probability is highly decreased: the chances that DNA parts without overhangs

are present for a full assembly is only 74 %. This error rate can be further increased by other DNA species which are able to hybridize with the BOs. This includes unspecific PCR products, PCR templates, PCR amplification primers and DNA debris from shearing.
For PCR purifications using no gel extraction it is highly recommended to perform a DpnI-restriction digestion (or other appropriate digestion) directly after each PCR with a methylated PCR template. This is not possible if a Dam-methylase deficient strain was used for plasmid propagation [67, 79]. If possible, to split the resistance marker gene or/and the ORI is recommended to avoid a carry-over of PCR template into the LCR. If the PCR products were purified by gel extraction, a digestion is not mandatory as long as the size of the PCR template is not similar to the specific product. Otherwise, a digestion have to be performed prior to the excision. To elute the DNA parts, TRIS-EDTA buffer of the commercial kits is necessary to ensure stable storage conditions and to prevent a digestion by nucleases [22]. For short-time usage or if they are aliquoted, the usage of TRIS-buffer without EDTA or *A. dest.* only is recommended. The ligase utilizes Mg^{2+}-ions for the ligation [98] and these divalent cations can be complexed by EDTA. This probably hampers the efficiency of the LCR.
For highly efficient assemblies, all DNA parts have to be added to the LCR mix in the same ratio. In order to achieve this, the precise measurement of the eluted DNA part concentration is important. Standard quantification by using spectrophotometric measurements based on absorbance is sufficient as long as no unspecific PCR products are present. This can be ensured by gel excision. To get more accurate concentrations, it is recommended to apply other methods like spectrofluorometry, quantitative PCR or capillar electrophoresis to measure the specific PCR product only. After the purification, aliquotation of the DNA parts is necessary to prevent a loss of function by repetitive freezing and thawing. Repeated freeze-thaw cycles of DNA parts [86, 93] and BOs [81] are negatively influencing the LCR efficiency and should be avoided.
In case of using *de novo* sequences for an assembly, gene synthesis is necessary. If the synthetic DNA parts should directly be used for the LCR, the sequences have to be ordered with 5'-phosphorylated ends. Enzymatic phosphorylation of double stranded DNA is less efficient and for this it is necessary to adjust the phosphorylation protocol described for ssDNA (protocol on page 131). Altough it was not investigated, a thermal denaturation for 5 min at 95 °C and cool-down in ice is recommended for DNA parts prior to the phosphorylation. Afterwards, to perform the phosphorylation for 1 h followed by the subsequent denaturation step should result in DNA parts with a high grade of phosphorylated ends. If unphosphorylated synthetic parts are used as template for a PCR, 5'-phosphorylated primers has to be utilized for the amplification.

3.2.4 Ligase cycling reaction

The LCR can be utilized for linear and circular assemblies. Nevertheless, to directly use an LCR for genetic engineering approaches is not recommended due to unspecific side products. Nevertheless, the LCR can be utilized as template for PCRs to generate the desired product.

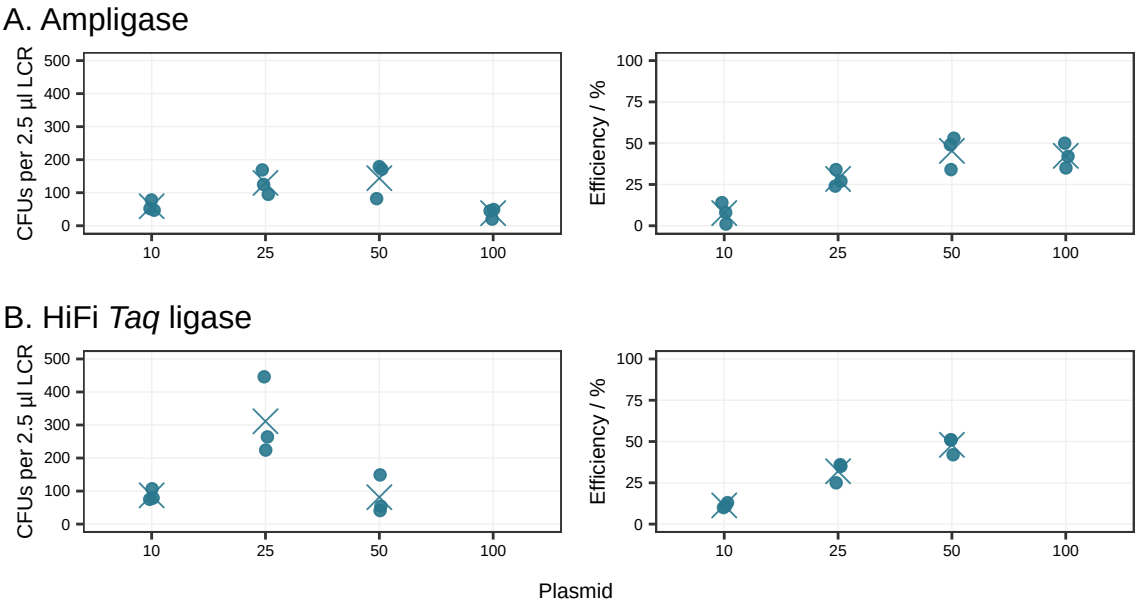

Figure 3.14: A three parted plasmid (Figure 3.1B) was assembled by the LCR in 10, 25, 50 and 100 cycles. For the HiFi *Taq* ligase, 100 cycles resulted in a total loss of volume due to the overall experimental duration of ca. 4 h although low-profile 96-PCR tubes were utilized. **A.** The standard ligase of this thesis 'Ampligase®' was utilized. **B.** To compare the influence of another thermostable ligase, the HiFi *Taq* ligase of NEB was utilized. After 100 cycles, the total volume of the LCR evaporated. The '×' symbolizes the mean. CFUs: colony forming units.

Afterwards, a purification by gel excision is recommended. As a general protocol for the LCR, the purified DNA parts are mixed with the buffer, BOs and NAD^+ as showed in the following list:

- 30 nM of each BO
- 3 nM of each DNA insert
- 0.3 nM of the backbone[1]
- 1× Ampligase® ligase buffer
- 0.5 mM NAD^+
- 0.3 U μL^{-1} U of Ampligase®
- fill up to 25 µL with *A. dest.*

The preparation of the LCR is based on standard handling for molecular *in vitro* reactions in the wet-lab. To thaw the DNA parts, BOs/BO master-mix, supplements and buffer following by mixing and spinning them down before the transfer to the LCR reaction is necessary to ensure homogeneous solutions by resolving precipitates. The LCR mix has to be prepared on ice and the ligase is added last. After mixing and spinning down the mix the thermal cycling is started. Afterwards, the direct transformation of the LCR into the host or a PCR with the LCR

[1] A 10× reduction of the vector concentration to 0.3 nM results in more correct colonies and higher efficiencies.

as a template is recommended. It is possible to freeze the LCR at −20 °C but it has to be mixed after thawing. To prepare the LCR mix and freeze it for a future cycling is not recommended. To utilize the LCR as a template for PCRs to amplify linear products is an appropriate route to generate linear copies for the genetic modification of microbial hosts or subcloning. The utilization of 1 µL of a 1:10 to 1:100 diluted LCR resulted in the expected PCR products. Mostly this LCR-PCR method results in several unspecific PCR products due the existence of intermediate products in the LCR-mix where the amplification primers can hybridize. Additionally, there is also a carry-over of the BOs because they are not incorporated during the LCR assembly. They will serve as forward-primers in the PCR. To perform a digestion with exonucleases I or VII before the PCR is helpful to reduce the effects of the BOs. Nevertheless, to transfer the PCR on a gel and perform an excision is highly recommended for the LCR-PCR approach.

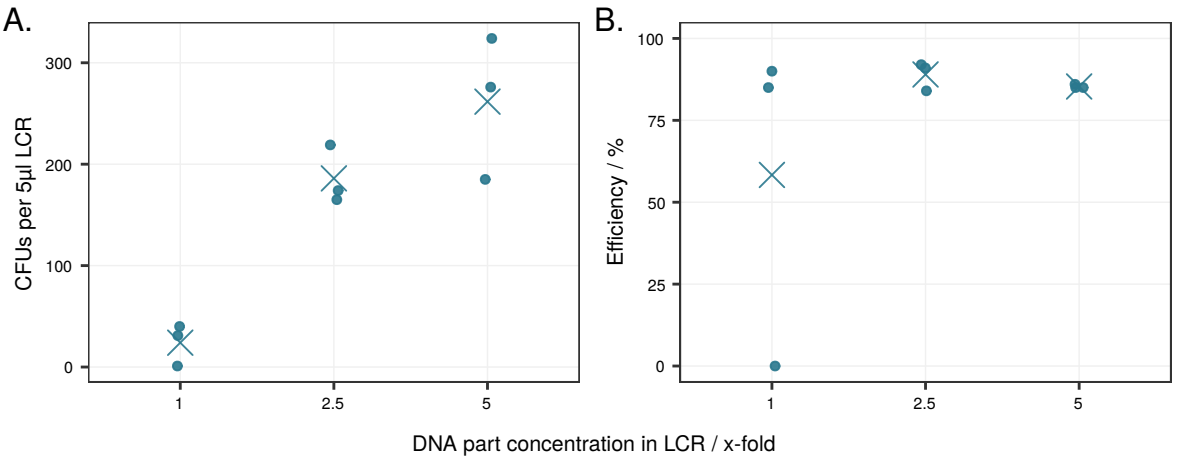

Figure 3.15: A two parted plasmid was assembled by the LCR. The DNA concentration of the DNA inserts and the plasmid backbone were increased and compared to the baseline concentration of 3 nM DNA inserts and 0.3 nM backbone (condition '1'). The '×' symbolizes the mean. CFUs: colony forming units.

Higher concentrations of DNA parts and higher transformation volumes are beneficial for LCR assemblies

The LCR enables high efficient DNA assemblies with low amount of DNA parts (3 nM in a standard reaction). Nevertheless, an increase of the DNA part concentration can improve the assembly. To demonstrate this, 2.5× and 5× higher concentrations of DNA parts (inserts and plasmid backbone) were used for an assembly of a two and three part split of the same plasmid. The concentration of the BOs was not varied. As shown in Figures 3.15 and 3.16, the increased DNA part concentrations yielded in more colonies but similar LCR efficiencies. Additionally, a heat-shock duration of 30 s is considered as sufficient for the chemical transformation (Figure 3.18). To transform 2.5 to 5 µL in 25 to 50 µL electro- or chemically competent cells normally results in colonies. The effects of transforming different volumes of LCR in 50 µL

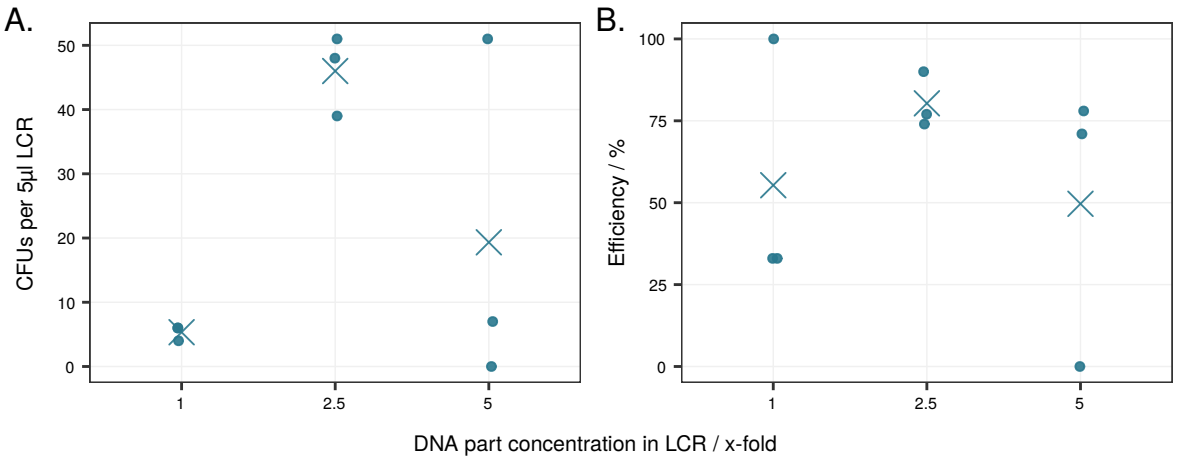

Figure 3.16: A three parted plasmid (Figure 3.1B) was assembled by the LCR without DMSO and betaine. The DNA concentration of the DNA inserts and the plasmid backbone were increased and compared to the baseline concentration of 3 nM DNA inserts and 0.3 nM backbone (condition '1'). The '×' symbolizes the mean. CFUs: colony forming units.

chemically competent cells are presented in Figure 3.17. The amount of colonies increased with an increasing transformation volume and was already described for transformations of *E. coli* [54]. A decrease of the number of CFUs were observed for volumes ≥6 µL. This is probably related to the increased of DMSO and betaine in transformation mix. In section 3.1 it was demonstrated that the transformation of 3 µL of an LCR with 8 % v/vDMSO/0.45 M betaine in 30 µL electrocompetent cells is decreasing the amount of colonies (Figure 6.11). Although this was not an issue for chemically transformations of the same volumes (Figure 6.14), DMSO and betaine probably negatively influences chemical transformations at higher concentrations. In general, the limiting effects for electroporations and chemical transformations can be circumvented by performing the dialysis of the LCR or to utilize at least a 10:1 ration of cells and LCR for chemical transformations. To perform a dialysis directly before the transformation by using a nitrocellulose membrane and *A. dest.* yields more colonies (not shown).

Storage of the Ampligase®, the 10× reaction buffer and 10 mM NAD^+

Two enable a robust usage of the LCR, the effects of two Ampligase® production batches (Lucigen, Wisconsin, USA) with different ages were investigated. After arrival, the ligase was aliquoted and stored at −20 °C. As shown in Figure 3.19, no impact of the batches was observed by comparing the assembly results of a three part split of the toy-model plasmid (plasmid shown in Figure 3.1B). Additionally, the influence of self-made Ampligase® buffer was investigated. According to the results shown in Figure 3.20, the utilized 10× buffer with 200 mM trihydroxyaminomethan (TRIS)-HCl (pH 8.3), 250 mM KCl and 0.1 % Triton® X-100 is stable at the storage conditions of 4 and −20 °C. Furthermore, the results of the two batches 'new' and '24 months' are similar. This suggests a robust production of a self-made buffer and

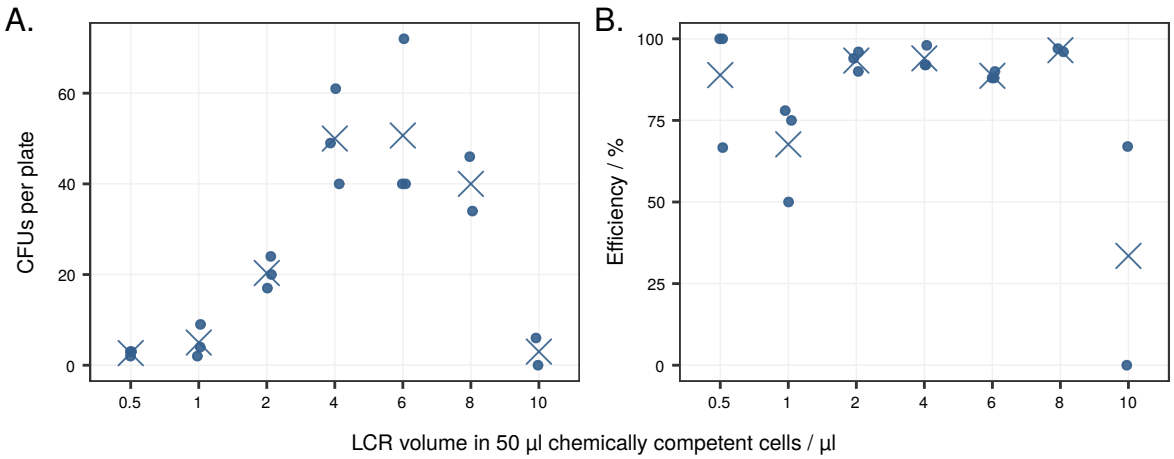

Figure 3.17: Different volumes of the same LCR with 8 % v/v DMSO and 0.45 M betaine were transformed in 50 µL chemically competent *E. coli* cells. A heat-shock of 30 s at 42 °C were applied for the transformation. The '×' symbolizes the mean. CFUs: colony forming units.

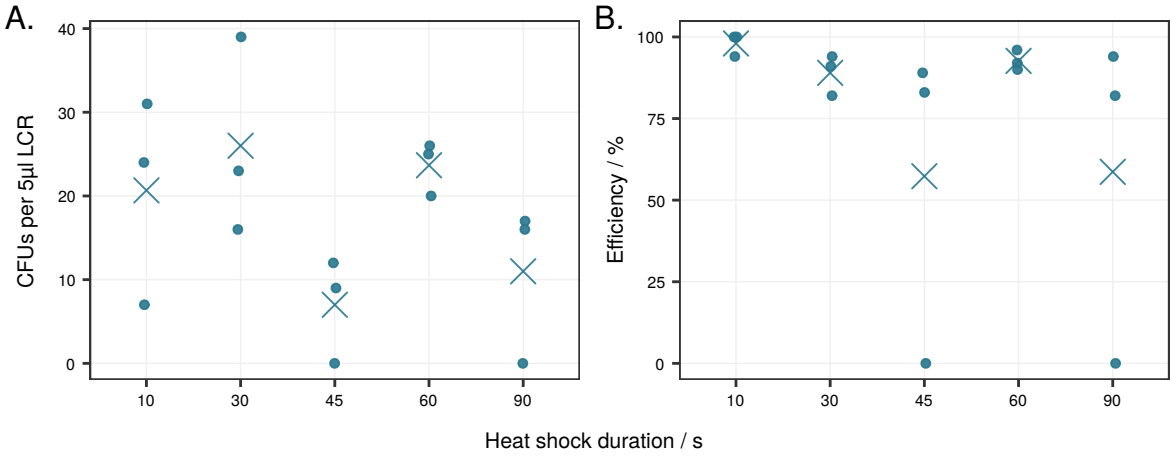

Figure 3.18: Heat-shock duration for chemical transformation. For each transformation, 5 µL LCR were transformed into 50 µL cells. The heat-shock was performed at 42 °C. The '×' symbolizes the mean. CFUs: colony forming units.

an unproblematic storage at ≤4 °C. The latter allows the continuous usage in a cooling position of a robotic platform as long the buffer is protected from evaporation.

For some ligases the NAD^+/ATP is already supplemented in the reaction buffer. NAD^+ is not stable for longtime and is sensitive to repeated freeze-thaw cycles, UV-light or heat [125]. To prepare a self-made buffer without the substrate based on the recipe of the ligase supplier is recommended for longterm usage. Both substrates should be freshly prepared or aliquoted and stored at −80 °C. The buffer without NAD^+/ATP can be aliquoted and stored for longtime at −20 °C or 4 °C (Figure 3.20). For the LCR reaction, the NAD^+/ATP is added separately to each LCR. To investigate the impact of the storage of NAD^+ for the ligase 'Ampligase®', several ages of 10 mM NAD^+ stock solutions were compared. The batches were prepared by solving NAD^+

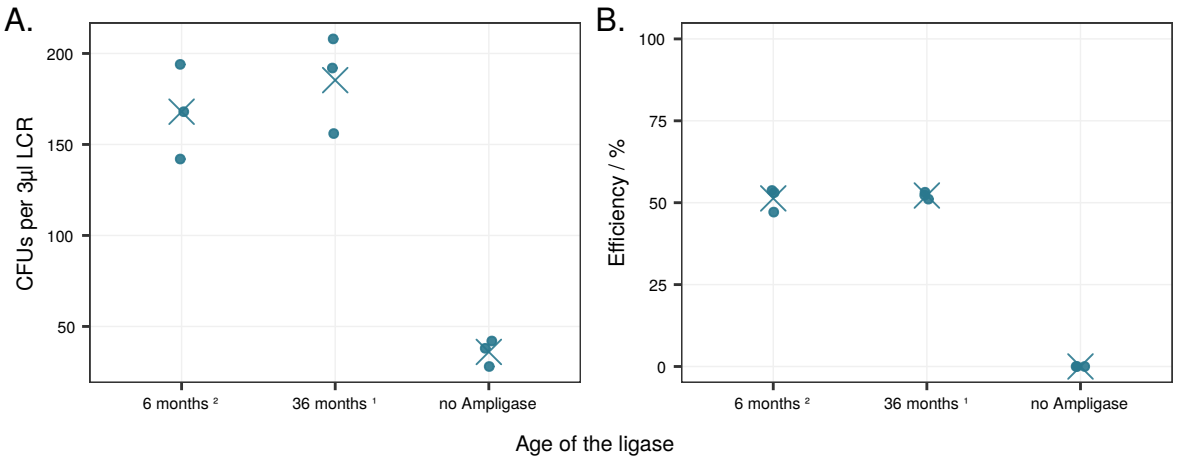

Figure 3.19: Two batches of different Ampligase® ages were used for the assembly of a three part split of a plasmid (Figure 3.1B) to investigate the influence of the storage at −20 °C and different production batches. For this, 3 µL LCR were transformed in 30 µL chemically competent *E. coli* cells. The Ampligase® was aliquoted after arrival and aliquoted before the storage at −20 °C. Fresh aliquots were used for the investigations. The '×' symbolizes the mean. [1]: Ampligase® production batch 1, [2]: Ampligase® production batch 2. CFUs: colony forming units.

in *A. dest.* by utilizing the same stock powder (stored at −20 °C) followed by aliquotation and storage at −20 °C. Aliquots from these batches were stored in the freezer and were thawed for the first time for an LCR assembly to obtain the stability. Interestingly, the impact of NAD^+ with an age $\leq$ 24 months does not have a clear influence on the LCR (Figure 3.21). A high impact of an age of 36 months and LCRs without the addition of NAD^+ was observed. The latter condition resulted in correct assembled plasmids and is probably related to residual NAD^+ in the purified Ampligase®. The reduced amount of colonies if the 36 months old NAD^+ is probably related to the fact, that the concentration of intact NAD^+ is lower in comparison to the NAD^+ in the purified enzyme. Nevertheless, a negative influence of a longterm storage of 10 mM NAD^+ at −20 °C was determined and have to be considered as a crucial bottleneck if a > 24 months old NAD^+ solution is used in LCRs.

To sum up, the success rate of LCR assemblies is influences by design rules and experimental settings. Mainly, the LCR is assumed as being most effective if the BOs and annealing temperature is nearby the optimum of the utilized ligase. In this thesis, the utilized ligase 'Ampligase®' has its highest activity around 70 °C and BOs with a similar value for each half resulted in the most efficient assemblies. To match the desired target T_m for a BO-half, the calculation algorithm have to be chosen carefully. Depending on the chosen formula, the sequence can differ significantly. Prior to the design, the chosen system have to be calibrated by utilizing a golden-standard BO-half. This sequence is known to be one of the best BO-halves for the described DMSO/betaine-free LCRs in this thesis with a T_m of 67.8 °C when the T_m calculation and salt correction of SantaLucia was applied [89]. If available in the utilized tool, the salt concentrations (monovalent: 50 mM, divalent: 10 mM), BO-concentration (30 nM) and DNA

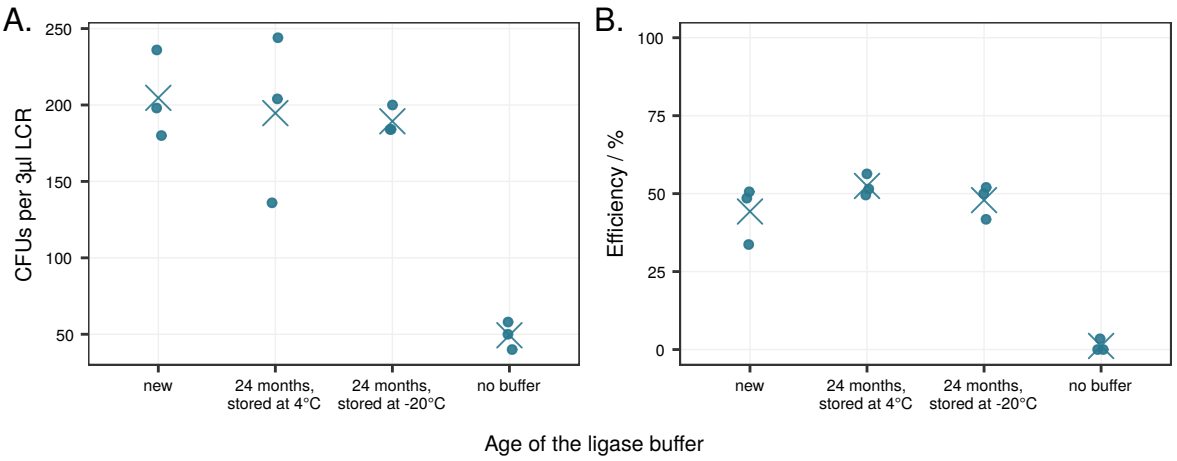

Figure 3.20: Two batches of different Ampligase® buffer ages were used for the assembly of a three part split of a plasmid (Figure 3.1B) to investigate the influence of storage at different temperatures and different production batches. The 24 months old buffers are derived from the same batch and were split for the storage in the fridge (4 °C) and freezer (−20 °C). For the LCRs, 3 µL LCR were transformed in 30 µL chemically competent *E. coli* cells. The buffers were prepared as 10× stocks according to the manufacturers instructions and included 200 mM TRIS-HCl (pH 8.3), 250 mM KCl and 0.1 % Triton® X-100. $MgCl_2$ was not included in the buffers but was added separately to the LCR mixes. Fresh aliquots of the buffers were used for the investigations. The '×' symbolizes the mean. CFUs: colony forming units.

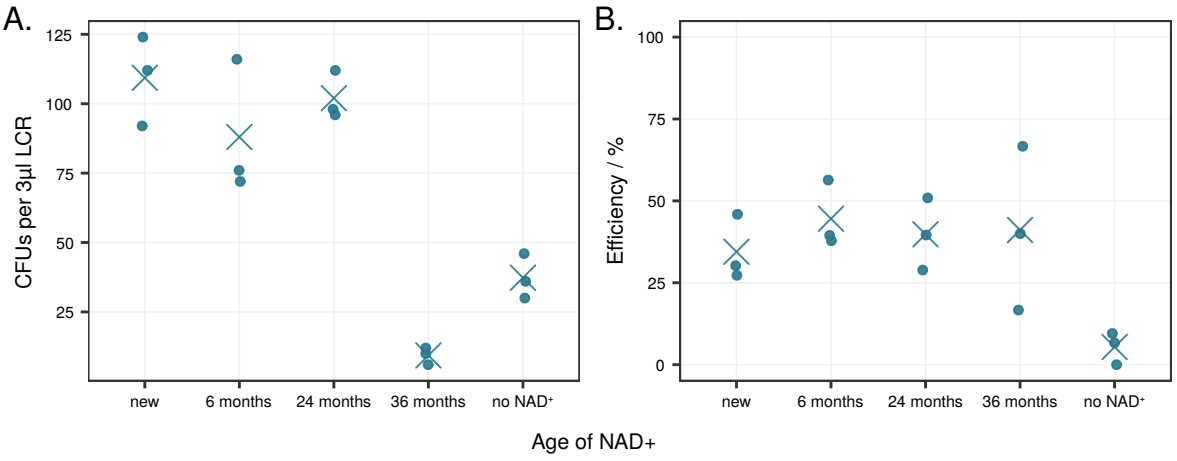

Figure 3.21: Four batches of 10 mM NAD^+ with different ages were compared by assembling a three part split of a plasmid (Figure 3.1B) to investigate the influence of the storage at −20 °C and different production batches. For this, 3 µL LCR were transformed in 30 µL chemically competent *E. coli* cells. Fresh aliquots of the different NAD^+ batches were used for the investigations. Each aliquot was derived from a separate production batch from the same NAD^+ stock (powder at −20 °C). The '×' symbolizes the mean. [1]: Ampligase® production batch, [2]: Ampligase® production batch 2. CFUs: colony forming units.

part concentration (3 nM) have to be set. The lowered concentration of the backbone (0.3 nM) is not considered for the calculations.
Unfortunately, the chosen workflow for the improved LCR protocol included the laborious utilization of transformations of *E. coli*, plating on agar plates and the colony screening by fluorescence microscopy. Additionally, the influence of *E. coli* in the assembly process and a hypothesized unspecific activity of the ligase are not distinguishable when this *in vivo* LCR screening is applied. To omit the transformation and the subsequent steps would tackle both drawbacks to further gain insights into this assembly method and to raise the rapid prototyping of genetic constructs to a next level. This can be achieved by substituting all *in vivo* steps of the current LCR workflow by utilizing a cell extract for a CFPS of the reporter genes.

3.3 *In vitro* LCR

The target-oriented and efficient implementation of synthetic genetic circuits into living organisms requires methods for the assembly of DNA. Of special importance are methods which enable a high throughput and are not prone to errors. As particularly promising, the LCR [11, 16] is a candidate to fulfill these prerequisites. Nevertheless, the LCR assembly still has a wide potential for optimization, especially with regard to yield, accuracy, speed and a larger number of DNA fragments. Unfortunately the DBTL cycle presented so far in this thesis is highly slowed down by the transformation of *E. coli*, the subsequent plating and colony screening. As a classical *in vivo* method, LCRs with varying parameters are transformed into *E. coli* followed by the determination of the assembly efficiency by fluorescence screening of the transformants (Figure 1.4 in chapter 1). This *in vivo* LCR readout is a limiting factor for high throughput approaches. Furthermore, no discrimination of *in vitro* and *in vivo* issues is possible due to the fact that the *in vitro* assembled DNA is processed by *E. coli*. To adress these limitations, an *in vitro* LCR method based on a TXTL system was developed. *In vitro* results are generated by combining the LCR, the rolling circle amplification (RCA) and CFPS by using a cell extract from *E. coli* [14, 106] (Figure 3.22). This method was developed with the support of the bachelor student Darius Zibulski (Entwicklung einer Zellextrakt-basierten *in vitro* Ligase-Cycling-Reaction. Bachelorarbeit, 2019, TU Darmstadt).

3.3.1 Cell free protein synthesis for rapid protoyping

To determine the effects of varying the parameters in the LCR assembly, an *in vitro* LCR method based on CFPS was developed by utilizing a cell extract of *E. coli*. This extract enables an *in vitro* transcription and translation of the assembled GOI followed by the fluorescence readout in 384-well PCR plates by a plate reader. By using the nanoliter dispenser I-DOT, a 384-well cycler and a 384-well PCR plate, the technically lowest LCR volume was experimentally determined. Less than 300 nL evaporated during the 25 LCR cycles if a foil made of aluminium was utilized

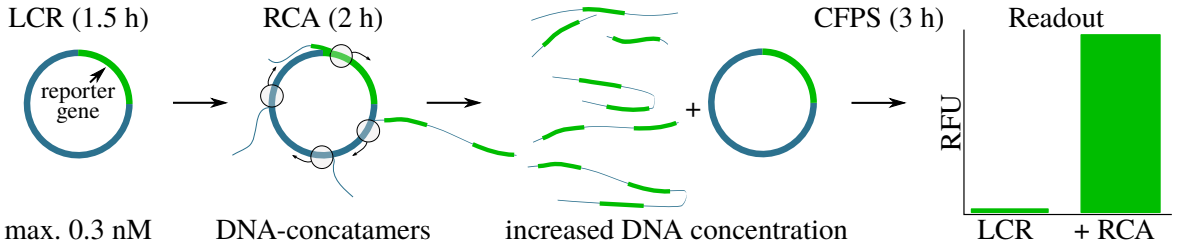

Figure 3.22: Workflow of the *in vitro* LCR. A circular construct is build by the LCR with a maximum DNA concentration of 0.3 nM. Afterwards the rolling circle amplification (RCA) is applied to randomly amplify the LCR product including the reporter gene. The increased DNA quantity enables the readout after a cell free protein synthesis via an *E. coli* cell extract for an *in vitro* transcription and translation (TXTL). h: hours, CFPS: cell free protein synthesis, RFU: relative fluorescence unit.

for sealing the 384-well PCR plate. Due to this, the lowest possible volume of one LCR are 300 nL. According to the manufacturer and literature, 5.7 µL of the RCA components (GenomiPhi™ V2 DNA Amplification Kit) and 20 µL of the *E. coli* extract are used for one *in vitro* LCR. To be more efficient, the reaction volume should be decreased to enable more CFPS reactions with the same batches of the RCA kit and self-made cell extract. To achieve this, several experimental setups were investigated to decrease the total volume with a high signal-to-noise ratio and are described in the following paragraphs. To set up the experimental workflow, 0.3 nL of a 0.3 nM plasmid with a known quantity was utilized. To use an LCR for those initial experiments would be inappropriate due to an unknown concentration of circular product. Afterwards this experimental setup has to be transferred to LCR assemblies. This is shown and discussed in section 3.3.4.

The CFPS is based on a cell extract and DNA or mRNA as template for the TXTL. The cell extract consists of the complete protein synthesis machinery and can be extracted from diverse prokaryotic and eukaryotic hosts [14]. By mixing the cell extract with nucleotides (e.g., adenosine triphosphate (ATP)), amico acids, tRNAs and coenzymes, the GOI can be transcribed and translated *in vitro* to the protein of interest in a scale of $\mu g\,\mu L^{-1}$ [14]. In comparison to the literature [106], the protocol for the production of the cell extract was shortened to one day with the help of Francois-Xavier Lehr from the AG Koeppl (step-to-step protocol in section 6.1.4). Additionally, for the sonification step two protocols were used to investigate if a higher input of energy increases the amount of cell extract (Supplementary Figure 6.20). The impact of 900 J attends to be less favorable. Because of this, the cell extract batch derived from the 700 J sonification step was used for all following *in vitro* LCRs. In general, to enable a readout by combining the LCR, RCA and CFPS seems to be plausible. As described in the literature, the maximal product concentration in the LCR (0.3 nM) is not sufficient to generate a signal in the CFPS [61, 106]. This was confirmed in an initial experiment (Figure 3.23). To increase the concentration in the LCR is possible but would lead to a higher consumption of DNA parts. To apply a dialysis step after the RCA improves the signal due to less salt perturbations during the CFPS (Figure 3.23) but this approach is not automation friendly and would limit the

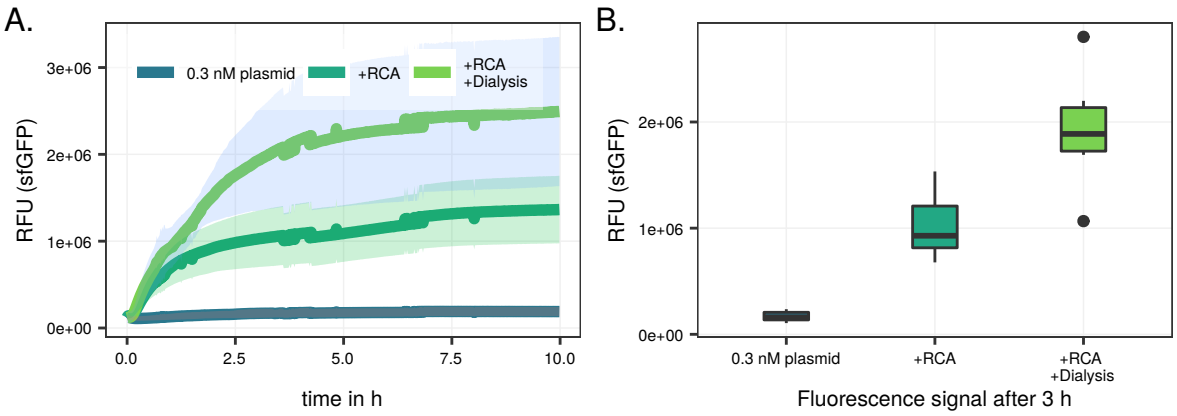

Figure 3.23: Kinetics and 3 h measurements with a plate reader of 0.3 nM plasmid p10024 (Supplementary Figure 6.19) and different experimental setups. **A.** Kinetics were determined by measuring the fluorescence signal of sfGFP every minute. The maximal product concentration in an LCR (0.3 nM), results in no significant signal in comparison to the negative control without plasmid (data of the control reaction not shown). By applying the RCA directly after the LCR, a signal was detectable. A dialysis step after the RCA for 20 min against *A. dest.* led to a 2× higher signal. The shading of the curves is representing the standard deviation. The fluorescence was measured every 60 s.**B.** The presented signals presenting the measurements after 3 h. All measurements were performed as sextuplicates (n=6). Control reactions without plasmid were negative and are not shown. RCA: rolling circle amplification, RFU: relative fluorescence unit, sfGFP: super folder green fluorescent protein.
This figure is plotted by using the raw data of the bachelor thesis of Darius Zibulski.

experimental throughput. To optimize the signal in the CFPS, the concentration of DNA has to be increased by an alternative way. For this, the RCA [17] was applied (Figure 3.22) by using the GenomiPhi™ V2 DNA Amplification Kit (GE Healthcare UK Limited, Buckinghamshire, UK). This kit consists of two buffers, the sample and reaction buffer, and the enzyme mix. Although the concentrations of salts, random oligonucleotide hexamers and enzyme concentration are unknown, this kit was applied for the signal amplification in the *in vitro* LCR method.

3.3.2 Signal amplification by the rolling circle amplification

Based on the RCA method, DNA can be amplified in high quantities by the phi29 polymerase. This polymerase was already applied for several molecular biology approaches [44, 48, 64, 78, 101], including cell free systems [56], and offers a possibility to increase the amount of template DNA for the LCR-CFPS method. The phi29 polymerase is highly processive and can amplify up to 70 kbp [87]. Additonally, and in comparison to other polymerases used for, *e.g.*, PCRs, this polymerase is able to convert dsDNA to ssDNA by strand displacement. The RCA takes advantage of both and enables an isothermal amplification of the LCR product at relative low temperatures (30 °C) (Figure 3.22). As shown in Figure 3.23, the utilization of the RCA increased the TXTL derived signal. A dialysis against *A. dest.* further doubles the signal but is not applicable for automation and will not be further considered in the investigations. For the

analysis of the following results, boxplots of the measurements after 3 h of the CFPS at 29 °C will be utilized as shown in Figure 3.23B. Furthermore, an optimal amplification time of 90 min was investigated and is the standard setting for the RCAs (Figure 3.25A).

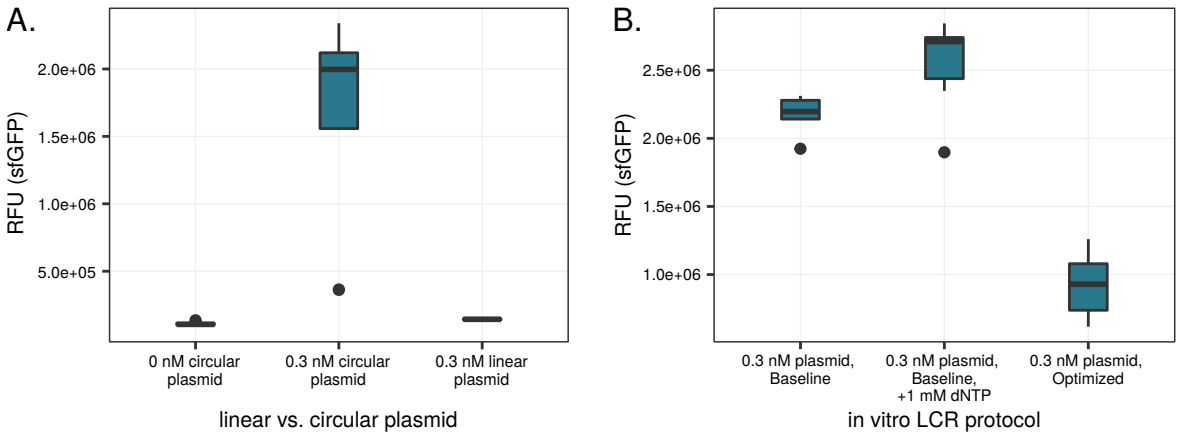

Figure 3.24: A. An *in vitro* LCR of a linear form of the plasmid p10024 with *sfGFP* does not result in a higher signal in comparison to the negative control without DNA ('0 nM circular plasmid'). For all, a total volume of 3.6 µL were used for the measurements in a plate reader. The presented signals presenting the measurements after 3 h. All measurements were performed as sextuplicates (n=6). As template for the RCA, 0.3 nM of the isolated plasmid p10024 or a linear PCR product was used. In the PCR product the *sfGFP* was split in the middle. **B.** The results of baseline protocol (according to the manufacturers) and the optimized *in vitro* LCR protocol. The signals represent the measurements after 3 h. All measurements were performed as sextuplicates (n=6). As template for the RCA 0.3 nM of the isolated plasmid p10024 was used. Control reactions without plasmid were negative and are not shown. RCA: rolling circle amplification, RFU: relative fluorescence unit, sfGFP: super folder green fluorescent protein.
This figure is plotted by using the raw data of the bachelor thesis of Darius Zibulski.

3.3.3 Defining the experimental setup

In several experiments the RCA and CFPS were altered to reduce the total volume of the final reaction. The main goal of the optimizations was related to design an experimental concept which allows an automated high throughput readout in 384-Well PCR plates with a low total volume to economize the volume of the expensive RCA kit and the self-made cell extract. As already discussed in section 3.3.1 the lowest volume for the LCR of 25 thermal cycles is technically limited to a volume of $\geq$300 nL. This volume automatically results in a total volume of 26 µL for one *in vitro* LCR reaction if the baseline protocol is utilized (Table 3.2). Although this generates to the highest signal, a trade-off between signal-to-noise ratio and the lowest reaction volume has to be found. Step-by-step the volume of the phi29 kit and cell extract were decreased. This resulted in a ca. 7$\times$ lower total volume and a 2.5$\times$ signal decrease (Figure 3.24B). A comparison between the baseline protocol, the protocol with recommended conditions by the manufacturers, and the optimized protocol for the automation approach is

shown in Table 3.2 and Figure 3.24B. Additionally, the data for all experimental modification steps are referenced in Table 3.2.

Table 3.2: Baseline and optimized protocol for the *in vitro* LCR. The LCR/plasmid was added to one well of a 384-well PCR plate and cycled for 25 cycles. Afterwards the RCA components were added to each well with the DNA and the plate was incubated for 90 min at 30 °C followed by the addition of the CFPS components into the same wells and an incubation for 3 h at 29 °C. The fluorescence measurements of both protocols are shown in Figure 3.24B. [1] in comparison to the volume used in the baseline protocol. [2] final concentration of dNTPs in the vitro LCR. CFPS: cell free protein synthesis, RCA: rolling circle amplification

	LCR protocol		
Factor	Baseline	Optimized (reduced volume)[1]	Corresponding data
0.3 nM LCR/DNA	0.30 µL	0.30 µL	macroscopic observation
RCA (GenomiPhi™ kit)			
sample buffer	2.7 µL	0.62 µL (23 %)	Figure 6.21
reaction buffer	2.7 µL	0.62 µL (23 %)	"
enzyme mix	0.30 µL	0.09 µL (30 %)	Figures 6.21 and 6.23
10 mM dNTPs [1 mM][2]	/	0.18 µL (/)	Figures 3.24B and 6.22
CFPS			
cell extract	9.09 µL	0.82 µL (9 %)	Figure 6.24
energy buffer	10.91 µL	0.98 µL (9 %)	"
Total volume	26 µL	3.61 µL (13 %)	
Normalized RFU signal	1	0.4	Figure 3.24B

3.3.4 *In vitro* LCR investigations

By applying the optimized *in vitro* LCR protocol (Table 3.2), several experimental parameters of the LCR were investigated to gain more insights into this assembly method. To investigate optimal parameters for the LCR, a quantification of an increasing or decreasing amount of circular product is mandatory prerequisite. This relation was shown by measuring the fluorescence signal of known plasmid concentrations in a range of 0-0.6 nM (Figure 3.25B). Unfortunately, the deviation was high and this specific workflow did not allow a precise quantification. Nevertheless, an internal comparison of varying the parameters by comparing the means/medians is possible. Besides the DNA quantification, it is a prerequisite that the linear form of the utilized reporter gene *sfGFP* results in no signal. This was investigated by performing an *in vitro* LCR of 0.3 nM circular plasmid and with a 0.3 nM linear PCR product of the plasmid. In the PCR product, the linear form of the plasmid p10024, the *sfGFP* was split in the middle. This resulted in a signal which was similar to a negative control without DNA (Figure 3.24A). This proofs the presented workflow of an *in vitro* LCR (Figure 3.22) as a method for rapid prototyping in a

small and automated scale in a 384-well PCR plate. As mentioned before in section 3.1 and

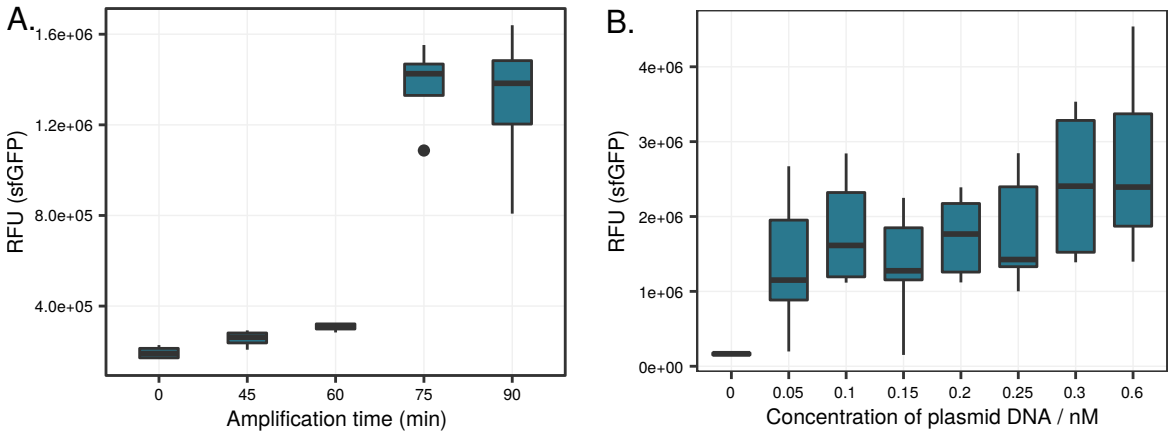

Figure 3.25: A. The amplification time for the RCA of 0.3 nM circular plasmid was varied between 0 and 90 min. The CFPS was measured in the plate reader. The signals represent the measurements after 3 h. All measurements were performed as sextuplicates (n=6). As template for the RCA 0.3 nM of the isolated plasmid p10024 was used. Control reactions without plasmid were negative and are not shown. **B.** Approach to quantify DNA by the fluorescence signals. In general more DNA in the CFPS results in higher signals until 0.3 nM plasmid and no further increase if the concentration is increased from 0.3 nM to 0.6 nM. Nevertheless, due to the small pipetting volumes and manual pipetting the deviation is high. No quantification is possible due to this but shows a proof of principle if a more accurate liquid handling is utilized. For all protocols, 3.6 µL were used for the measurements in the plate reader. The presented signals presenting the measurements after 3 h. All measurements were performed as sextuplicates (n=6). As template for the RCA 0.3 nM of the isolated plasmid p10024 was used. RCA: rolling circle amplification, RFU: relative fluorescence unit, sfGFP: super folder green fluorescent protein. This figure is plotted by using the raw data of the bachelor thesis of Darius Zibulski.

section 3.2, a prolonged annealing step at 66 °C is advantageous for *in vivo* LCRs. This was also utilized as a validation experiment for the *in vitro* LCR. For this, the annealing time was varied in five steps from 20 to 40 sec. As expected the shortest annealing step of 20 sec resulted in a lower signal in comparison to the baseline condition of 30 sec and an even longer step of 40 sec (Figure 3.26A). Furthermore, the concentration of BOs was modified in a range of 0 to 60 nM. Interestingly the Ampligase™ seems to have an unspecific activity which can be observed from the control reaction without BOs and the reaction without BOs and Ampligase™ in Figure 3.26B. The signal of the first experimental setup was higher than the negative signal without DNA at all (not shown). The addition of BOs still increases the signal as expected. As hypothesized by de Kok *et al.* [16], a lower concentration of BOs than 30 nM is disadvantageous. This was not confirmed or dis-confirmed in the *in vitro* LCR: lower concentrations (10 and 20 nM) resulted in similar or slightly higher signals. Furthermore, a higher concentration of 40 nM is regarded as advantageous but a further increase lowered the signals.

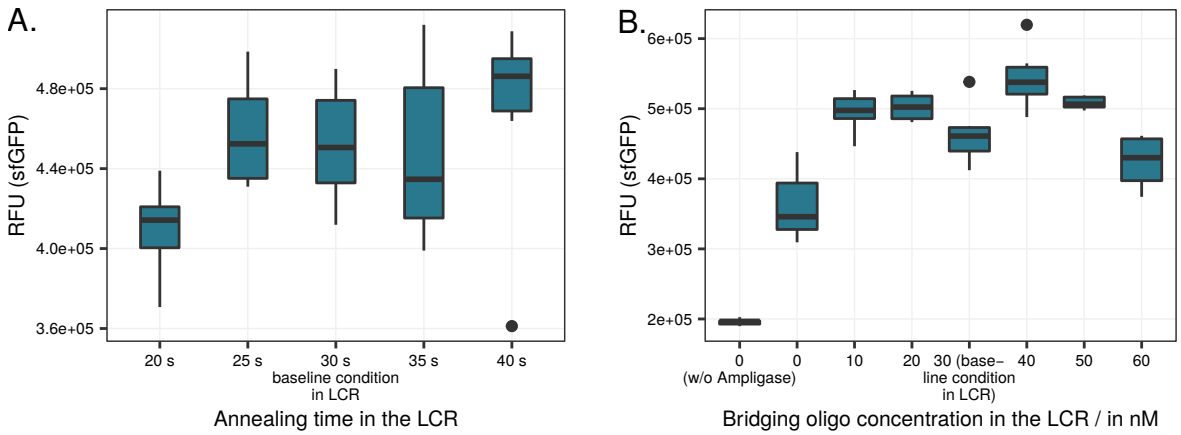

Figure 3.26: A. A linear form of the plasmid p10024 were ligated via the optimized *in vitro* LCR protocol (Table 3.2) followed by the *in vitro* readout. Shorter annealing in comparison to the baseline condition in the LCR (30 sec) resulted in less signal. An annealing step of 40 sec increased the signal. For all, a total volume of 3.6 µL were used for the measurements in the plate reader. The presented signals presenting the measurements after 3 h. All measurements were performed as sextuplicates (n=6). Control reactions without DNA and an LCR without Ampligase™ were negative and are not shown. **B.** A linear form of the plasmid p10024 was ligated with several bridging oligo concentrations and measured via the optimized *in vitro* LCR protocol (Table 3.2). The control reaction without bridging oligos and Ampligase™ resulted in less signal in comparison to the LCR without bridging oligos only. Probably the enzyme ligates the linear plasmid. Nevertheless, the addition of bridging oligos increases the signal. Bridging oligo concentrations higher than 10 nM are not improving the *in vitro* LCR. For all, a total volume of 3.6 µL were used for the measurements in the plate reader. The presented signals presenting the measurements after 3 h. All measurements were performed as sextuplicates (n=6). A control reaction without DNA was negative and is not shown. RFU: relative fluorescence unit, sfGFP: super folder green fluorescent protein, w/o: without.
This figure is plotted by using the raw data of the bachelor thesis of Darius Zibulski.

3.3.5 Cell free *in vitro* LCR for high throughput approaches

To accelerate LCR investigations an CFPS system was utilized and combined with the RCA. The volume for one reaction was decreased to 3.6 µL and enables a high throughput DBTL-cycle in non-optical 384-well PCR plates. All steps for one *in vitro* LCR can be performed serially in one well: first the LCR including the cycling followed by the addition of the RCA components and the isothermal amplification and, finally, the addition of the *E. coli* cell extract for the CFPS. This procedure takes up to ca. 6 h from assembly to the readout. In comparison to the *in vivo* method, this *in vitro* approach allows the generation of results in a shorter time period with more robust results due to the ease of performing more experimental replicates. To conclude, the *in vitro* LCR is the favorable approach in comparison to the *in vivo* workflow to investigate this assembly method and can also be transferred to other cloning techniques.
So far, proof of principle experiments for the LCR were performed and confirmed by published data and/or hypotheses for *in vivo* LCR optimizations. Furthermore, this *in vitro* method can be utilized for diverse applications like, *e.g.*, the characterization of genetic circuits and elements, protein engineering, library screening of promoters and other regulatory elements or to gain

knowledge to build an *in silico* model for the LCR. To further optimize and cheapen the *in vitro* LCR, the GenomiPhi™ V2 DNA Amplification Kit for the RCA has to be substituted by a defined buffer, oligonucleotide concentration, dNTP concentration and by using the $phi29$ polymerase from an enzyme stock solution.

3.4 Automated bridging oligo design and DNA assembly

3.4.1 `CloneFlow`: Software Platform for LCR assemblies

The robust and correct assembly of DNA is one of the main bottlenecks in synthetic biology. In the last decades, many tools for *in vitro* or *in vivo* assemblies were developed and used to build DNA constructs (e.g. Gibson assembly [34], Golden Gate assembly [24, 25], CPEC [80], BASIC [102], etc.). For synthetic biology most of these methods have limitations in reuseability of DNA parts (e.g., specific modifications, remnant scars in the final construct, maximum of parts, total size). The modification- and scar-free ligase cycling reaction (LCR [11, 16, 74]) offers the chance to overcome these limitations. The LCR fits perfect for automated one-pot gene assemblies and robotic platforms. To optimize the assembly, an improved LCR protocol was already investigated in section 3.1. Besides the optimized *in vitro* reaction conditions, the defined, reproducible, automated and fast design of BOs is another crucial part. Currently, no software tool for the design of BOs is available and all oligos have to be designed manually by the experimenter. This is prone to errors due to the impact of the utilized formulas for the T_m calculation and a tremendous limitation for automation approaches.
To support the SynBio community, software solutions were build in interdisciplinary cooperations with Felix Reinhardt, Sven Jager and Michael Schmidt from the Computational Biology and Systems group of Prof. Dr. Kay Hamacher (Fakultät der Biologie, TU Darmstadt), Prof. Dr. Johannes Kabisch and the help of bachelor students of informatics (Bachelorinformatiker-Praktikum, TU Darmstadt). Two tools will be described in the next sections. These tools are used to design and create BOs and/or to guide the wet-lab experimenter to achieve high-efficient LCR assemblies. Both tools are named `CloneFlow`. First, a `Java`-based `Geneious`[1] plugin was developed to generate BOs for linear and circular LCR assemblies. These BOs are designed by choosing the target T_m and user defined parameters. This software tool was already published in Schlichting *et al.* [95]. As a second software tool, a `Django`[2] and `Python3.5`-based server named '`CloneFlow`' was build which allows the design of BOs with low inter- and intramolecular crosstalk within a specific T_m range for linear and circular LCR constructs. Further, the `CloneFlow`-Server allows the user to build DNA libraries consisting of DNA parts and already designed BOs. In the next sections, the `CloneFlow` plugin for `Geneious` and the `CloneFlow` server are presented in more details.

[1] >v. 11, http://www.geneious.com, [52]
[2] `Django` (Version 2.2.6) [Computer Software]. (2013). Retrieved from https://djangoproject.com

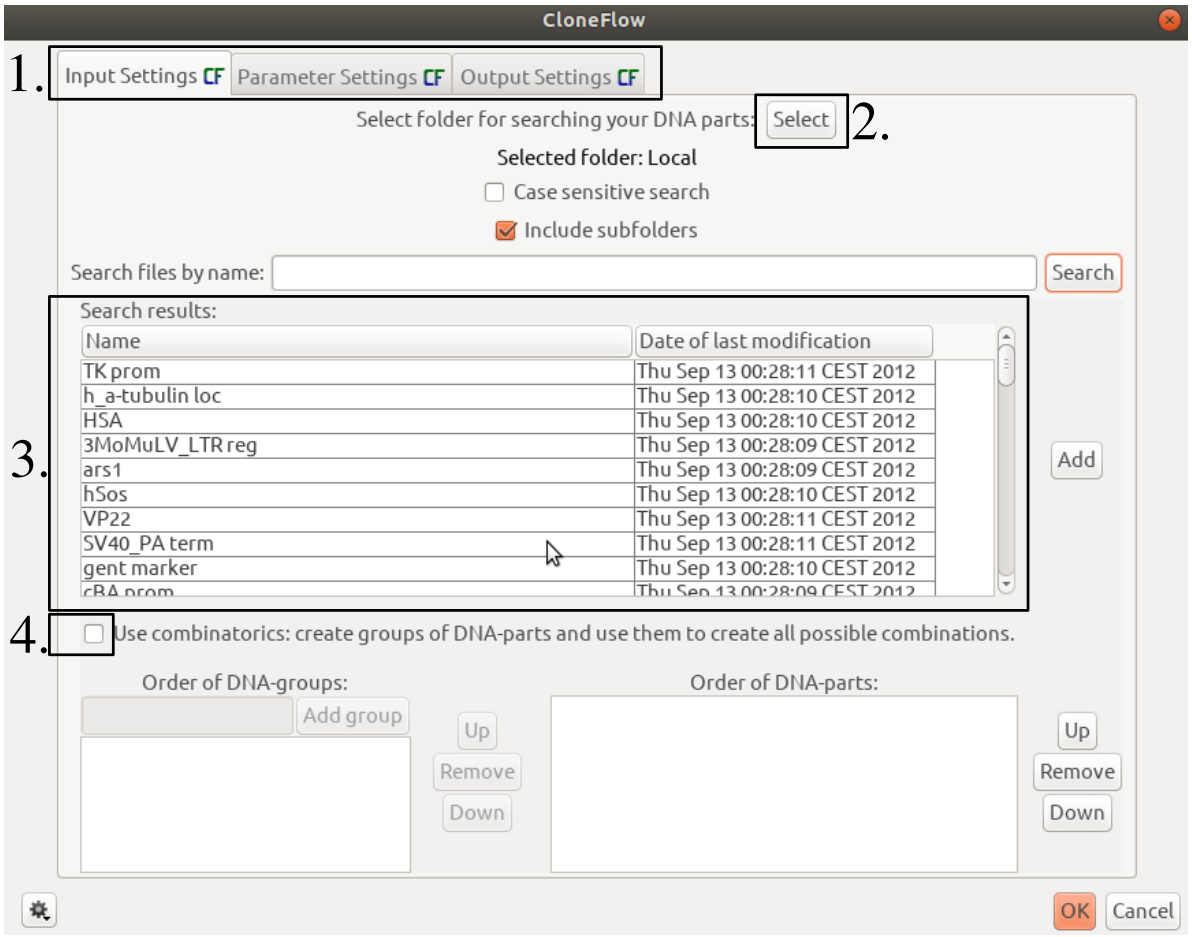

Figure 3.27: `CloneFlow` plugin for `Geneious`. **1.** On startup, a window with three tabs is visible. The 'Input Settings' tab is an area to choose the DNA parts for the BO design. The content of the second and third tab will be shown in Figures 3.30 and 3.31. **2.** The 'Local' folder of `Geneious` was chosen as the working directory to search for DNA parts.**3.** All linear sequences of the folder and all subfolders are shown. Sequences of the category 'oligonucleotide' are not included. Only dsDNA parts with a size $\geq$ 100 bp appear. **4.** By enabling the combinatorics, groups of DNA parts can be defined. More information in Figure 3.29.

3.4.2 `CloneFlow` plugin for the *in silico* software `Geneious`

Based on the findings for the *in vivo* LCR optimization in section 3.1, a plugin for the *in silico* cloning software `Geneious` was developed to automate the BO design and was published in Schlichting *et al.* [95]. The default parameters for LCRs without 8 % DMSO and 0.45 M betaine and the optimized annealing and ligation at 66 °C are considered. The target T_m for each BO-half is 68 °C in the calculation system of SantaLucia [89]. After the installation of the plugin, DNA parts can be selected by searching in folders of `Geneious` or by preselecting the parts of interest before starting the plugin. The preselected sequences are imported automatically into the `CloneFlow` plugin. After setting the order of assembly, the BOs are created and saved in the actual working folder of `Geneious`. As an additional feature, groups of DNA parts and their

logical order can be defined (e.g., promoter, CDS, terminator). The members of these groups are used for a combinatorial LCR design with the predefined assembly order. Furthermore, the LCR constructs are generated with the annotations of each DNA part and additionally the designed BOs are mapped on the assembled sequence. Allover, this plugin enables an automated *in silico* LCR assembly for the improved LCR protocol shown in Table 3.1.

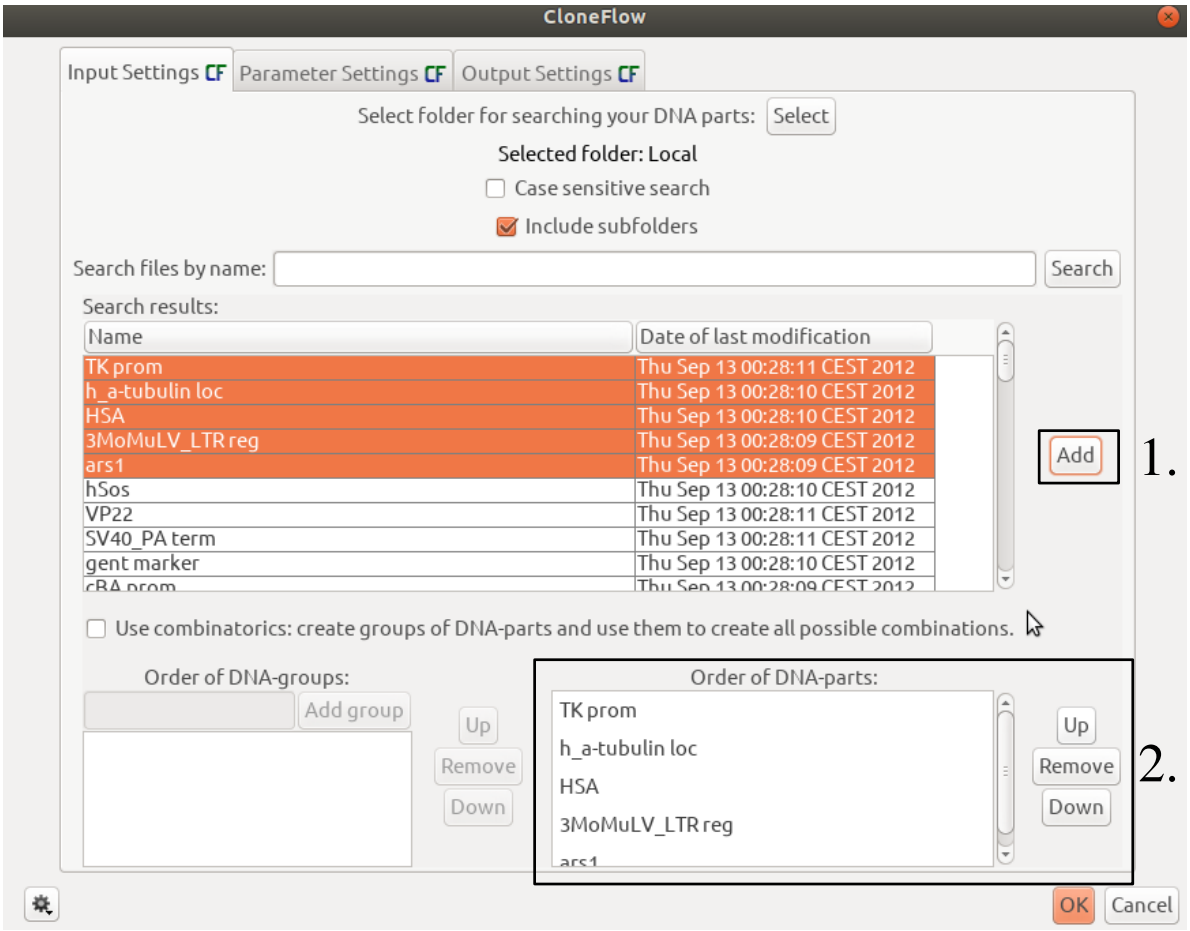

Figure 3.28: Defining the order of assembly in the `CloneFlow` plugin. **1.** Five sequences were chosen for the assembly of one construct and added to the assembly list presented in **2.**. The assembly order is defined by the order showed here (from top to bottom). The order can be modified by clicking on a part and shifting it up or down or to delete it. More parts from other folders can be added by repeating the steps shown here and in Figure 3.27.

Automated bridging oligo design for LCR assemblies

To support the robust DNA assembly by the LCR, the design of BOs with a defined target T_m is a crucial step due to the broad presence of calculation formulas and salt corrections [4, 72, 73, 89, 91, 92, 94, 104, 105, 120]. Depending on the utilized system, the T_m calculation of the same sequence differs significantly and has an impact on the experimental reproducibility [75].

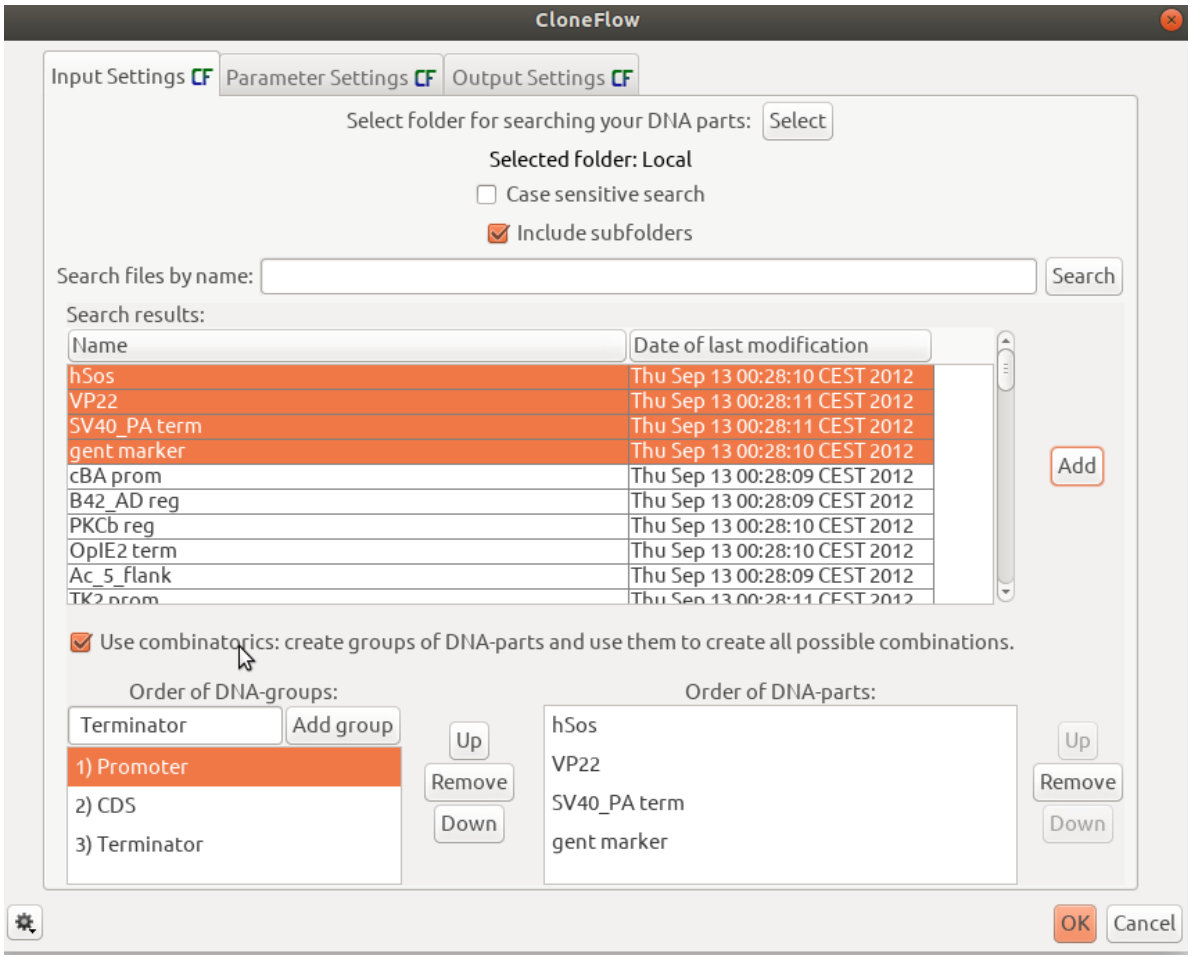

Figure 3.29: Combinatorial LCR design with `CloneFlow`. DNA groups can be defined (e.g., promoter, CDS, terminator). To each DNA group, DNA parts can be assigned by clicking on 'Add' while the desired DNA parts and DNA group is marked. The order of DNA groups specifies the order of assembly. Each member of group 1 'Promoter' will be ligated with each member of group 2 'CDS' and each member of group 2 will be ligated to each member of group 3 'Terminator'. This allows a combinatorial and rational LCR design.

The effects of miscalculated BOs were also shown in section 3.1 (for example in Supplementary Figure 3.4). Due to this, the importance of an in silco BO design tool, which considers the improved *in vivo* LCR conditions presented in section 3.1, prevents the user to utilize falsely created BOs and low efficient LCR assemblies. The first approach to generate BOs with the `CloneFlow` plugin is to select the DNA parts of interest and to start the tool. The parts are directly assigned to the list 'Order of DNA-parts' (Figure 3.28). Afterwards, more parts are assignable by selecting a folder of interest and to utilize the search funtion. Another approach is to start the plugin without a preselection and to utilize the search function only. The latter method is mandatory for combinatorial LCR designs. All dsDNA sequences with a size $\geq$ 100 bp are listed and can be added to the DNA part list consisting of the preselected sequences or to an empty list (Figure 3.28).

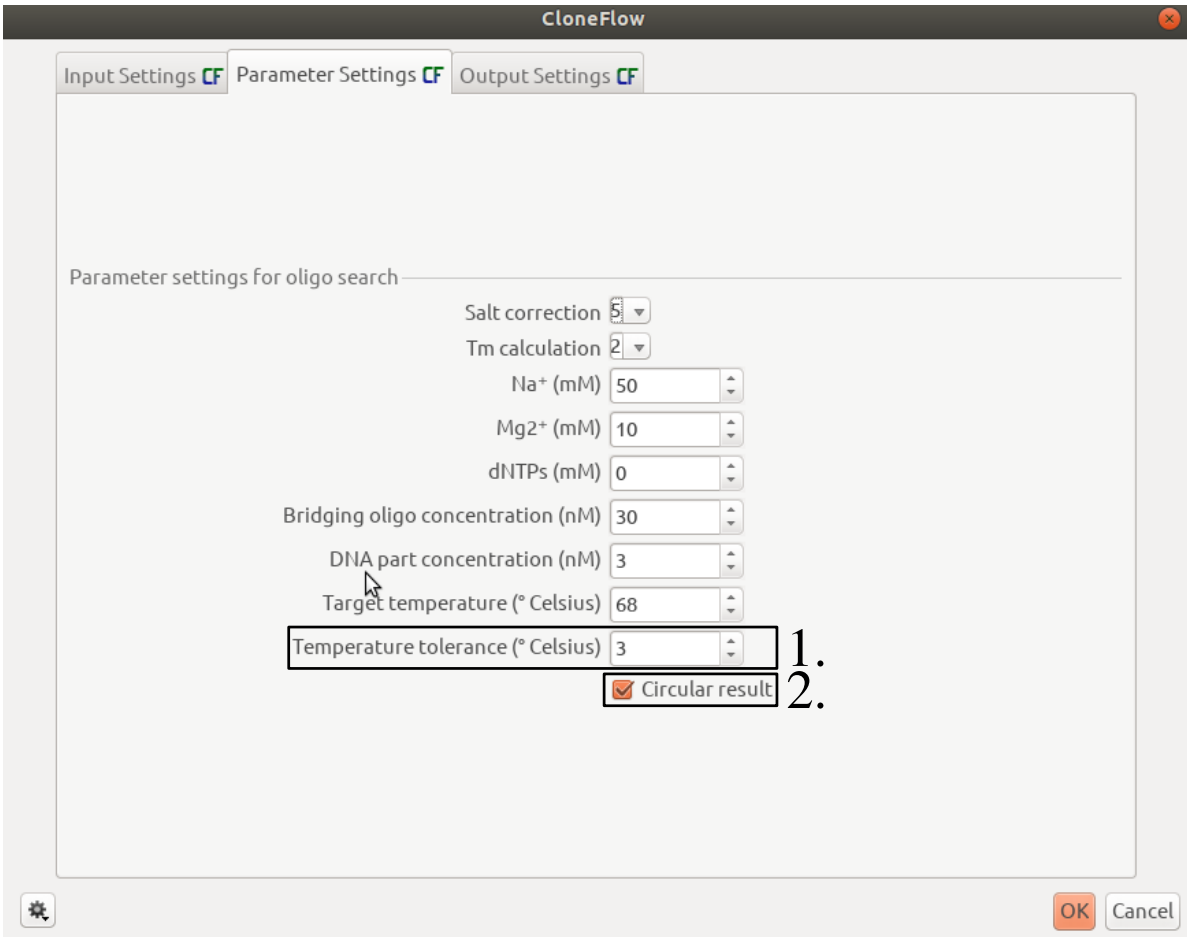

Figure 3.30: Parameter settings for the BO design. The recommended parameters for LCRs without DMSO and betaine (improved protocol in Table 3.1) are utilized automatically as default parameters. **1.** A leeway to generate BOs with the target T_m is mandatory due to the rare event that a BO perfectly matches the adjusted target. **2.** `CloneFlow` can design circular or linear LCR products. By disabling this checkbox, the LCR assemblies are linear.

As depicted in Figure 3.27, `CloneFlow` can be utilized to search for the desired DNA sequences. All double stranded sequences in `Geneious` are regarded as a DNA part as long as the size is equal or larger than 100 bp. Less basepairs than this limit possibly lead to overlapping BOs or to BOs with a too low target T_m. To create one BO-half with a target T_m of 68 °C for a DNA part with a GC-content of ca. 45 %, 33 bp are needed. This amount of basepairs is also mandatory for the design of another BO-half at the other end of the same DNA part. Otherwise, the BOs for the bridge from part A to B and B to C are overlapping and this probably hampers the LCR. Furthermore, the limit of 100 bp per DNA part is necessary to enable a leeway for other sequences with, *e.g.*, a lower GC-content than the mentioned one. A lower GC-content lowers the effective T_m per base [89] and more basepairs are needed to fulfill the target T_m criteria of 68 °C. Concluding this, the search mode of this plugin only shows dsDNA sequences with a size $\geq$100 bp. If a too short or ssDNA sequence is selected before starting the `CloneFlow` plugin,

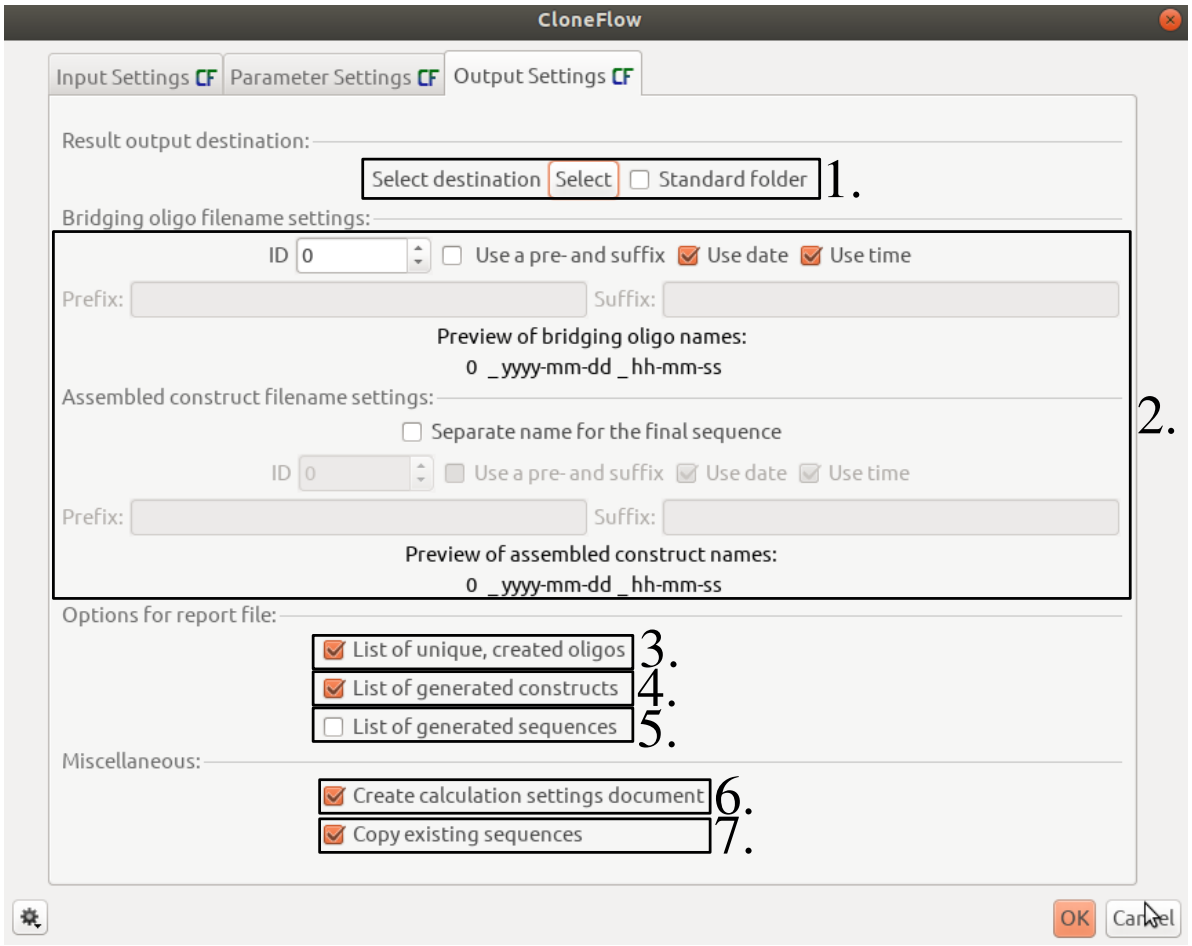

Figure 3.31: Output settings of the `CloneFlow` Plugin. **1.** The output folder can be chosen. If 'standard folder' is activated, the files will be saved in the current working directory in `Geneious`. **2.** Bridging oligos and the automatically designed LCR constructs are saved in the chosen output destination. By default, the BOs and the constructs are named with a unique numeric ID, the date and time of the design. The ID is upcounted by 1. A user-defined pre- and suffix can be added to the name and the starting value for the ID-counter can be adjusted. The assembled constructs are named by the same pattern and a user-defined pre- and suffix can be defined. One tsv-file is generated and saved in the chosen destination folder to summarize the design with the utilized design values adjusted in the 'parameter settings' tab, the BO names and sequences, the DNA part names and the sequence of the assembled construct. **3.** For a combinatorial design, the output files can be modified by enabling or disabling the checkboxes. **4.-7.** If unchecked, no information about the utilized parameters will be created. Furthermore, the utilized DNA parts sequences are not copied.

the sequence will be ignored and an error message with additional information is shown.

Combinatorial design is a feature to allow the rapid design process of *e.g.*, synthetic circuits, and was already utilized for other DNA assembly techniques [26, 69, 100, 109]. For the LCR, no combinatoric design tool is described. `CloneFlow` offers this feature by selecting the combinatorics option shown in Figure 3.29. The DNA groups are defined by typing user-defined group names, for example promoter, CDS and terminator, followed by the assignment

of members. This can be achieved by following the assignment steps in the previous paragraphs.

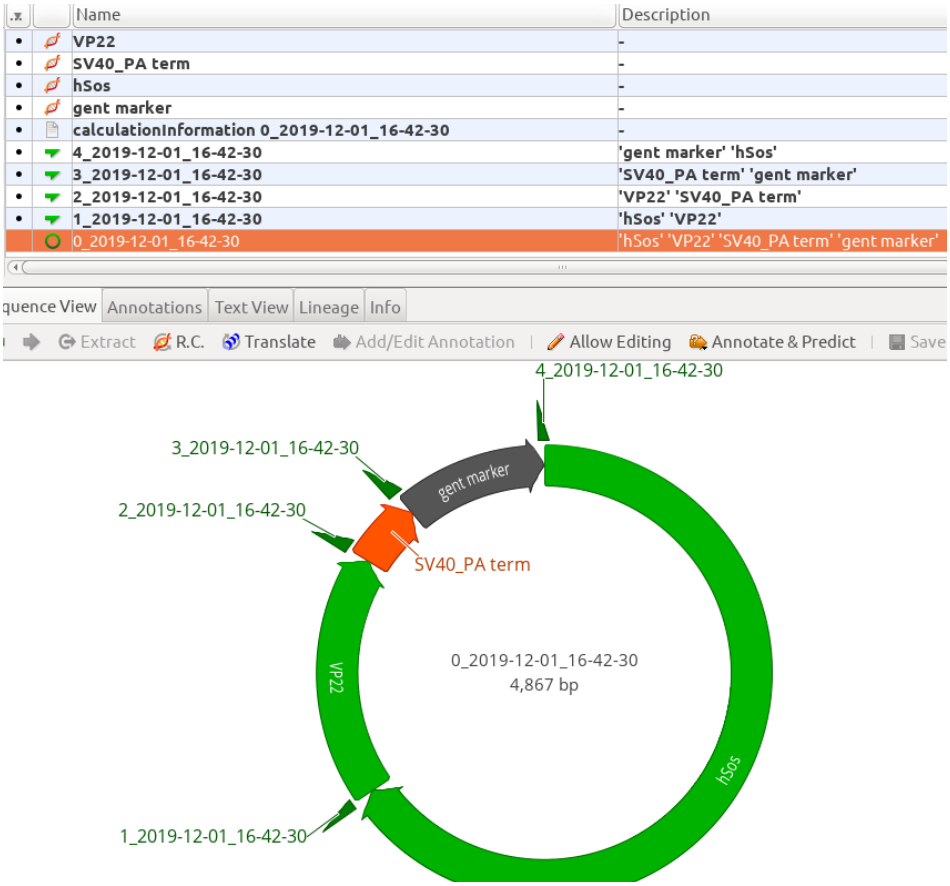

Figure 3.32: Output of the `CloneFlow` plugin. The utilized DNA parts for the assembly, the BOs, the product and the file with the design parameters are generated as the default output for the circular assembly of one construct. The annotation and the direction of each DNA part is transferred to the circular product. Furthermore, the BOs are mapped on the sequence. In the description of a BO it is written which DNA parts the BO spans.

Each DNA group can contain an unlimited amount of DNA parts and even duplicates. Further, a part can be assigned to one, several or all groups. After the assignment of the members, all possible combinations are designed whereby the order of the DNA groups is fixed according to the adjustments of the user ('Order of DNA-groups' in Figure 3.29). `CloneFlow` is not able to use logical design rules for the combinatorics. As shown in Figure 3.29, each member of the first group 'Promoter' is ligated to each member of the second group 'CDS', each member of the seconds group 'CDS' is ligated to each member of the group 'Terminator'. To swap the order of the first and second DNA group would also result in all possible assemblies but the design would not be logical. If linear constructs are designed, the ligation of the last and first group members will be omitted and no BOs are created. Before the BO design is started, the design rules can be modified (Figure 3.30). The default parameters are loaded automatically by the `CloneFlow` plugin and are based on the LCR optimizations described in section 3.1

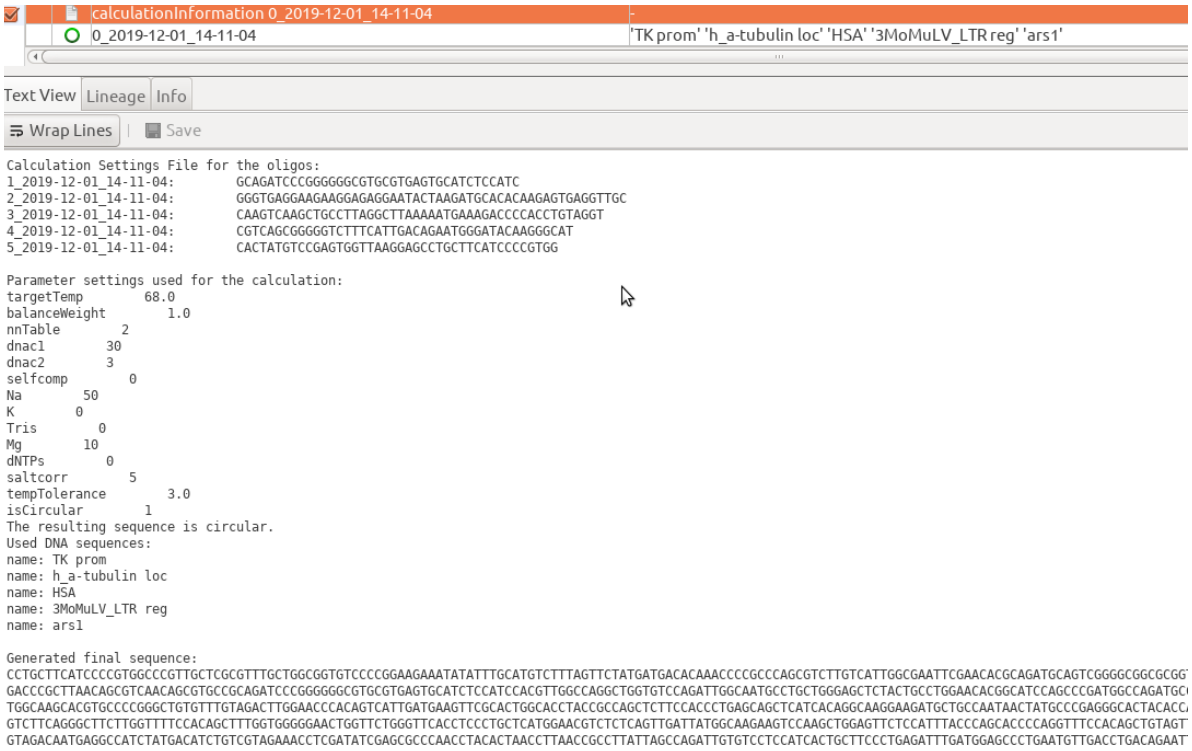

Figure 3.33: Calculation information file of `CloneFlow`. In this file, the sequences and names of the designed BOs, the utilized parameters and the assembled sequence is shown. This is the default output for the output settings shown in Figure 3.31. The parameter 'nnTable' represents the utilized T_m calculation formula, 'dnac1' the BO concentration and 'dnac2' the DNA part concentration. 'Tris' and 'K' are not utilized in the LCR but values are expected from the formulas.

and on the salt concentrations of the utilized Ampligase® buffer. Nevertheless, all parameters are adjustable to allow user-defined designs. Circular LCR designs are the default setting but can be disabled to enable linear constructs. To enable a curtain leeway for the calculation of BOs, a 'Temperature tolerance' parameter was included in the T_m calculations. The utilized calculation formulas design BOs with non-integer values and it is a rare event, that the T_m of a BO-half matches exactly the target T_m. The tolerance value of $\pm 3\,°C$ is mandatory to enable the `CloneFlow` tool to find BOs with the closest T_m to the target T_m. To choose a higher tolerance interval would increase the calculation time needed to create the pool of all possible BO-halves for one ligation site. The chosen BO-half would be the same but the overall duration for the design would be prolonged. A smaller tolerance value would increase the risk to find no BO.
After choosing the DNA parts, the order of assembly, the design parameters for the BOs and the output folder can be modified (Figure 3.31). To create custom names of the BOs and constructs is available. For both, a counter function is utilized which upcounts each designed BO and construct to prevent redundant IDs. By default, the same counter function is utilized for the results. For example, for the circular assembly of three DNA parts, this results in a construct with the ID '1' and the BOs '2', '3' and '4'. In addition to this, the feature 'Separate name for the

final sequence' creates two independent counters and this would result in construct '1' with the BOs '1', '2' and '3'. Furthermore, a report file is generated with details of the assembly. The user can modify this file as shown in Figure 3.31. Last, the report file can be disabled at all and the user can choose if the utilized DNA parts are copied into the output folder or not. Finally, the design can be started. `CloneFlow` generates circular or linear constructs of one

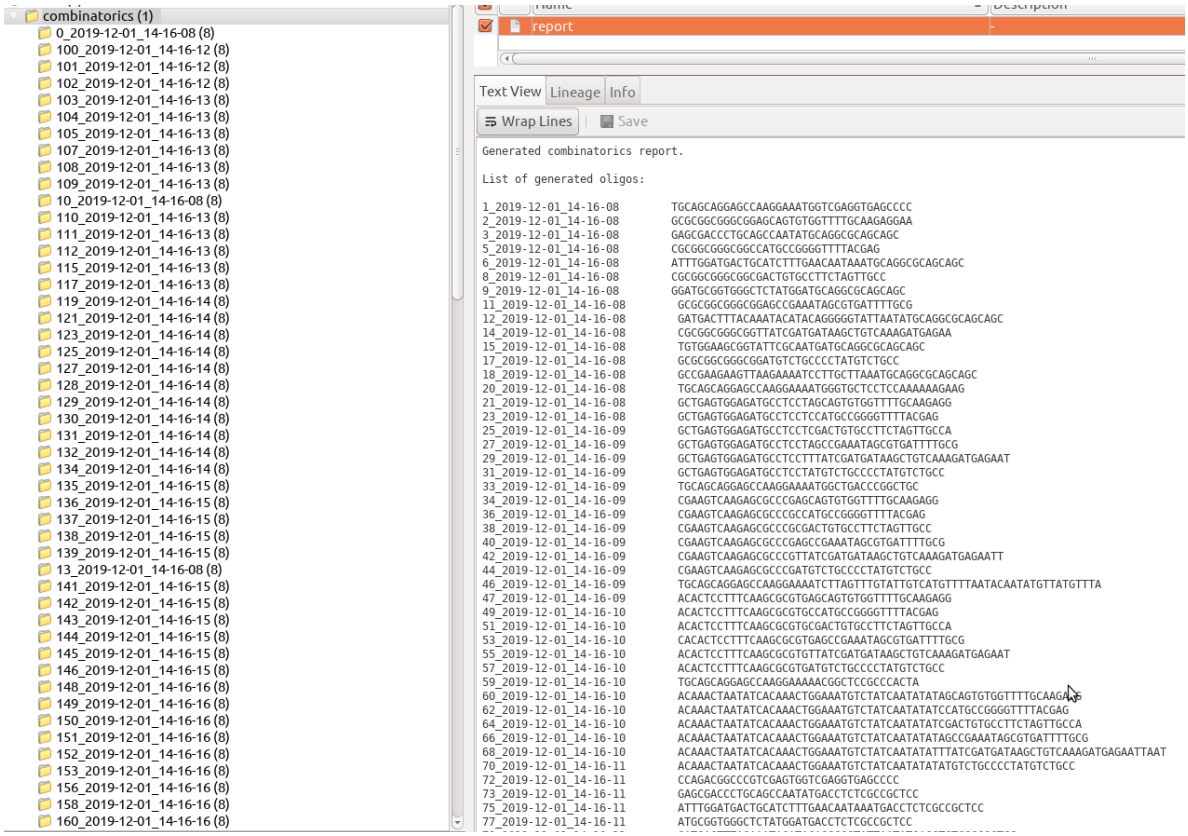

Figure 3.34: Combinatoric *in silico* LCR assembly with the `CloneFlow` plugin. A report file is generated in the folder 'combinatorics' with the list of the unique BOs of all designs. Each subfolder consists of one assembly and the output presented in Figure 3.32.

or combinatorial assemblies. The designed BOs and the assembled sequence are saved in the chosen output folder of `Geneious` or the current working directory. The default output of a four part assembly is shown in Figure 3.32. The utilized DNA parts are also copied into the folder to backtrace the design. As an additional feature, the names of the DNA parts are utilized for the description of each BO and the assembled construct. The latter sequence is generated by the plugin including the annotations of the DNA parts and the mapped BOs. Furthermore, a report file with more metadata is provided (Figure 3.33). In case of a combinatorial design, an additional report file is printed and saved in the parent folder (Figure 3.34). This file consists of checks all designed BOs for all processed combinations of one assembly and only the unique BOs are listed. Redundant BOs are deleted in this list if, for example, one DNA part is substituted by another one and the other parts are still the same. In this case, two other BOs are created and

the others remain. This offers the possibility to reduce the financial costs for the LCR designs when the same DNA parts are used multiple times in the same order.
Overall, the `CloneFlow` plugin supports the rapid build process of LCRs by the *in silico* design of BOs and assembled sequences by considering the improved conditions presented in section 3.1. Combinatorial approaches are supported to allow a fast generation of synthetic circuits and is based on DNA libraries. Nevertheless, no logical combinations are designed by this tool itself and depends on the knowledge of the user. In the future, the plugin can be further improved by implementing design rules for the construction of more rational designs. On the other hand, the DNA groups can be populated logically if existing switches, gates and computational design tools are utilized to build logical synthetic circuits [51, 69, 116, 123]. For those tools it is mandatory to follow the annotation and design rules of the synthetic biology open language (SBOL) approach [30]. To utilize the existing tools to build the DNA groups, including the sequences and annotations, and import them into `CloneFlow` offers a chance to build logical circuits with the `CloneFlow` plugin.

3.4.3 Stand-alone `CloneFlow` server

`CloneFlow` offers the user to create DNA part libraries and to use them for the design of BOs. For this it is necessary to upload the DNA parts before the user can start with the design process. Usage of a fasta or mfasta-file is possible in the upload area of the server (Figure 3.35B). All parts of one fasta/mfasta-file can be assigned to a group (i.e., if all parts in the file are promoters, they can be assigned to the group 'promoters'). Each DNA part can also be added to at least one group afterwards or it can be removed from groups. Further, every part will get a unique ID from the `CloneFlow` system. One more advantage of `CloneFlow` is to save, search, find and regroup every member of the DNA library. If required, only special members can be assigned to an admin group to get permissions for renaming and regrouping the libraries. Based on these libraries, the parts can be chosen for *in silico* assemblies in the calculation area. After choosing the DNA parts of interest, the order of the LCR assembly and the design parameters can be adjusted to design the BOs.
For the design of BOs several parameters has to be adjusted like the T_m, different salt concentrations of the utilized buffers and the calculation formulas (Figure 3.35B). `CloneFlow` provides default parameter tables for the BO design and optimization and can be seen or edited in the admin area. The admin has to name a design parameter set. Automatically, this parameter set can be utilized from all other users. Otherwise, no calculation of BOs is possible so far. The utilized parameters for every design can also be observed after the job is done in the home area. Nevertheless, the admin can edit the default parameters and share them with all other users or can create new parameter sets. Users with restricted rights are allowed to use the provided parameter sets from the admin after they were assigned to these users/groups or to create and save their own parameter sets in the calculation area. The parameter sets are chosen directly

before starting the jobs and will be described in the next paragraphs.
Single stranded oligonucleotides in the LCR are building a stable 'bridge' between the denatured ends of two DNA parts and are called BOs. One strain of two DNA parts and the connecting BO are presenting a double stranded DNA with a single nick (shown in Figure 1.3 on page 6). This serves as a template for an enzymatic ligation and will end in the desired construct. To specify the assembly order of the assembly, the BOs are utilized. In contrast to other cloning techniques, there is no need to reamplify or resynthesize the DNA parts with specific overhangs to build more than one construct. By using the same DNA parts of the library, new BOs have to be ordered only to redefine the order of the assembly. This advantage is depicted in Figure 1.1. An additional amplification or order is avoided and this lowers the costs and allows a high sustainable way to save time, workload and money. Every BO in `CloneFlow` has a system-defined and numeric unique ID which can be used to label the BO. After the `CloneFlow` job is done, the user will get an e-mail notification and a link to the BOs, design parameters, used DNA parts and sequences. The BOs and the parameters can be downloaded as a csv-file. For a high stability of the hybridized BO and DNA part the T_m of the BOs have to fit the experimental temperatures and is a trade-off of specificity and efficiency. Further, the utilization of secondary structure inhibitors like or betaine can increase the assembly efficiencies for some LCR designs [16]. The target T_m for each BO-half depends on the experimental conditions and utilized calculation formulas, This is based on a comprehensive theoretical and experimental research and is described in more details in section 3.2.

Outlook

The `CloneFlow` plugin is functionable and was already utilized for some BO design in this thesis. In contrast, the server is still under development to enable a construction of DNA libraries and BO libraries where. The combinatorial design has to be implemented as described for the `CloneFlow` plugin in subsection 3.4.2. Additionally, the design of amplification primers can be another useful feature to further strengthen the server. Further, only a prototype feature to generate a human-readable LCR dispensing protocol is implemented. This protocol is based on the experimental parameters of de Kok *et al.* [16] and the published protocol with DMSO and betaine. In the `CloneFlow` server, the BO design is optimized to calculate the minimal folding energies. As shown in section 3.1, this crosstalk seems to be negligible for LCR assemblies with predefined parts. Nevertheless, for *de novo* assemblies where the final construct is designed but not the DNA parts themselves, this feature is a promising approach for optimized LCRs. This was already shown to be beneficial for Golden Gate assemblies [37]. The final construct was designed *in silico* by joining the desired DNA parts. Afterwards this sequence was split into subparts by detecting 4 bases long linkers with the lowest ΔG of all possible junctions. According to this study, a ca. $4\times$ increase of the efficiency and amount of colonies were obtained for the assembly with the ΔG optimized linker A non-functional prototype of the software is

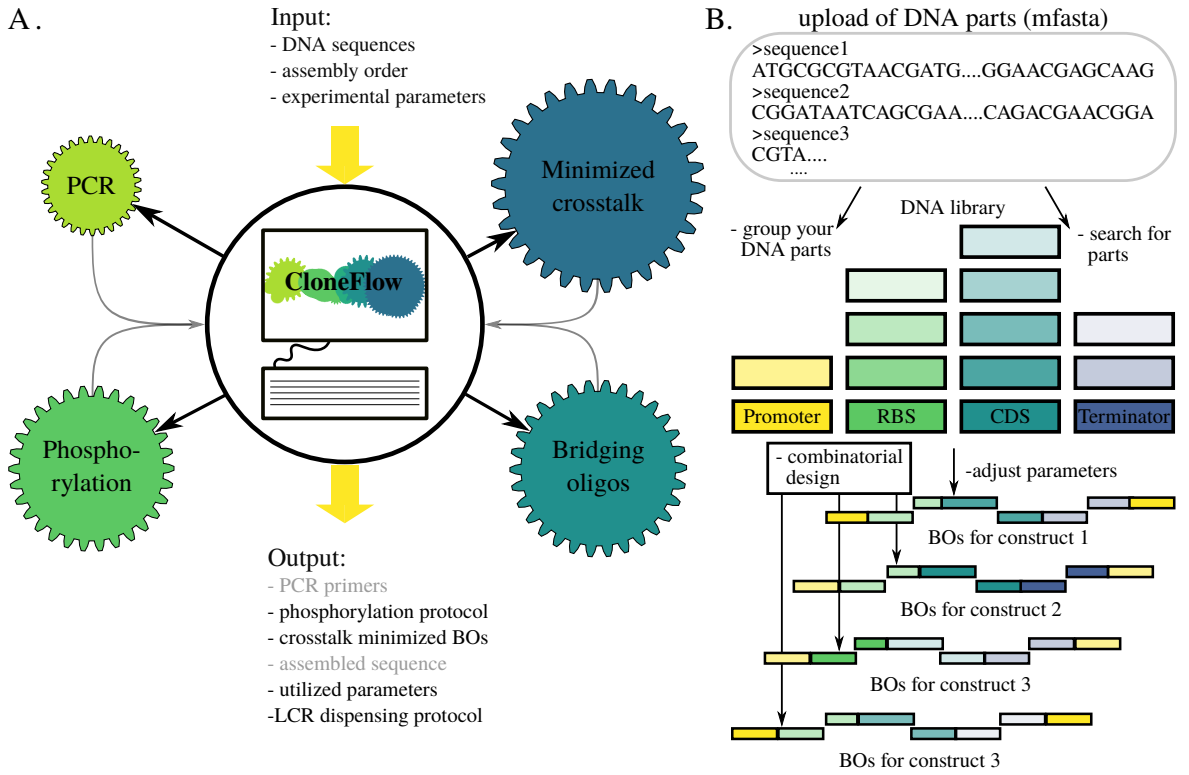

Figure 3.35: A. Input and the supposed output of the `CloneFlow` server. After a user input, several modules can be utilized to create the output of a phosphorylation protocol for amplification primers, crosstalk optimized BOs with a specific target T_m and an LCR protocol in `csv`-format. The design of the amplification primers and the assembled sequence is not implemented so far. **B.** `CloneFlow` serves as a DNA archive for the scientist and the whole group. All DNA part sequences can be uploaded in a (m)fasta format. They can be named and assigned to self-defined groups (origin of replication, promoter, RBS or CDS). `CloneFlow` also offers an adjustable right management to rename, delete or regroup every entry. Based on this library, linear and circular DNA constructs can be designed. Bridging oligos are designed automatically for linear or circular constructs following user-specified parameters (target T_m, salt and DNA concentrations, kinetic parameters). Otherwise, the general rules published in the literature will be used by default [16]. The combinatorial design is not implemented so far. BO: bridging oligo, CDS: coding sequence, RBS: ribosome binding site.

offered for *de novo* LCR designs by the authors[1] and further supports the need for ΔG optimized BOs of assemblies without a predefined split.

In the future, the `CloneFlow` server can offer the design of crosstalk minimized BOs for LCR designs but mainly addresses assemblies of synthetic constructs with a total size of more than 2000 bp. This size is approximately the maximum of current synthetic genes [43]. If the designed construct is smaller, the sequence can be ordered synthetically without a need of a DNA assembly. To calculate several splits with high and low BO crosstalk, the toy-model plasmid sequence for the LCR optimization in section 3.1 can be utilized. By utilizing the *in vitro* LCR described in section 3.3, the success rates of the assemblies can be quantified

[1] http://ibiocad.igb.illinois.edu/ (no https allowed for the homepage!)

to determine the influence of the splits. Afterwards, the *in vivo* LCR should be applied for the most diverse results to verify them. Based on this, the `CloneFlow` server can be further developed to optimize this random split model and to automate the BO design and ordering and to generate machine-readable LCR protocols. The improved LCR protocol investigated in section 3.1 and the computer-aided design of BOs presented in subsection 3.4.1 are the scaffold for the rapid and automated LCR assembly of genetic constructs. A low efficiency results in a higher screening effort after the transformation. In case of an assembly efficiency of 10 %, 29 colonies have to be picked to obtain the correct sequence with a probability level of 95 %, six colonies with the efficiency of 40 % and only two CFUs if 80 % of the colonies contain the correct sequence. For non-automated assemblies, the efficiency has no significant impact due to the fact that picking a few colonies after one assembly is a routine. In contrast to this, a rapid assembly via automation approaches highly suffers from low efficiencies. For example, for 100 assemblies with an efficiency of 40 %, the plasmid of 600 colonies have to be analyzed to obtain the correct sequence. This is accompanied by 600 plasmid cultivations, isolations, restriction analysis and sequencing, and would increase the need for additional space for, *e.g.*, picking robots and incubators. An increased efficiency of 80 % would tremendously lower the screening effort to 200 colonies. To tackle this, the LCR protocol was optimized for a high efficient assembly by omitting DMSO and betaine and by adjusting the BO-T_m and annealing temperature (section 3.1). Furthermore, the automated and combinatorial design of BOs and LCR constructs were achieved to standardize and accelerate the design-build steps of the DBTL-cycle (subsection 3.4.1).
For the automation, the robotic platform of the CompuGene project and Prof. Dr. Johannes Kabisch was utilized for the automated LCR assembly (platform is shown in Figure 2.3 of chapter 2). The workflow for the assembly results in the plating of the transformed LCRs into *E. coli* (Figure 3.36). The maximum amount of transformations for one assembly round is 96. Additionally, the transformed cells can be split into two user-defined volumes after the recovery two enable a plating of two plating dilutions per transformation. So far, the automated workflow presented in the following abstracts was only validated without performing LCRs and transformations. Nevertheless, the workflow was developed and verified by utilizing dummy dispensing protocols and empty MTPs to simulate the assembly.

3.4.4 Automation of the LCR with a robotic platform

To utilize DNA libraries is mandatory for a high sustainable and rapid automated DNA assembly. It reduces the hands-on time for the experimenter to amplify DNA parts or to reorder BOs. Nevertheless, the stability of DNA libraries is doubtful due to the negative impact of repeated freeze-thaw cycles, contaminations with nucleases [82] or cross-contaminations and was regarded as a crucial limitation in the *in vivo* LCR investigations (section 3.1). To store the DNA at 4 °C is possible but increases the effects of DNA degradation by nucleases [82] and

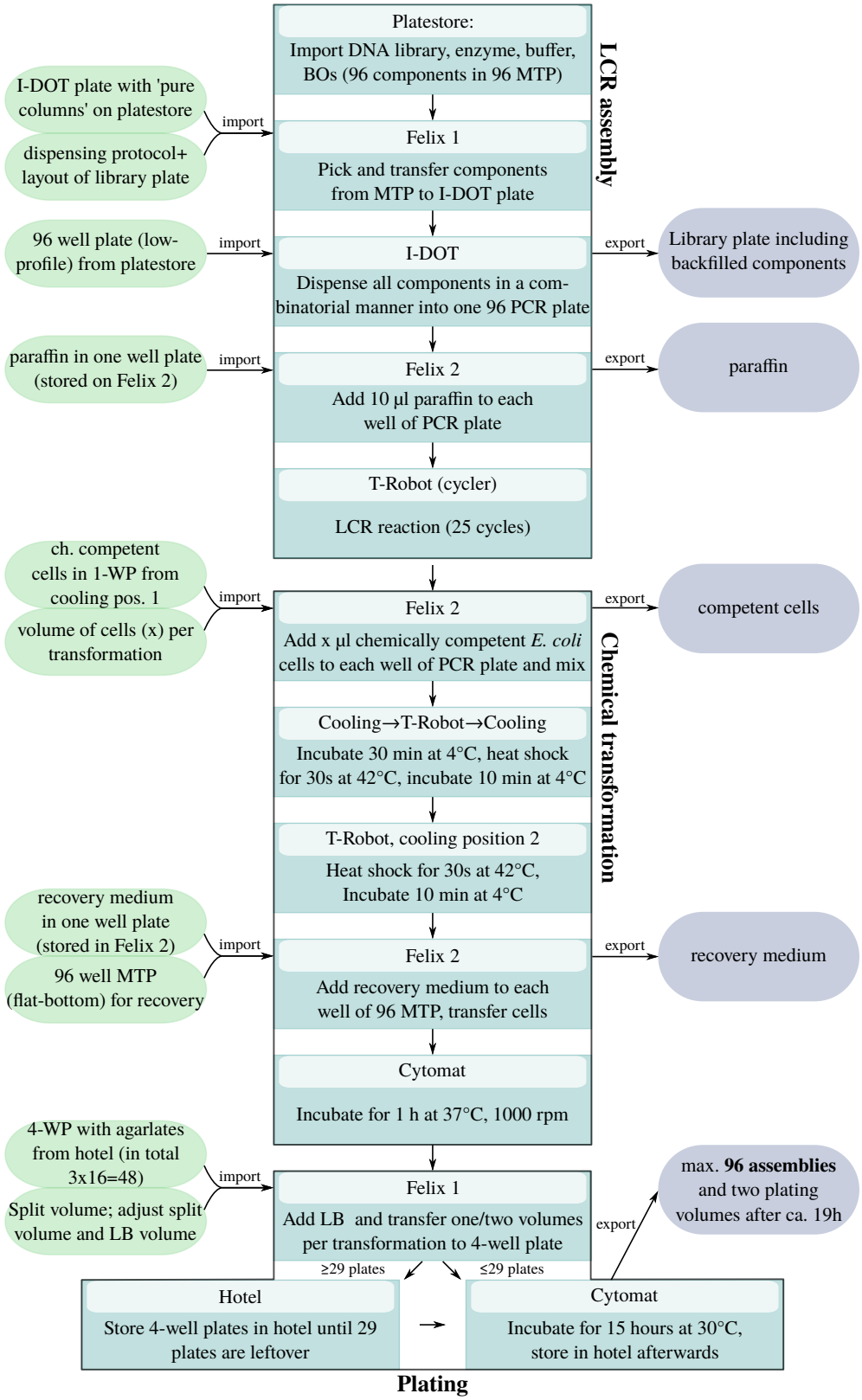

Figure 3.36: Workflow design for the automated *in vivo* LCR with the robotic platform. In total, 96 constructs could be assembled and transformed automatically within 19 h. So far, the workflow presented here was validated by running the platform with plates without liquids or agar. 1-WP: 1-well plate, 4-WP: 4-well plate.

an evaporation of the solvent. As a radical solution, Robinson *et al.* [81] automated the LCR by amplifying the DNA parts on demand by the platform itself or for one assembly round to circumvent the described limitations.
According to the complexity of the freeze-thaw cycles and storage effects, the influence of reusing the same aliquots of DNA parts is assumed to be disadvantageous for the LCR assembly efficiency. The overall impact has to be validated in additional investigations with the scope on freeze-thaw cycles, storage temperature, storage buffer and DNA part size. Furthermore, the degradation of oligonucleotides, respectively, BOs, and the repeated freeze-thaw cycles of NAD^+ are known issues [15, 81, 125] and these further decrease the approach of utilizing library plates. As a trade-off, all components can be split into several library plates with the same layout to reduce the amount of freeze-thaw cycles. This workaround is more laborious and needs additional storage capacities. Another approach would include the utilization of automated PCRs and a synthesizer for the BOs. Furthermore, an accessible freezer is mandatory to automatically get and store the library plates.

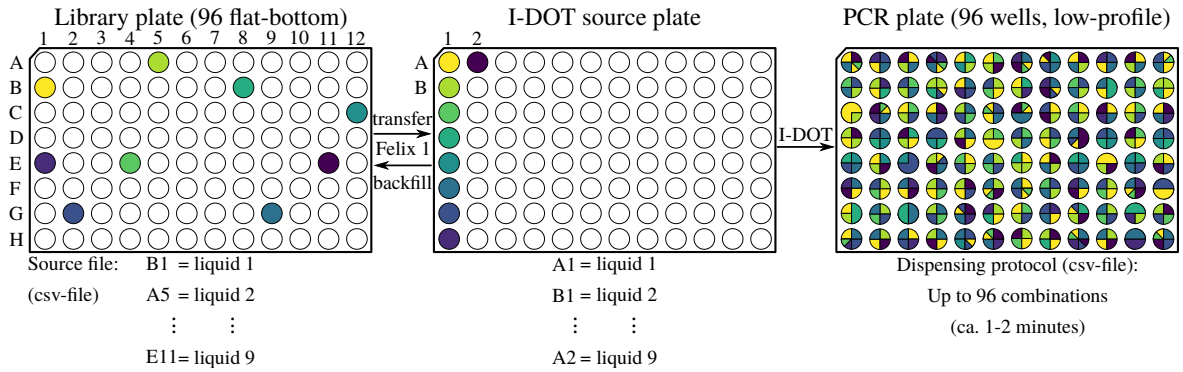

Figure 3.37: Combinatorial LCR design in the robotic platform. A 96-well library plate with DNA parts, BOs, enzyme buffer, enzyme, water and NAD^+ is utilized to transfer the desired liquids to the pure columns of the I-DOT source plate. For this, the position of each liquid in the library plate is specified by a source file (`csv`-format). This file consists of the names and positions of the desired liquids and is manually created beforehand by the user for the automated and column-wise transfer to the I-DOT source plate. Afterwards, the source plate is utilized by the I-DOT for a dispensing into a 96-well PCR plate. The volumes and combinations are specified by a dispensing protocol (`csv`-file). Up to 96 combinations are mixed in 1-2 min. Afterwards, the PCR plate is transferred to the cycler. Finally, the liquids in the I-DOT source plate are backfilled into the corresponding wells of the library plate.

3.4.5 Transformation of *E. coli*

To utilize chemically competent cells and the heat-shock for transformations of *E. coli* is an easy-to-automate method but results in a lower transformation efficiency in comparison to electroporations [38]. Additionally, the transformation efficiency tremendously decreases if thawed cells are refrozen and utilized an additional time [36]. Residual cells should be discarded or reused soon without an additional freeze-thaw cycle in between. Due to this it is recommended to prepare a 96 MTP or 96 PCR plate with cell aliquots equal to the amount

of LCRs and an excess cell volume of 10 %. Furthermore, the cells are stored on the cooling position before starting the robotic workflow. Until their utilization, ca. 2 h elapses. An impact of this duration on the transformation efficiency is not described in the literature and was not investigated. *Escherichia coli* adapts to the lower temperature after a few hours [2]. This reactivated metabolism assumes an impact on the transformation efficiency by, *i.e.*, alterations of the cell membrane. Nevertheless, a technical solution by utilizing an accessible freezer for automated thawing in close temporal proximity to the heat-shock is recommended.
The volume of recovery medium depends on the humidity of the agar plates and the percentage of the agar. So far, to add the default volume of 250 µL medium is considered as sufficient to receive agar plates with evenly distributed colonies after the growth. Nevertheless, the plating is still a bottleneck of the automated LCR workflow. Too high volumes of the recovery medium result in a liquid layer on the agar plates at the end of the incubation step. This hampers the formation of colonies. This is probably related to the humidity chamber of the incubator. To incubate the agar plates with an empty water reservoir is suggested to accelerate the evaporation of the liquid without compromising the output of evenly distributed colonies.
In case of the maximal amount of 96 transformations and two dilutions for each transformation, 48 4-well agar plates have to be prepared for the sum of 192 platings. The height of the agar and the added recovery medium for the plating is influencing the probability of cross-contaminations. Due to this, the maximal agar volume per well was investigated. The volume has to be 5 mL to 10 mL to ensure no cross-mixing during the shaking and no drying of the agar. Furthermore, more than 29 agar plates can not be stored in the incubator due to the limited storing positions. By calculating the amount of LCRs from the dispensing protocol and by considering if the plating volume is split into one or two volumes, the amount of total 4-well agar plates are automatically calculated. Before populating the incubator, the agar plates with plated cells are stored in an empty stack of the hotel. Only the last 29 agar plates will then be stored in the incubator. This workaround enables the automated assembly of 96 constructs. Further, the user can remove the agar plates with cells from the hotel and incubate them somewhere else. Afterwards, the residual plates are automatically stored and incubated by the robotic platform.
The presented LCR workflow was developed by utilizing the corresponding devices of the plattform and the software suite of Analytik Jena. So far, all steps were tested by running the workflow in a dry mode with no liquids. To validate the workflow, 96 assemblies have to be designed to assemble them by the robotic platform.

4 Conclusion and outlook

The DNA assembly of desired genetic constructs is the scaffold of modern biology. A broad variety of techniques are described and utilized all over the world. In most laboratories, the assembly method of choice mainly depends on one decision-making step in early days of each facility. Each method has a right to exist and normally results in the desired sequence within a few days. Nevertheless, the assembly technique for automation approaches underlies curtain demands. As prerequisites for this laborious build-process, one-pot assemblies of an unlimited number of modular building bricks, the DNA parts, low pre-planning and low post-assembly screening effort are desirable. Unfortunately, most automation approaches are utilizing error-prone methods by inserting DNA bias into the final sequence or by the limited reusage of DNA parts due to specific DNA part modifications. Furthermore, the design of the DNA parts is cumbersome or requires a construct-specific and sequential assembly strategy. To overcome these limitations, a universal and simple DNA assembly method was utilized in this thesis and is based on concatenating unmodified DNA parts. This is achieved by guiding a prokaryotic ligase to the nicks in between two DNA parts by temporarily connecting them by a complementary bridge made of DNA. These bridges are called bridging oligos (BOs) and are 40 to 70 bases long single-stranded DNA. To shuffle the order of DNA parts in the final sequence, only new BOs are added to the reaction mixture. In contrast to other methods, there is no need to reorder or reamplify the DNA parts. Allover, this assembly method supports the rapid build process for biology by fulfilling the criteria 'reusable' and 'scarless' and is named ligase cycling reaction (LCR) [11, 16, 74, 83].
The automation of the LCR includes the

1. *in silico* design of BOs and final constructs followed by the
2. device-aided assembly in the wet-lab to generate constructs.

Both were addressed by utilizing the software `Geneious` and the robotic platform of the CompuGene project and Prof. Dr. Johannes Kabisch. First, the protocol of the LCR assembly was optimized to ensure more efficient DNA assemblies and to decrease the screening effort to a minimal level (section 3.1). The optimization experiments based on a plasmid with two fluorescent reporter genes to determine the assembly efficiency and the total number of colonies. Both reporter genes consisted of the same terminator sequence. The plasmid was split into 79 to 2974 bp subparts to simulate a challenging assembly. Based on this toy-model plasmid, the

efficiency and total number of colonies were determined to rate the success of each assembly condition. Although the protocol was validated by assemblies of additional plasmids, the robustness of the LCR is still related to unknown issues. The ability of *E. coli* to utilize and alter the DNA in the following transformation step and the blunt-end activity of the utilized ligase 'Ampligase®' are thought to cause an unpredictable assembly behavior. Both were observed in the results of this thesis and are shown in Figures 3.19 (page 60) and, respectively, Figure 3.13 (page 54). Nevertheless, the optimized protocol is clearly improving the results of *in vivo* LCRs even if *E. coli* and the ligase are utilized (Figure 3.9). If the improved protocol is beneficial for all LCR assemblies has to be validated. According to the results presented in this thesis the reasons for the improved LCR protocol seem to be related to sequence-unspecific issues like the omission of DMSO/betaine and the more favorable reaction temperature for the involved ligase. Nevertheless, the three utilized plasmids for the assemblies are not covering a broad range in total size or amount of parts. More plasmids need to be designed and assembled by using several protocols.

The speed of the *in vivo* LCR workflow is limited by the associated effort of transforming each LCR in *E. coli* and to screen the so derived colonies (both workflows shown in Figure 1.4 on page 7). Instead, a cell-free LCR was developed by linking the cell free protein synthesis with a DNA amplification step, the rolling circle amplification (RCA). A protocol was designed to enable high-throughput assays in a total volume of 3.6 µL (section 3.3). Furthermore, all steps of the *in vitro* LCR are performed in non-optical 384-well PCR-plates instead of using significantly more expensive optical plates. To conclude, the time-consuming transformation, plating and colony screening steps were substituted by the addition of a cell extract of *E. coli*. This enabled an *in vitro* readout of LCRs whereby the assembly criteria of the *in vivo* LCR 'efficiency' and 'total CFUs' were substituted by quantifying a fluorescent signal derived by a cell free protein synthesis (CFPS). As another feature, a high number of biological repetitions can be achieved to avoid underpowered experimental designs. By this, the influence of the annealing time in the LCR and the blunt-end activity of the ligase were validated (Figure 3.26) as hypothesized for the *in vivo* LCR. Unfortunately, the *in vitro* LCR is performed with undefined conditions due to the RCA kit. This kit has to be substituted by a polymerase and defined reac¸tion buffers to lower the financial effort for this method and to further optimize the protocol. Furthermore, it is highly recommended to utilize a nanoliter dispensing unit to mix the reactions. By this, a lower deviation of the results was observed (Supplementary Figure 6.25).

Second, the new LCR protocol was validated and the derived new rules and parameters were included in the development of a software plugin for `Geneious` (subsection 3.4.2). This tool enables the automated design of BOs and the final sequence of the construct. As a special feature, the plugin is capable of performing a combinatorial design with members of predefined DNA groups including the output of all final sequences and unique BOs. Unfortunately, the minimal DNA part size is limited to 100 bp in the current version of the plugin due to an increased the risk of overlapping BOs. Further, the default target T_m can probably not be reached during the

design. Due to both issues, the software plugin automatically omits too small sequences for LCR designs. To further increase the flexibility of the LCR, the lower size limit has to be investigated experimentally or an appropriate specific strategy has to be developed. For latter, a part with a size of 6 bp was successfully incorporated in initial experiments by utilizing the vivo LCR approach. The BO design was performed manually by ignoring the small part. The designed BO was spanning from the 3'-end of the previous part to the 5'-start of the next part with the desired target T_m each. A control reaction without the ligase also resulted in the desired construct and supports the theory, that *E. coli* participate in the assembly. By this, the host can be utilized to assemble small DNA parts and to enable a strategy for the *in silico* and *in vivo* LCR assembly.
Finally, the optimized LCR protocol was transferred to the robotic platform for an hypothetical and automated assembly approach (section 3.4). Besides the cytometer, all devices of the platform (shown in Figure 2.3 on 31) are utilized for the automated assembly of 96 constructs within 19 h. A nanoliter liquid handling unit, the I-DOT, automatically dispenses liquids from a DNA library plate into a 96-well PCR plate by following a user-defined dispensing protocol. Afterwards, all residual volumes of the utilized liquids are refilled into the library plate. This supports the automated multiple usage of DNA parts and increases the sustainability of already amplified or synthesized building bricks. Nevertheless, the automated design of the dispensing protocol and linking it to the positions of the liquids in the DNA library plate is not incorporated in the workflow. This increases the risk to transfer the false liquids into the source wells of the I-DOT plate. One workaround to prevent this is to add the desired liquids and their initial volumes to a database first. The user should only design the dispensing protocol with the unique names or IDs of the liquids. By a search, the liquid will be automatically transferred from the library plate to the I-DOT plate followed by the dispensing. After the backfill from the I-DOT plate to the library plate, the volumes of each utilized liquid has to be recalculated and is based on the dispensed volume plus an additional volume due to loss during the liquid transfer processes in the platform. For future applications, a fridge or freezer has to be incorporated into the robotic platform to enable the automatic handling of the library plates. For transforming more than 96 LCRs into *E. coli*, additional space for storing the agar plates is required. This would also include the utilization of additional PCR plates with LCRs. So far, the workflow can generate only one 96-well PCR plate with the maximum of 96 LCRs. In the case of more LCRs, the existing workflow has to be further developed and an accessible freezer or fridge and an additional thermal cycler has to be implemented. Another option to increase the number of LCRs in one run is to utilize a 384-well cycler (heating-block) and corresponding PCR plates. Nevertheless, the automated LCR workflow enables the user to assemble 96 LCRs in one run. To pick and screen the derived colonies, fluorescent genes can be incorporated as a visual selection marker to enable a fluorescence based colony screening. For this, a UV-light chamber and a colony picker has to be incorporated into the platform. Another approach utilizes the plate reader of the platform to detect colonies and their fluorescence and to use the pipetting robot 'Felix 1' for the colony picking. This is already under development in the group of Prof. Dr. Kabisch and the

PhD student Thomas Zoll. A successful implementation would increase the flexible usage of the platform, would circumvent the implementation of additional devices and enable the automated colony screening, picking and cultivation directly after the growth of colonies. To gain more insights into the LCR, the *in vitro* approach offers a chance to accelerate the rapid prototyping of DNA-constructs, the characterization of synthetic circuits and to generate statistically robust results for modeling approaches. For this, the already implemented workflow for the *in vivo* LCR can be adapted.

In total, the automated DNA assembly was achieved by a) investigating an improved LCR protocol and potential bottlenecks, b) by an automated, fast and combinatorial design of LCR assemblies and BOs and c) by transferring the improved LCR to a robotic platform to design a hypothetical workflow for the assembly of 96 3 µL LCR-reactions within 19 h. So far, the automated LCR workflow was tested by running all steps without liquids, cells and agar. This still has to be validated by performing the full capacity of 96 assemblies to prove the applicability of the hypothetical workflow.

5 Bibliography

[1] **Albert**, K.J., **Bradshaw**, J.T., **Knaide**, T.R. and **Rogers**, A.L., 2006. *Verifying Liquid-Handler Performance for Complex or Nonaqueous Reagents: A New Approach*. JALA: Journal of the Association for Laboratory Automation, vol. 11(4):pp. 172–180. ISSN 1535-5535. doi:10.1016/j.jala.2006.06.003.

[2] **Barria**, C., **Malecki**, M. and **Arraiano**, C.M., 2013. *Bacterial adaptation to cold*. Microbiology (Reading, England), vol. 159(Pt 12):pp. 2437–2443. ISSN 1465-2080. doi:10.1099/mic.0.052209-0.

[3] **Bode**, M., **Khor**, S., **Ye**, H., **Li**, M.H. and **Ying**, J.Y., 2009. *TmPrime: fast, flexible oligonucleotide design software for gene synthesis*. Nucleic Acids Research, vol. 37(suppl_2):pp. W214–W221. ISSN 1362-4962, 0305-1048. doi:10.1093/nar/gkp461.

[4] **Breslauer**, K.J., **Frank**, R., **Blöcker**, H. and **Marky**, L.A., 1986. *Predicting DNA duplex stability from the base sequence*. Proceedings of the National Academy of Sciences of the United States of America, vol. 83(11):pp. 3746–3750. ISSN 0027-8424. doi:10.1073/pnas.83.11.3746.

[5] **Bzymek**, M. and **Lovett**, S.T., 2001. *Instability of repetitive DNA sequences: the role of replication in multiple mechanisms*. Proceedings of the National Academy of Sciences, vol. 98(15):pp. 8319–8325. ISSN 0027-8424, 1091-6490. doi:10.1073/pnas.111008398.

[6] **Cardelli**, L., **Hernansaiz-Ballesteros**, R.D., **Dalchau**, N. and **Csikász-Nagy**, A., 2017. *Efficient Switches in Biology and Computer Science*. PLOS Computational Biology, vol. 13(1):p. e1005100. ISSN 1553-7358. doi:10.1371/journal.pcbi.1005100.

[7] **Cardinale**, S. and **Arkin**, A.P., 2012. *Contextualizing context for synthetic biology – identifying causes of failure of synthetic biological systems*. Biotechnology Journal, vol. 7(7):pp. 856–866. ISSN 1860-7314. doi:10.1002/biot.201200085.

[8] **Carpenter**, A.E., **Jones**, T.R., **Lamprecht**, M.R., **Clarke**, C., **Kang**, I.H., **Friman**, O., **Guertin**, D.A., **Chang**, J.H., **Lindquist**, R.A., **Moffat**, J., **Golland**, P. and **Sabatini**, D.M., 2006. *CellProfiler: image analysis software for identifying and quantifying cell phenotypes*. Genome Biology, vol. 7(10):p. R100. ISSN 1474-760X. doi:10.1186/gb-2006-7-10-r100.

[9] **Cermak**, T., **Doyle**, E.L., **Christian**, M., **Wang**, L., **Zhang**, Y., **Schmidt**, C., **Baller**, J.A., **Somia**, N.V., **Bogdanove**, A.J. and **Voytas**, D.F., 2011. *Efficient design and assembly of custom TALEN and other TAL effector-based constructs for DNA targeting*. Nucleic Acids Research, vol. 39(12):p. e82. ISSN 1362-4962. doi:10.1093/nar/gkr218.

[10] **Chai**, S.C., **Goktug**, A.N., **Cui**, J., **Low**, J. and **Chen**, T., 2013. *Practical Considerations of Liquid Handling Devices in Drug Discovery*. Drug Discovery. doi:10.5772/52546.

[11] **Chandran**, S., 2017. *Rapid assembly of DNA via ligase cycling Reaction (LCR)*. In R.A. Hughes, ed., Synthetic DNA, vol. 1472, pp. 105–110. Springer New York, New York, NY. ISBN 978-1-4939-6341-6 978-1-4939-6343-0. doi:10.1007/978-1-4939-6343-0_8.

[12] **Chase**, J.W. and **Richardson**, C.C., 1974. *Exonuclease VII of Escherichia coli PURIFICATION AND PROPERTIES*. Journal of Biological Chemistry, vol. 249(14):pp. 4545–4552. ISSN 0021-9258, 1083-351X.

[13] **Cho**, N., **Hwang**, B., **Yoon**, J.K., **Park**, S., **Lee**, J., **Seo**, H.N., **Lee**, J., **Huh**, S., **Chung**, J. and **Bang**, D., 2015. *De novo assembly and next-generation sequencing to analyse full-length gene variants from codon-barcoded libraries*. Nature Communications, vol. 6:p. 8351. ISSN 2041-1723. doi:10.1038/ncomms9351.

[14] **Chong**, S., 2014. *Overview of Cell-Free Protein Synthesis: Historic Landmarks, Commercial Systems, and Expanding Applications*. Current Protocols in Molecular Biology, vol. 108(1):pp. 16.30.1–16.30.11. ISSN 1934-3647. doi:10.1002/0471142727.mb1630s108.

[15] **Davis**, D.L., **O'Brie**, E.P. and **Bentzley**, C.M., 2000. *Analysis of the degradation of oligonucleotide strands during the freezing/thawing processes using MALDI-MS*. Analytical Chemistry, vol. 72(20):pp. 5092–5096. ISSN 0003-2700. doi:10.1021/ac000225s.

[16] **de Kok**, S., **Stanton**, L.H., **Slaby**, T., **Durot**, M., **Holmes**, V.F., **Patel**, K.G., **Platt**, D., **Shapland**, E.B., **Serber**, Z., **Dean**, J., **Newman**, J.D. and **Chandran**, S.S., 2014. *Rapid and reliable DNA assembly via ligase cycling reaction*. ACS Synthetic Biology, vol. 3(2):pp. 97–106. ISSN 2161-5063, 2161-5063. doi:10.1021/sb4001992.

[17] **Dean**, F.B., **Nelson**, J.R., **Giesler**, T.L. and **Lasken**, R.S., 2001. *Rapid Amplification of Plasmid and Phage DNA Using Phi29 DNA Polymerase and Multiply-Primed Rolling Circle Amplification*. Genome Research, vol. 11(6):pp. 1095–1099. ISSN 1088-9051. doi:10.1101/gr.180501.

[18] **Del Vecchio**, D., **Ninfa**, A.J. and **Sontag**, E.D., 2008. *Modular cell biology: retroactivity and insulation*. Molecular Systems Biology, vol. 4(1):p. 161. ISSN 1744-4292. doi:10.1038/msb4100204.

[19] **Doherty**, A.J. and **Dafforn**, T.R., 2000. *Nick recognition by DNA ligases11Edited by K. Nagai*. Journal of Molecular Biology, vol. 296(1):pp. 43–56. ISSN 0022-2836. doi: 10.1006/jmbi.1999.3423.

[20] **Doherty**, A.J. and **Suh**, S.W., 2000. *Structural and mechanistic conservation in DNA ligases*. Nucleic Acids Research, vol. 28(21):pp. 4051–4058. ISSN 0305-1048.

[21] **Dutra**, B.E., **Sutera**, V.A. and **Lovett**, S.T., 2007. *RecA-independent recombination is efficient but limited by exonucleases*. Proceedings of the National Academy of Sciences, vol. 104(1):pp. 216–221. ISSN 0027-8424, 1091-6490. doi:10.1073/pnas.0608293104.

[22] **El-Ashram**, S., **Al Nasr**, I. and **Suo**, X., 2016. *Nucleic acid protocols: Extraction and optimization*. Biotechnology Reports, vol. 12:pp. 33–39. ISSN 2215-017X. doi:10.1016/j.btre.2016.10.001.

[23] **Ellis**, T., **Adie**, T. and **Baldwin**, G.S., 2011. *DNA assembly for synthetic biology: from parts to pathways and beyond*. Integrative Biology: Quantitative Biosciences from Nano to Macro, vol. 3(2):pp. 109–118. ISSN 1757-9708. doi:10.1039/c0ib00070a.

[24] **Engler**, C., **Gruetzner**, R., **Kandzia**, R. and **Marillonnet**, S., 2009. *Golden gate shuffling: a one-pot DNA shuffling method based on type IIs restriction enzymes*. PLoS ONE, vol. 4(5):p. e5553. ISSN 1932-6203. doi:10.1371/journal.pone.0005553.

[25] **Engler**, C., **Kandzia**, R. and **Marillonnet**, S., 2008. *A one pot, one step, precision cloning method with high throughput capability*. PLoS ONE, vol. 3(11):p. e3647. ISSN 1932-6203. doi:10.1371/journal.pone.0003647.

[26] **Engler**, C. and **Marillonnet**, S., 2013. *Combinatorial DNA Assembly Using Golden Gate Cloning*. In K.M. Polizzi and C. Kontoravdi, eds., Synthetic Biology, Methods in Molecular Biology, pp. 141–156. Humana Press, Totowa, NJ. ISBN 978-1-62703-625-2. doi: 10.1007/978-1-62703-625-2_12.

[27] **Enroth**, C.H., **Fehler**, A.O., **Poulsen**, L.D. and **Vinther**, J., 2019. *Excess primer degradation by Exo I improves the preparation of 3' cDNA ligation-based sequencing libraries*. BioTechniques, vol. 67(3):pp. 110–116. ISSN 1940-9818. doi:10.2144/btn-2018-0178.

[28] **Falk**, J., **Bronstein**, L., **Hanst**, M., **Drossel**, B. and **Koeppl**, H., 2019. *Context in synthetic biology: Memory effects of environments with mono-molecular reactions*. The Journal of Chemical Physics, vol. 150(2):p. 024106. ISSN 0021-9606, 1089-7690. doi:10.1063/1.5053816.

[29] **Freemont**, P.S., 2019. *Synthetic biology industry: data-driven design is creating new opportunities in biotechnology*. Emerging Topics in Life Sciences, vol. 3(5):pp. 651–657. ISSN 2397-8554. doi:10.1042/ETLS20190040.

[30] **Galdzicki**, M., **Clancy**, K.P., **Oberortner**, E., **Pocock**, M., **Quinn**, J.Y., **Rodriguez**, C.A., **Roehner**, N., **Wilson**, M.L., **Adam**, L., **Anderson**, J.C., **Bartley**, B.A., **Beal**, J., **Chandran**, D., **Chen**, J., **Densmore**, D., **Endy**, D., **Grünberg**, R., **Hallinan**, J., **Hillson**, N.J., **Johnson**, J.D., **Kuchinsky**, A., **Lux**, M., **Misirli**, G., **Peccoud**, J., **Plahar**, H.A., **Sirin**, E., **Stan**, G.B., **Villalobos**, A., **Wipat**, A., **Gennari**, J.H., **Myers**, C.J. and **Sauro**, H.M., 2014. *The Synthetic Biology Open Language (SBOL) provides a community standard for communicating designs in synthetic biology*. Nature Biotechnology, vol. 32(6):pp. 545–550. ISSN 1546-1696. doi:10.1038/nbt.2891.

[31] **Garamella**, J., **Garenne**, D. and **Noireaux**, V., 2019. *TXTL-based approach to synthetic cells*. Methods in Enzymology, vol. 617:pp. 217–239. ISSN 1557-7988. doi:10.1016/bs.mie.2018.12.015.

[32] **Geissmann**, Q., 2013. *OpenCFU, a new free and open-source software to count cell colonies and other circular objects*. PLOS ONE, vol. 8(2):p. e54072. ISSN 1932-6203. doi:10.1371/journal.pone.0054072.

[33] **Gibriel**, A.A. and **Adel**, O., 2017. *Advances in ligase chain reaction and ligation-based amplifications for genotyping assays: Detection and applications*. Mutation Research/Reviews in Mutation Research, vol. 773:pp. 66–90. ISSN 1383-5742. doi:10.1016/j.mrrev.2017.05.001.

[34] **Gibson**, D.G., **Young**, L., **Chuang**, R.Y., **Venter**, J.C., **Hutchison**, C.A. and **Smith**, H.O., 2009. *Enzymatic assembly of DNA molecules up to several hundred kilobases*. Nature Methods, vol. 6(5):pp. 343–345. ISSN 1548-7091, 1548-7105. doi:10.1038/nmeth.1318.

[35] **Giladi**, H., **Goldenberg**, D., **Koby**, S. and **Oppenheim**, A.B., 1995. *Enhanced activity of the bacteriophage lambda PL promoter at low temperature.* Proceedings of the National Academy of Sciences of the United States of America, vol. 92(6):pp. 2184–2188. ISSN 0027-8424.

[36] **Green**, M.R. and **Sambrook**, J., 2018. *The Hanahan Method for Preparation and Transformation of Competent Escherichia coli: High-Efficiency Transformation*. Cold Spring Harbor Protocols, vol. 2018(3):p. pdb.prot101188. ISSN 1940-3402, 1559-6095. doi:10.1101/pdb.prot101188.

[37] **HamediRad**, M., **Weisberg**, S., **Chao**, R., **Lian**, J. and **Zhao**, H., 2019. *Highly Efficient Single-Pot Scarless Golden Gate Assembly*. ACS Synthetic Biology, vol. 8(5):pp. 1047–1054. ISSN 2161-5063, 2161-5063. doi:10.1021/acssynbio.8b00480.

[38] **Hanahan**, D., 1983. *Studies on transformation of Escherichia coli with plasmids*. Journal of Molecular Biology, vol. 166(4):pp. 557–580. ISSN 0022-2836. doi:10.1016/S0022-2836(83)80284-8.

[39] **Hanahan**, D., **Jessee**, J. and **Bloom**, F.R., 1991. *Plasmid transformation of Escherichia coli and other bacteria*. Methods in Enzymology, vol. 204:pp. 63–113. ISSN 0076-6879. doi:10.1016/0076-6879(91)04006-a.

[40] **Hendling**, M., **Pabinger**, S., **Peters**, K., **Wolff**, N., **Conzemius**, R. and **Barišić**, I., 2018. *Oli2go: an automated multiplex oligonucleotide design tool*. Nucleic Acids Research, vol. 46(W1):pp. W252–W256. ISSN 0305-1048. doi:10.1093/nar/gky319.

[41] **Hillson**, N.J., **Rosengarten**, R.D. and **Keasling**, J.D., 2012. *j5 DNA Assembly Design Automation Software*. ACS Synthetic Biology, vol. 1(1):pp. 14–21. doi:10.1021/sb2000116.

[42] **Hong**, S.H., 2019. *"Cell-Free Synthetic Biology": Synthetic Biology Meets Cell-Free Protein Synthesis*. Methods and Protocols, vol. 2(4):p. 80. doi:10.3390/mps2040080.

[43] **Hughes**, R.A. and **Ellington**, A.D., 2017. *Synthetic DNA Synthesis and Assembly: Putting the Synthetic in Synthetic Biology*. Cold Spring Harbor Perspectives in Biology, vol. 9(1). ISSN 1943-0264. doi:10.1101/cshperspect.a023812.

[44] **Hutchison**, C.A., **Smith**, H.O., **Pfannkoch**, C. and **Venter**, J.C., 2005. *Cell-free cloning using phi29 DNA polymerase*. Proceedings of the National Academy of Sciences of the United States of America, vol. 102(48):pp. 17332–17336. ISSN 0027-8424. doi:10.1073/pnas.0508809102.

[45] **Iverson**, S.V., **Haddock**, T.L., **Beal**, J. and **Densmore**, D.M., 2016. *CIDAR MoClo: Improved MoClo Assembly Standard and New E. coli Part Library Enable Rapid Combinatorial Design for Synthetic and Traditional Biology*. ACS Synthetic Biology, vol. 5(1):pp. 99–103. doi:10.1021/acssynbio.5b00124.

[46] **Jacobus**, A.P. and **Gross**, J., 2015. *Optimal cloning of PCR fragments by homologous recombination in Escherichia coli*. PLOS ONE, vol. 10(3):p. e0119221. ISSN 1932-6203. doi:10.1371/journal.pone.0119221.

[47] **Jessop-Fabre**, M.M. and **Sonnenschein**, N., 2019. *Improving Reproducibility in Synthetic Biology*. Frontiers in Bioengineering and Biotechnology, vol. 7. ISSN 2296-4185. doi:10.3389/fbioe.2019.00018.

[48] **Jung**, H., **Pena-Francesch**, A., **Saadat**, A., **Sebastian**, A., **Kim**, D.H., **Hamilton**, R.F., **Albert**, I., **Allen**, B.D. and **Demirel**, M.C., 2016. *Molecular tandem repeat strategy for elucidating mechanical properties of high-strength proteins*. Proceedings of the National Academy of Sciences of the United States of America, vol. 113(23):pp. 6478–6483. ISSN 0027-8424. doi:10.1073/pnas.1521645113.

[49] **Kamens**, J., 2014. *Addgene: Making Materials Sharing "Science As Usual"*. PLOS Biology, vol. 12(11):p. e1001991. ISSN 1545-7885. doi:10.1371/journal.pbio.1001991.

[50] **Kamens**, J., 2015. *The Addgene repository: an international nonprofit plasmid and data resource*. Nucleic Acids Research, vol. 43(Database issue):pp. D1152–D1157. ISSN 0305-1048. doi:10.1093/nar/gku893.

[51] **Karamasioti**, E., **Lormeau**, C. and **Stelling**, J., 2017. *Computational design of biological circuits: putting parts into context*. Molecular Systems Design & Engineering, vol. 2(4):pp. 410–421. ISSN 2058-9689. doi:10.1039/C7ME00032D.

[52] **Kearse**, M., **Moir**, R., **Wilson**, A., **Stones-Havas**, S., **Cheung**, M., **Sturrock**, S., **Buxton**, S., **Cooper**, A., **Markowitz**, S., **Duran**, C., **Thierer**, T., **Ashton**, B., **Meintjes**, P. and **Drummond**, A., 2012. *Geneious basic: an integrated and extendable desktop software platform for the organization and analysis of sequence data*. Bioinformatics, vol. 28(12):pp. 1647–1649. ISSN 1367-4803. doi:10.1093/bioinformatics/bts199.

[53] **Khatib**, S.E. and **Yassine**, N.A., 2019. *Advances in Synthetic Biology and Metabolic Engineering in the Production of Biofuel*. International Journal of Current Microbiology and Applied Sciences, vol. 8(09):pp. 1762–1772. ISSN 23197692, 23197706. doi:10.20546/ijcmas.2019.809.204.

[54] **Kostylev**, M., **Otwell**, A.E., **Richardson**, R.E. and **Suzuki**, Y., 2015. *Cloning Should Be Simple: Escherichia coli DH5α-Mediated Assembly of Multiple DNA Fragments with Short End Homologies*. PloS One, vol. 10(9):p. e0137466. ISSN 1932-6203. doi:10.1371/journal.pone.0137466.

[55] **Kouprina**, N. and **Larionov**, V., 2016. *Transformation-associated recombination (TAR) cloning for genomics studies and synthetic biology*. Chromosoma, vol. 125(4):pp. 621–632. ISSN 1432-0886. doi:10.1007/s00412-016-0588-3.

[56] **Kumar**, G. and **Chernaya**, G., 2009. *Cell-free protein synthesis using multiply-primed rolling circle amplification products*. BioTechniques, vol. 47(1):pp. 637–639. ISSN 0736-6205. doi:10.2144/000113171.

[57] **Kunjapur**, A.M., **Pfingstag**, P. and **Thompson**, N.C., 2018. *Gene synthesis allows biologists to source genes from farther away in the tree of life*. Nature Communications, vol. 9(1):pp. 1–11. ISSN 2041-1723. doi:10.1038/s41467-018-06798-7.

[58] **Lee**, H.H., **Molla**, M.N., **Cantor**, C.R. and **Collins**, J.J., 2010. *Bacterial charity work leads to population-wide resistance*. Nature, vol. 467(7311):pp. 82–85. ISSN 1476-4687. doi:10.1038/nature09354.

[59] **Lee**, M.E., **DeLoache**, W.C., **Cervantes**, B. and **Dueber**, J.E., 2015. *A highly characterized yeast toolkit for modular, multipart assembly*. ACS Synthetic Biology, vol. 4(9):pp. 975–986. ISSN 2161-5063, 2161-5063. doi:10.1021/sb500366v.

[60] **Lehman**, I.R. and **Nussbaum**, A.L., 1964. *THE DEOXYRIBONUCLEASES OF ESCHERICHIA COLI. V. ON THE SPECIFICITY OF EXONUCLEASE I (PHOSPHODIESTERASE)*. The Journal of biological chemistry, vol. 239:pp. 2628–2636.

[61] **Lehr**, F.X., **Hanst**, M., **Vogel**, M., **Kremer**, J., **Göringer**, H.U., **Suess**, B. and **Koeppl**, H., 2019. *Cell-Free Prototyping of AND-Logic Gates Based on Heterogeneous RNA Activators*. ACS Synthetic Biology, vol. 8(9):pp. 2163–2173. doi:10.1021/acssynbio.9b00238.

[62] **Li**, H., **Cui**, X. and **Arnheim**, N., 1991. *Eliminating primers from completed polymerase chain reactions with exonuclease VII*. Nucleic Acids Research, vol. 19(11):pp. 3139–3141. ISSN 0305-1048. doi:10.1093/nar/19.11.3139.

[63] **Ma**, S., **Tang**, N. and **Tian**, J., 2012. *DNA synthesis, assembly and applications in synthetic biology*. Current Opinion in Chemical Biology, vol. 16(3-4):pp. 260–267. ISSN 1879-0402. doi:10.1016/j.cbpa.2012.05.001.

[64] **Marincevic-Zuniga**, Y., **Gustavsson**, I. and **Gyllensten**, U., 2012. *Multiply-primed rolling circle amplification of human papillomavirus using sequence-specific primers*. Virology, vol. 432(1):pp. 57–62. ISSN 1096-0341. doi:10.1016/j.virol.2012.05.030.

[65] **Markarian**, S.A., **Asatryan**, A.M., **Grigoryan**, K.R. and **Sargsyan**, H.R., 2006. *Effect of diethylsulfoxide on the thermal denaturation of DNA*. Biopolymers, vol. 82(1):pp. 1–5. ISSN 1097-0282. doi:10.1002/bip.20454.

[66] **Marshall**, R. and **Noireaux**, V., 2018. *Synthetic Biology with an All E. coli TXTL System: Quantitative Characterization of Regulatory Elements and Gene Circuits*. Methods in Molecular Biology (Clifton, N.J.), vol. 1772:pp. 61–93. ISSN 1940-6029. doi:10.1007/978-1-4939-7795-6_4.

[67] **Mierzejewska**, K., **Siwek**, W., **Czapinska**, H., **Kaus-Drobek**, M., **Radlinska**, M., **Skowronek**, K., **Bujnicki**, J.M., **Dadlez**, M. and **Bochtler**, M., 2014. *Structural basis of the methylation specificity of R.DpnI*. Nucleic Acids Research, vol. 42(13):pp. 8745–8754. ISSN 0305-1048. doi:10.1093/nar/gku546.

[68] **Nandakumar**, J., **Nair**, P.A. and **Shuman**, S., 2007. *Last Stop on the Road to Repair: Structure of E. coli DNA Ligase Bound to Nicked DNA-Adenylate*. Molecular Cell, vol. 26(2):pp. 257–271. ISSN 1097-2765. doi:10.1016/j.molcel.2007.02.026.

[69] **Nielsen**, A.A.K., **Der**, B.S., **Shin**, J., **Vaidyanathan**, P., **Paralanov**, V., **Strychalski**, E.A., **Ross**, D., **Densmore**, D. and **Voigt**, C.A., 2016. *Genetic circuit design automation*. Science, vol. 352(6281). ISSN 0036-8075, 1095-9203. doi:10.1126/science.aac7341.

[70] **Nowak**, R.M., **Wojtowicz-Krawiec**, A. and **Plucienniczak**, A., 2015. *DNASynth: a computer program for assembly of artificial gene parts in decreasing temperature*.

BioMed Research International, vol. 2015:pp. 1–8. ISSN 2314-6133, 2314-6141. doi: 10.1155/2015/413262.

[71] **Odell**, M. and **Shuman**, S., 1999. *Footprinting of Chlorella virus DNA ligase bound at a nick in duplex DNA*. The Journal of Biological Chemistry, vol. 274(20):pp. 14032–14039. ISSN 0021-9258. doi:10.1074/jbc.274.20.14032.

[72] **Owczarzy**, R., **Moreira**, B.G., **You**, Y., **Behlke**, M.A. and **Walder**, J.A., 2008. *Predicting stability of DNA duplexes in solutions containing magnesium and monovalent cations*. Biochemistry, vol. 47(19):pp. 5336–5353. ISSN 0006-2960. doi:10.1021/bi702363u.

[73] **Owczarzy**, R., **You**, Y., **Moreira**, B.G., **Manthey**, J.A., **Huang**, L., **Behlke**, M.A. and **Walder**, J.A., 2004. *Effects of Sodium Ions on DNA Duplex Oligomers: Improved Predictions of Melting Temperatures*. Biochemistry, vol. 43(12):pp. 3537–3554. ISSN 0006-2960, 1520-4995. doi:10.1021/bi034621r.

[74] **Pachuk**, C.J., **Samuel**, M., **Zurawski**, J.A., **Snyder**, L., **Phillips**, P. and **Satishchandran**, C., 2000. *Chain reaction cloning: a one-step method for directional ligation of multiple DNA fragments*. Gene, vol. 243(1-2):pp. 19–25. ISSN 0378-1119.

[75] **Panjkovich**, A. and **Melo**, F., 2005. *Comparison of different melting temperature calculation methods for short DNA sequences*. Bioinformatics, vol. 21(6):pp. 711–722. ISSN 1367-4803. doi:10.1093/bioinformatics/bti066.

[76] **Paoli**, H.C.D., **Tuskan**, G.A. and **Yang**, X., 2016. *An innovative platform for quick and flexible joining of assorted DNA fragments*. Scientific Reports, vol. 6(1):pp. 1–14. ISSN 2045-2322. doi:10.1038/srep19278.

[77] **Pedrolli**, D.B., **Ribeiro**, N.V., **Squizato**, P.N., **de Jesus**, V.N., **Cozetto**, D.A., **Tuma**, R.B., **Gracindo**, A., **Cesar**, M.B., **Freire**, P.J.C., **da Costa**, A.F.M., **Lins**, M.R.C.R., **Correa**, G.G. and **Cerri**, M.O., 2019. *Engineering Microbial Living Therapeutics: The Synthetic Biology Toolbox*. Trends in Biotechnology, vol. 37(1):pp. 100–115. ISSN 0167-7799. doi:10.1016/j.tibtech.2018.09.005.

[78] **Pena-Francesch**, A. and **Demirel**, M.C., 2019. *Squid-Inspired Tandem Repeat Proteins: Functional Fibers and Films*. Frontiers in Chemistry, vol. 7. ISSN 2296-2646. doi: 10.3389/fchem.2019.00069.

[79] **Pingoud**, A. and **Jeltsch**, A., 2001. *Structure and function of type II restriction endonucleases*. Nucleic Acids Research, vol. 29(18):pp. 3705–3727. ISSN 0305-1048.

[80] **Quan**, J. and **Tian**, J., 2009. *Circular polymerase extension cloning of complex gene libraries and pathways*. PLoS ONE, vol. 4(7):p. e6441. ISSN 1932-6203. doi:10.1371/journal.pone.0006441.

[81] **Robinson**, C.J., **Dunstan**, M.S., **Swainston**, N., **Titchmarsh**, J., **Takano**, E., **Scrutton**, N.S. and **Jervis**, A.J., 2018. *Chapter Thirteen - Multifragment DNA Assembly of Biochemical Pathways via Automated Ligase Cycling Reaction*. In N. Scrutton, ed., Methods in Enzymology, vol. 608 of *Enzymes in synthetic biology*, pp. 369–392. Academic Press. doi:10.1016/bs.mie.2018.04.011.

[82] **Rossmanith**, P., **Röder**, B., **Frühwirth**, K., **Vogl**, C. and **Wagner**, M., 2011. *Mechanisms of degradation of DNA standards for calibration function during storage*. Applied Microbiology and Biotechnology, vol. 89(2):pp. 407–417. ISSN 1432-0614. doi:10.1007/s00253-010-2943-2.

[83] **Roth**, T.L., **Milenkovic**, L. and **Scott**, M.P., 2014. *A rapid and simple method for DNA engineering using cycled ligation assembly*. PLOS ONE, vol. 9(9):p. e107329. ISSN 1932-6203. doi:10.1371/journal.pone.0107329.

[84] **Roy**, S. and **Caruthers**, M., 2013. *Synthesis of DNA/RNA and their analogs via phosphoramidite and H-phosphonate chemistries*. Molecules (Basel, Switzerland), vol. 18(11):pp. 14268–14284. ISSN 1420-3049. doi:10.3390/molecules181114268.

[85] **Rustad**, M., **Eastlund**, A., **Jardine**, P. and **Noireaux**, V., 2018. *Cell-free TXTL synthesis of infectious bacteriophage T4 in a single test tube reaction*. Synthetic Biology, vol. 3(1). doi:10.1093/synbio/ysy002.

[86] **Röder**, B., **Frühwirth**, K., **Vogl**, C., **Wagner**, M. and **Rossmanith**, P., 2010. *Impact of Long-Term Storage on Stability of Standard DNA for Nucleic Acid-Based Methods*. Journal of Clinical Microbiology, vol. 48(11):pp. 4260–4262. ISSN 0095-1137. doi:10.1128/JCM.01230-10.

[87] **Salas**, M., **Blanco**, L., **Lázaro**, J.M. and **de Vega**, M., 2008. *The bacteriophage phi29 DNA polymerase*. IUBMB Life, vol. 60(1):pp. 82–85. ISSN 1521-6543. doi:10.1002/iub.19.

[88] **Salis**, H.M., **Mirsky**, E.A. and **Voigt**, C.A., 2009. *Automated design of synthetic ribosome binding sites to control protein expression*. Nature Biotechnology, vol. 27(10):pp. 946–950. ISSN 1546-1696. doi:10.1038/nbt.1568.

[89] **SantaLucia**, J., 1998. *A unified view of polymer, dumbbell, and oligonucleotide DNA nearest-neighbor thermodynamics*. Proceedings of the National Academy of Sciences, vol. 95(4):pp. 1460–1465. ISSN 0027-8424, 1091-6490. doi:10.1073/pnas.95.4.1460.

[90] **SantaLucia**, J., 2007. *Physical principles and visual-OMP software for optimal PCR design*. In J.M. Walker and A. Yuryev, eds., PCR Primer Design, vol. 402, pp. 3–33. Humana Press, Totowa, NJ. ISBN 978-1-58829-725-9 978-1-59745-528-2. doi:10.1007/978-1-59745-528-2_1.

[91] **SantaLucia**, J., **Allawi**, H.T. and **Seneviratne**, P.A., 1996. *Improved Nearest-Neighbor Parameters for Predicting DNA Duplex Stability †*. Biochemistry, vol. 35(11):pp. 3555–3562. ISSN 0006-2960, 1520-4995. doi:10.1021/bi951907q.

[92] **SantaLucia**, J. and **Hicks**, D., 2004. *The thermodynamics of DNA structural motifs*. Annual Review of Biophysics and Biomolecular Structure, vol. 33:pp. 415–440. ISSN 1056-8700. doi:10.1146/annurev.biophys.32.110601.141800.

[93] **Schaudien**, D., **Baumgärtner**, W. and **Herden**, C., 2007. *High preservation of DNA standards diluted in 50% glycerol*. Diagnostic Molecular Pathology: The American Journal of Surgical Pathology, Part B, vol. 16(3):pp. 153–157. ISSN 1052-9551. doi:10.1097/PDM.0b013e31803c558a.

[94] **Schildkraut**, C. and **Lifson**, S., 1965. *Dependence of the melting temperature of DNA on salt concentration*. Biopolymers, vol. 3(2):pp. 195–208. ISSN 0006-3525, 1097-0282. doi:10.1002/bip.360030207.

[95] **Schlichting**, N., **Reinhardt**, F., **Jager**, S., **Schmidt**, M. and **Kabisch**, J., 2019. *Optimization of the experimental parameters of the ligase cycling reaction*. Synthetic Biology, vol. 4(1). doi:10.1093/synbio/ysz020.

[96] **Shin**, J. and **Noireaux**, V., 2012. *An E. coli cell-free expression toolbox: application to synthetic gene circuits and artificial cells*. ACS Synthetic Biology, vol. 1(1):pp. 29–41. doi:10.1021/sb200016s.

[97] **Shuman**, S., 1995. *Vaccinia virus DNA ligase: specificity, fidelity, and inhibition*. Biochemistry, vol. 34(49):pp. 16138–16147. ISSN 0006-2960. doi:10.1021/bi00049a029.

[98] **Shuman**, S., 2009. *DNA Ligases: Progress and Prospects*. The Journal of Biological Chemistry, vol. 284(26):pp. 17365–17369. ISSN 0021-9258. doi:10.1074/jbc.R900017200.

[99] **Silbersack**, J., **Juergen**, B., **Hecker**, M., **Schneidinger**, B., **Schmuck**, R. and **Schweder**, T., 2006. *An acetoin-regulated expression system of Bacillus subtilis*. Applied Microbiology and Biotechnology, vol. 73(4):pp. 895–903. ISSN 1432-0614. doi:10.1007/s00253-006-0549-5.

[100] **Smanski**, M.J., **Bhatia**, S., **Zhao**, D., **Park**, Y., **B A Woodruff**, L., **Giannoukos**, G., **Ciulla**, D., **Busby**, M., **Calderon**, J., **Nicol**, R., **Gordon**, D.B., **Densmore**, D. and **Voigt**, C.A., 2014. *Functional optimization of gene clusters by combinatorial design and assembly*. Nature Biotechnology, vol. 32(12):pp. 1241–1249. ISSN 1546-1696. doi:10.1038/nbt.3063.

[101] **Stevens**, H., **Rector**, A. and **Ranst**, M.V., 2010. *Multiply Primed Rolling-Circle Amplification Method for the Amplification of Circular DNA Viruses*. Cold Spring Harbor Protocols, vol. 2010(4):p. pdb.prot5415. ISSN 1940-3402, 1559-6095. doi:10.1101/pdb.prot5415.

[102] **Storch**, M., **Casini**, A., **Mackrow**, B., **Fleming**, T., **Trewhitt**, H., **Ellis**, T. and **Baldwin**, G.S., 2015. *BASIC: A new biopart assembly standard for idempotent cloning provides accurate, single-tier DNA assembly for synthetic biology*. ACS Synthetic Biology, vol. 4(7):pp. 781–787. ISSN 2161-5063, 2161-5063. doi:10.1021/sb500356d.

[103] **Storch**, M., **Haines**, M.C. and **Baldwin**, G.S., 2019. *DNA-BOT: A low-cost, automated DNA assembly platform for synthetic biology*. bioRxiv, p. 832139. doi:10.1101/832139.

[104] **Sugimoto**, N., **Nakano**, S., **Katoh**, M., **Matsumura**, A., **Nakamuta**, H., **Ohmichi**, T., **Yoneyama**, M. and **Sasaki**, M., 1995. *Thermodynamic parameters to predict stability of RNA/DNA hybrid duplexes*. Biochemistry, vol. 34(35):pp. 11211–11216. ISSN 0006-2960. doi:10.1021/bi00035a029.

[105] **Sugimoto**, N., **Nakano**, S., **Yoneyama**, M. and **Honda**, K., 1996. *Improved thermodynamic parameters and helix initiation factor to predict stability of DNA duplexes*. Nucleic Acids Research, vol. 24(22):pp. 4501–4505. ISSN 0305-1048. doi:10.1093/nar/24.22.4501.

[106] **Sun**, Z.Z., **Hayes**, C.A., **Shin**, J., **Caschera**, F., **Murray**, R.M. and **Noireaux**, V., 2013. *Protocols for Implementing an Escherichia coli Based TX-TL Cell-Free Expression System for Synthetic Biology*. JoVE (Journal of Visualized Experiments), vol. 0(79):p. e50762. ISSN 1940-087X. doi:10.3791/50762.

[107] **Swainston**, N., **Dunstan**, M., **Jervis**, A.J., **Robinson**, C.J., **Carbonell**, P., **Williams**, A.R., **Faulon**, J.L., **Scrutton**, N.S. and **Kell**, D.B., 2018. *PartsGenie: an integrated tool for optimizing and sharing synthetic biology parts*. Bioinformatics, vol. 34(13):pp. 2327–2329. ISSN 1367-4803. doi:10.1093/bioinformatics/bty105.

[108] **Tang**, Z., **Wang**, K., **Tan**, W., **Ma**, C., **Li**, J., **Liu**, L., **Guo**, Q. and **Meng**, X., 2005. *Real-time investigation of nucleic acids phosphorylation process using molecular beacons*. Nucleic Acids Research, vol. 33(11):p. e97. ISSN 0305-1048. doi:10.1093/nar/gni096.

[109] **Taylor**, G.M., **Mordaka**, P.M. and **Heap**, J.T., 2019. *Start-Stop Assembly: a functionally scarless DNA assembly system optimized for metabolic engineering*. Nucleic Acids Research, vol. 47(3):pp. e17–e17. ISSN 0305-1048. doi:10.1093/nar/gky1182.

[110] **Tew**, D., 2019. *Synthetic biology and healthcare*. Emerging Topics in Life Sciences, vol. 3(5):pp. 659–667. ISSN 2397-8554. doi:10.1042/ETLS20190086.

[111] **Untergasser**, A., **Cutcutache**, I., **Koressaar**, T., **Ye**, J., **Faircloth**, B.C., **Remm**, M. and **Rozen**, S.G., 2012. *Primer3-new capabilities and interfaces*. Nucleic Acids Research, vol. 40(15):p. e115. ISSN 0305-1048. doi:10.1093/nar/gks596.

[112] **Vasudevamurthy**, M.K., **Lever**, M., **George**, P.M. and **Morison**, K.R., 2009. *Betaine structure and the presence of hydroxyl groups alters the effects on DNA melting temperatures*. Biopolymers, vol. 91(1):pp. 85–94. ISSN 1097-0282. doi:10.1002/bip.21085.

[113] **Vazquez-Vilar**, M., **Orzaez**, D. and **Patron**, N., 2018. *DNA assembly standards: Setting the low-level programming code for plant biotechnology*. Plant Science, vol. 273:pp. 33–41. ISSN 0168-9452. doi:10.1016/j.plantsci.2018.02.024.

[114] **Walsh**, D.I., **Pavan**, M., **Ortiz**, L., **Wick**, S., **Bobrow**, J., **Guido**, N.J., **Leinicke**, S., **Fu**, D., **Pandit**, S., **Qin**, L., **Carr**, P.A. and **Densmore**, D., 2019. *Standardizing Automated DNA Assembly: Best Practices, Metrics, and Protocols Using Robots*. SLAS TECHNOLOGY: Translating Life Sciences Innovation, vol. 24(3):pp. 282–290. ISSN 2472-6303. doi:10.1177/2472630318825335.

[115] **Wang**, L., **Jiang**, S., **Chen**, C., **He**, W., **Wu**, X., **Wang**, F., **Tong**, T., **Zou**, X., **Li**, Z., **Luo**, J., **Deng**, Z. and **Chen**, S., 2018. *Synthetic Genomics: From DNA Synthesis to Genome Design*. Angewandte Chemie International Edition, vol. 57(7):pp. 1748–1756. ISSN 1521-3773. doi:10.1002/anie.201708741.

[116] **Wang**, Y.H., **Wei**, K.Y. and **Smolke**, C.D., 2013. *Synthetic biology: advancing the design of diverse genetic systems*. Annual review of chemical and biomolecular engineering, vol. 4:pp. 69–102. ISSN 1947-5438. doi:10.1146/annurev-chembioeng-061312-103351.

[117] **Watson**, J.F. and **García-Nafría**, J., 2019. *In vivo DNA assembly using common laboratory bacteria: A re-emerging tool to simplify molecular cloning*. The Journal of Biological Chemistry, vol. 294(42):pp. 15271–15281. ISSN 0021-9258. doi:10.1074/jbc.REV119.009109.

[118] **Wenzel**, M. and **Altenbuchner**, J., 2015. *Development of a markerless gene deletion system for Bacillus subtilis based on the mannose phosphoenolpyruvate-dependent phosphotransferase system*. Microbiology (Reading, England), vol. 161(10):pp. 1942–1949. ISSN 1465-2080; 1350-0872. doi:10.1099/mic.0.000150.

[119] **Werle**, E., **Schneider**, C., **Renner**, M., **Völker**, M. and **Fiehn**, W., 1994. *Convenient single-step, one tube purification of PCR products for direct sequencing.* Nucleic Acids Research, vol. 22(20):pp. 4354–4355. ISSN 0305-1048.

[120] **Wetmur**, J.G., 1991. *DNA Probes: Applications of the Principles of Nucleic Acid Hybridization*. Critical Reviews in Biochemistry and Molecular Biology, vol. 26(3-4):pp. 227–259. ISSN 1040-9238, 1549-7798. doi:10.3109/10409239109114069.

[121] **Wiedmann**, M., **Wilson**, W.J., **Czajka**, J., **Luo**, J., **Barany**, F. and **Batt**, C.A., 1994. *Ligase chain reaction (LCR)–overview and applications.* Genome Research, vol. 3(4):pp. S51–S64. ISSN 1088-9051, 1549-5469.

[122] **Wilson**, E.H., **Sagawa**, S., **Weis**, J.W., **Schubert**, M.G., **Bissell**, M., **Hawthorne**, B., **Reeves**, C.D., **Dean**, J. and **Platt**, D., 2016. *Genotype Specification Language*. ACS Synthetic Biology, vol. 5(6):pp. 471–478. ISSN 2161-5063, 2161-5063. doi:10.1021/acssynbio.5b00194.

[123] **Xiang**, Y., **Dalchau**, N. and **Wang**, B., 2018. *Scaling up genetic circuit design for cellular computing: advances and prospects*. Natural Computing, vol. 17(4):pp. 833–853. ISSN 1572-9796. doi:10.1007/s11047-018-9715-9.

[124] **Yang**, J., **Kim**, B., **Kim**, G.Y., **Jung**, G.Y. and **Seo**, S.W., 2019. *Synthetic biology for evolutionary engineering: from perturbation of genotype to acquisition of desired phenotype*. Biotechnology for Biofuels, vol. 12(1):p. 113. ISSN 1754-6834. doi:10.1186/s13068-019-1460-5.

[125] **Yoshino**, J. and **Imai**, S.i., 2013. *Accurate measurement of nicotinamide adenine dinucleotide (NAD+) with high-performance liquid chromatography*. Methods in molecular biology (Clifton, N.J.), vol. 1077:pp. 203–215. ISSN 1064-3745. doi:10.1007/978-1-62703-637-5_14.

[126] **Zhang**, Y., **Werling**, U. and **Edelmann**, W., 2012. *SLiCE: a novel bacterial cell extract-based DNA cloning method*. Nucleic Acids Research, vol. 40(8):p. e55. ISSN 0305-1048. doi:10.1093/nar/gkr1288.

6 Supplement

6.1 LCR Optimization

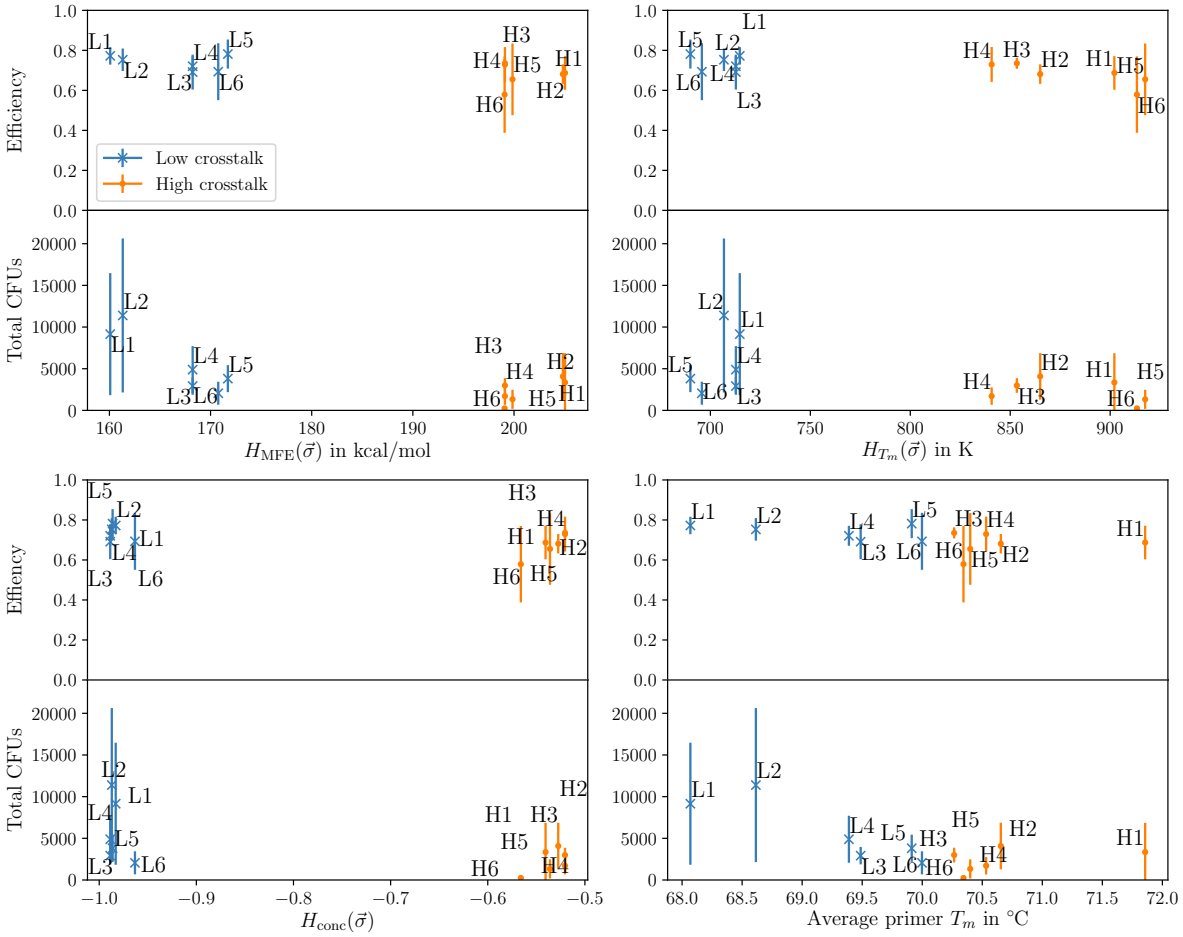

Supplementary Figure 6.1: Efficiency and total number of CFUs depending on crosstalk and melting temperatures. The data is from the LCRs without DMSO and betaine of the seven parted toy-plasmid. All LCRs were performed as quintuplets. Sets with a minimized folding energy perform better than the remaining sets, but the reason is likely their low melting temperature and not their low crosstalk. Their crosstalk evaluated by H_{T_m} and H_{conc} does not differ from the other low-crosstalk sets, which further suggests that the melting temperature is the main reason for the performance. This figure is adapted from Schlichting *et al.* [95].

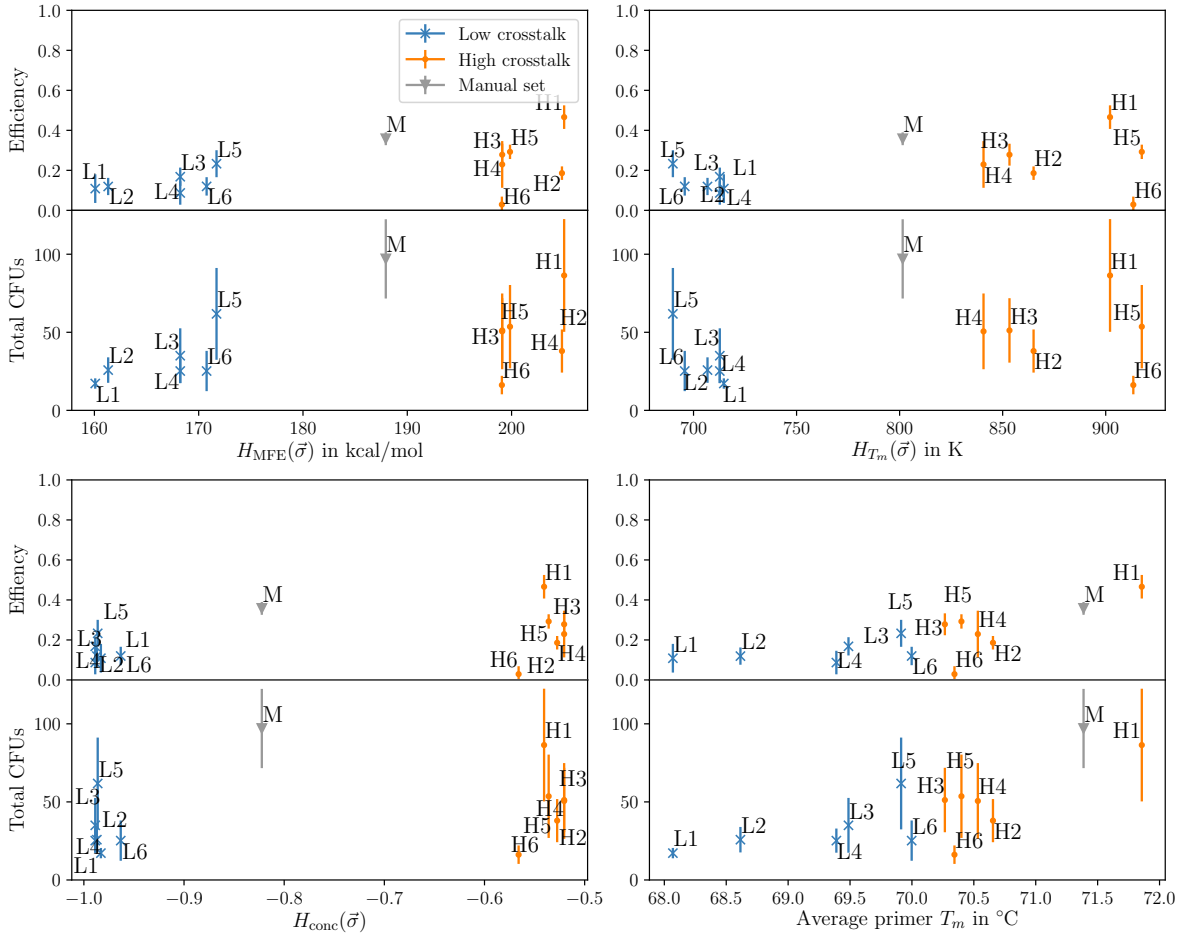

Supplementary Figure 6.2: Efficiency and total number of CFUs depending on crosstalk and melting temperatures of BO sets with crosstalk optimized towards high (H) or low (L) values plus one manually designed set (M). The data is from the LCRs with 8 % v/v DMSO and 0.45 M betaine of the seven parted toy-plasmid. All LCRs were performed as quintuplets. The optimization criterion for each set can be seen in the crosstalk plots, e.g. sets L1 and L2 appear at the very left of the MFE crosstalk plot because they were optimized for low MFE crosstalk. High-crosstalk sets perform better than low-crosstalk sets because greater crosstalk is usually accompanied by greater melting temperatures; this counteracts the effect of DMSO and betaine, which lower the melting temperature. Ultimately, secondary structure was inhibited so much by DMSO and betaine that crosstalk could not occur and the BOs could barely attach to their complementary DNA parts. Thus the melting temperatures were a better criterion for performance than crosstalk. MFE: minimal folding energy. This figure is adapted from Schlichting *et al.* [95].

6.1.1 Phenotypes of the colonies obtained by the LCRs with the toy-model plasmid

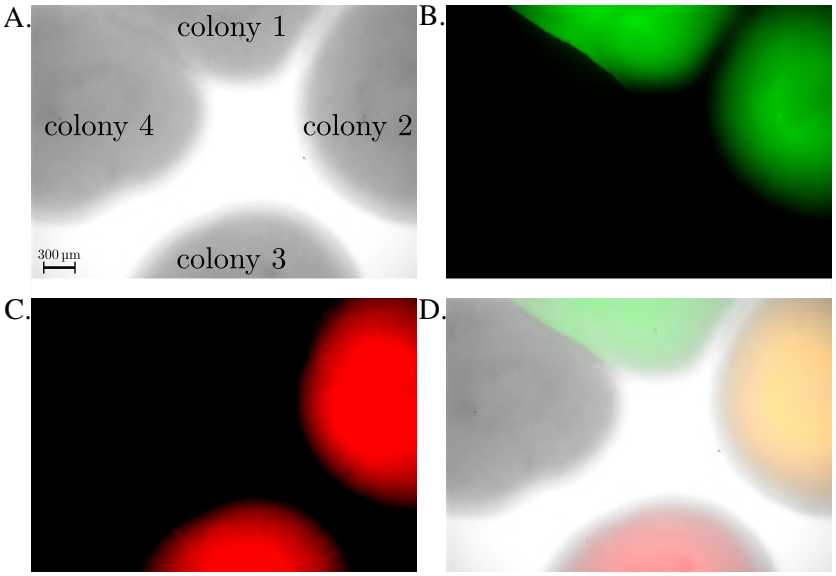

Supplementary Figure 6.3: The four observed phenotypes of CFUs after the transformation of the LCRs of the toy-model plasmid. The "colony 2" with the red and green phenotype contained the correct sequence of the toy-model plasmid. The magnification of the images is 40×. **A**. Brightfield image of four colonies. **B**. Image of the colonies shown in A with (colonies 1 and 2) and without sfGFP. **C**. Image of colonies shown in A and B with and without mRFP1 (colonies 2 and 3). **D**. Overlay of the images A-C. CFU: colony forming unit, mRFP1: monomeric red fluorescent protein 1, sfGFP: superfolder green fluorescent protein. This figure is adapted from Schlichting *et al.* [95].

6.1.2 Optimization experiments with the toy-model plasmid

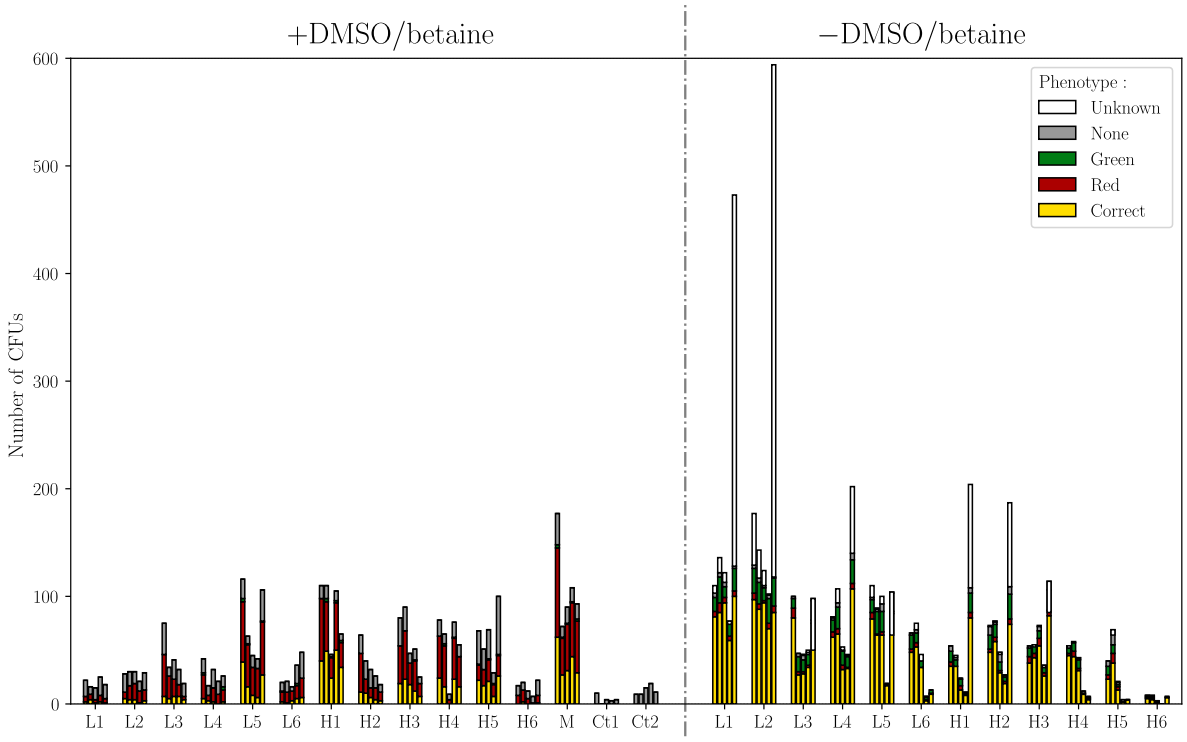

Supplementary Figure 6.4: Overview of raw data of the experiments to investigate and calculate the influence/omission of DMSO and betaine of the seven parted toy-plasmid (Supplementary Figure 3.2). All LCRs were performed as quintuplets. Bridging oligo sets with minimized (L1-L6) crosstalk, maximized (H1-H6) crosstalk and the manually designed set (M) are presented. The negative control reactions with BOs without ligase (Ct1) and without BOs and ligase (Ct2) resulted in no fluorescent colonies and were only performed for the LCRs with DMSO/betaine. For the LCRs without DMSO and betaine the amount of CFUs presented here were corrected by multiplying them with the correction factor of 50. All CFUs were counted, but only the phenotypes of about 100 CFUs per LCR were determined. White bars indicate CFUs where the phenotype was not determined. All BO sequences are shown in Supplementary Table 6.2. BO: bridging oligo, CFU: colony forming unit, DMSO: dimethyl sulfoxide, T_m: melting temperature of a BO-half. This figure is adapted from Schlichting *et al.* [95].

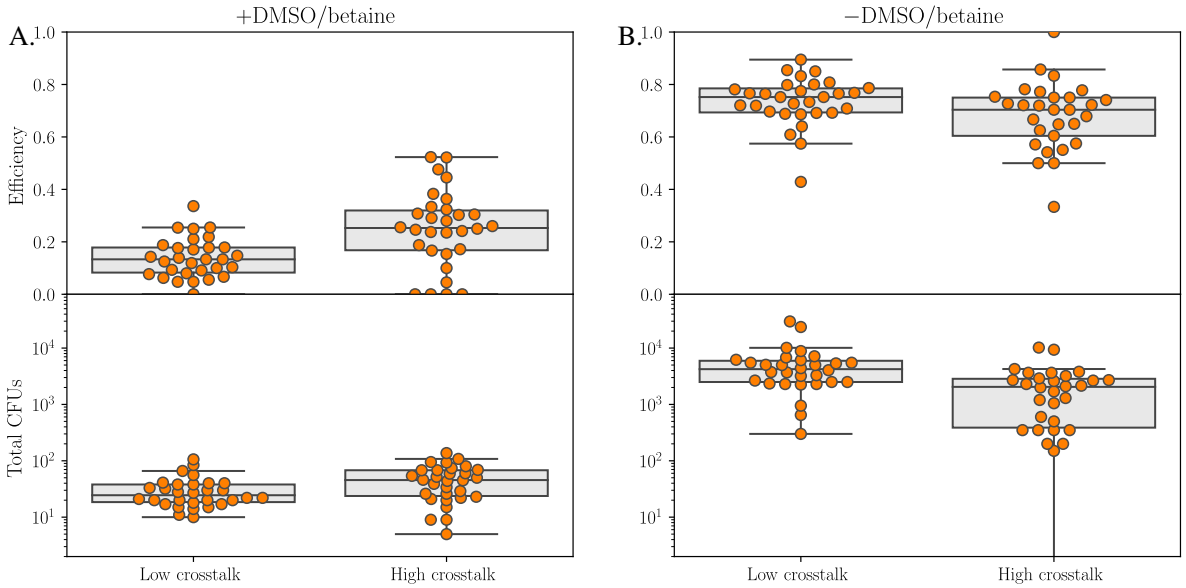

Supplementary Figure 6.5: Overview of the seven parted LCR of the toy-model plasmid by utilizing six bridging oligo-sets (BO-sets) with low crosstalk and six BO-sets with high crosstalk. Each BO-set was used five times to assemble the toy-model plasmid (Figure 3.1B) by using the baseline-conditions with 8 % v/v DMSO/0.45 M betaine and without both detergents. For all LCRs, 3 µL were transformed by electroporation in 30 µL NEB® 10-β *E. coli* cells. For more detailed results of each BO-set refer to Supplementary Figures 6.4 and 3.2. **A.** The baseline-conditions with DMSO and betaine resulted in low efficiencies and low amounts of colonies. No correlation between crosstalk and BO performance was found. **B.** LCRs without DMSO and betaine resulted in more colonies and higher efficiencies in comparison to the baseline-conditions. The sequences of all BO-sets are shown in Supplementary Table 6.2. BO: bridging oligo, CFU: colony forming unit, DMSO: dimethyl sulfoxide. This figure is adapted from Schlichting *et al.* [95].

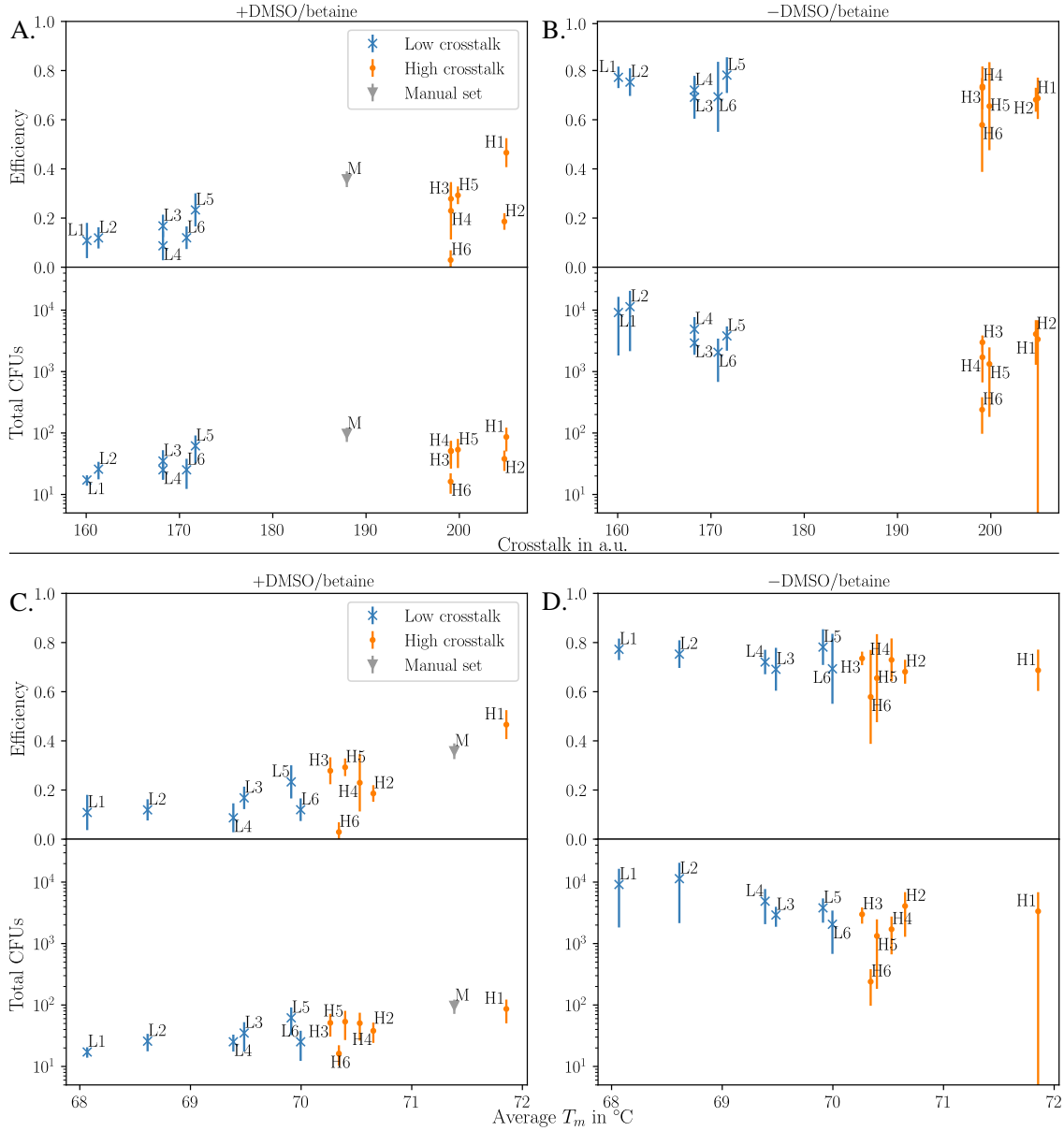

Supplementary Figure 6.6: Graphical analysis of the bridging oligo sets (BO-sets) utilized for the assembly of a seven parted toy-plasmid, based on the results shown in Supplementary Figure 3.2. **A+B.** No crosstalk-dependent effects of the BOs were observed for the LCR with (A) and without (B) DMSO/betaine. Both clusters (L1-L6 and H1-H6) were distinguishable by the crosstalk but without affecting the LCR efficiency and total amount of colonies. Slightly higher efficiencies and more colonies were observed for the cluster of the sets H1-H6 when DMSO/betaine was used. **C+D.**: The average melting temperature of the BO-sets influenced the LCRs. Higher T_ms resulted in higher efficiencies and more colonies when DMSO and betaine were used (C). Without DMSO and betaine, all BO-sets resulted in similar efficiencies suggesting no impact of crosstalk of BOs with the DNA parts in the LCR-assembly of the seven parted toy-plasmid. More colonies were observed for sets L1-L6. In contrast to LCRs with DMSO and betaine (C), the total amount of colonies was found to be increasing with decreasing melting temperatures. All T_ms presented here were calculated by using the formula of SantaLucia [89] for the T_m calculation and salt correction. The manual set ("M", used for LCRs with DMSO and betaine) was designed in `Geneious` with the same algorithms and a target temperature of 70 °C. The difference of ~1.5 °C in comparison to the target T_m of 70 °C is due to the lack of an option to specify the DNA part concentration in the software. The raw data of the LCRs presented here are shown in Supplementary Figure 6.4. This figure is adapted from Schlichting *et al.* [95].

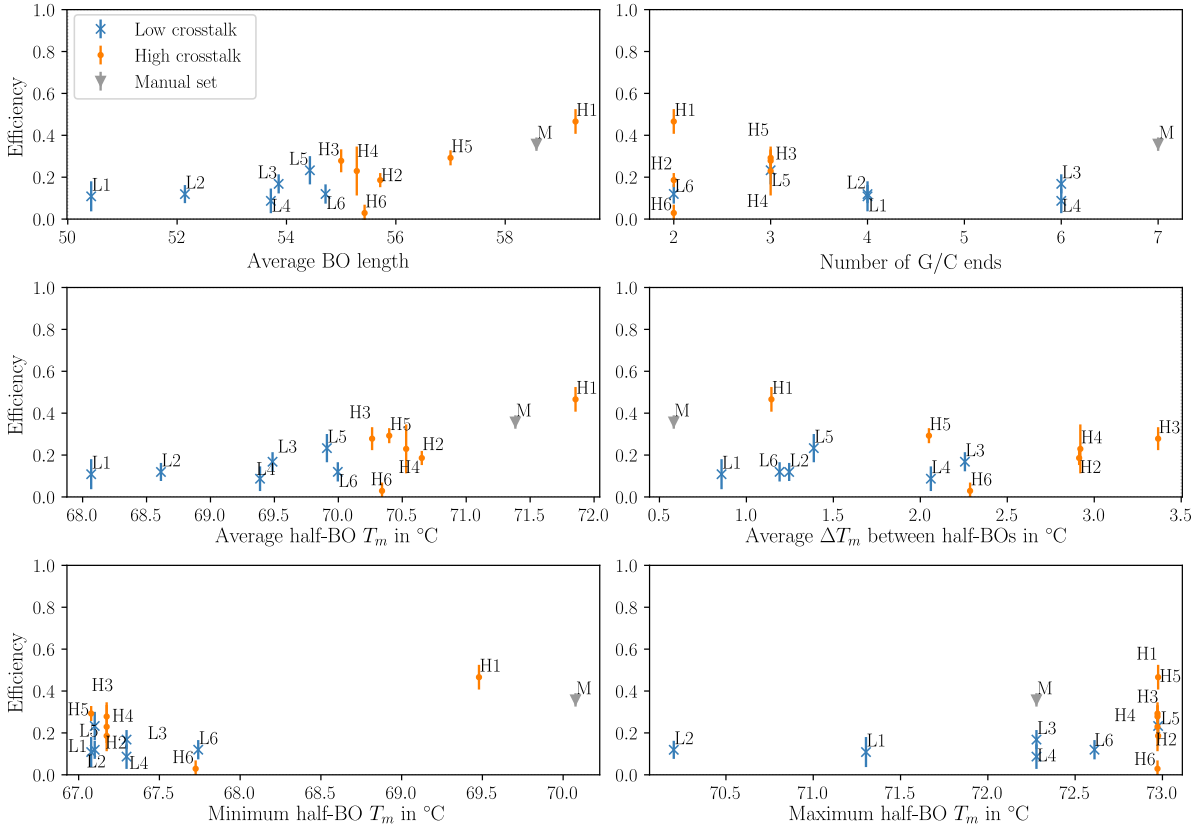

Supplementary Figure 6.7: Graphical analysis of LCRs with 8 % v/v DMSO and 0.45 M betaine of the seven parted toy-plasmid and the influence of various predictors on the efficiencies by utilizing different bridging oligo sets. All LCRs were performed as quintuplets. The standard deviation for each LCR is indicated by error bars. All BO sequences are shown in Supplementary Table 6.2. BO: bridging oligo, DMSO: dimethyl sulfoxide, G/C end: 3'-end of one BO ending with the nucleobase guanine or cytosine, T_m: melting temperature. This figure is adapted from Schlichting *et al.* [95].

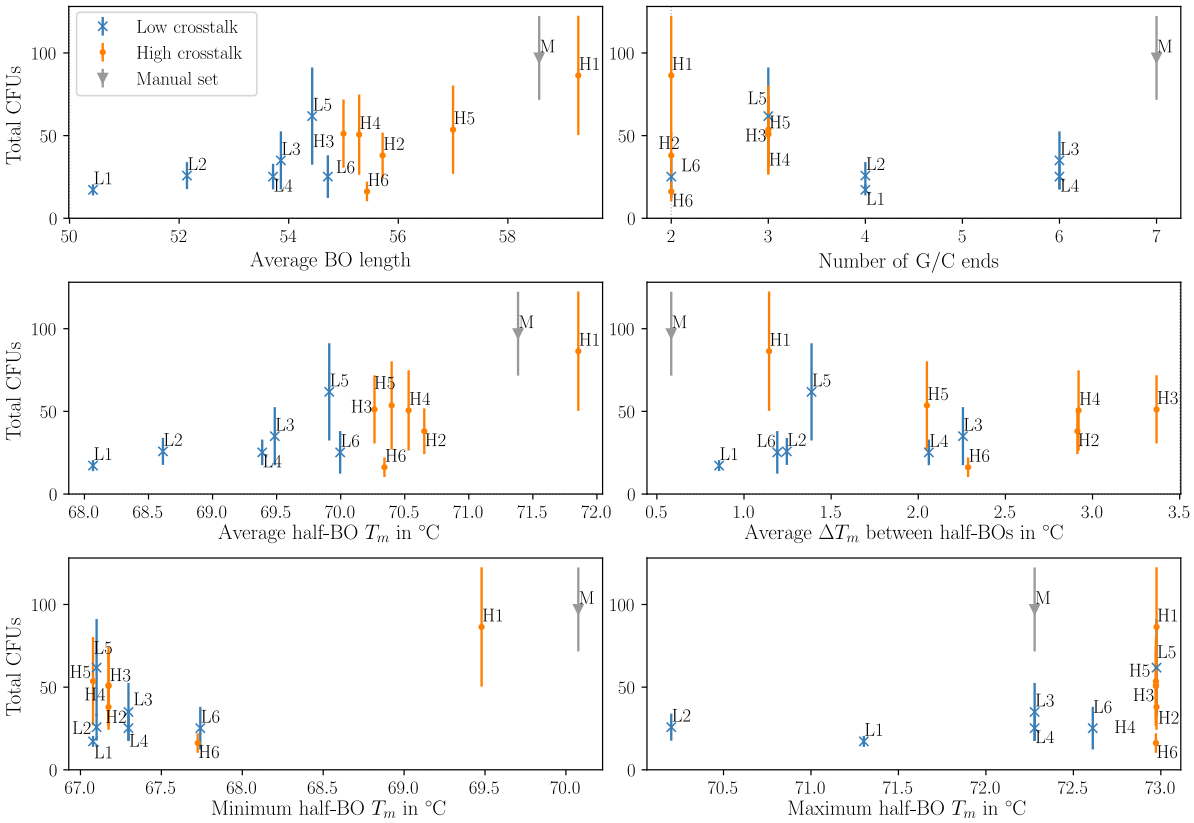

Supplementary Figure 6.8: Graphical analysis of LCRs with 8 %v/v DMSO and 0.45 M betaine of the seven parted toy-plasmid and the influence of various predictors on the total amount of colonies by utilizing different bridging oligo sets. All LCRs were performed as quintuplets. The standard deviation for each LCR is indicated by error bars. All BO sequences are shown in Supplementary Table 6.2. BO: bridging oligo, CFU: colony forming unit, DMSO: dimethyl sulfoxide, G/C end: 3'-end of one BO ending with the nucleobase guanine or cytosine, T_m: melting temperature. This figure is adapted from Schlichting *et al.* [95].

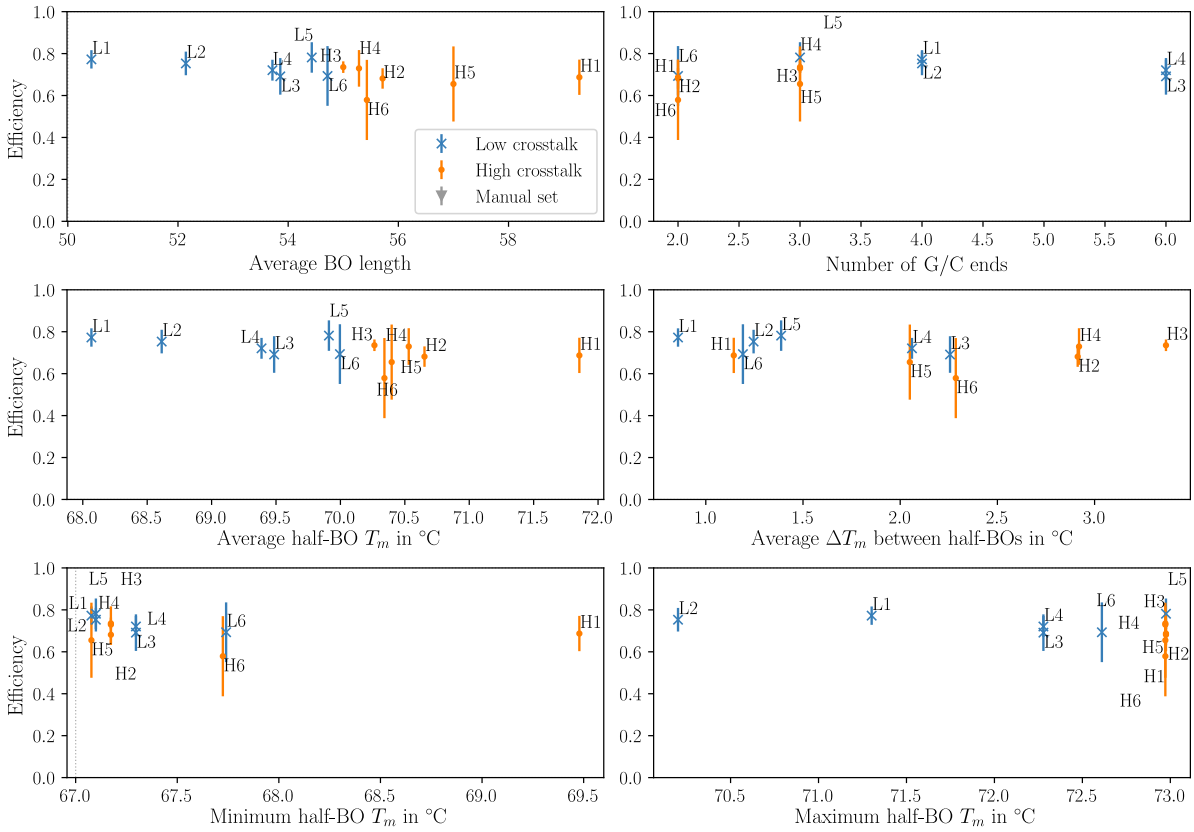

Supplementary Figure 6.9: Graphical analysis of LCRs without 8 % v/v DMSO and 0.45 M betaine of the seven parted toy-plasmid and the influence of various predictors on the efficiencies by utilizing different bridging oligo sets. All LCRs were performed as quintuplets. The standard deviation for each LCR is indicated by error bars. All BO sequences are shown in Supplementary Table 6.2. BO: bridging oligo, DMSO: dimethyl sulfoxide, G/C end: 3'-end of one BO ending with the nucleobase guanine or cytosine, T_m: melting temperature. This figure is adapted from Schlichting *et al.* [95].

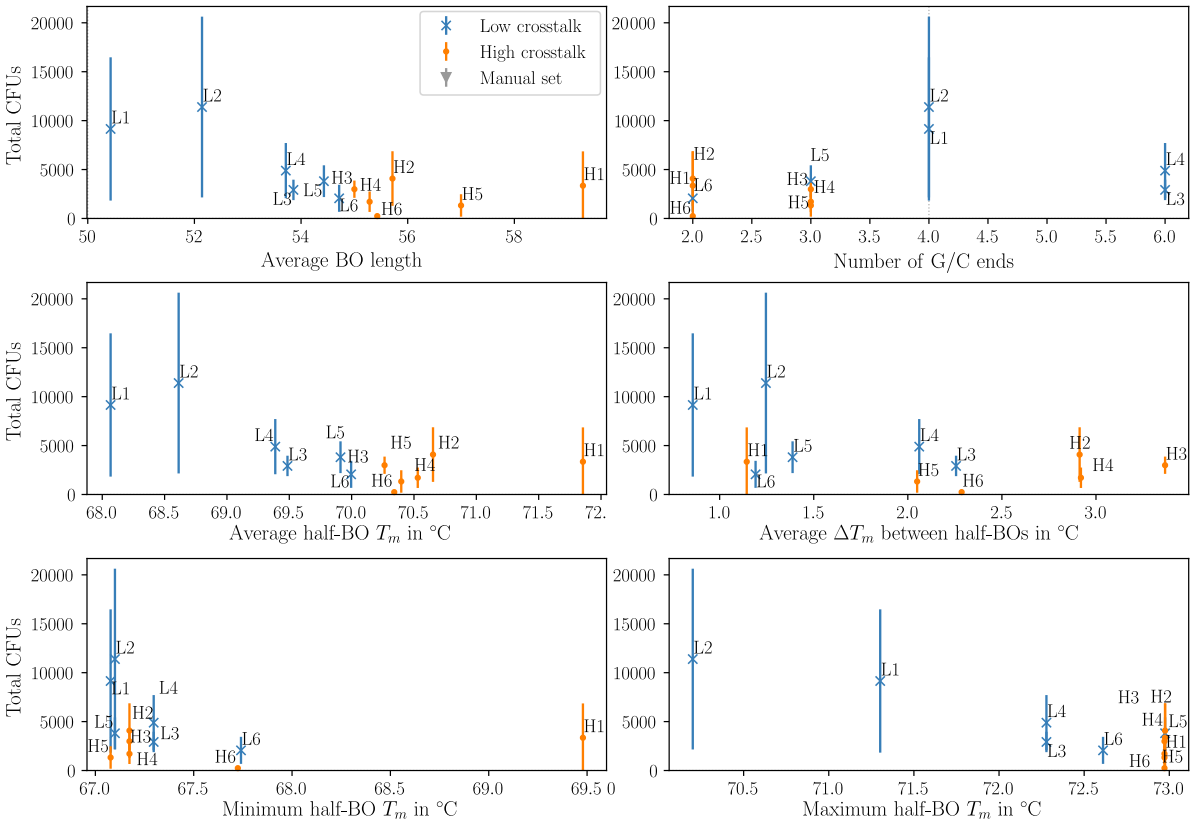

Supplementary Figure 6.10: Graphical analysis of LCRs without 8 % v/v DMSO and 0.45 M betaine of the seven parted toy-plasmid and the influence of various predictors on the total amount of colonies by utilizing different bridging oligo sets. All LCRs were performed as quintuplets. The standard deviation for each LCR is indicated by error bars. All BO sequences are shown in Supplementary Table 6.2. BO: bridging oligo, CFU: colony forming unit, DMSO: dimethyl sulfoxide, G/C end: 3'-end of one BO ending with the nucleobase guanine or cytosine, T_m: melting temperature. This figure is adapted from Schlichting *et al.* [95].

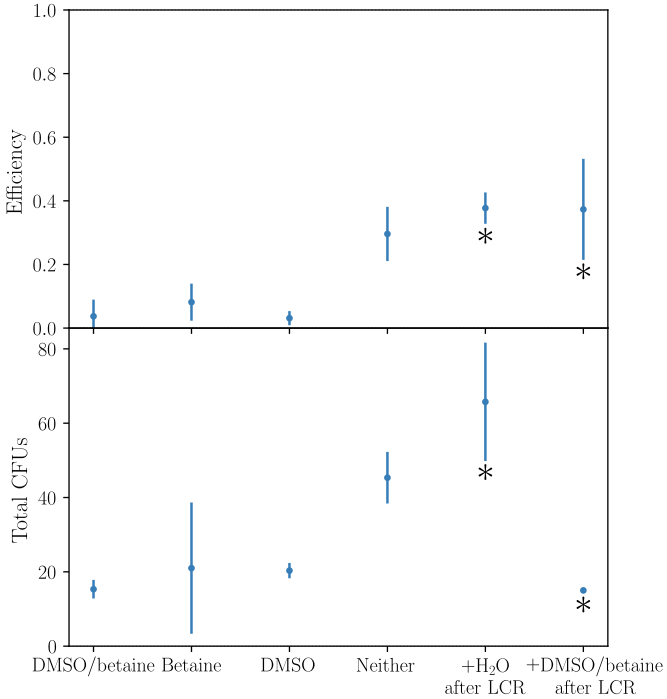

Supplementary Figure 6.11: DMSO and betaine negatively affect the LCR of the seven parted plasmid. The LCRs to investigate the impact of DMSO and/or betaine were performed as triplicates. To investigate the direct influence of DMSO and betaine on the electroporation process, the LCRs were performed as quadruplets (indicated with an *). The standard deviation for each LCR is indicated by error bars and the manual set "M" was used. The combination of DMSO and betaine negatively affects the efficiency and the total amount of colonies (comparing the results for DMSO/betaine with none of both). Further investigation revealed a direct negative impact of DMSO/betaine in the electroporation. An LCR was performed without DMSO/betaine. Both detergents were added before the electroporation to simulate the transformation conditions (8 % v/v DMSO and 0.45 M betaine, mix of 3 µL LCR and 30 µL competent cells). As a control *dd*H_2O was added. All BO sequences are shown in Supplementary Table 6.2. BO: bridging oligo, CFU: colony forming unit, DMSO: dimethyl sulfoxide. This figure is adapted from Schlichting *et al.* [95].

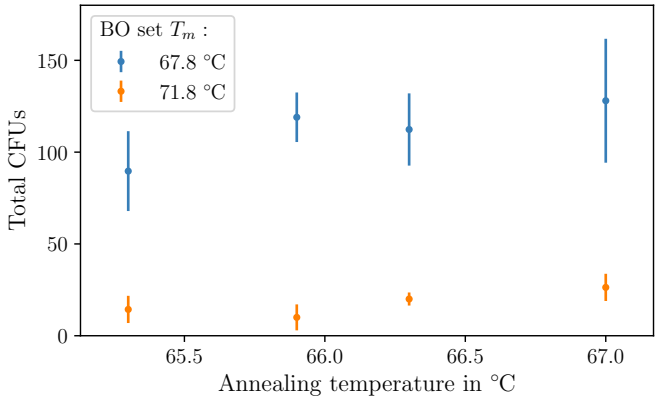

Supplementary Figure 6.12: Total amount of colonies for the bridging oligo sets "67.8 °C" and "71.8 °C" in the annealing temperature range of 65-67 °C (larger temperature range shown in Figure 3.6A+B). All LCRs were performed as triplicates. The standard deviation for each LCR is indicated by error bars. All BO sequences are shown in Supplementary Table 6.3. BO: bridging oligo, CFU: colony forming unit, DMSO: dimethyl sulfoxide, T_m: melting temperature of one BO-half. This figure is adapted from Schlichting *et al.* [95].

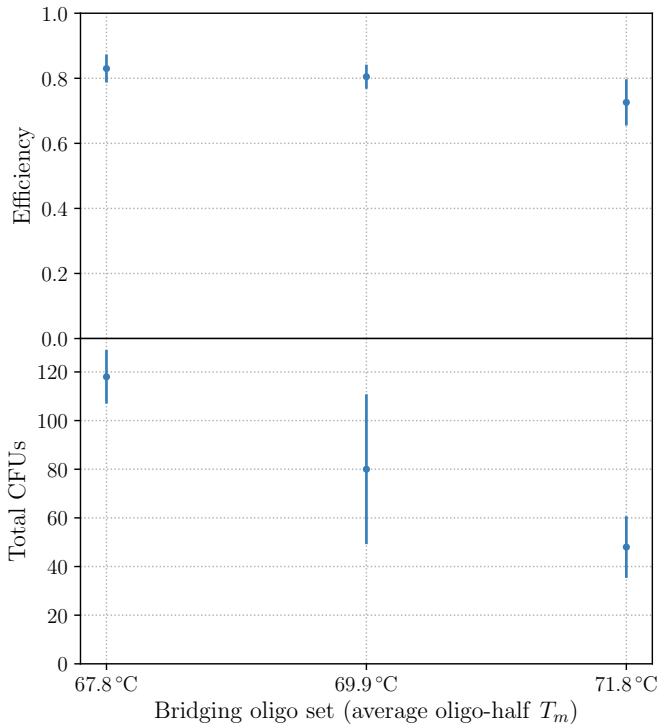

Supplementary Figure 6.13: LCR without DMSO and betaine at the annealing temperature of 67.9 °C using three bridging oligo sets (T_m = 67.8, 69.9 and 71.8 °C). All LCRs were performed as triplicates. The standard deviation for each LCR is indicated by error bars. A larger range of the annealing temperature is shown in Figure 3.6A+B. **A.** The efficiencies of the LCRs were similar. **B.** The total amount of colonies increased with lower melting temperatures of the BOs. BO: bridging oligo, CFU: colony forming unit, DMSO: dimethyl sulfoxide, T_m: melting temperature of one BO-half. This figure is adapted from Schlichting *et al.* [95].

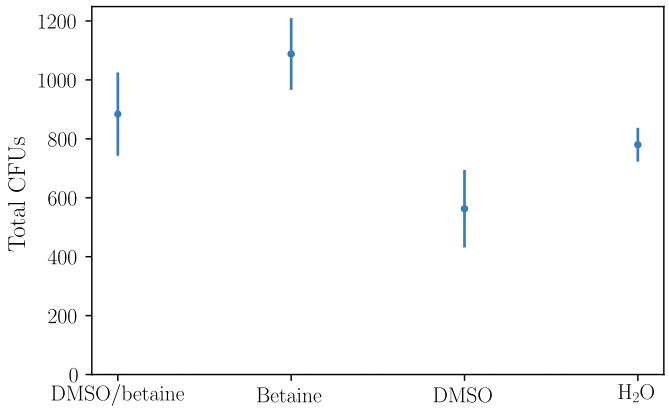

Supplementary Figure 6.14: DMSO and betaine in chemical transformations. All transformations were performed as triplicates. The standard deviation for each LCR is indicated by error bars. The plasmid pUC19 was mixed with DMSO and/or betaine or *aq. dest.* followed by chemical transformation of *E. coli*. DMSO had a negative impact whereas betaine had a positive impact on the number of colonies. Adding both yielded similar results as adding neither. CFU: colony forming unit, DMSO: dimethyl sulfoxide. This figure is adapted from Schlichting *et al.* [95].

6.1.3 Sequences of the toy-model plasmid and the utilized amplification primers and bridging oligos

Supplementary Table 6.1: Oligonucleotides for the amplification of all toy-model plasmid parts (shown in Figure 3.1B). [1] The complete part was ordered as two oligonucleotides, which were phosphorylated and annealed to double stranded DNA before the LCR (described in the methods). [2] For sequencing from the vector into the inserts. fw: forward direction, *mRFP1*: monomeric red fluorescent protein 1, rv: reverse direction, *sfGFP*: superfolder green fluorescent protein. This table is adapted from Schlichting *et al.* [95].

Toy-Plasmid Part	OligoID	Sequence (5'→3')
mRFP1 (Addgene: pYTK090)		
part 1 (*mRFP1*-part 1)[1]	10141-fw	TCCCTATCAGTGATAGAGATTGACATCCCT ATCAGTGATAGAGATACTGAGCACGGATC TGAAAGAGGAGAAAGGATCT
	10142-rv	AGATCCTTTCTCCTCTTTCAGATCCGTGCT CAGTATCTCTATCACTGATAGGGATGTCAA TCTCTATCACTGATAGGGA
part 2 (*mRFP1*-part 2)	10127-fw	ATGGCGAGTAGCGAAGACG
	10128-rv	GTCCTGGGTAACGGTAACAAC
part 3 (*mRFP1*-part 3)	10129-fw	TCCTCCCTGCAAGACGG
	10132-rv	TATAAACGCAGAAAGGCCCAC
sfGFP (Addgene: pYTK001)		
part 4 (*sfGFP*-part 1)	10108-fw	GAAAGTGAAACGTGATTTCATGCG
	10110-rv	TGAACTTCAGCGTCAGTTTAC
part 5 (*sfGFP*-part 2)	10111-fw	TCTGTACTACTGGTAAACTGC
	10112-rv	TGTGGCTGTTAAAATTGTATTCC
part 6 (*sfGFP*-part 3)	10113-fw	ATGTTTACATCACCGCCG
	10109-rv	TATAAACGCAGAAAGGCCCAC
pJET1.2/blunt (Thermo Fisher)		
part 7	23043-fw	ATCTTGCTGAAAAACTCGAGC
	23044-rv	ATCTTTCTAGAAGATCTCC
Sequencing Primers[2]		

Supplementary Table 6.1: Oligonucleotides for the amplification of all toy-model plasmid parts (continued)

Toy-Plasmid Part	OligoID	Sequence (5'→3')
forward	14013	CGACTCACTATAGGGAGAGCGGC
reverse	14014	AAGAACATCGATTTTCCATGGCAG

Supplementary Table 6.2: Oligonucleotides for crosstalk LCRs (results shown in Supplementary Figures 3.2 and 6.6). All melting temperatures (T_ms) presented here are calculated for each BO-half using the formula of SantaLucia [89] for the T_m-calculation and the salt correction. T_m: melting temperature of a BO-half. This table is adapted from Schlichting *et al.* [95].

Bridging Oligo Set (T_m per BO-half)	**OligoID**	**Sequence (5'→3')**
Manually Designed		
M ($71.4 \pm 0.7\,^{\circ}\mathrm{C}$)	10133	CGGATGGCTCGAGTTTTTCAGCAAGATTCCCTATCAGTGATAGAGATTGACATCCCTATCAG
	10134	GCACGGATCTGAAAGAGGAGAAAGGATCTATGGCGAGTAGCGAAGACGTTATCAAAG
	10135	GTGGTGTTGTTACCGTTACCCAGGACTCCTCCCTGCAAGACGGTGAGTTC
	10137	CGGCCGCGTGTTACAACCAATGAAAGTGAAACGTGATTTCATGCGTCATTTTGAAC
	10116	GCAACTAATGGTAAACTGACGCTGAAGTTCATCTGTACTACTGGTAAACTGCCGGTTCC
	10117	CCATAAGCTGGAATACAATTTTAACAGCCACAATGTTTACATCACCGCCGATAAACAAAAAAATG
	10118	CGGGTGGGCCTTTCTGCGTTTATAATCTTTCTAGAAGATCTCCTACAATATTCTCAGCTGC
Low Crosstalk		
L1 ($68.1 \pm 1.1\,^{\circ}\mathrm{C}$)	10232	TGGCTCGAGTTTTTCAGCAAGATTCCCTATCAGTGATAGAGATTGACATCC
	10233	CGGATCTGAAAGAGGAGAAAGGATCTATGGCGAGTAGCGAAGACGT
	10234	GTGTTGTTACCGTTACCCAGGACTCCTCCCTGCAAGACGGTG
	10235	GGCCGCGTGTTACAACCAATGAAAGTGAAACGTGATTTCATGCGT
	10236	AATGGTAAACTGACGCTGAAGTTCATCTGTACTACTGGTAAACTGCCGG
	10237	CATAAGCTGGAATACAATTTTAACAGCCACAATGTTTACATCACCGCCGATAAACAAAAAAA
	10238	CGGGTGGGCCTTTCTGCGTTTATAATCTTTCTAGAAGATCTCCTACAATATTCTCAGC
L2 ($68.6 \pm 0.9\,^{\circ}\mathrm{C}$)	10235	GGCCGCGTGTTACAACCAATGAAAGTGAAACGTGATTTCATGCGT
	10239	GATGGCTCGAGTTTTTCAGCAAGATTCCCTATCAGTGATAGAGATTGACATCCCT

Supplementary Table 6.2: Oligonucleotides for crosstalk LCRs (continued).

Bridging Oligo Set (T_m per BO-half)	**OligoID**	**Sequence (5'→3')**
	10240	ACGGATCTGAAAGAGGAGAAAGGATCTATGGCGAGTAGCGAAGACGTTATC
	10241	GGTGTTGTTACCGTTACCCAGGACTCCTCCCTGCAAGACGGTG
	10242	CAACTAATGGTAAACTGACGCTGAAGTTCATCTGTACTACTGGTAAACTGCCGG
	10243	ATAAGCTGGAATACAATTTTAACAGCCACAATGTTTACATCACCGCCGATAAACAAAAAA
	10244	GGGTGGGCCTTTCTGCGTTTATAATCTTTCTAGAAGATCTCCTACAATATTCTCAGC
L3 ($69.5 \pm 1.7\,^{\circ}\mathrm{C}$)	10244	GGGTGGGCCTTTCTGCGTTTATAATCTTTCTAGAAGATCTCCTACAATATTCTCAGC
	10268	GGCCGCGTGTTACAACCAATGAAAGTGAAACGTGATTTCATGCGTC
	10283	GGATGGCTCGAGTTTTTCAGCAAGATTCCCTATCAGTGATAGAGATTGACATCCC
	10284	GCACGGATCTGAAAGAGGAGAAAGGATCTATGGCGAGTAGCGAAGACGTTATC
	10285	GTGTTGTTACCGTTACCCAGGACTCCTCCCTGCAAGACGGTGAGTTC
	10286	GCAACTAATGGTAAACTGACGCTGAAGTTCATCTGTACTACTGGTAAACTGCCGGT
	10287	TAAGCTGGAATACAATTTTAACAGCCACAATGTTTACATCACCGCCGATAAACAAAAAAATGG
L4 ($69.4 \pm 1.6\,^{\circ}\mathrm{C}$)	10244	GGGTGGGCCTTTCTGCGTTTATAATCTTTCTAGAAGATCTCCTACAATATTCTCAGC
	10268	GGCCGCGTGTTACAACCAATGAAAGTGAAACGTGATTTCATGCGTC
	10283	GGATGGCTCGAGTTTTTCAGCAAGATTCCCTATCAGTGATAGAGATTGACATCCC
	10284	GCACGGATCTGAAAGAGGAGAAAGGATCTATGGCGAGTAGCGAAGACGTTATC
	10285	GTGTTGTTACCGTTACCCAGGACTCCTCCCTGCAAGACGGTGAGTTC
	10286	GCAACTAATGGTAAACTGACGCTGAAGTTCATCTGTACTACTGGTAAACTGCCGGT
	10288	TAAGCTGGAATACAATTTTAACAGCCACAATGTTTACATCACCGCCGATAAACAAAAAAATG

Supplementary Table 6.2: Oligonucleotides for crosstalk LCRs (continued).

Bridging Oligo Set (T_m per BO-half)	**OligoID**	**Sequence (5'→3')**
L5 ($69.9 \pm 2.1\,^{\circ}\mathrm{C}$)	10235	GGCCGCGTGTTACAACCAATGAAAGTGAAACGTGATTTCATGCGT
	10260	CGGATGGCTCGAGTTTTTCAGCAAGATTCCCTATCAGTGATAGAGATTGACATCCCTAT
	10261	CGGATCTGAAAGAGGAGAAAGGATCTATGGCGAGTAGCGAAGACGTTATC
	10262	TGGTGTTGTTACCGTTACCCAGGACTCCTCCCTGCAAGACGGTGAGTTC
	10263	GCAACTAATGGTAAACTGACGCTGAAGTTCATCTGTACTACTGGTAAACTGCCGGTTCCTT
	10264	TAAGCTGGAATACAATTTTAACAGCCACAATGTTTACATCACCGCCGATAAACAAA
	10265	GGGTGGGCCTTTCTGCGTTTATAATCTTTCTAGAAGATCTCCTACAATATTCTCAGCTGCC
L6 ($70.0 \pm 1.7\,^{\circ}\mathrm{C}$)	10259	GTGGTGTTGTTACCGTTACCCAGGACTCCTCCCTGCAAGACGGTGAGTT
	10266	CGGATGGCTCGAGTTTTTCAGCAAGATTCCCTATCAGTGATAGAGATTGACATCCCTA
	10267	CGGATCTGAAAGAGGAGAAAGGATCTATGGCGAGTAGCGAAGACGTT
	10268	GGCCGCGTGTTACAACCAATGAAAGTGAAACGTGATTTCATGCGTC
	10269	CAACTAATGGTAAACTGACGCTGAAGTTCATCTGTACTACTGGTAAACTGCCGGTT
	10270	GCCATAAGCTGGAATACAATTTTAACAGCCACAATGTTTACATCACCGCCGATAAACAAAAAAATG
	10271	TTCGGGTGGGCCTTTCTGCGTTTATAATCTTTCTAGAAGATCTCCTACAATATTCTCAGCT
High Crosstalk		
H1 ($71.9 \pm 1.1\,^{\circ}\mathrm{C}$)	10245	CGGATGGCTCGAGTTTTTCAGCAAGATTCCCTATCAGTGATAGAGATTGACATCCCTATCAGT
	10246	GCACGGATCTGAAAGAGGAGAAAGGATCTATGGCGAGTAGCGAAGACGTTATCAAAG
	10247	GTGGTGTTGTTACCGTTACCCAGGACTCCTCCCTGCAAGACGGTGAGT
	10248	GCGGCCGCGTGTTACAACCAATGAAAGTGAAACGTGATTTCATGCGTCATTTTGAACA

Supplementary Table 6.2: Oligonucleotides for crosstalk LCRs (continued).

Bridging Oligo Set (T_m per BO-half)	OligoID	Sequence (5'→3')
	10249	CAACTAATGGTAAACTGACGCTGAAGTTCATCTGTACTACTGGTAAACTGCCGGTTCCTT
	10250	GCCATAAGCTGGAATACAATTTTAACAGCCACAATGTTTACATCACCGCCGATAAACAAAAAAAT
	10251	TTCGGGTGGGCCTTTCTGCGTTTATAATCTTTCTAGAAGATCTCCTACAATATTCTCAGCTGCC
H2 ($70.7 \pm 2.4\,^{\circ}\mathrm{C}$)	10248	GCGGCCGCGTGTTACAACCAATGAAAGTGAAACGTGATTTCATGCGTCATTTTGAACA
	10252	ATGGCTCGAGTTTTTCAGCAAGATTCCCTATCAGTGATAGAGATTGACATCCCTATCAGT
	10253	AGCACGGATCTGAAAGAGGAGAAAGGATCTATGGCGAGTAGCGAAGACGTT
	10254	GTGGTGTTGTTACCGTTACCCAGGACTCCTCCCTGCAAGACGGTGAGTTC
	10255	AATGGTAAACTGACGCTGAAGTTCATCTGTACTACTGGTAAACTGCCGGTTCCTT
	10256	AAGCTGGAATACAATTTTAACAGCCACAATGTTTACATCACCGCCGATAAACAA
	10257	TTCGGGTGGGCCTTTCTGCGTTTATAATCTTTCTAGAAGATCTCCTACAATATTCTCAGCTG
H3 ($70.3 \pm 2.3\,^{\circ}\mathrm{C}$)	10248	GCGGCCGCGTGTTACAACCAATGAAAGTGAAACGTGATTTCATGCGTCATTTTGAACA
	10265	GGGTGGGCCTTTCTGCGTTTATAATCTTTCTAGAAGATCTCCTACAATATTCTCAGCTGCC
	10289	GATGGCTCGAGTTTTTCAGCAAGATTCCCTATCAGTGATAGAGATTGACATCCCTATCA
	10290	AGCACGGATCTGAAAGAGGAGAAAGGATCTATGGCGAGTAGCGAAGACGTTA
	10291	GTGGTGTTGTTACCGTTACCCAGGACTCCTCCCTGCAAGACGGTG
	10292	AATGGTAAACTGACGCTGAAGTTCATCTGTACTACTGGTAAACTGCCGGTTC
	10293	GCCATAAGCTGGAATACAATTTTAACAGCCACAATGTTTACATCACCGCCGATAAACA
H4 ($70.5 \pm 2.2\,^{\circ}\mathrm{C}$)	10248	GCGGCCGCGTGTTACAACCAATGAAAGTGAAACGTGATTTCATGCGTCATTTTGAACA
	10265	GGGTGGGCCTTTCTGCGTTTATAATCTTTCTAGAAGATCTCCTACAATATTCTCAGCTGCC

Supplementary Table 6.2: Oligonucleotides for crosstalk LCRs (continued).

Bridging Oligo Set (T_m per BO-half)	OligoID	Sequence (5'→3')
	10290	AGCACGGATCTGAAAGAGGAGAAAGGATCTATGGCGAGTAGCGAAGACGTTA
	10291	GTGGTGTTGTTACCGTTACCCAGGACTCCTCCCTGCAAGACGGTG
	10292	AATGGTAAACTGACGCTGAAGTTCATCTGTACTACTGGTAAACTGCCGGTTC
	10293	GCCATAAGCTGGAATACAATTTTAACAGCCACAATGTTTACATCACCGCCGATAAACA
	10294	CGGATGGCTCGAGTTTTTCAGCAAGATTCCCTATCAGTGATAGAGATTGACATCCCTATCA
H5 ($70.4 \pm 1.9\,^{\circ}\mathrm{C}$)	10248	GCGGCCGCGTGTTACAACCAATGAAAGTGAAACGTGATTTCATGCGTCATTTTGAACA
	10272	TGGCTCGAGTTTTTCAGCAAGATTCCCTATCAGTGATAGAGATTGACATCCCTATCAGT
	10273	CACGGATCTGAAAGAGGAGAAAGGATCTATGGCGAGTAGCGAAGACGTTATCAAAGA
	10274	GTGTTGTTACCGTTACCCAGGACTCCTCCCTGCAAGACGGTGA
	10275	CAACTAATGGTAAACTGACGCTGAAGTTCATCTGTACTACTGGTAAACTGCCGGTTC
	10276	CATAAGCTGGAATACAATTTTAACAGCCACAATGTTTACATCACCGCCGATAAACAAAAAAAATGG
	10277	CGGGTGGGCCTTTCTGCGTTTATAATCTTTCTAGAAGATCTCCTACAATATTCTCAGCTG
H6 ($70.3 \pm 2.2\,^{\circ}\mathrm{C}$)	10242	CAACTAATGGTAAACTGACGCTGAAGTTCATCTGTACTACTGGTAAACTGCCGG
	10248	GCGGCCGCGTGTTACAACCAATGAAAGTGAAACGTGATTTCATGCGTCATTTTGAACA
	10278	GATGGCTCGAGTTTTTCAGCAAGATTCCCTATCAGTGATAGAGATTGACATCCCTATCAGT
	10279	AGCACGGATCTGAAAGAGGAGAAAGGATCTATGGCGAGTAGCGAAGACGTTATCAA
	10280	GTGGTGTTGTTACCGTTACCCAGGACTCCTCCCTGCAAGACGGTGA
	10281	AGCTGGAATACAATTTTAACAGCCACAATGTTTACATCACCGCCGATAAACAA
	10282	TTCGGGTGGGCCTTTCTGCGTTTATAATCTTTCTAGAAGATCTCCTACAATATTCTCAGC

Supplementary Table 6.3: Bridging oligo sets for the gradient-LCR (composed of bridging oligos for crosstalk experiments; Supplementary Table 6.2). The results of the gradient-LCRs are shown in Figure 3.6A+B. All melting temperatures (T_ms) presented here are calculated for each BO-half using the formula of SantaLucia [89] for the T_m-calculation and the salt correction. T_m: melting temperature of a BO-half. This table is adapted from Schlichting *et al.* [95].

Bridging Oligo Set (T_m per BO-half)	**OligoID**	**Sequence (5'→3')**
$67.8 \pm 0.5\,^{\circ}\mathrm{C}$	10232	TGGCTCGAGTTTTTCAGCAAGATTCCCTATCAGTGATAGAGATTGACATCC
	10233	CGGATCTGAAAGAGGAGAAAGGATCTATGGCGAGTAGCGAAGACGT
	10234	GTGTTGTTACCGTTACCCAGGACTCCTCCCTGCAAGACGGTG
	10236	AATGGTAAACTGACGCTGAAGTTCATCTGTACTACTGGTAAACTGCCGG
	10244	GGGTGGGCCTTTCTGCGTTTATAATCTTTCTAGAAGATCTCCTACAATATTCTCAGC
	10268	GGCCGCGTGTTACAACCAATGAAAGTGAAACGTGATTTCATGCGTC
	10281	AGCTGGAATACAATTTTAACAGCCACAATGTTTACATCACCGCCGATAAACAA
$69.9 \pm 1.3\,^{\circ}\mathrm{C}$	10117	CCATAAGCTGGAATACAATTTTAACAGCCACAATGTTTACATCACCGCCGATAAACAAAAAAATG
	10118	CGGGTGGGCCTTTCTGCGTTTATAATCTTTCTAGAAGATCTCCTACAATATTCTCAGCTGC
	10240	ACGGATCTGAAAGAGGAGAAAGGATCTATGGCGAGTAGCGAAGACGTTATC
	10247	GTGGTGTTGTTACCGTTACCCAGGACTCCTCCCTGCAAGACGGTGAGT
	10268	GGCCGCGTGTTACAACCAATGAAAGTGAAACGTGATTTCATGCGTC
	10269	CAACTAATGGTAAACTGACGCTGAAGTTCATCTGTACTACTGGTAAACTGCCGGTT
	10283	GGATGGCTCGAGTTTTTCAGCAAGATTCCCTATCAGTGATAGAGATTGACATCCC
$71.8 \pm 0.8\,^{\circ}\mathrm{C}$	10116	GCAACTAATGGTAAACTGACGCTGAAGTTCATCTGTACTACTGGTAAACTGCCGGTTCC
	10117	CCATAAGCTGGAATACAATTTTAACAGCCACAATGTTTACATCACCGCCGATAAACAAAAAAATG
	10133	CGGATGGCTCGAGTTTTTCAGCAAGATTCCCTATCAGTGATAGAGATTGACATCCCTATCAG
	10134	GCACGGATCTGAAAGAGGAGAAAGGATCTATGGCGAGTAGCGAAGACGTTATCAAAG
	10248	GCGGCCGCGTGTTACAACCAATGAAAGTGAAACGTGATTTCATGCGTCATTTTGAACA
	10251	TTCGGGTGGGCCTTTCTGCGTTTATAATCTTTCTAGAAGATCTCCTACAATATTCTCAGCTGCC

Supplementary Table 6.3: Bridging oligo sets for the gradient-LCR (continued)

Bridging Oligo Set (T_m per BO-half)	OligoID	Sequence (5'→3')
	10259	GTGGTGTTGTTACCGTTACCCAGGACTCCTCCCTGCAAGACGGTGAGTT

Supplementary Table 6.4: Bridging oligo sets with temperatures in the range of 62.0 °C to 67 °C. The results of the LCRs are shown in Figure 3.7. All melting temperatures (T_ms) presented here are calculated for each BO-half using the formula of SantaLucia [89] for the T_m-calculation and the salt correction. T_m: melting temperature of a BO-half. This table is adapted from Schlichting *et al.* [95].

Bridging Oligo Set (T_m per BO-half)	**OligoID**	**Sequence (5'→3')**
$62.0 \pm 0.9\,^{\circ}\mathrm{C}$	10331	GGAATACAATTTTAACAGCCACAATGTTTACATCACCGCCG
	10333	GCTCGAGTTTTTCAGCAAGATTCCCTATCAGTGATAGAGATTGAC
	10334	ATCTGAAAGAGGAGAAAGGATCTATGGCGAGTAGCGAAGAC
	10335	TGTTACCGTTACCCAGGACTCCTCCCTGCAAGACG
	10336	CCGCGTGTTACAACCAATGAAAGTGAAACGTGATTTCATGC
	10337	AAACTGACGCTGAAGTTCATCTGTACTACTGGTAAACTGC
	10338	GGGCCTTTCTGCGTTTATAATCTTTCTAGAAGATCTCCTACAATAT
$63.3 \pm 0.7\,^{\circ}\mathrm{C}$	10333	GCTCGAGTTTTTCAGCAAGATTCCCTATCAGTGATAGAGATTGAC
	10336	CCGCGTGTTACAACCAATGAAAGTGAAACGTGATTTCATGC
	10339	GATCTGAAAGAGGAGAAAGGATCTATGGCGAGTAGCGAAGAC
	10340	GTTGTTACCGTTACCCAGGACTCCTCCCTGCAAGACGG
	10341	GTAAACTGACGCTGAAGTTCATCTGTACTACTGGTAAACTGCC
	10342	TGGAATACAATTTTAACAGCCACAATGTTTACATCACCGCCGATA
	10343	TGGGCCTTTCTGCGTTTATAATCTTTCTAGAAGATCTCCTACAATATTCT
$65.1 \pm 0.6\,^{\circ}\mathrm{C}$	10340	GTTGTTACCGTTACCCAGGACTCCTCCCTGCAAGACGG
	10344	GGCTCGAGTTTTTCAGCAAGATTCCCTATCAGTGATAGAGATTGACATC
	10345	GGATCTGAAAGAGGAGAAAGGATCTATGGCGAGTAGCGAAGACG
	10346	GCCGCGTGTTACAACCAATGAAAGTGAAACGTGATTTCATGCG
	10347	GGTAAACTGACGCTGAAGTTCATCTGTACTACTGGTAAACTGCCG
	10348	CTGGAATACAATTTTAACAGCCACAATGTTTACATCACCGCCGATAAA
	10349	GTGGGCCTTTCTGCGTTTATAATCTTTCTAGAAGATCTCCTACAATATTCTC
$66.0 \pm 0.5\,^{\circ}\mathrm{C}$	10344	GGCTCGAGTTTTTCAGCAAGATTCCCTATCAGTGATAGAGATTGACATC
	10345	GGATCTGAAAGAGGAGAAAGGATCTATGGCGAGTAGCGAAGACG

Supplementary Table 6.4: Bridging oligo sets with temperatures in the range of 62.0 °C to 67.3 °C (continued).

Bridging Oligo Set (T_m per BO-half)	**OligoID**	**Sequence (5'→3')**
	10346	GCCGCGTGTTACAACCAATGAAAGTGAAACGTGATTTCATGCG
	10350	TGTTGTTACCGTTACCCAGGACTCCTCCCTGCAAGACGGT
	10351	TGGTAAACTGACGCTGAAGTTCATCTGTACTACTGGTAAACTGCCG
	10352	GCTGGAATACAATTTTAACAGCCACAATGTTTACATCACCGCCGATAAAC
	10353	GGTGGGCCTTTCTGCGTTTATAATCTTTCTAGAAGATCTCCTACAATATTCTCAG
$67.3 \pm 0.6\,^{\circ}\mathrm{C}$	10350	TGTTGTTACCGTTACCCAGGACTCCTCCCTGCAAGACGGT
	10353	GGTGGGCCTTTCTGCGTTTATAATCTTTCTAGAAGATCTCCTACAATATTCTCAG
	10354	ATGGCTCGAGTTTTTCAGCAAGATTCCCTATCAGTGATAGAGATTGACATCC
	10355	CGGATCTGAAAGAGGAGAAAGGATCTATGGCGAGTAGCGAAGACGT
	10356	GGCCGCGTGTTACAACCAATGAAAGTGAAACGTGATTTCATGCGTC
	10357	CTAATGGTAAACTGACGCTGAAGTTCATCTGTACTACTGGTAAACTGCCGG
	10358	GCTGGAATACAATTTTAACAGCCACAATGTTTACATCACCGCCGATAAACA

6.1.4 Validation experiments

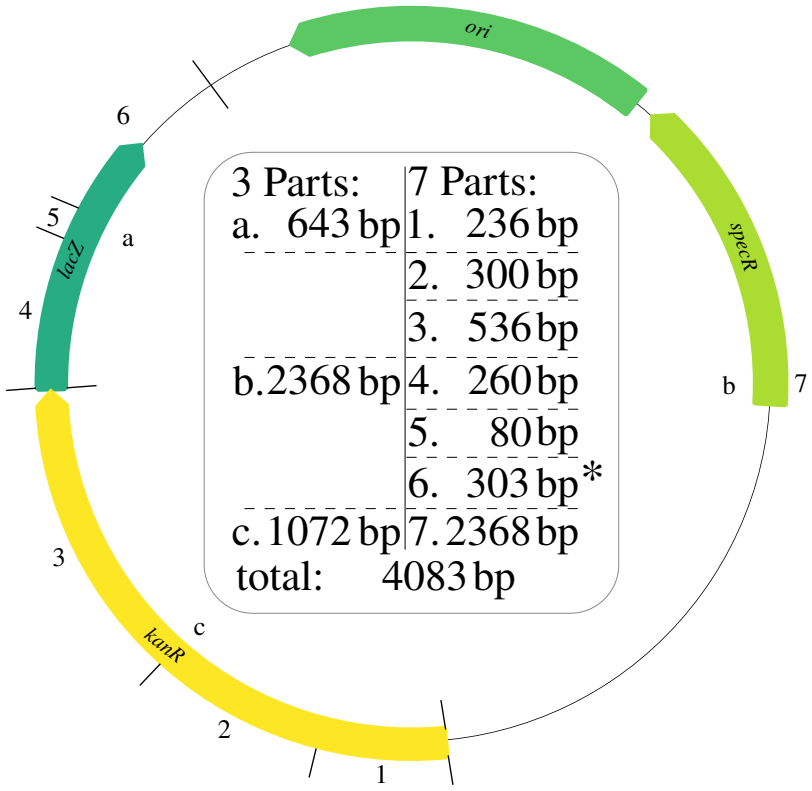

Supplementary Figure 6.15: Plasmid 1 ("VP1") for the validation experiments of the improved LCR conditions (Figure 3.9, Table 3.1). The plasmid was split in three and seven parts. Only if all parts were assembled the cells were able to replicate, were resistant to spectinomycin and turned blue by using the blue-white screening. Part 7 was PCR-amplified from the already existing plasmid build for scar-free deletions in *Bacillus subtilis* [118]. The *lacZ* gene was inserted to enable a blue-white screening and was derived from the TALEN Kit 2.0 from Addgene [9]. In comparison to the original flanking regions of the *lacZ* some mutations were present due to subcloning. *: Part 6 was amplified from the existing validation plasmid 2 ("VP2") shown in Supplementary Figure 6.16. The *kanR* gene was derived from [99]. Before PCR-amplification, all templates were digested by restriction enzymes. Afterwards, all PCR-products were additionally digested by a DpnI-digestion. *lacZ*: β-galactosidase, *ori*: origin of replication, *specR*: spectinomycin resistance gene. This figure is modified after Schlichting *et al.* [95].

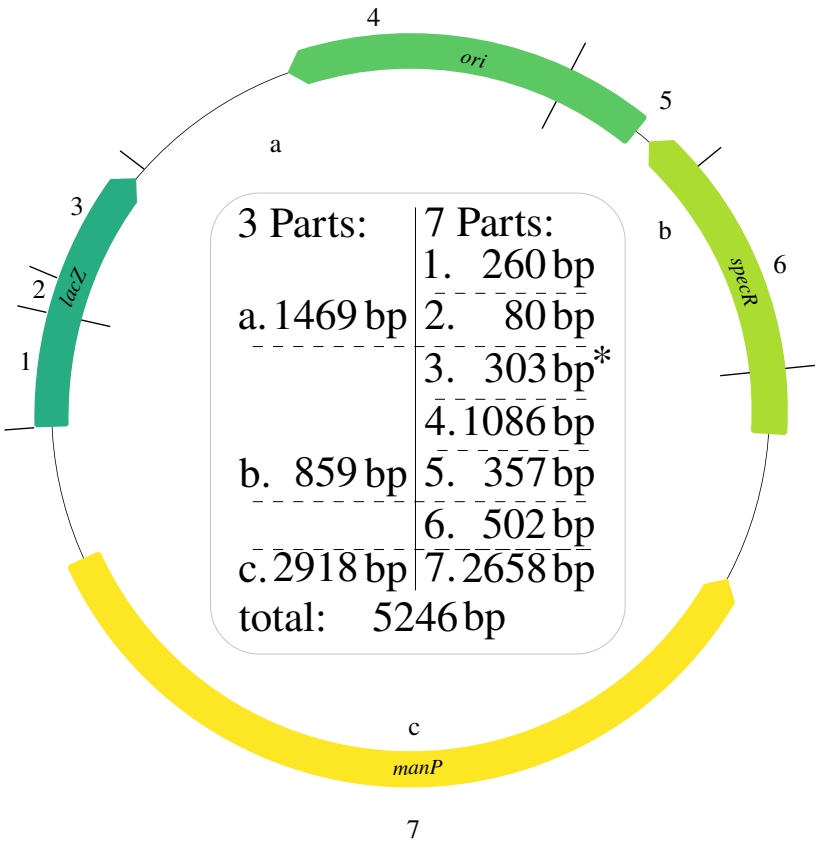

Supplementary Figure 6.16: Plasmid 2 ("VP2") for the validation experiments of the improved LCR conditions (Figure 3.9, Table 3.1). The plasmid was split in three and seven parts. Only if all parts were assembled the cells were able to replicate, were resistant to spectinomycin and kanamycin and turned blue by using blue-white screening. Parts 1-3 were derived by PCR-amplification of a plasmid from Wenzel *et al.* [118] and . Part 3 (*) begins in the *lacZ* of the plasmid derived from TALEN Kit 2.0 from Addgene [9] and ends in the plasmid derived from Wenzel *et al.* [118]. Parts 4-7 were PCR-amplified from the already existing plasmid build for scar-free deletions in *Bacillus subtilis* [118]. Before PCR-amplification, all templates were digested by restriction enzymes. Afterwards, all PCR-products were digested by DpnI. *lacZ*: β-galactosidase, *manP*: D-mannose permease (for *Bacillus* spp.), *ori*: origin of replication), *specR*: spectinomycin resistance gene. This figure is modified after Schlichting *et al.* [95].

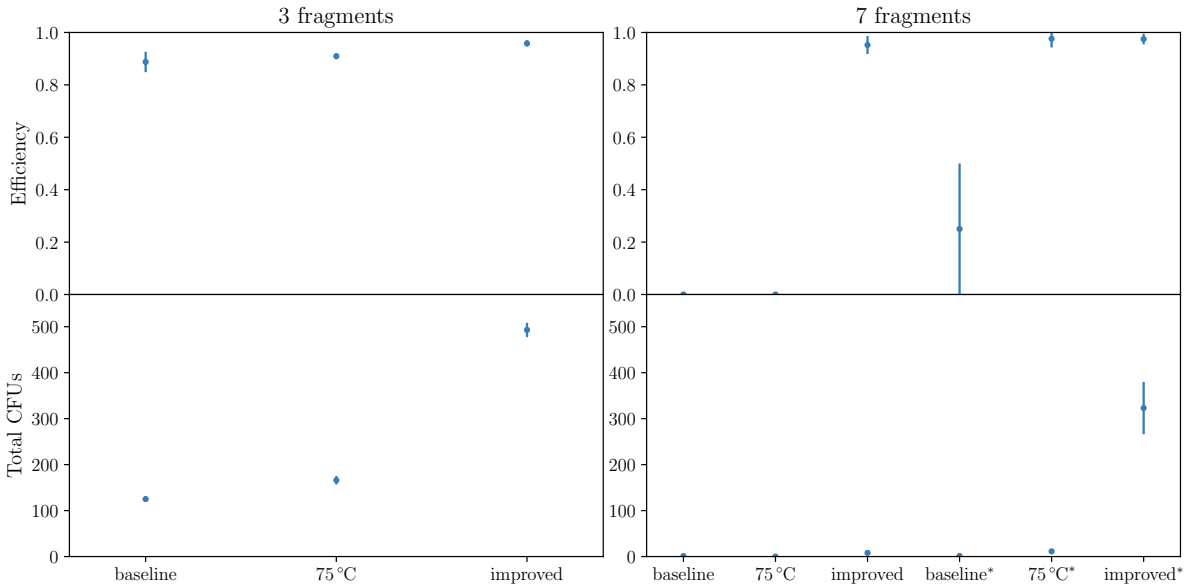

Supplementary Figure 6.17: Results of the baseline, 75 °C and improved LCR-protocol for the validation plasmid 1 ("VP1"). For the seven part split the same LCRs were transformed in chemical cells and electrocompetent cells (indicated by an *) due to no CFUs for the baseline and 75 °C protocol when chemical transformation was used. For all LCRs, 3 µL were transformed in 30 µL cells. As a negative control, the LCR-mix without BOs and without Ampligase® was used and resulted in no colonies (not shown). All LCRs were performed as triplicates. CFU: colony forming unit. This figure is adapted from Schlichting *et al.* [95].

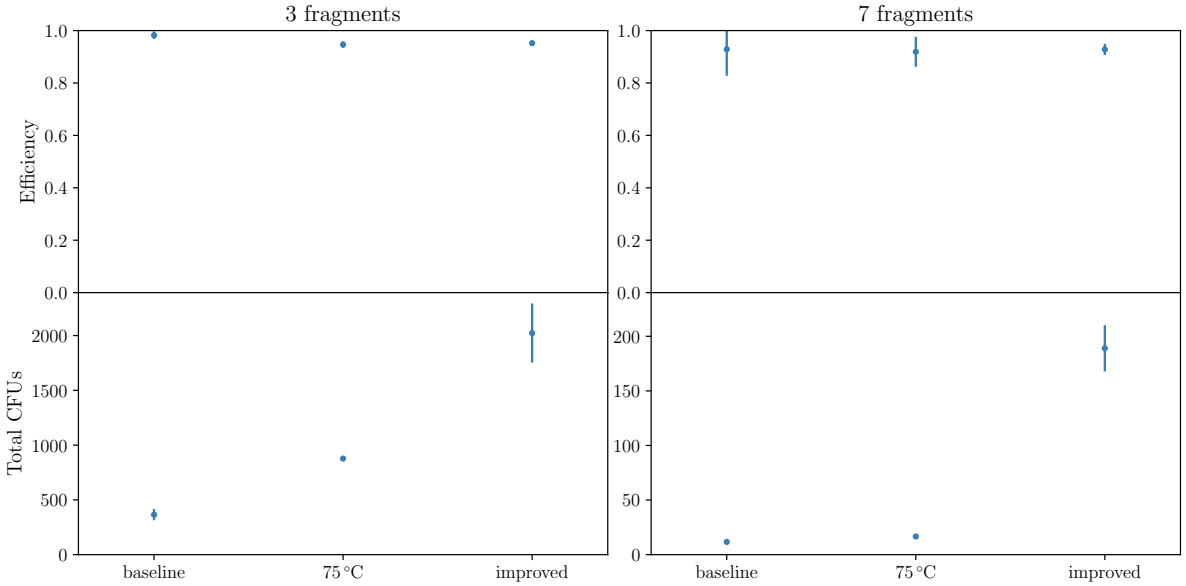

Supplementary Figure 6.18: Results of the baseline, 75 °C and improved LCR-protocol for the validation plasmid 2 ("VP2"). All LCRs were transformed in chemical competent cells. For this, 3 µL were transformed in 30 µL cells. As a negative control, the LCR mix without BOs and without Ampligase® were used and resulted in no colonies (not shown). All LCRs were performed as triplicates. BO: bridging oligo, CFU: colony forming unit. This figure is adapted from Schlichting *et al.* [95].

6.1.5 Protocol for the LCR assembly

Step-by-step protocol for the ligase cycling reaction

Niels Schlichting, Felix Reinhardt, Sven Jager, Michael Schmidt, Johannes Kabisch

Correspondence: johannes@kabisch-lab.de

Abstract

The ligase cycling reaction (LCR) is a scarless and efficient method to assemble plasmids from fragments of DNA. This assembly method is based on the hybridization of DNA fragments with complementary oligonucleotides, so-called bridging oligos (BOs), and an experimental procedure of thermal denaturation, annealing and ligation. In this study, we explore the effect of molecular crosstalk of BOs and various experimental parameters on the LCR by utilizing a fluorescence-based screening system. The results indicate an impact of the melting temperatures of BOs on the overall success of the LCR assembly. Secondary structure inhibitors, such as DMSO and betaine, are shown to negatively impact the number of correctly assembled plasmids. Adjustments of the annealing, ligation and BO-melting temperature further improved the LCR. The optimized LCR was confirmed by validation experiments. Based on these findings, a step-by-step protocol is offered within this study to ensure a routine for high efficient LCR assemblies.

Reagents

- amplification of DNA fragments:
  - proof-reading polymerase, no T/A overhangs
  - phosphorylated primers for the amplification of DNA fragments (use T4-polynucleotide kinase (T4-PNK; New England Biolabs, Ipswich, USA) and T4-PNK buffer (10×) or order as synthetically modified oligos
- LCR:
  - Ampligase® thermostable DNA (Lucigen, Wisconsin, USA) ligase (Epicentre) and 10×-buffer
  - *aq. dest.*
  - competent cells

Amplification of DNA fragments

- use phosphorylated amplification primers for the amplification of DNA fragments (inserts and backbone)
- phosphorylation of the amplification primers by T4-PNK (on ice):

  2 µL of 100 µM primer
  + 5 µL 10× T4-PNK buffer (1x)
  + 1 µL 10 000 U ml^{-1} T4-PNK (10 U)
  + 2 µL 100 mM ATP (4 mM)
  + 41.0 µL *aq. dest*/MilliQ

  $\sum$ 50 µL of 4 µM primer
- incubate for 1 h at 37 °C and 20 min at 65 °C
- use 6.25 µL of each phosphorylated amplification primer in a 50 µL PCR (primer concentration in PCR: 500 nM)[1,2]
- Recommended: DpnI digestion of all parts before the purification
- store parts at −20 °C; prepare aliquots for multiple usage of the same part (loss of function due to repeated freeze-thaw cycles [1, 2])

Bridging Oligo Design

For the LCRs the addition of DMSO/betaine is NOT recommended. The target-T_m of the BO design depends on the algorithms you are applying (1):

- SantaLucia 1998 (T_m calculation and salt correction [3])
  - target $T_m \approx 67.8$ °C

or

- SantaLucia 1998 (T_m calculation [3]) and Owczarzy 2008 (salt correction [4])
  - target $T_m \approx 65.2$ °C

or

- `Geneious` (www.geneious.com, [5]):
  - a Geneious-plugin for the design of bridging oligos is available at www.gitlab.com/kabischlab.de/lcr-publication-synthetic-biology

  To use Geneious without the plugin (utilization of `Primer3` [6]):

- restrictions in adjusting parameters for DNA-part concentration (only "Oligo" can be adjusted)
- to get correct melting temperatures use 114 nM for the input of "Oligo"
- then use SantaLucia 1998 [3] for the T_m calculation and salt correction (Owczarzy 2008 [4] is not available for the calculations in `Geneious` versions$\leq$ 11.0.5)
- target $T_m \approx 67.8\,^{\circ}\mathrm{C}$

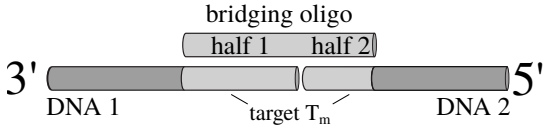

Figure 1: Scheme of the bridging oligo design. Half 1: 100% complementary to the 5-end of the first DNA part. Half 2: 100% complementary to the 3-end of the second DNA part.

Ligation

- use inserts:vector ratio of 10:1 (use 0.3 nM of the backbone) to reduce the background (religation of the backbone occurs due to the phosphorylation of all parts)
- for 25 µl (in brackets: final concentration):

  DNA inserts (3 nM of each fragment)
  + vector (0.3 nM)
  + 0.5 µL of each 1.5 µM bridging oligo (30 nM of each oligo)
  + 2.5 µL 10× Ampligase® buffer (includes 0.5 mM NAD^+)
  (+ 1.25 µL of 10 mM NAD^+ (0.5 mM))[3]
  + 1.5 µL of 5 U μL^{-1} Ampligase® (7.5 U)

  fill up with *aq. dest* to 25 µL
- use low-profile tubes or low-profile PCR plates (96-well) in a cycler for volumes of less than 10 µL
- for more than 25 cycles of small volumes ($\leq$ 10 µL): use 384-well plates
- start cycling (figure 2)

Initial denaturation:	94 °C 2 min	
Denaturation:	94 °C 10 s	⎫
Annealing:	66 °C 30 s	⎬ 25-50x
Ligation:	66 °C 1 min	⎭
Hold:	10 °C ∞	

Figure 2: Cycling parameters for the LCR.

– store at -20 °C or directly use for transformation of chemically- or electrocompetent cells or use LCR-mix as template in a PCR (1 µl of 1:100 dilution works in general)

Notes

1. This is the recommended primer concentration for the Q5® High-Fidelity Polymerase (New England Biolabs, Ipswich, USA). Probably, the concentration has to be adjusted for your polymerase. For this please ask your supplier.
2. For some PCRs the sum of the forward and reverse primers 12.5 µL in a total PCR-volume of 50 µL can result in no product. In those cases, a dialysis of the phosphorylated primers for 20 min with *aq. dest.* and a floating membrane (Merck-Millipore™Membrane Filter, 0.025 µm; order-#: VSWP02500) is helpful.
3. Self-made 10×-buffer without NAD^+ is recommended. NAD^+ is sensitive to freeze-thaw cycles, long-term storage and light exposure. Prepare a stock solution of NAD^+ and store in aliquots at −80 °C up to 6 months. 10× Ampligase® buffer: 200 mM TRIS-HCl (pH 8.3), 250 mM KCl, 100 mM $MgCl_2$, 0.1% Triton X-100.

References

[1] Robinson, C. J., Dunstan, M. S., Swainston, N., Titchmarsh, J., Takano, E., Scrutton, N. S., and Jervis, A. J. (January, 2018) Chapter Thirteen - Multifragment DNA Assembly of Biochemical Pathways via Automated Ligase Cycling Reaction. In Scrutton, N., (ed.), *Methods in Enzymology*, Vol. 608 of Enzymes in synthetic biology, pp. 369–392 Academic Press.

[2] Davis, D. L., O'Brie, E. P., and Bentzley, C. M. (October, 2000) Analysis of the degradation of oligonucleotide strands during the freezing/thawing processes using MALDI-MS. *Analytical Chemistry,* **72**(20), 5092–5096.

[3] SantaLucia, J. (February, 1998) A unified view of polymer, dumbbell, and oligonucleotide DNA nearest-neighbor thermodynamics. *Proceedings of the National Academy of Sciences,* **95**(4), 1460–1465.

[4] Owczarzy, R., Moreira, B. G., You, Y., Behlke, M. A., and Walder, J. A. (May, 2008) Predicting stability of DNA duplexes in solutions containing magnesium and monovalent cations. *Biochemistry,* **47**(19), 5336–5353.

[5] Kearse, M., Moir, R., Wilson, A., Stones-Havas, S., Cheung, M., Sturrock, S., Buxton, S., Cooper, A., Markowitz, S., Duran, C., Thierer, T., Ashton, B., Meintjes, P., and Drummond, A. (June, 2012) Geneious basic: an integrated and extendable desktop software platform for the organization and analysis of sequence data. *Bioinformatics,* **28**(12), 1647–1649.

[6] Untergasser, A., Cutcutache, I., Koressaar, T., Ye, J., Faircloth, B. C., Remm, M., and Rozen, S. G. (August, 2012) Primer3-new capabilities and interfaces. *Nucleic Acids Research,* **40**(15), e115.

Supplementary Table 6.5: Oligonucleotides for the amplification of all validation plasmid 1 parts (shown in Supplementary Figure 6.15). For the amplification of the parts of the three part split, the oligonucleotides of parts 1 (fw)+3 (rv), 4 (fw)+6 (rv) and 7 (fw and rv) were used. [1] The complete part was ordered as two oligonucleotides, which were phosphorylated and annealed to double stranded DNA before the LCR (described in the methods). [2] Part 6 begins in the *lacZ* of the plasmid derived from the TALEN Kit 2.0 from Addgene [9] and ends in the plasmid derived from Wenzel *et al.* [118]. [3] For sequencing from the vector into the inserts. fw: forward direction, *kanR*: kanamycin resistance gene, *lacZ*: β-galactosidase, rv: reverse direction. This table is adapted from Schlichting *et al.* [95].

Part	OligoID	Sequence (5'→3')
kanR (pMSE3, [99])		
part 1 (*kanR*-part 1)	10404-fw	GTCGATACTATGTTATACGCCAAC
	10407-rv	TTCCGTATCTTTTACGCAGC
part 2 (*kanR*-part 2)	10408-fw	GGAATGTCTCCTGCTAAGG
	10409-rv	GGAGTGAAAGAGCCTGATG
part 3 (*kanR*-part 3)	10410-fw	ATCGACATATCGGATTGTCC
	10433-rv	TGAGTACGGTTATTTTAGCTGAAAAACCAAGCCAGGCATTAGC
lacZ (pTAL3_His, Addgene: TALEN Kit 2.0)		
part 4 (*lacZ*-part 1)	10185-fw	CGCTGCACCGTTTCGAAG
	10382-rv	GGGCGAATTGGGTACCG
part 5 (*lacZ*-part 2)[1]	10387-fw	TATAGTGAGTCGTATTACGCGCGCTCACTGGCCGTCGTTTTACAACGTCGTGACTGGGAAAACCCTGGCGTTACCCAACT
	10388-rv	AGTTGGGTAACGCCAGGGTTTTCCCAGTCACGACGTTGTAAAACGACGGCCAGTGAGCGCGCGTAATACGACTCACTATA
part 6 (*lacZ*-part 3)[2]	10187-fw	TAATCGCCTTGCAGCACATC
	10383-rv	CGATGAAACGAGAGAGGATG
Backbone (pJOE8739.1, [118])		
part 7	10384-fw	GTATCATTACCCCCATGAACAG

Supplementary Table 6.5: Oligonucleotides for the amplification of all validation plasmid 1 parts (continued)

Part	OligoID	Sequence (5'→3')
	10406-rv	ACCCCTGGCGAATGGC
Sequencing primers[3]		
forward	10419-fw	CTTGCCAGTCACGTTACG
reverse	10420-rv	CCTGTTTGGTCACTGATGCC

Supplementary Table 6.6: Oligonucleotides for the amplification of all validation plasmid 2 parts (shown in Supplementary Figure 6.16). For the amplification of the parts of the three part split the oligonucleotides of parts 2 (fw)+4 (rv), 5 (fw)+6 (rv) and 7 (fw)+1 (rv) were used. [1] The complete part was ordered as two oligonucleotides, which were phosphorylated and annealed to double stranded DNA before the LCR (described in the methods). [2] Part 3 begins in the *lacZ* of the plasmid derived from the TALEN Kit 2.0 from Addgene [9] and ends in the plasmid derived from Wenzel *et al.* [118]. [3] For sequencing from the vector into the inserts. fw: forward direction, *ori*: origin of replication, *lacZ*: β-galactosidase, rv: reverse direction, *specR*: spectinomycin resistance gene. This table is adapted from Schlichting *et al.* [95].

Part	OligoID	Sequence (5'→3')
lacZ (pTAL3_His, Addgene: TALEN Kit 2.0)		
part 1 (*lacZ*-part 1)	10185-fw	CGCTGCACCGTTTCGAAG
	10382-rv	GGGCGAATTGGGTACCG
part 2 (*lacZ*-part 2)[1]	10387-fw	TATAGTGAGTCGTATTACGCGCGCTCACTGGCCGTCGTTTTACAACGTCGTGACTGGGAAAACCCTGGCGTTACCCAACT
	10388-rv	AGTTGGGTAACGCCAGGGTTTTCCCAGTCACGACGTTGTAAAACGACGGCCAGTGAGCGCGCGTAATACGACTCACTATA
part 3 (*lacZ*-part 3)[2]	10187-fw	TAATCGCCTTGCAGCACATC
	10383-rv	CGATGAAACGAGAGAGGATG
Backbone (pJOE8739.1, [118])		
part 4 (ori-part 1)	10384-fw	GTATCATTACCCCCATGAACAG
	11313-rv	CCACCACTTCAAGAACTCTGTAG
part 5 (*ori*-part 2+*specR*-part 1)	11315-fw	CCTAACTACGGCTACACTAGAAGG
	11308-rv	CCATTAGAACATAGGGAGAGAATTTTG
part 6 (*specR*-part 2)	10385-fw	AGAAGATTCAGCCACTGCATTTC
	10389-rv	TGACTTTTTAGTCGTCGTATCTG
part 7 (*specR*-part 3+*manP*)	10381-fw	AGATCACTATTTGGTTTTAGTCCAC
	10386-rv	GATATCTTGCTGAAAAACTCGAGC

Supplementary Table 6.6: Oligonucleotides for the amplification of all validation plasmid 2 parts (continued)

Part	OligoID	Sequence (5'→3')
Sequencing primers[3]		
forward	11253	GCAGAGCGAGGTATGTAGG
reverse	10420	CCTGTTTGGTCACTGATGCC

Supplementary Table 6.7: Bridging oligonucleotides for the assembly of the three parted and seven parted toy-plasmid consisting of *mRFP1*, *sfGFP* and pJET1.2/blunt by using the baseline and improved protocol (results and protocols shown in Figure 3.9). The BO-set for the baseline LCR consists of BOs of the manual set shown in Supplementary Table 6.2. The BO-set for the improved LCR consists of BOs of the "67.8 °C"-set of the gradient-LCR (Supplementary Table 6.3). All melting temperatures (T_ms) presented here are calculated for each BO-half using the formula of SantaLucia [89] for the T_m-calculation and the salt correction. [1] Bridging oligos with a target T_m of 70.0 °C for each half, with 8 % v/v DMSO and 0.45 M betaine and the experimental annealing temperature of 55 °C. [2] Bridging oligos with a target T_m of 67.8 °C for each half, without DMSO and betaine and the experimental annealing temperature of 66 °C. T_m: melting temperature of a BO-half. This table is adapted from Schlichting *et al.* [95].

Bridging Oligo Set (T_m per BO-half)	**OligoID**	**Sequence (5'→3')**
Three part split		
Baseline (71.4 ± 0.6 °C)[1]	10133	CGGATGGCTCGAGTTTTTCAGCAAGATTCCCTATCAGTGATAGAGATTGACATCCCTATCAG
	10137	CGGCCGCGTGTTACAACCAATGAAAGTGAAACGTGATTTCATGCGTCATTTTGAAC
	10118	CGGGTGGGCCTTTCTGCGTTTATAATCTTTCTAGAAGATCTCCTACAATATTCTCAGCTGC
Improved (67.9 ± 0.7 °C)[2]	10232	TGGCTCGAGTTTTTCAGCAAGATTCCCTATCAGTGATAGAGATTGACATCC
	10244	GGGTGGGCCTTTCTGCGTTTATAATCTTTCTAGAAGATCTCCTACAATATTCTCAGC
	10268	GGCCGCGTGTTACAACCAATGAAAGTGAAACGTGATTTCATGCGTC
Seven part split		
Baseline (71.4 ± 0.7 °C)[1]	10133	CGGATGGCTCGAGTTTTTCAGCAAGATTCCCTATCAGTGATAGAGATTGACATCCCTATCAG
	10134	GCACGGATCTGAAAGAGGAGAAAGGATCTATGGCGAGTAGCGAAGACGTTATCAAAG
	10135	GTGGTGTTGTTACCGTTACCCAGGACTCCTCCCTGCAAGACGGTGAGTTC
	10137	CGGCCGCGTGTTACAACCAATGAAAGTGAAACGTGATTTCATGCGTCATTTTGAAC
	10116	GCAACTAATGGTAAACTGACGCTGAAGTTCATCTGTACTACTGGTAAACTGCCGGTTCC
	10117	CCATAAGCTGGAATACAATTTTAACAGCCACAATGTTTACATCACCGCCGATAAACAAAAAAATG
	10118	CGGGTGGGCCTTTCTGCGTTTATAATCTTTCTAGAAGATCTCCTACAATATTCTCAGCTGC
Improved (67.8 ± 0.5 °C)[2]	10232	TGGCTCGAGTTTTTCAGCAAGATTCCCTATCAGTGATAGAGATTGACATCC
	10233	CGGATCTGAAAGAGGAGAAAGGATCTATGGCGAGTAGCGAAGACGT

Supplementary Table 6.7: Oligonucleotides for crosstalk LCRs (continued).

Bridging Oligo Set (T_m per BO-half)	OligoID	Sequence (5'→3')
	10234	GTGTTGTTACCGTTACCCAGGACTCCTCCCTGCAAGACGGTG
	10236	AATGGTAAACTGACGCTGAAGTTCATCTGTACTACTGGTAAACTGCCGG
	10244	GGGTGGGCCTTTCTGCGTTTATAATCTTTCTAGAAGATCTCCTACAATATTCTCAGC
	10268	GGCCGCGTGTTACAACCAATGAAAGTGAAACGTGATTTCATGCGTC
	10281	AGCTGGAATACAATTTTAACAGCCACAATGTTTACATCACCGCCGATAAACAA

Supplementary Table 6.8: Bridging oligos for the assembly of the validation plasmid 1 (Supplementary Figure 6.15; results shown in Figure 3.9). All melting temperatures (T_ms) presented here are calculated for each BO-half using the formula of SantaLucia [89] for the T_m-calculation and the salt correction. [1] Bridging oligos with a target T_m of 70.0 °C for each half, with 8 % v/v DMSO and 0.45 M betaine and the experimental annealing temperature of 55 °C. [2] Bridging oligos with a target T_m of 74.8 °C for each half, with 8 % v/v DMSO and 0.45 M betaine and the experimental annealing temperature of 55 °C. [3] Bridging oligos with a target T_m of 67.8 °C for each half, without DMSO and betaine and the experimental annealing temperature of 66 °C. DMSO: dimethyl sulfoxide, T_m: melting temperature of a BO-half, w/o: without. This table is adapted from Schlichting *et al.* [95].

Bridging Oligo Set (T_m per BO-half)	**OligoID**	**Sequence (5'→3')**
Three part split		
Baseline (70.8 ± 0.4 °C)[1]	10425	CGTGAGCATCCTCTCTCGTTTCATCGGTATCATTACCCCCATGAACAGAAATCCCC
	10429	AAATCGCCATTCGCCAGGGGTGTCGATACTATGTTATACGCCAACTTTGAAAACAAC
	10432	GCTTGGTTTTTCAGCTAAAATAACCGTACTCACGCTGCACCGTTTCGAAGAGAC
75 °C (74.5 ± 0.9 °C)[2]	10396	CCGTATCGTGAGCATCCTCTCTCGTTTCATCGGTATCATTACCCCCATGAACAGAAATCCCCCTTACA
	10411	CGAAAATCGCCATTCGCCAGGGGTGTCGATACTATGTTATACGCCAACTTTGAAAACAACTTTGAAA
	10417	GCCTGGCTTGGTTTTTCAGCTAAAATAACCGTACTCACGCTGCACCGTTTCGAAGAGACCG
Improved (68.1 ± 0.4 °C)[3]	10400	TGAGCATCCTCTCTCGTTTCATCGGTATCATTACCCCCATGAACAGAAATCC
	10412	CGCCATTCGCCAGGGGTGTCGATACTATGTTATACGCCAACTTTGAAA
	10418	TGGTTTTTCAGCTAAAATAACCGTACTCACGCTGCACCGTTTCGAAGAG
Seven part split		
Baseline (70.9 ± 0.6 °C)[1]	10429	AAATCGCCATTCGCCAGGGGTGTCGATACTATGTTATACGCCAACTTTGAAAACAAC
	10430	GAAAAATACCGCTGCGTAAAAGATACGGAAGGAATGTCTCCTGCTAAGGTATATAAGCTGG
	10431	GGAGTGCATCAGGCTCTTTCACTCCATCGACATATCGGATTGTCCCTATACGAATAG
	10432	GCTTGGTTTTTCAGCTAAAATAACCGTACTCACGCTGCACCGTTTCGAAGAGAC
	10423	GCCCGGTACCCAATTCGCCCTATAGTGAGTCGTATTACGCGCGCTC
	10424	GGAAAACCCTGGCGTTACCCAACTTAATCGCCTTGCAGCACATCCCC

Supplementary Table 6.8: Bridging oligos for the assembly of the validation plasmid 1 (continued)

Bridging Oligo Set (T_m per BO-half)	**OligoID**	**Sequence (5'→3')**
	10425	CGTGAGCATCCTCTCTCGTTTCATCGGTATCATTACCCCCATGAACAGAAATCCCC
75 °C (74.6 ± 0.7 °C)[2]	10411	CGAAAATCGCCATTCGCCAGGGGTGTCGATACTATGTTATACGCCAACTTTGAAAACAACTTTGAAA
	10413	ACTGATCGAAAAATACCGCTGCGTAAAAGATACGGAAGGAATGTCTCCTGCTAAGGTATATAAGCTGGTGGG
	10415	GCGGAGTGCATCAGGCTCTTTCACTCCATCGACATATCGGATTGTCCCTATACGAATAGCTTAGAC
	10417	GCCTGGCTTGGTTTTTCAGCTAAAATAACCGTACTCACGCTGCACCGTTTCGAAGAGACCG
	10399	GGCCCGGTACCCAATTCGCCCTATAGTGAGTCGTATTACGCGCGCTCACTGG
	10390	CTGGGAAAACCCTGGCGTTACCCAACTTAATCGCCTTGCAGCACATCCCCCTTT
	10396	CCGTATCGTGAGCATCCTCTCTCGTTTCATCGGTATCATTACCCCCATGAACAGAAATCCCCCTTACA
Improved (68.2 ± 0.5 °C)[3]	10412	CGCCATTCGCCAGGGGTGTCGATACTATGTTATACGCCAACTTTGAAA
	10414	ACCGCTGCGTAAAAGATACGGAAGGAATGTCTCCTGCTAAGGTATATAAGCT
	10416	GTGCATCAGGCTCTTTCACTCCATCGACATATCGGATTGTCCCTATACG
	10418	TGGTTTTTCAGCTAAAATAACCGTACTCACGCTGCACCGTTTCGAAGAG
	10403	CCCGGTACCCAATTCGCCCTATAGTGAGTCGTATTACGCGCGC
	10393	AACCCTGGCGTTACCCAACTTAATCGCCTTGCAGCACATCC
	10400	TGAGCATCCTCTCTCGTTTCATCGGTATCATTACCCCCATGAACAGAAATCC

Supplementary Table 6.9: Bridging oligos for the assembly of the validation plasmid 2 (Supplementary Figure 6.16; results shown in Figure 3.9). All melting temperatures (T_ms) presented here are calculated for each BO-half using the formula of SantaLucia [89] for the T_m-calculation and the salt correction. [1] Bridging oligos with a target T_m of 70.0 °C for each half, with 8 % v/v DMSO and 0.45 M betaine and the experimental annealing temperature of 55 °C. [2] Bridging oligos with a target T_m of 74.8 °C for each half, with 8 % v/v DMSO and 0.45 M betaine and the experimental annealing temperature of 55 °C. [3] Bridging oligos with a target T_m of 67.8 °C for each half, without DMSO and betaine and the experimental annealing temperature of 66 °C. DMSO: dimethyl sulfoxide, T_m: melting temperature of a BO-half. This table is adapted from Schlichting *et al.* [95].

Bridging Oligo Set (T_m per BO-half)	**OligoID**	**Sequence (5'→3')**
Three part split		
Baseline (70.8 ± 0.8 °C)[1]	10423	GCCCGGTACCCAATTCGCCCTATAGTGAGTCGTATTACGCGCGCTC
	10426	GGTGCTACAGAGTTCTTGAAGTGGTGGCCTAACTACGGCTACACTAGAAGGACAG
	10428	GTCAATGGTTCAGATACGACGACTAAAAAGTCAAGATCACTATTTGGTTTTAGTCCACTCTCAACTC
75 °C (74.2 ± 0.5 °C)[2]	10399	GGCCCGGTACCCAATTCGCCCTATAGTGAGTCGTATTACGCGCGCTCACTGG
	10391	GCGGTGCTACAGAGTTCTTGAAGTGGTGGCCTAACTACGGCTACACTAGAAGGACAGTATTTGGTAT
	10392	TTGATCTGTCAATGGTTCAGATACGACGACTAAAAAGTCAAGATCACTATTTGGTTTTAGTCCACTCTCAACTCCTGAT
Improved (68.7 ± 0.4 °C)[3]	10403	CCCGGTACCCAATTCGCCCTATAGTGAGTCGTATTACGCGCGC
	10394	TGCTACAGAGTTCTTGAAGTGGTGGCCTAACTACGGCTACACTAGAAGGACA
	10395	TGGTTCAGATACGACGACTAAAAAGTCAAGATCACTATTTGGTTTTAGTCCACTCTCA
Seven part split		
Baseline (70.8 ± 0.7 °C)[1]	10422	GGATGGCTCGAGTTTTTCAGCAAGATATCCGCTGCACCGTTTCGAAGAGAC
	10423	GCCCGGTACCCAATTCGCCCTATAGTGAGTCGTATTACGCGCGCTC
	10424	GGAAAACCCTGGCGTTACCCAACTTAATCGCCTTGCAGCACATCCCC
	10425	CGTGAGCATCCTCTCTCGTTTCATCGGTATCATTACCCCCATGAACAGAAATCCCC
	10426	GGTGCTACAGAGTTCTTGAAGTGGTGGCCTAACTACGGCTACACTAGAAGGACAG
	10427	ACTGCTAACAAAATTCTCTCCCTATGTTCTAATGGAGAAGATTCAGCCACTGCATTTCCC

Supplementary Table 6.9: Bridging oligos for the assembly of the validation plasmid 2 (continued)

Bridging Oligo Set (T_m per BO-half)	**OligoID**	**Sequence (5'→3')**
	10428	GTCAATGGTTCAGATACGACGACTAAAAAGTCAAGATCACTATTTGGTTTTAGTCCACTCTCAACTC
75 °C (74.5 ± 0.5 °C)[2]	10398	TCTTCCGGATGGCTCGAGTTTTTCAGCAAGATATCCGCTGCACCGTTTCGAAGAGACCG
	10399	GGCCCGGTACCCAATTCGCCCTATAGTGAGTCGTATTACGCGCGCTCACTGG
	10390	CTGGGAAAACCCTGGCGTTACCCAACTTAATCGCCTTGCAGCACATCCCCCTTT
	10396	CCGTATCGTGAGCATCCTCTCTCGTTTCATCGGTATCATTACCCCCATGAACAGAAATCCCCCTTACA
	10391	GCGGTGCTACAGAGTTCTTGAAGTGGTGGCCTAACTACGGCTACACTAGAAGGACAGTATTTGGTAT
	10397	ACTACGAACTGCTAACAAAATTCTCTCCCTATGTTCTAATGGAGAAGATTCAGCCACTGCATTTCCCGCAATATC
	10392	TTGATCTGTCAATGGTTCAGATACGACGACTAAAAAGTCAAGATCACTATTTGGTTTTAGTCCACTCTCAACTCCTGAT
Improved (68.3 ± 0.5 °C)[3]	10402	ATGGCTCGAGTTTTTCAGCAAGATATCCGCTGCACCGTTTCGAAGAG
	10403	CCCGGTACCCAATTCGCCCTATAGTGAGTCGTATTACGCGCGC
	10393	AACCCTGGCGTTACCCAACTTAATCGCCTTGCAGCACATCC
	10400	TGAGCATCCTCTCTCGTTTCATCGGTATCATTACCCCCATGAACAGAAATCC
	10394	TGCTACAGAGTTCTTGAAGTGGTGGCCTAACTACGGCTACACTAGAAGGACA
	10401	GCTAACAAAATTCTCTCCCTATGTTCTAATGGAGAAGATTCAGCCACTGCATTTCC
	10395	TGGTTCAGATACGACGACTAAAAAGTCAAGATCACTATTTGGTTTTAGTCCACTCTCA

6.2 *In vitro* LCR

6.2.1 Protocol for the cell extract production and the *in vitro* LCR

Cell extract from *E. coli* and cell free protein synthesis (CFPS) of LCRs

Niels Schlichting, Darius Zibulski

Abstract

To produce the cell extract from *E. coli* a short version of the published protocol [1] was developed. The cell extract can be generated within one day and is closely related to the protocol for competent *E. coli*. Afterwards the extract can be utilized to analyze the LCR *in vitro*. Before adding the cell extract an additonal DNA amplification by the rolling circle amplification is necessary. The workflow of the *in vitro* LCR is depicted in Figure 1.

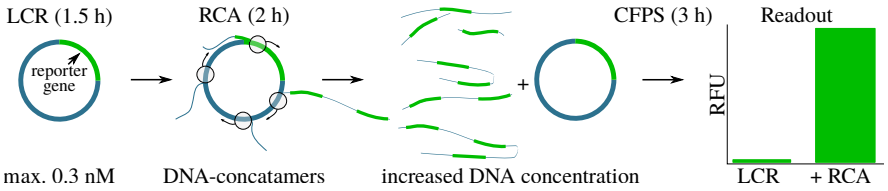

Figure 1: Scheme of the *in vitro* LCR. A LCR will be amplified by the rolling circle amplification (RCA) followed by an *in vitro* transcription and translation step (TXTL) for a cell free protein synthesis (CFPS) by adding the cell extract from *E. coli*.

Reagents

- LCR:

  as described in Schlichting *et al.* [2]
- rolling circle amplification (RCA):

  GenomiPhi™ V2 DNA Amplification Kit (GE Healthcare UK Limited, Buckinghamshire, UK)
- cell extract and buffer:

  all reagents were ordered as described in the protocol of Sun *et al.* [1]

1 Cell extract generation

Preculture

- 50 mL 2x YT+phosphate medium
- add appropriate antibiotics; for *E. coli* Rosetta EL22 add 34 µg mL^{-1} chloramphenicol and 50 µg mL^{-1} kanamycin
- inoculate preculture and incubate overnight at 37 °C and 200 rpm

Main culture

- 800 mL 2x YT+phosphate medium + antibiotics + 50 mL preculture in a 5 L flask
- inoculate main culture at 37 °C and 200 rpm
- let grow to OD_{600} of 3 to 3.5 (3.5 to 4.5 h)
- prepare ice boxes and cool down the centrifuge for the harvesting and 1 L S30A buffer without DTT
- put 2 mL of 1 M DTT on ice for thawing

Harvesting

- all following steps are performed on ice/4 °C!
- split the suspension in 4 centrifuge beakers with 200 mL each and centrifuge them for 12 min at 5000 g to get pellets
- decant the supernatant and put the beakers on ice
- add 2 mL of 1 M DTT to prechilled 1 L S30A buffer to get a final concentration of 2 mM DTT
- resuspend each pellet with 40 mL S30A-buffer + 2 mM DTT by shaking or vortexing (cool down after ca. 10 sec of shaking/vortexing)
- centrifuge for 12 min at 5000 g to get pellets and repeat the resuspension and centrifugation step (same volume of S30A buffer + DTT)
- after the two washing steps resuspend each pellet with 10 mL S30A-buffer + DTT
- weigh two 50 mL centrifuge falcons and cool them in ice
- pool the suspensions in the weighed 50 mL centrifuge falcons and centrifuge them for 20 min at 3499 g (max. g of the utilized rotor) to get pellets
- decant supernatant and centrifuge again for 2 min at 2000 g
- remove residual supernatant with a pipette and weigh the falcons to calculate the mass of the pellets
- add a volume of S30A buffer + DTT to each pellet which is equal to the mass of the pellet (e.g.: 1 g pellet = 1 mL buffer)
- resuspend the pellets by vortexing/shaking; put on ice in between as often as possible!

- make sure that the suspension is homogenous and no clumps are leftover
- split the suspension in 2 mL microcentrifuge tubes with max. 1 mL per tube

Lysis

- put the 2 mL microcentrifuge tubes in a beaker with ice water
- ensure that the tubes are in contact with the ice water during the sonification!
- place the tip of the sonotrode into the upper third of the tube
- make sure that the sonotrode has no contact to the tube
- lyse the cells: 10 sec pulse-10 sec pause with an amplitude of 50 %; check in between if the wall of the tube is still in full contact to the ice water and if the ice is not already melted!
- the sum of energy for each tube should be around 700 J
- after the sonification the suspension should be more aqueous and close to transparent
- the success of the sonification can be checked by observing the cell viability by microscopy

Extract

- centrifuge the 2 mL microcentrifuge tubes for 10 min at 12 000 g and 4 °C
- use pipettes to save the supernatant and transfer it to new 2 mL microcentrifuge tubes
- avoid the transfer of cell debris/clumbs! Repeat the centrifugation step if necessary
- incubate the tubes with the supernatant for 80 min at 37 °C and 220 rpm in a thermoshaker
- centrifuge the tubes for 10 minutes at 12 000 g and 4 °C
- pool all supernatants and aliquote the cell extract on ice
- freeze the cell extract with liquid nitrogen
- store the tubes at −80 °C

2 Ligase cycling reaction

- follow the protocol published in Schlichting *et al.* [2]
- the maximum product concentration of one LCR is 0.3 nM (concentration of the backbone in the LCR)
- use 0.3 µL of each LCR for one *in vitro* assay
- the concentration of 0.3 nM does not lead to a detectable signal in the CFPS
- the DNA has to be amplified in an additional step before the CFPS (Figure 1): the rolling circle amplification (RCA)

3 Rolling circle amplification

Reagents

- 0.3 nM LCR
- GenomiPhi™ V2 DNA Amplification Kit (GE Healthcare UK Limited, Buckinghamshire, UK):
  - sample buffer (stored at −20 °C)
  - reaction buffer (stored at −20 °C)
  - enzyme mix (stored at −80 °C)
- 10 mM dNTPs
- low-profile PCR tube or 384-Well PCR plate

Amplification

- use 0.3 µL of a 0.3 nM LCR per reaction
- add 0.62 µL of the sample buffer
- incubate for 3 min at 95 °C
- put tube/plate on ice and add
  - 0.62 µL of the reaction buffer
  - 0.18 µL of 10 mM dNTPs
  - 0.09 µL of the enzyme mix
- incubate for 90 min at 30 °C
- incubate for 10 min at 65 °C
- put tube/plate on ice and prepare the *in vitro* cell extract

4 Cell free protein synthesis with the cell extract

Reagents

- RCA-amplified LCR
- CFPS:
  - cell extract (stored at −80 °C)
  - cell extract buffer (stored at −80 °C)
- plate reader, optical sealing foil, top measurement if non-optical plates/tubes are used

Cell extract buffer

- this buffer is prepared as described in Sun *et al.* [1]
- the buffer consists of an amino acid solution, energy solution, Mg-glutamate, K-glutamate, PEG-8000 and DTT
- amino acid solution (4× stock solution in *A. dest.*, stored at −80 °C):
  - 5 mM leucine
  - 6 mM of all other amino acids
- energy buffer (14× stock solution in *A. dest.*, stored at −80 °C):

  - 700 mM HEPES (pH 8)
  - 21 mM ATP
  - 21 mM GTP
  - 12.6 mM CTP
  - 12.6 mM UTP
  - 2.8 mg mL^{-1} tRNA
  - 3.64 mM CoA
  - 4.62 mM NAD
  - 10.5 mM cAMP
  - 0.95 mM folinic acid
  - 14 mM spermidine
  - 420 mM 3-PGA
- to get ca. 2 mL of cell extract buffer:
  - 532 µL 4× amino acid solution
  - 459 µL *A. dest.*
  - 337 µL 14× energy buffer
  - 236 µL 40 % − m/v PEG-8000
  - 251 µL 3000 mM K-glutamate
  - 94 µL 500 mM Mg-glutamate
  - 70 µL 100 mM DTT
- the cell extract buffer can be stored at −80 °C

CFPS

- perform all steps on ice
- prepare a mastermix of cell extract and buffer:

  for one reaction:
  - 0.82 µL cell extract
  - 0.98 µL cell extract buffer
- add on ice 1.8 µL of the cell extract + cell extract buffer mix to each RCA-amplified LCR (1.8 µL)
- cover the plate with an optical plate
- the total volume of 3.6 µL has to be mixed
- spin down the volume for ca. 1 min and place the *in vitro* LCR reaction at 29 to 30 °C for 3 h
- an increase of fluorescence can be observed after ca. 30 to 40 min if a fluorescent reporter gene is utilized

References

[1] Sun, Z. Z., Hayes, C. A., Shin, J., Caschera, F., Murray, R. M., and Noireaux, V. (September, 2013) Protocols for Implementing an *Escherichia coli* Based TX-TL Cell-Free Expression System for Synthetic Biology. *JoVE (Journal of Visualized Experiments),* (79), e50762.

[2] Schlichting, N., Reinhardt, F., Jager, S., Schmidt, M., and Kabisch, J. (January, 2019) Optimization of the experimental parameters of the ligase cycling reaction. *Synthetic Biology,* **4**(1).

6.2.2 Investigations for the *in vitro* LCR workflow

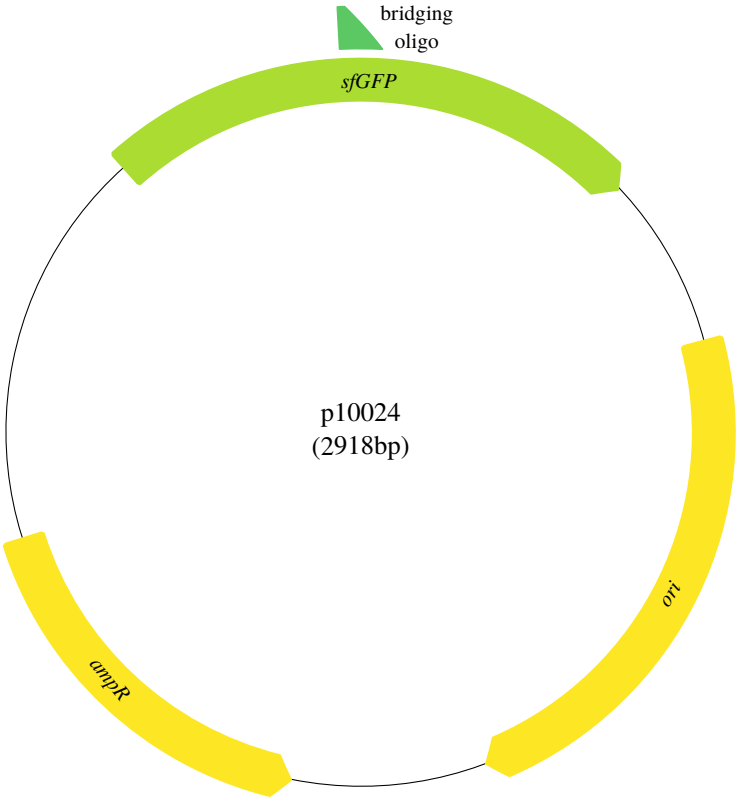

Supplementary Figure 6.19: Plasmid 'p10024' for the *in vitro* LCR investigation. For the LCRs of this plasmid, the plasmid was split in the middle of the *sfGFP*. *ampR*: gene for ampicillin resistance, *ori*: *origin of replication*, *sfGFP*: *super folder green fluorescent protein*.

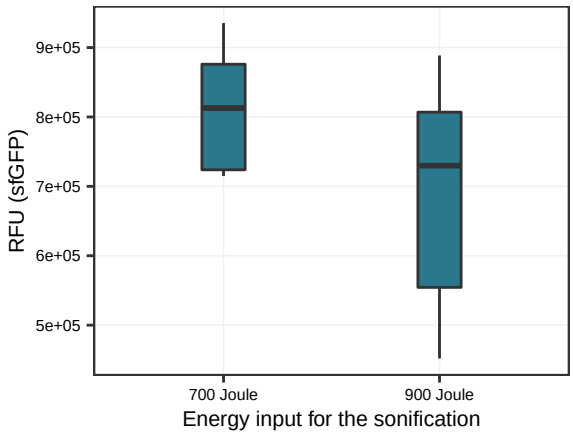

Supplementary Figure 6.20: For the preparation of the cell extract the cells were split before the sonification step. One batch of cell extract was produced by using 700 J, the other one by applying 900 J. Based on the results, the energy of 700 J for the sonification resulted in a slightly better cell extract. RCA-amplified plasmid was used in the CFPS for the measurements in the plate reader. The signals represent the measurements after 3 h. All measurements were performed as sextuplicates (n=6). As template for the RCA 0.3 nM of the isolated plasmid p10024 was used. Control reactions without plasmid were negative and are not shown. CFPS: cell free protein synthesis, RCA: rolling circle amplification, RFU: relative fluorescence unit, sfGFP: super folder green fluorescent protein.

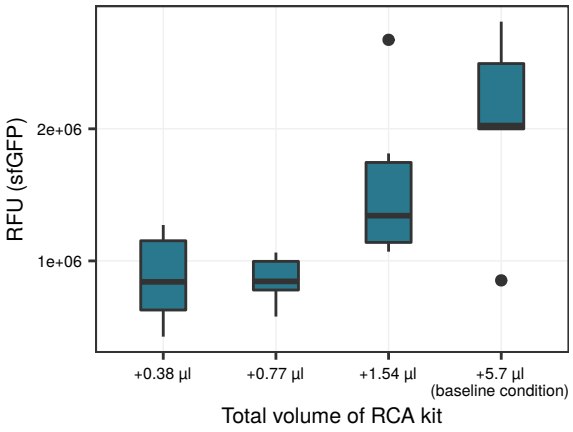

Supplementary Figure 6.21: The reduction of the RCA volume resulted in lower signal. The volume of 1.54 µL was chosen as the new improved RCA for the volume of sample and reaction buffer. The volume of the enzyme mix is still 0.3 µL in this experimental setup. The effects of lowering the enzyme mix volume is shown in Supplementary Figure 6.23. The signals represent the measurements after 3 h. All measurements were performed as sextuplicates (n=6). As template for the RCA 0.3 nM of the isolated plasmid p10024 was used. Control reactions without plasmid were negative and are not shown. RCA: rolling circle amplification, RFU: relative fluorescence unit, sfGFP: super folder green fluorescent protein.

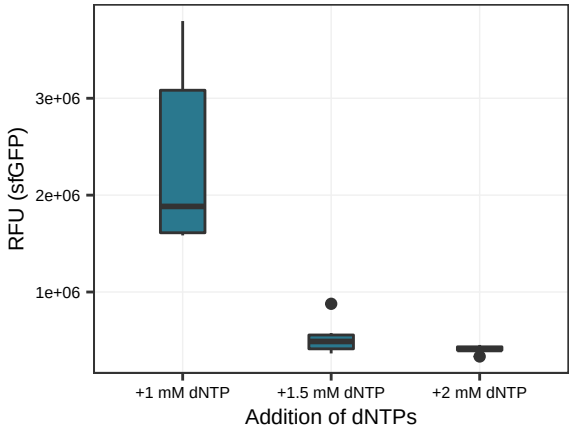

Supplementary Figure 6.22: Influence of the addition of dNTPs in the RCA. The positive effect of 1 mM dNTPs in comparison to no additional dNTPs is shown in Figure 3.24B. For all, 2 µL were used for the measurements in the plate reader. The signals represent the measurements after 3 h. All measurements were performed as sextuplicates (n=6). As template for the RCA 0.3 nM of the isolated plasmid p10024 was used. Control reactions without plasmid were negative and are not shown. RCA: rolling circle amplification, RFU: relative fluorescence unit, sfGFP: super folder green fluorescent protein.

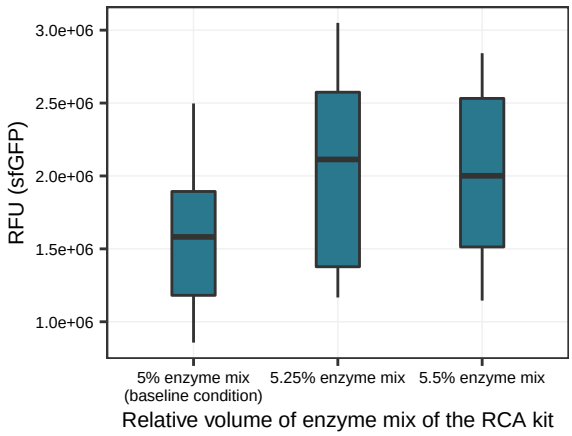

Supplementary Figure 6.23: Volume of enzyme mix in the RCA. Higher concentrations of the recommended 5 % v/v enzyme mix (manufacturers protocol) per RCA reaction mix (sample buffer + reaction buffer + enzyme mix) do not clearly improve the signal. As a baseline condition, the volumes for the sample and reaction buffer were already reduced as shown in Supplementary Figure 6.21. For all, 2 µL were used for the measurements in the plate reader. The signals represent the measurements after 3 h. All measurements were performed as sextuplicates (n=6). As template for the RCA 0.3 nM of the isolated plasmid p10024 was used. Control reactions without plasmid were negative and are not shown. RCA: rolling circle amplification, RFU: relative fluorescence unit, sfGFP: super folder green fluorescent protein.

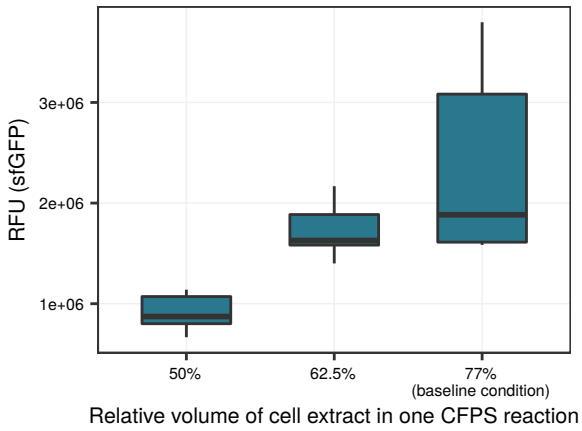

Supplementary Figure 6.24: Volume of cell extract in the *in vitro* LCR. Although the signal of the baseline condition is ca. 2× higher, the 50 % mix will be used for the optimized *in vitro* protocol. As a baseline condition, the volumes for the sample, reaction buffer and enzyme mix were already reduced as shown in Supplementary Figures 6.21 and 6.23. For all, 2 µL were used for the measurements in the plate reader. The presented signals presenting the measurements after 3 h. All measurements were performed as sextuplicates (n=6). As template for the RCA 0.3 nM of the isolated plasmid p10024 was used. Control reactions without plasmid were negative and are not shown. CFPS: cell free protein synthesis, RCA: rolling circle amplification, RFU: relative fluorescence unit, sfGFP: super folder green fluorescent protein.

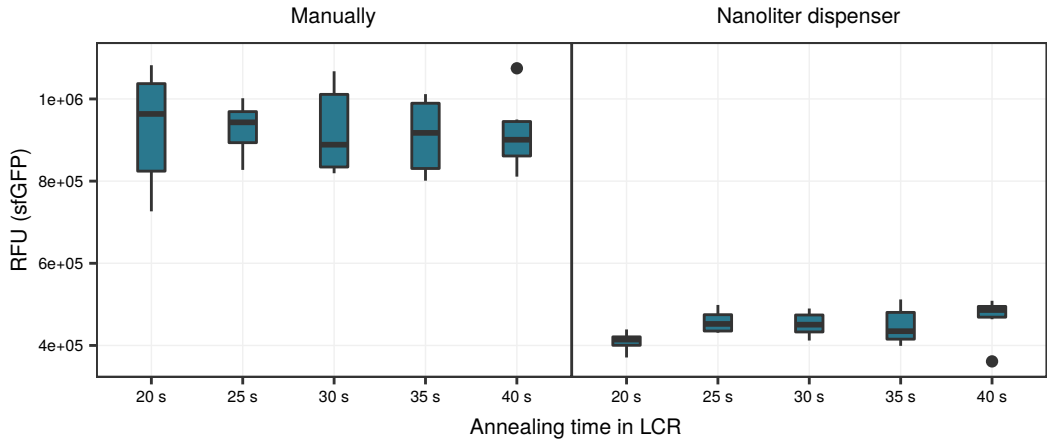

Supplementary Figure 6.25: A nanoliter dispensing unit decreases the absolute deviation of the *in vitro* LCR results. Although the fluorescence signals are lower for the investigation with the nanoliter dispenser (right plot), a higher reproducibility is observable. For all, 2 µL were used for the measurements in the plate reader. The presented signals presenting the measurements after 3 h. All measurements were performed as sextuplicates (n=6). As template for the RCA 0.3 nM LCR was used. Control reactions without DNA were negative and are not shown. CFPS: cell free protein synthesis, RCA: rolling circle amplification, RFU: relative fluorescence unit, sfGFP: super folder green fluorescent protein.

6.3 CloneFlow

6.3.1 Installation code for the CloneFlow Server

This code was mainly written by Felix Reinhardt (AG Koeppl).

```
"""Assist the user with setting up the server.
Call in terminal: python3 installer.py
"""

import sys,os, time
import getpass

if "/" in __file__:
stop = input("""It seems that Python is not run from the terminal.
The setup may fail. Proceed: y/n """)
if not stop.lower() in ("y","yes"):
print("Aborting execution.")
sys.exit(1)


DIR = os.path.dirname(os.path.abspath(__file__))+"/site/env1"
os.chdir(DIR)


RED    = '\033[91m'
GREEN  = '\033[92m'
YELLOW = '\033[93m'
BLUE   = '\033[94m'
HEADER = '\033[95m'
END    = '\033[0m'
BOLD   = '\033[1m'
BAD = YELLOW+BOLD

def print2(typ,s): print(typ+s+END)

def Replace(path, *placeholders):
"""Take a placeholder file and fill out the PLACEHOLDER strings to
   create the actual file.
```

```
E.g. Replace("file.txt","test") will use the file fileplaceholder.
    txt and
replace all"PLACEHOLDER0" with "test"."""
name, ext = os.path.splitext(path)
data = open(name+"placeholder"+ext,"r").read()
for i,new in enumerate(placeholders):
data = data.replace("PLACEHOLDER"+str(i),new)
open(path,"w").write(data)

# Install all required packages:

rv = os.system("sudo apt-get install python3.5 build-essential
    python3.5-dev python3-tk python3-pip libxml2-dev libz-dev qt5-
    default postgresql postgresql-contrib nginx rabbitmq-server")
if rv: print2(BAD,"Something went wrong with installing packages.
    This might be bad.")

rv = os.system("sudo python3 -m pip install Biopython python-igraph
     matplotlib django celery uwsgi psycopg2")
if rv: print2(BAD,"Could not install anything with pip.")


# Set up the database:
print("")
print2(YELLOW,"Creating DB named cloneflow.")

rv = os.system("sudo -u postgres psql -c 'CREATE DATABASE cloneflow
    '")
if rv: print2(BAD, "Could not create database.")
print("")
print(YELLOW+"Setting postgres password.")
rv = os.system("sudo -u postgres psql -d cloneflow -c '\password'")
postgresPassword = getpass.getpass("Enter password once more: ")
# Create a settings.py with the database password.
print(END)
Replace("env1/settings.py", postgresPassword)
print2(GREEN+BOLD, "Added the password to env1/settings.py.")
```

```
# Create env1_nginx.conf from template. Feed in the current
    directory (it does not accept relative paths).
assert os.path.exists("/etc/nginx/sites-enabled"), "nginx
    installation not found."
Replace("env1_nginx.conf", DIR)

# Make a symbolic link from env1_nginx.conf to etc/nginx/sites-
    enabled/.

# Create softlink only if it does not exist.
if not os.path.exists("/etc/nginx/sites-enabled/env1_nginx.conf"):
assert not os.system("sudo ln -s "+DIR+"/env1_nginx.conf /etc/nginx
    /sites-enabled/env1_nginx.conf"), "Could not create softlink for
     nginx."

# Set the uwsgi paths:
Replace("env1_uwsgi.ini",DIR)



# Tell Django about it:
rv = os.system("python3 manage.py makemigrations")
if rv: print2(BAD, "Could not make migrations. Did you type the
    wrong password in the previous step?")

rv = os.system("python3 manage.py migrate")
if rv: print2(BAD, "Could not migrate.")



# Create django user.
print("")
print2(YELLOW,"Create superuser for Django (ctrl+c to skip this
    step):")
rv = os.system("python3 manage.py createsuperuser")
if rv: print2(BAD, "Superuser not created.")


os.system("chmod 777 ./restart.sh")
```

```
rv = os.system("./restart.sh")
if rv: print2(YELLOW, "Could not restart nginx and rabbitmq.")

os.system("chmod 777 ./start.sh")
rv = os.system("./start.sh")
if rv: print2(BAD, "Could not start the server.")
```